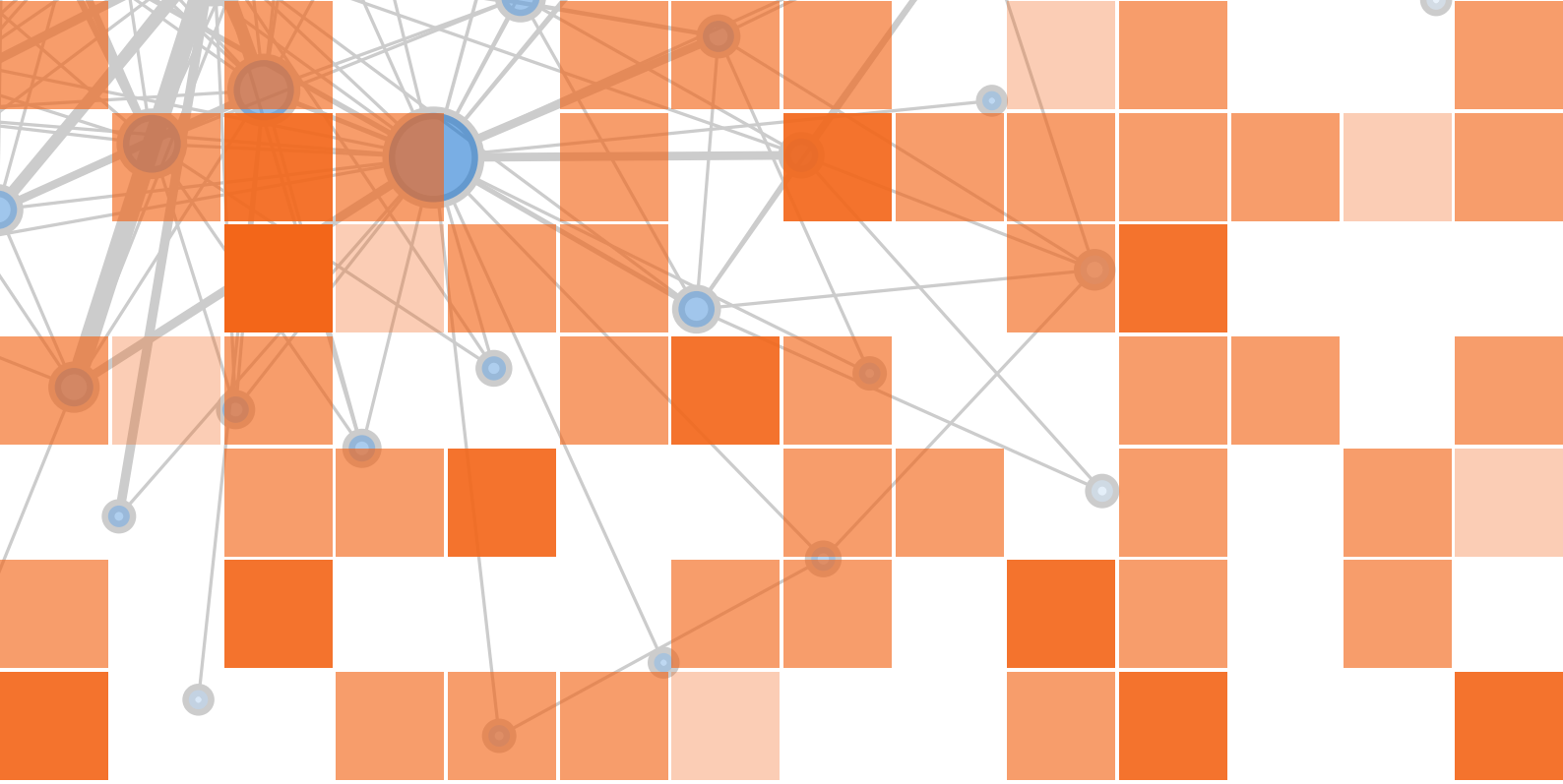

Dynamical properties of gene regulatory networks involved in long-term potentiation

a thesis submitted for the degree of Doctor of Philosophy

Gonzalo Sánchez Nido

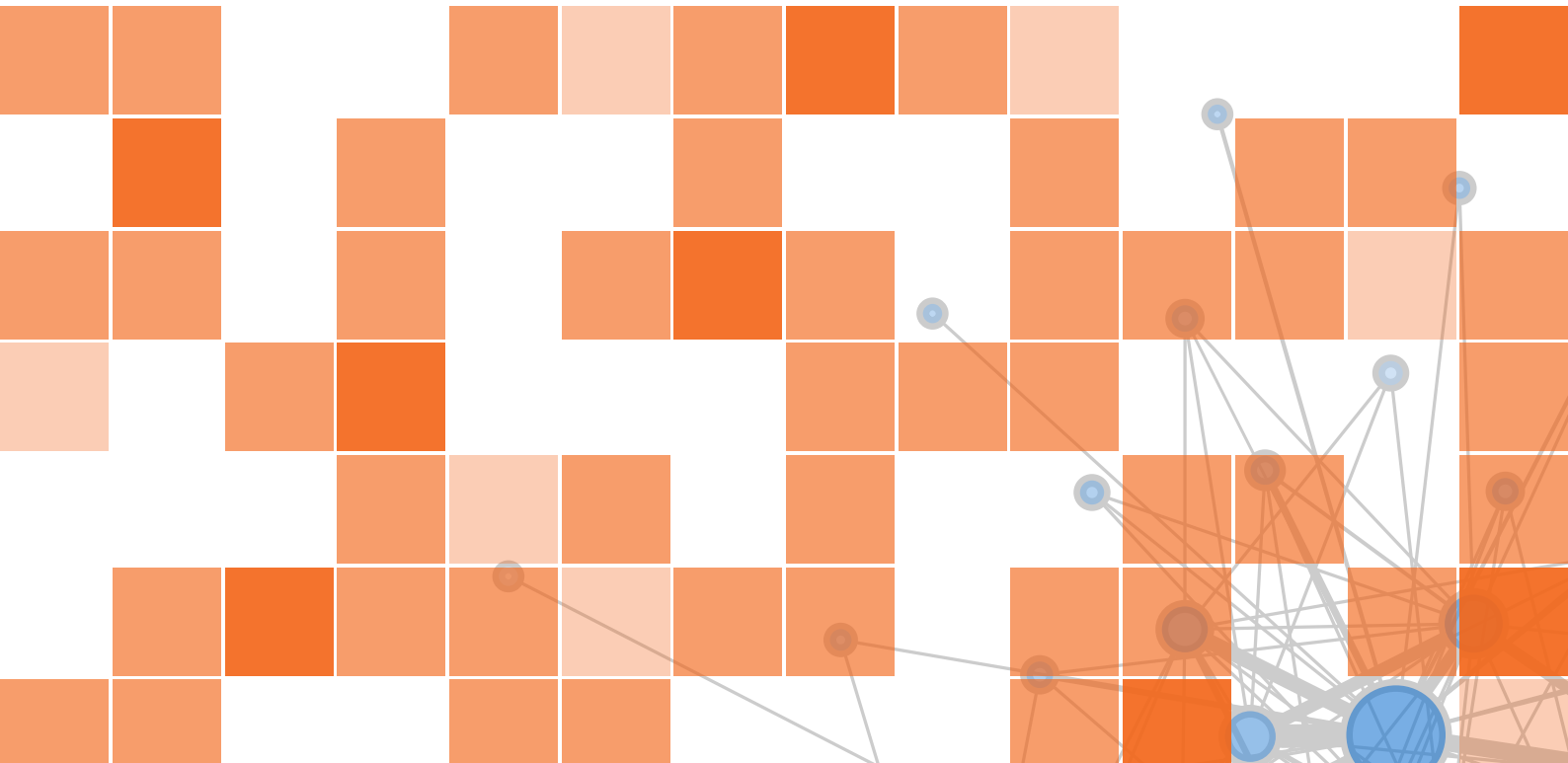

Dynamical properties of gene regulatory networks involved in long-term potentiation

DEPARTMENT OF COMPUTER SCIENCE, UNIVERSITY OF OTAGO

The research work presented on this thesis has been partially published and portions of these publications are reused. Textual portions and figures of these publications are reused with permission.

- Nido, G., Williams, J., and Benuskova, L. (2012). Bistable properties of a memory-related gene regulatory network. In Neural Networks (IJCNN), The 2012 International Joint Conference on, 1602–1607. IEEE.

  "The IEEE does not require individuals working on a thesis to obtain a formal reuse license"

- Nido, G., Ryan, M., Benuskova, L., and Williams, J. (2015). Dynamical properties of gene regulatory networks involved in long-term potentiation. Frontiers in Molecular Neuroscience, 8(42).

  "Under the Frontiers Terms and Conditions, authors retain the copyright to their work. All Frontiers articles are Open Access and distributed under the terms of the Creative Commons Attribution License, (CC-BY 3,0), which permits the use, distribution and reproduction of material from published articles, provided the original authors and source are credited, and subject to any copyright notices concerning any third-party content"

First submitted, March 2015
Hardbound copy deposited, July 2015

Abstract

The significant increase in the availability of postgenomic data has stimulated the growth of hypothesis-generating strategies to unravel the molecular basis of nature. The application of systems theory to biological problems emerged in the early 1970s, and yet the computational methods developed to model biological networks and analyse their functionality have been seldom used for understanding the neurogenetic basis of cognition. The main interests of this thesis are the application of computational models to microarray expression data for the identification and analysis of biological networks related with long-term potentiation (LTP), the cellular correlate of learning and memory in mammals. The models include the analysis of co-expression and studies of dynamical stability.

The thesis starts with the application of established methods on gene expression analysis on the available expression data from LTP in order to identify networks of closely correlated genes in their patterns of expression to ultimately pinpoint putative key regulators not identified previously by classical differential expression analysis.

The thesis continues with the analysis of previously identified gene networks regulated 20 min, 5 h, and 24 h post-LTP induction. A dynamical stability analysis using weight matrices suggests that the early network has a significant sensitivity to perturbations compared with randomly generated networks of similar characteristics. In addition, using random Boolean networks, we study the differential sensitivity to perturbations of these networks and we find that our results are consistent with a model of LTP as a complex cellular switch. In such a scenario, earlier networks are dynamically more unstable than later regulatory networks, which are proposed to be responsible for the new homeostatic state reached by the stimulated neurons. Key genes responsible for the dynamic properties observed are identified and discussed. In particular, we found that Egr2, a member of the Egr family of transcription factors was crucial to the bistability observed in the early-response network. Other genes previously associated with LTP have a more modest contribution.

A functional analysis of these networks is presented and integrated with previous knowledge on the molecular basis of LTP.

A Miki y a Javi

Acknowledgements

This thesis would not have been possible without emotional support. I left family and friends behind when I started my PhD at the University of Otago. I have to thank each member of the P.B. group of WhatsApp, made up of my Biology classmates from Uni, now scattered all over the world – Jero, Djordje, Pin, Carol, Pablulu, Palo, Ainhoa, Rincho, Mery, Manolo, Isa, Paula and Paulita.

I would also like to extend my thanks to the members of the P.H. group on Telegram, set up during a quick encounter in Berlin with Molly, Pako and David Lee. They helped me to keep up with music and politics, and at the same time share desperation and joy.

I would like to express my very great appreciation to the members of the Bioinformatics Unit of the Centre for Molecular Biology Severo Ochoa, where I worked as a research assistant before starting my PhD – Ugo, Alberto, David, Klett, Antonio, Ruben, Fons and Amigo.

"Survival" in Dunedin has been possible thank to local friends, of course. Throughout these years, people have come and gone, but some of them have been there for quite a long time. I am deeply grateful to Sam and Andrew. You have made me feel at home up in the summits and back home in Dunedin and I feel a great deal of admiration for you. Also, thank you Dave for being always there when I needed a place to stay or someone to talk to. Pretty much all my friends in New Zealand are amazing climbers – Sarah, Kate, Dani, Rocio, Martin, Paul and Michelle. It has been delightful to climb mountains, ice and rock with you during these years (and the years to come).

I would also like to thank Lech for the conversations during coffee breaks and lunches. Your enthusiasm and company have definitely made a difference to my life in the Department.

Central to this thesis are my main and co-supervisors, Lubica and Joanna. I would like to express my deep gratitude for the opportunity to embark this journey. Thank you for your help, knowledge and encouragement throughout these years. I would also like to thank Margaret for her advice and assistance with the microarray data.

My family, of course, despite the distance, has always been *there* for me. Mum, dad, Miguel and Javi – thank you so much.

I am particularly grateful to Maud, who has been there pretty much every day during my PhD, dealing with my unbearable personality, my ups and downs, and my contradictions.

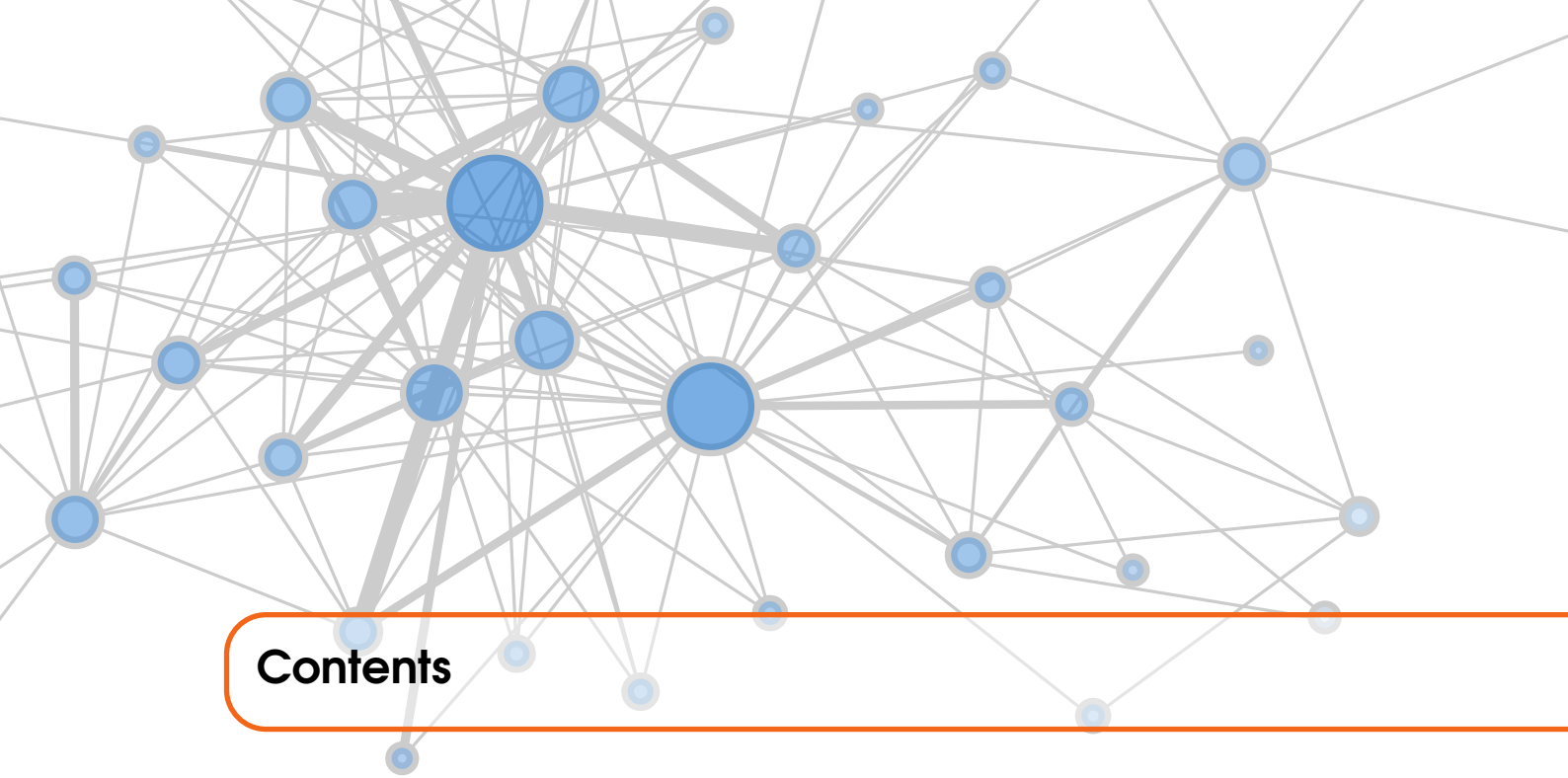

Contents

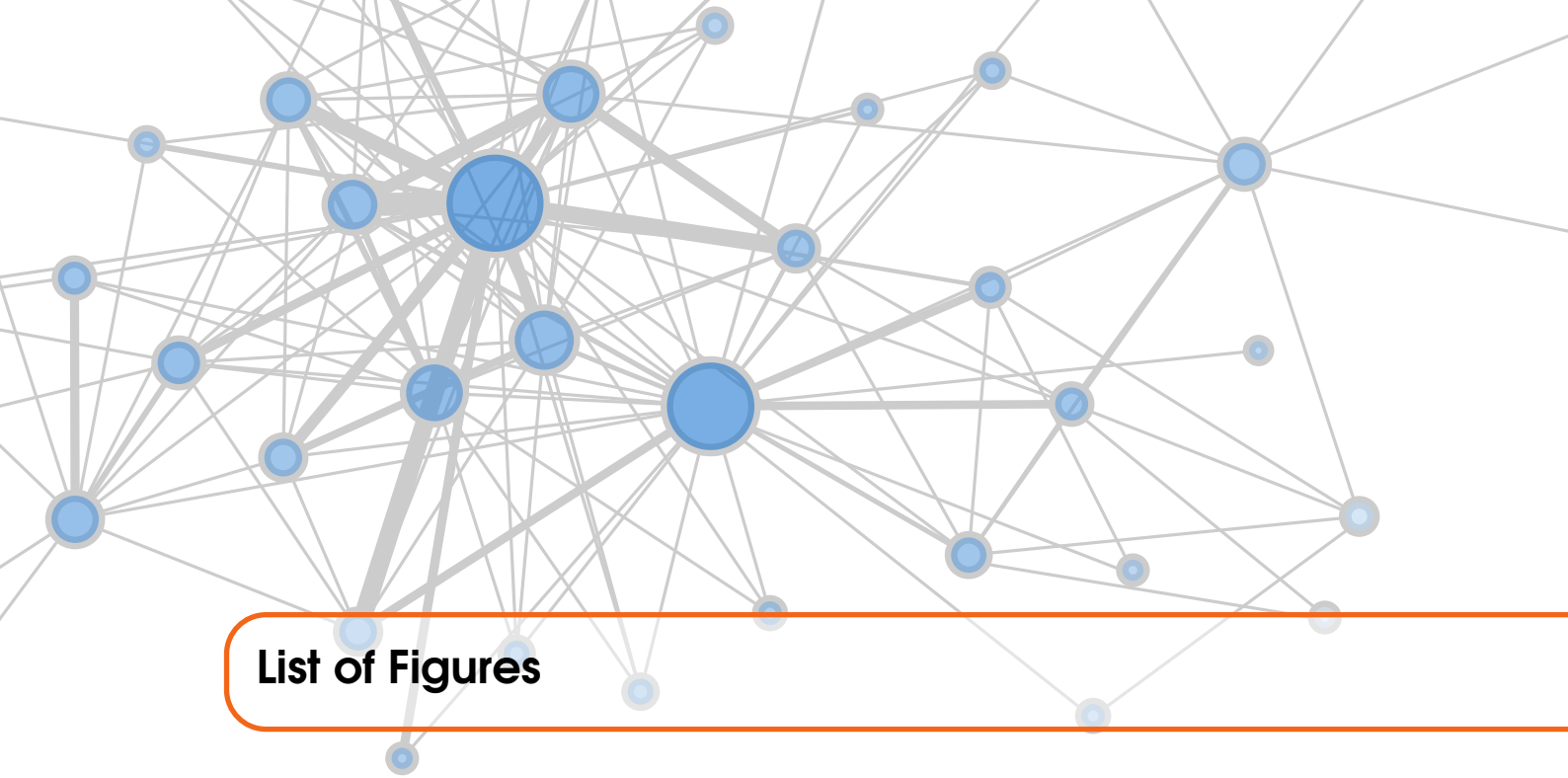

List of Figures

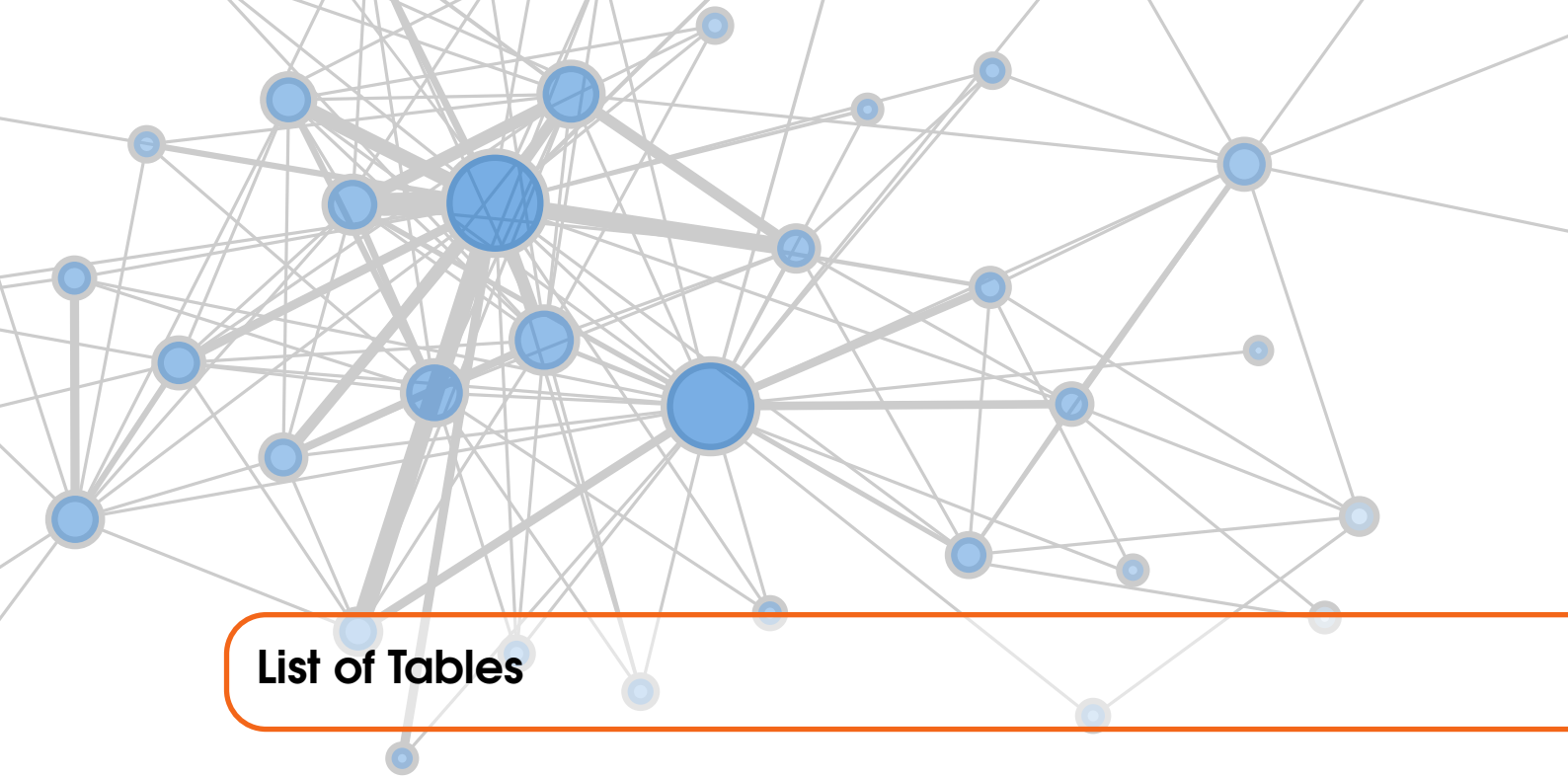

List of Tables

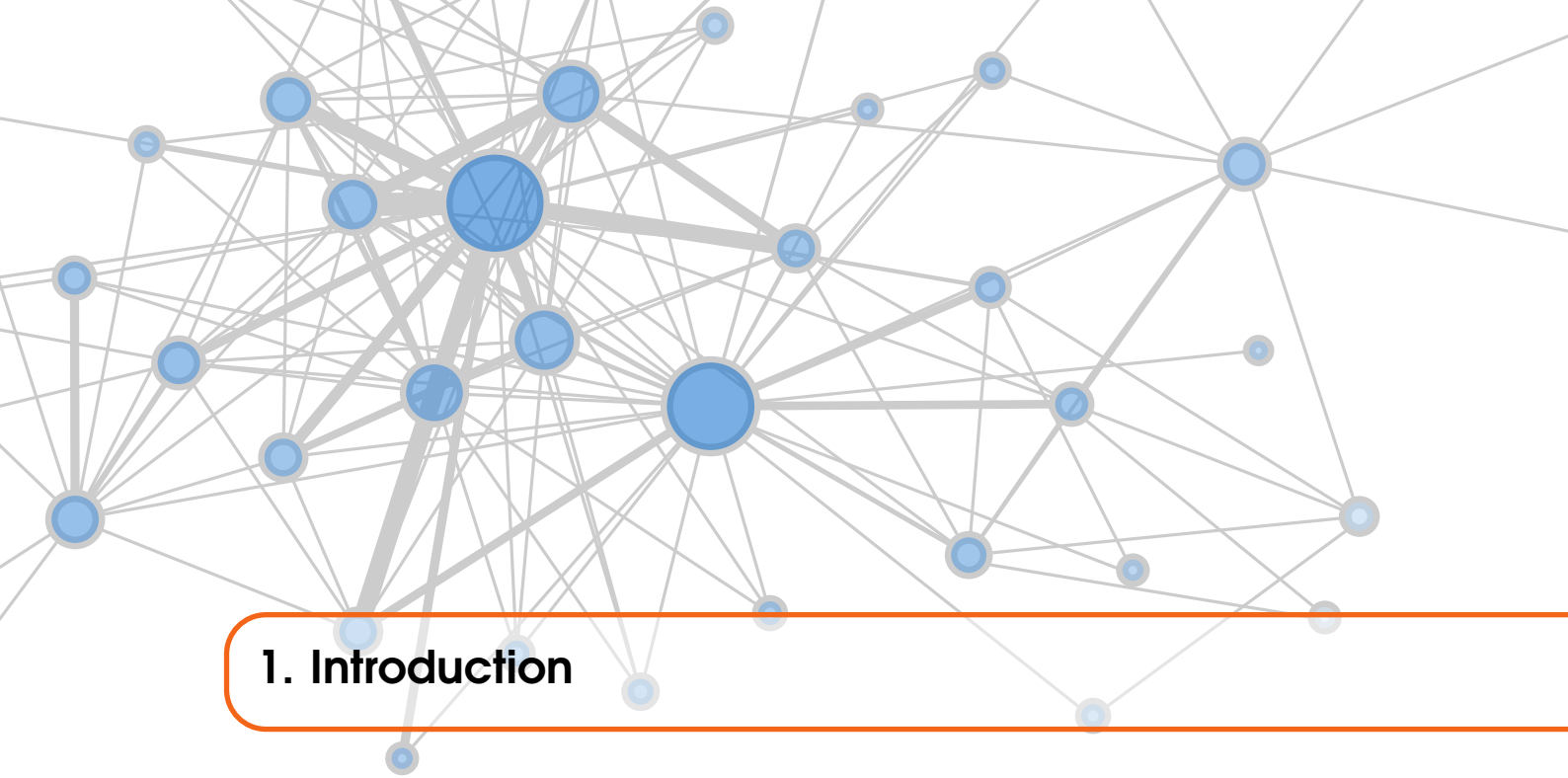

1. Introduction

If a man carries many such memories into life with him, he is saved for the rest of his days. And even if only one good memory is left in our hearts, it may also be the instrument of our salvation one day

Fyodor Dostoyevsky

1.1 Neuroscience and the study of the brain

The brain is the centre of the nervous system and is localised in close proximity to the main sensory organs. Information from the sensory organs is integrated by the brain to elicit adequate responses. The ability to learn and retain memories represents an evolutionary advantage for the success of a species in a changing environment. Whereas the capacity to retain information over long periods of time is not exclusive to the mammalian brain, some notable differences exist between their brains and the other vertebrates.

Perhaps the most striking feature of the mammalian brain is its larger size when compared to other vertebrates. But more interestingly, the brain of mammals is structurally different as well. The mammalian brain possesses a highly complex structure called *neocortex*, which differs from the more simple *pallium* found in other vertebrates (Aboitiz, Morales, and Montiel, 2003). Other areas such as the *amygdala* and the *hippocampus* are more developed. The hippocampus, in particular, is a brain region that, as such, is only present in mammals.

Differences also exist between human brain and their close relatives – the great apes. The human brain is remarkably large in size. Despite their similar overall body size, our brain is about three times heavier. The brain represents around 20% of the total body oxygen consumption and around 25% of the glucose.

The complexity of the nervous system is difficult to conceive. For example, an average human adult brain consists of around 85 billion neurons connected in a network of around 10^{14}-10^{15} connections, known as synapses (Herculano-Houzel, 2009). The brain of a rat, on the other hand, consists of 200 million neurons and between 10^{11} and 10^{12} synapses (Herculano-Houzel and Lent, 2005). The computational capabilities that such a network of processing units can hold is fascinating.

Especially considering that each of those synaptic connections possesses an extraordinary plasticity subject to fine tuning dependent on the specific requirements. Furthermore, neurons are able to create new connections with other neurons, reconfiguring the wiring of the network as we interact with the environment. At the same time, the brain withstands a disruption of the neural connectivity across the major neurodegenerative diseases. Indeed, these changes can be specific to the syndromes to some extent and track the pattern of the pathological development (Zhang, Wang, Wu, Kuang, Huang, He, and Gong, 2011; Pievani, de Haan, Wu, Seeley, and Frisoni, 2011).

While the first references to the human brain can be traced back as far as the times of the Ancient Egyptians, the consideration of the brain as a seat of intelligence dates to the times of the Ancient Greeks. The structural characterisation of the brain was a subject of study since the Hellenistic period, and knowledge of the anatomy of the brain has steadily accumulated ever since.

It was, however, during the late 19th Century that the field of neuroscience, benefiting from technical advances, broadened more greatly and incorporated different disciplines. The seminal work carried by Ramón y Cajal using the staining technique developed by Camillo Golgi represents perhaps the most influential breakthrough in the field of neuroscience. Their results lead to the neuron doctrine – the hypothesis that the functional unit of the brain is the neuron (Kandel, Schwartz, Jessell, *et al.*, 2000). Additional support for this theory came from the field of modern electrophysiology and the introduction of electron microscopy. While these experiments were carried out using animal models, other studies were focused on language disorders. French neurologist Pierre Paul Broca identified particular regions in the brain responsible for language. These results served as starting point for a number of subsequent studies to characterise functionally the different anatomical regions of the brain.

The advent of molecular biology and the 20th Century together with the consequent movement of the "gene" to the spotlight of biology brought an interest in the role of genes in behaviour. The first large-scale experiments where conducted in flies by the group of Seymour Benzer in the early 1970s, studying the effects of mutations in the circadian rhythm. Joseph Takahashi, in the 1990s, conducted similar studies on mice. Although human genetics represent a much more challenging scenario, there has been exceptional progress in the last decades in this regard, with a variety of mutations being identified with neurological disorders. These genes have been put into the context of molecular pathways and have shed light on the genetic basis of neurological and psychiatric disorders. Aside disease-oriented research, studies at the molecular level have characterised in great detail the mechanisms underlying neuronal function. Molecular biology and genetics methods have been adopted to understand neuronal development and how genetic changes influence biological functions.

The genomic and proteomic revolutions of the 1990s, together with the advent of other *-omic* fields has fired the popularisation of the discipline of systems biology in the late 1990s. The fast accumulation of genomic data has led to the development of a class of methodologies at the systems-level, with the aim to provide a more integrative understating of the nervous system function (Geschwind and Konopka, 2009; De Schutter, 2008). The adoption of functional genomics or molecular-systems methods that allow a dynamic measurement of gene products in a highly parallel manner, coupled with an underlying systems-level knowledge of the organization of these gene products, has the potential to provide a more integrative understanding of nervous system function.

1.2 Learning and memory

Somewhere within that complex network of neurons that constitute the brain, we encode, store, and retrieve information. This brain function is what we define as "memory". Memory is, in other words, the ability of the mind to hold and recall past experiences, and represents one of the most intensively studied subjects in the field of neuroscience.

The historic case of Henry Molaison (H.M.) is perhaps the most paradigmatic in the study of the neural basis of memory. In 1953, H.M. underwent a brain surgery to alleviate a case of severe intractable epilepsy in the medial temporal lobe. The surgery included the resection of the hippocampus and the adjoining regions in both hemispheres, which resulted in a very specific and severe anterograde amnesia. H.M. was able to recall memories of the times before the operation, including his normal vocabulary. He was, however, unable to form new memories. He would be able to retain new information for short periods of time, but he would forget after some minutes. H.M. had lost the ability to form new long-term memories, even though his short-term working memory was intact.

Despite not being able to remember new episodes after the surgery, H.M. was able to form a very specific type of long-term memories. He was able to improve his motor skills upon training, yet he would not be able to remember the training itself (Squire, 2009). This form of memory is what we know today as *implicit* memory (Kandel *et al.*, 2000; Roediger, 1990).

The case of H.M. case showed that new memories that require a conscious retrieval (*explicit* or declarative memories) were formed in the medial temporal lobe. Other cases narrowed the anatomical location for the formation of new explicit memories down to the hippocampus and more specifically highlighted the importance of the CA1 region. Long-term memories, however, are thought to be ultimately stored in the cerebral cortex. While the capacity of neurons to fix short-term events into long-term memories has been attributed to activity-dependent changes in the efficacy of synaptic connections throughout the 20th century, the experimental evidence did not come until 1966 by the hand of Terje Lømo. Lømo observed in the rabbit hippocampus that repetitive activation of excitatory synapses resulted in an increase in synaptic strength that could last for long periods of time (Lømo, 1966, 2003). This form of synaptic plasticity is known as LTP.

As it shall be discussed in more depth in Chapter 3, LTP represents the cellular mechanism responsible for long-term memories in mammals. Although some of their basic molecular mechanisms have been described, the molecular basis of LTP is an active field of research. Perhaps one of the most active discussions on LTP lies on the role of gene expression in the mechanistically different phases, and is the central topic of this thesis.

1.3 Motivation

It is known that the maintenance of LTP depends on gene expression (Abraham, Mason, Demmer, Williams, Richardson, Tate, Lawlor, and Dragunow, 1993; Abraham and Williams, 2003; Goelet, Castellucci, Schacher, and Kandel, 1986; Bramham, Alme, Bittins, Kuipers, Nair, Pai, Panja, Schubert, Soule, Tiron, *et al.*, 2010), but the mechanisms are still far from being well understood. Efforts towards a deeper understanding of the gene regulatory networks underlying LTP have been undertaken by Ryan, Mason-Parker, Tate, Abraham, and Williams (2011); Ryan, Ryan, Kyrke-Smith, Logan, Tate, Abraham, and Williams (2012) among many others. The new high-throughput methods developed in recent times have rendered available a great amount of valuable data on gene expression that is yet to be fully studied.

As we have mentioned, LTP is the change in synaptic efficiency most likely to be one of the cellular mechanisms responsible for long-term memory storage in the mammalian brain. From an experimental perspective, LTP behaves as a cellular switch whose output on/off value can be measured by the means of recording electrodes. Namely, cells that do not receive a stimulus sufficient to induce LTP will not show a significant change in their field excitatory post-synaptic potential. Figure 3.4 in Chapter 3 represents the effect of a high-frequency stimulus on the field excitatory post-synaptic potential (see also Chapter 3). As any other biological switch, a compromise between (a) robustness to genetic and environmental noise and (b) sensitivity to discriminate meaningful signals, is likely to be embedded in its structure. Furthermore, these

characteristics are expected to be distributed at different levels of biological organisation, requiring of an integrative, systems-level approach to its study.

From a genetic control perspective, attractors have been postulated to represent a specific pattern of protein expression that defines the cell's character (Kauffman, 1969b), and LTP offers an attractive model of biological switch – LTP can be experimentally measured and at the same time its long-lasting effect overlaps through different spatial and temporal scales of organisation.

1.4 Thesis goals

This thesis aims to:

(1) Identify additional regulators expressed at different times post-LTP by the use of available tools for the analysis of gene expression data. In particular the classical differential expression methodology is compared with the co-expression networks (Chapters 5 and 6)

(2) Study the modules of co-expressed genes to identify the functions that are significantly enriched. Discuss the relevance of central genes and functions within the context of LTP (Chapter 6)

(3) Characterize from a dynamical stability perspective the biological networks previously identified (Chapters 7 and 8)

1.5 Thesis outline

The present **Chapter 1** offers a brief introduction to the thesis and the motivation behind the experimental work carried out. Aims and problem statement are described. An overview on cellular biology focused on gene expression and microarray technology is presented throughout **Chapter 2**. LTP is then reviewed in **Chapter 3**, together with the basic biology of neurons and neural systems. **Chapter 4** describes the methodology for gene regulatory networks. The models used in this thesis – random Boolean networks and transcription regulation modelling using weight matrices are described in particular depth. These chapters should be considered introductory since they mostly cover a literature review of the field. Note, however, that Chapter 4 reviews *methodologies* in gene regulatory networks and hence provides a methodological ground for subsequent chapters. A description of the microarray data used is given in **Chapter 5**, which also replicates the classical differential expression analysis. The results presented in this chapter do not contain novel findings and are not thoroughly discussed in the thesis although they are referred to when relevant. The aim of the chapter is to describe the data processing conducted with the microarray datasets used as a starting point for the analyses performed subsequently.

Differential expression analysis introduced in Chapter 5 is extended and complemented by a co-expression analysis using the weighted gene co-expression network analysis tool at different times post-LTP induction in **Chapter 6**. **Chapter 7** focuses on a previously identified early network (20 min after LTP induction) by Ryan *et al.* (2011) and characterises its dynamics by implementing transcription regulation modelling using weight matrices. Results of the stability analysis of the network are described. **Chapter 8** further extends the analysis of gene expression underlying LTP by characterising the dynamic regime of the networks identified by Ryan *et al.* (2011) and Ryan *et al.* (2012) at different times post-LTP (20 min, 5 h, and 24 h). Conclusions are outlined in **Chapter 9**.

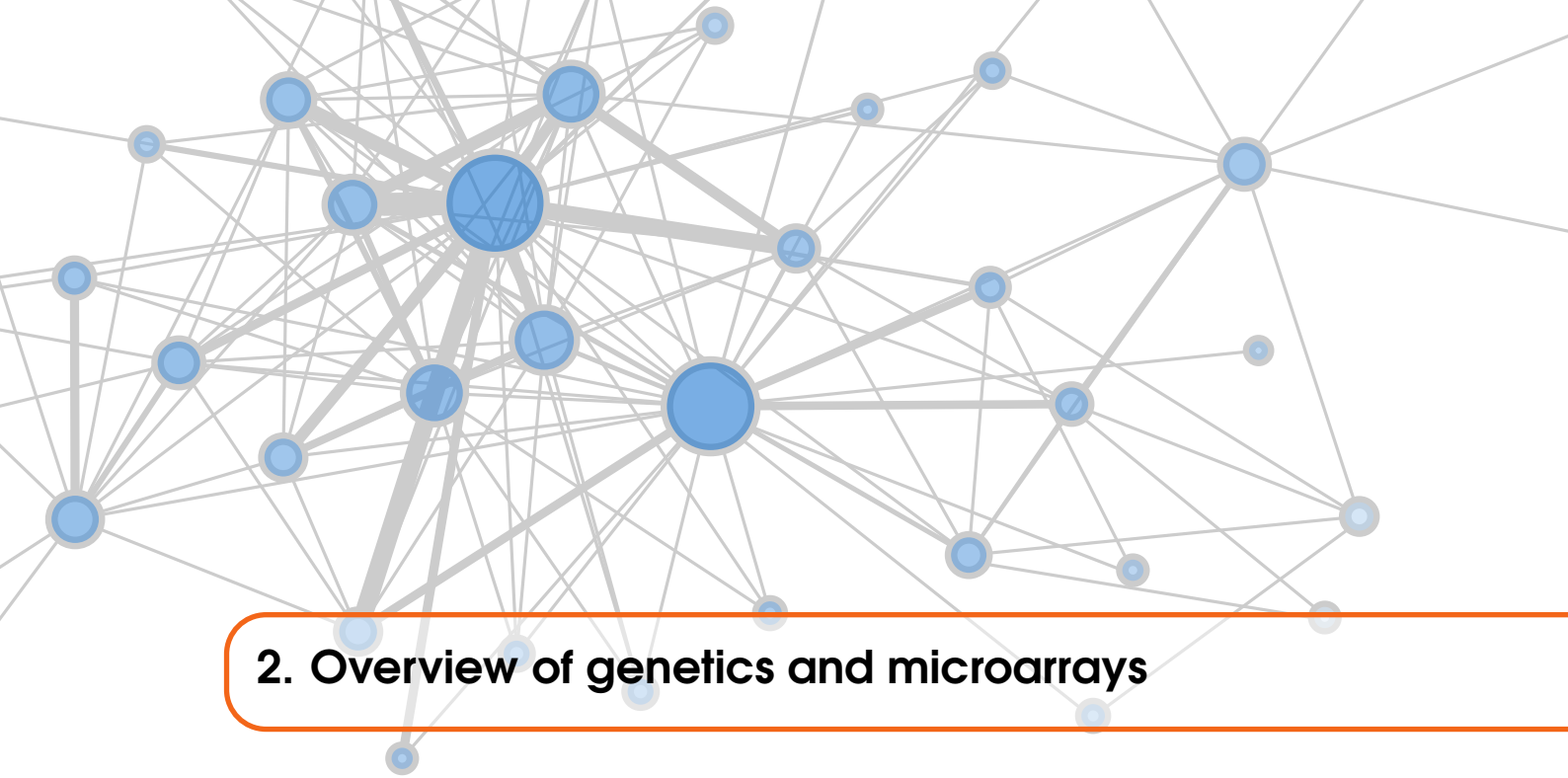

2. Overview of genetics and microarrays

Memories warm you up from the inside. But they also tear you apart

Haruki Murakami

2.1 Introduction

Just as the vast majority of cell types in mammals, neurons possess a nucleus within their cell body. In the nucleus, the whole genome encodes the blueprint of life. The molecule in charge of storing the inheritable genetic information is the DNA. According to the more classical view, inserted along the linear DNA molecule there are "coding regions" that encode functional proteins. These segments are *transcribed* to an intermediate molecule (RNA) which is subsequently *translated* into proteins by complex molecular machineries. Proteins are the actual effectors and in this regard, responsible for the maintenance of the cell homeostasis. Protein functions range from the formation of the structural scaffolding of cells and tissues to the processing and implementation of complex intra- and extra-cellular signals.

The regulation of gene transcription becomes of fundamental importance to understand the different cellular mechanisms. The key role of the regulation of gene expression is exemplified by the differentiation programs that cells undergo, which constitutes the basis of the difference in complexity between humans and lower organisms. Distinct cell types of the same organism differ thoroughly structurally and functionally, yet they possess the same exact copy of DNA. It is owing to the differential gene expression driven by key regulators that cells undergo differentiation to liver cells or neurons during the developmental stages of an individual.

In this chapter an overview on the biology of gene expression is given, together with a brief review on the methods for measuring gene expression levels. The emphasis will be on the DNA microarray technology owing to the scope of the present thesis.

2.2 Biology of gene expression

The necessary information for life is encoded in the DNA, and the complete complement of DNA for a species is referred to as its *genome*. The genome represents a blueprint for the development and maintenance of a living organism. The molecule of DNA consists of subunits known as nucleotides of which there are four different types: adenine, cytosine, guanine and thymine. The nucleotides are combined linearly in a single long string. With few exceptions, every human cell contains a copy of the whole genome in a cellular compartment called nucleus. Prior to cell division, the DNA replicates so that each of the daughter cells holds a complete copy of the genome.

Proteins, on the other hand, represent the structural and functional mediators between the living organism and the environment. Proteins, like DNA, are constituted of similar units bound in a linear fashion. The units of proteins are called amino acids, and there are 20 different of them. The particular combination of different amino acids in the chain will be reflected in the 3-dimensional structure of the protein. In fact, the different amino acids possess different physicochemical properties and it is owing to their interactions that a particular sequence folds to a particular protein structure. The 3-dimensional structure is responsible for the particular cellular function of the protein.

The concept of *gene* has changed significantly throughout history. The notion of "one gene-one protein" was originally proposed by Beadle and Tatum in 1941, referring to the fact that one strand of DNA coding for a protein would only make one protein – a one-to-one mapping. However, as a result of alternative splicing, trans-splicing, and other protein modifications that take place within the cell, we know today that rarely that is the case. Furthermore, DNA is not the only unit of inheritance, and some important RNA molecules are in fact passed to daughter cells and function as inheritance units. To make the picture even more complicated, proteins can be built up from different genomic sequences located far apart in the genome. The patterns of regulation at the different levels of biological organisation make difficult to physically delineate the gene. And yet, the operational definitions adopted by the scientific organisations still rely on the sequence – the Sequence Ontology Consortium defines the gene as the "locatable region of genomic sequence, corresponding to a unit of inheritance, which is associated with regulatory regions, transcribed regions and/or other functional sequence regions" (Pearson, 2006).

A more recent definition (or reinterpretation) of the notion of gene comes as a computational metaphor. Genes can be thought of as subroutines in the transcription/translation operating system (Gerstein, Bruce, Rozowsky, Zheng, Du, Korbel, Emanuelsson, Zhang, Weissman, and Snyder, 2007). For the sake of clarity, in this thesis we adopt a definition which, although overly simplistic, is still deeply rooted in contemporary narrative. According to such a definition, a gene represents a blueprint for a molecule (generally for a protein) which operates as a functional unit, either interacting with other biological units (DNA, RNA, or protein) or by having an effect on the cell and/or its environment.

During replication, an exact copy of the genome is synthesised by a dedicated cellular machinery. Proteins, however, do not replicate. Based on the cellular needs, they are synthesised using the corresponding DNA segment as a template. From a reductionist point of view, a gene is said to encode a protein, since the information in the DNA strand is translated from the 4-letter alphabet of nucleotides to the 20-letter alphabet of amino acids (the one-to-one mapping). The set of rules that map these alphabets is known as the genetic code. Each consecutive set of three nucleotides (also known as codon) is translated to one of the 20 amino acids. As there are four different nucleotides, there are 64 possible codons mapping to a total of only 20 amino acids. Hence, some of the codons map for the same amino acid (the genetic code is said to be *redundant*) but a given codon maps to only one amino acid (the genetic code is *non ambiguous*). Three of the codons are *stop codons* and signal a termination of translation.

In reality, the synthesis of a protein sequence from DNA passes through another intermediate

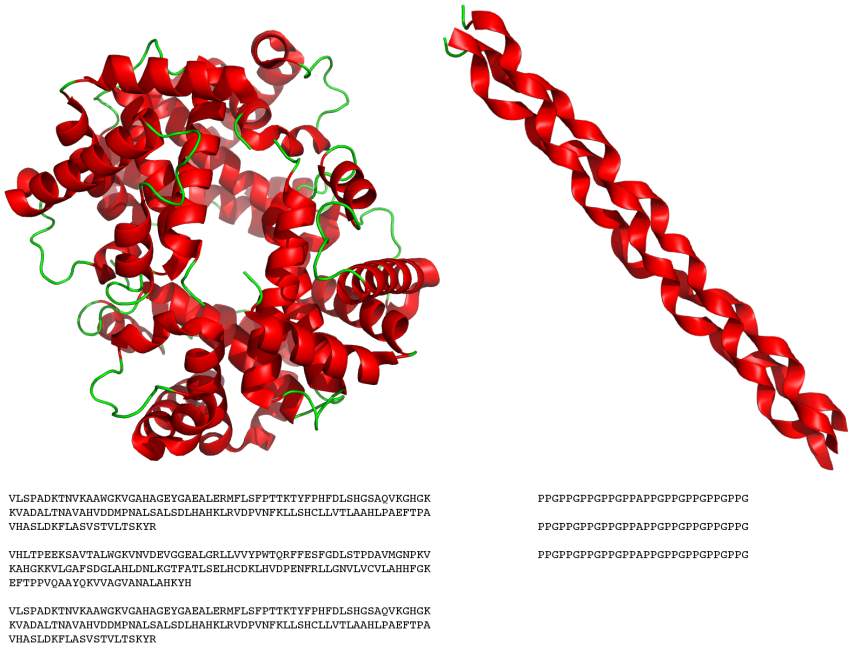

Figure 2.1: *The protein structures depicted correspond to collagen (left) and haemoglobin A (right). The corresponding sequences are also represented. Collagen is the most abundant protein in mammals. It is of a fibrous nature and represents the main component of connective tissue. Its function is of structural support. Haemoglobin A is a protein found in the red blood cells of vertebrates and responsible for carrying oxygen from the respiratory organs to the tissues. It is made up of four subunits that bind together forming a pocket that accommodates the so-called heme group. The latter contains an atom of iron that bounds to the protein subunit. Oxygen binds to the heme component during respiration. Sequences and coordinates obtained from PDB database (IDs 1hhb and 1cag, Fermi* et al.*, 1984; Bella* et al.*, 1994)*

molecule known as RNA, constituted by similar units (ribonucleotides) and depicted in Figure 2.2. RNA molecules are said to be *transcribed* from the gene with a complementary mapping – adenosine, cytosine, guanine, and thymine residues of the DNA segment are transcribed into uracil, guanine, cytosine, and adenine respectively to form the RNA string. In contrast to DNA, the messenger RNA (mRNA) molecules transcribed from a gene travel outside of the nucleus. The protein will be synthesised by yet another cellular machinery, the ribosome, by using the aforementioned genetic code mapping table to *translate* the sequence of mRNA. Although the whole picture is hardly as simple as summarised so far, the fundamental concepts of replication, transcription and translation suffice to give a general intuition of the basic protein synthesis mechanisms needed to understand the following sections.

In summary, the gene expression taking place in the nucleus leads to the synthesis of mRNA which is in turn translated into the functional effectors, proteins. The rate of gene expression of the different genes of the genome is responsible for the cellular levels of mRNA, and hence for the amount of each protein. Morphological and functional differences between cell types, such as liver cells and neurons, are in fact a result of different rates of expression (transcription) of

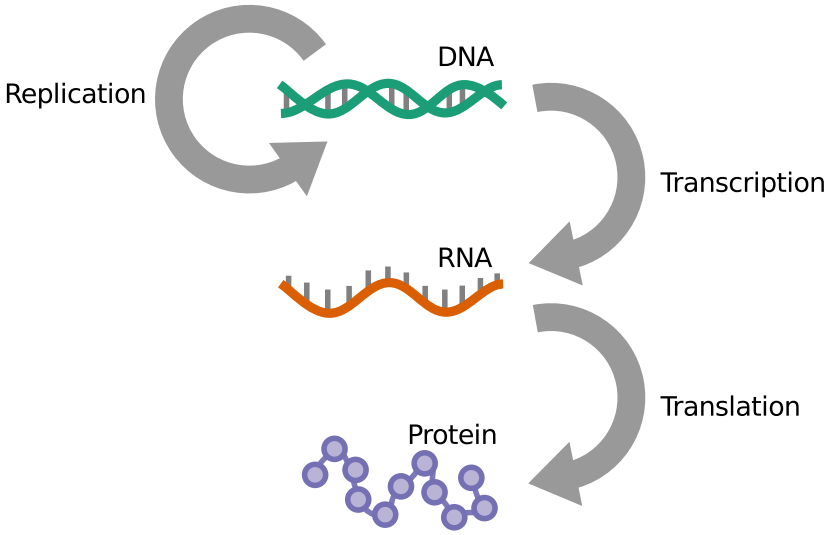

Figure 2.2: *The diagrams shows the main pathways of information within the cell. Once referred to as "the Central Dogma of Molecular Biology", this scheme is nowadays considered incomplete. It is represented here for its simplicity and relevance to the work presented in this thesis*

different key genes. While the expression of the haemoglobin genes is enhanced in the precursor cells that will eventually become mature red blood cells, cells that form the connective tissue will upregulate the expression of collagen. Such different expression profiles in different cell types is the result of a differentiation process from less differentiated cells guided by specific signals. Gene regulation during the differentiation process is crucial. In this regard, the traditional picture of the genotype-phenotype relationship, in which the observable characteristics of an individual are mapped to the particular sequence in his DNA, may be further complemented with the consideration of the expression profiles.

2.3 Regulation of transcription

There are a number of mechanisms adopted by living cells to regulate the specific needs in terms of gene expression. These mechanisms can modulate the final concentration levels of a protein at different levels:

- Transcription
- mRNA processing
- mRNA transport
- Translation

In general terms, the control at these different steps is mediated by proteins whose expression levels are, in turn, regulated by other up-regulated genes. Some RNA molecules such as microRNAs and small interfering RNAs are not translated into proteins but can still regulate gene output at

the transcriptional, translational and mRNA-stability level. However, we will focus here on the regulation that occurs at the transcriptional level by a direct effect of regulatory proteins acting on the genome. Later on in the discussion we will introduce the function of the RNA regulators.

At the transcriptional level, the regulation of the cellular concentration of a given protein happens indirectly through the control of RNA synthesis. Firstly, chemical modifications on the DNA, such as methylation and acetylation, are used to unpack the DNA molecules and allow access of the transcriptional machinery. This represents a first coarse level of regulation. Mediating this local uncoiling of the DNA structure are two classes of proteins, the histone acetyltransferases and methyltransferases (Kouzarides, 2007). A perhaps finer control of transcription is carried by the binding of proteins to specific sequences of the DNA, which are generally outside the coding regions. These DNA regions can be at different distances from the actual coding region upon they have an effect, both upstream and downstream of the direction of translation. A protein bound to its corresponding DNA sequence can have an effect on the rate of transcription of only one gene or act on a number of targets. The ultimate expression level of a given gene will therefore be the result of the combined effect of the different regulatory elements acting on it and their strength. The whole expanse of DNA involved in regulating the transcription of a gene is known as *gene control region*.

Note that the presence of some DNA-binding proteins will influence the target gene by effectively increasing its expression (activators) while some others will lead to the opposite effect, inhibiting gene expression (repressors). In the literature, these proteins are often referred to as transcription factors. Genomic responses to intra- and extracellular signals are represented by the complexity in the regulation of expression, rather than by the absolute number or genes. This regulation is, in fact, a good indicator of the anatomical and developmental complexity of an organism (Pilpel, Sudarsanam, and Church, 2001; Markstein, Markstein, Markstein, and Levine, 2002).

As mentioned earlier in the discussion, the complexity of the regulation further increases due to other regulators acting on the subsequent steps of gene expression. This large class of non-coding RNAs, (the microRNAs) act as repressors on the already synthesised mRNA by binding to it and promoting its degradation (Mattick and Makunin, 2006). The last stage of control happens after the mRNA has been translated into protein. Chemical modifications to the proteins themselves, mediated by other enzymes, can modulate their levels of activity, without directly affecting their cellular concentrations. This post-translational control is carried by kinases and phosphatases, which chemically add or remove, respectively, a phosphate group. These modifications change the activity of the protein by enhancing or inhibiting its function. Other post-translational modifications have an effect on the actual level of protein by promoting their degradation.

2.4 Cell homeostasis

The internal conditions of multicellular organisms, such as blood temperature in endothermic animals, blood pH and water content, are under strict control. The regulation of these variables is commonly known as homeostasis, and it operates at different hierarchical levels – organs, tissues, and cells, including unicellular organisms. This hierarchical and overlapping organisation of the different control levels poses serious difficulties to the systematic study of the different contribution of each component.

From a cellular perspective, the maintenance of the intracellular variables within their respective ranges includes the concentration of proteins needed to maintain a normal cellular physiology. Protein turnover is compensated by a tightly regulated gene expression profile, which ensures cell survival and, ultimately, organism survival. Regulation of gene expression serves as a homeostatic control mechanism: changes in the environment will be sensed by the appropriate receptor systems and subsequently processed. A response to correct the deviation of the particular variable will be then triggered resulting in changes in gene expression and protein levels. Some authors have

proposed the concept of *proteostasis* to refer to this cellular homeostatic control system (Powers, Morimoto, Dillin, Kelly, and Balch, 2009; Balch, Morimoto, Dillin, and Kelly, 2008).

Whereas housekeeping proteins tend to show similar expression profiles throughout different cell types, the homeostatic expression profiles for different tissues will differ according to the specific functional and structural needs of the tissue. Similarly, some genetic cellular subsystems will be activated only under particular circumstances, such as changes in metabolism. These changes in gene expression profiles between different cell states can be transient or last for long periods of time. Long-lasting changes such as the one triggered by the high frequency stimulus leading to LTP require the gene expression machinery to shift from one homeostatic state to another in a semi-permanent fashion. In this respect, an interesting hypothesis was raised by Kauffman (1969a) in 1969 – If we consider gene expression as a dynamic system, cell fates can be seen as high-dimensional attractor states in the gene expression space. The long-lasting changes following LTP can be interpreted from such a perspective.

The evident complexity of the circuitry integrated by the different cellular mechanisms remains a major technical difficulty to approach by classic experimental means. There exist a range of methods to infer, model, and analyse gene regulatory networks, and some will be described further on in Chapter 4.

2.5 Gene expression profiling

According to the scheme depicted in Figure 2.2, gene expression consists in the conversion of the information stored in the coding DNA segments into the actual protein, via the intermediate mRNA. The cellular concentration of a given protein is hence dependent on the rate of gene transcription and protein turnover. Mass spectrometry and two-dimensional gel electrophoresis are the main methods to quantify protein level. However, compared to measuring protein levels, it is technically easier to profile the amount of RNA. While in some cases mRNA levels are considered as an indirect measurement of protein levels, this is an oversimplification which, especially in the case of neurons, has to be taken into consideration as will become clear in Chapter 3.

The experimental techniques available nowadays to measure RNA levels in a cell can be classified according to different criteria. In terms of the overall strategy, some techniques rely on *sequencing* the RNA output, such as the serial analysis of gene expression (SAGE; Velculescu, Zhang, Vogelstein, Kinzler, *et al.*, 1995) and its variants (Matsumura, Ito, Saitoh, Winter, Kahl, Reuter, Krüger, and Terauchi, 2005), RNA-seq (Khan, Wei, Ringner, Saal, Ladanyi, Westermann, Berthold, Schwab, Antonescu, Peterson, *et al.*, 2001), and massively parallel signature sequencing (MPSS; Brenner, Johnson, Bridgham, Golda, Lloyd, Johnson, Luo, McCurdy, Foy, Ewan, *et al.*, 2000). Other techniques are based on *hybridization* of RNA to probes. This is the case of microarrays (Schena, Shalon, Davis, and Brown, 1995; Schulze and Downward, 2001), Northern Blot (Alberts, 2008), and quantitative polymerase chain reaction (qPCR; VanGuilder, Vrana, and Freeman, 2008). Microarrays are significantly cheaper to perform on large-scale studies and hence generally preferred in genome-wide experiments.

In terms of the number of genes that can be studied in each assay, the different techniques can be classified into low- or high-throughput. The former allows the study of a limited number of genes at the same time, while the second group embodies those technologies with the potential to encompass the whole transcriptome in the same assay. From the high-throughput technologies, microarrays and RNA-seq are by far the most widely used nowadays.

2.6 Oligonucleotide microarrays

A microarray consists of a set of DNA spots attached to a solid surface which can hybridise in a specific manner to complementary sequences in the sample. The hybridisation can be detected and

quantified to measure the expression levels of large numbers of genes (Heller, 2002). While it is possible to prepare custom microarrays in regular research facilities, the popularity of microarrays owes to the availability of commercial platforms, mass-produced by industrial companies. The precision of the commercially available microarrays allows the comparison between two (or more) identical arrays hybridized with different samples. This parallel microarray experiments can be used to measure the relative abundance of RNA in different tissues or different conditions, such as developmental stages or carcinogenic *versus* healthy tissues. The gene expression profiles constructed using parallel experiments are represented in a matrix where the rows represent genes and the columns represent samples. The cells of the matrix contain the values of expression of a single gene (Schulze and Downward, 2001).

The term "oligonucleotide microarrays" is often used to refer to the *GeneChip* class of microarrays developed by *Affymetrix*. They consist of a solid surface onto which a collection of DNA spots are attached. Each of these spots contains molecules of DNA with a specific sequence that corresponds to a section of a particular DNA element. Among those elements, many of them are complementary gene-coding sequences. Typically, microarray platforms may have tens of thousands of spots in a single array, and this size makes it possible to detect and quantify the expression of every known gene in the genome.

In an Affymetrix oligonucleotide microarray experiment, the RNA from the sample is extracted, purified, and subsequently transcribed back into its complementary DNA sequence (cDNA). Next, the second-strand of the cDNA is synthesised and the purified double-stranded cDNA is used as a template for an *in vitro* transcription reaction in the presence of labelled ribonucleotides. After filtering out the double-stranded cDNA, the resulting labelled RNA is fragmented and hybridized onto the microarray. The molecules will bind to their complementary probes attached onto the surface of the array. The strength of the signal from a spot will be proportional to the amount of cDNA present in the sample (Schena *et al.*, 1995; Brazma and Vilo, 2000). A summary is provided in Figure 2.3.

Each probeset is actually comprised of two signals – a set of 11-20 "PM" (perfect match) probes with a length of around 25 nucleotides, and a "MM" (mismatch) signal, resulting from another set of probes with a single nucleotide substitution in the centre of the probe, which can be used to account for non-specific probe binding. In fact, the average of the PM-MM differences for all probe pairs in a probe set ("average difference") is generally used as an expression index. Indeed, this is often the starting point for the so-called high-level analysis (see Section 2.7.2).

These platforms capture an additional layer of complexity which cannot be grasped solely by gene sequencing. The capacity to carry a systematic and comprehensive analysis of gene expression in a fast and reproducible manner, together with its relative low costs, makes of microarray technologies a remarkably valuable tool.

2.7 Analysis of microarray data

2.7.1 Low-level analysis

Low-level data analysis deals with extraction of the signal from the high level of noise and experimental artefacts, and includes image analysis, gene filtering, background correction, probe level analysis and gene summarisation. Although the present thesis focuses on the high-level analysis of microarray data, we will briefly summarize some basic low-level analysis procedures.

Following the experimental procedure for hybridization, the array is scanned and the resulting image (the DAT file) is inspected for defects. In general terms, if these defective areas represent less than 10% of the total probes, the areas can be masked as outliers (Li and Wong, 2001). The probe array image is then analysed to obtain a set of expression indices associated to each probeset. The probe intensity data for the chip is recorded in a text file (the CEL file), of which there will be one

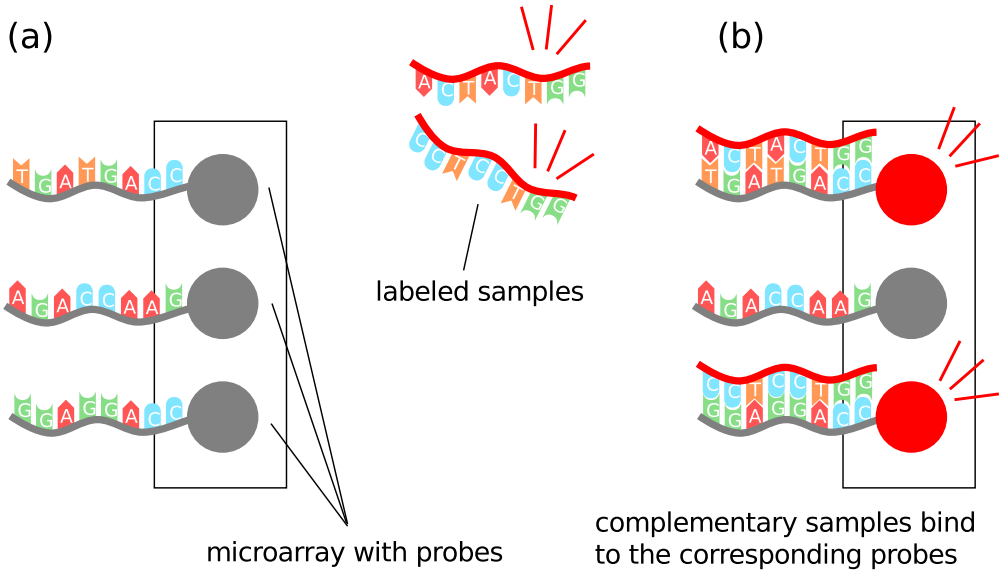

Figure 2.3: *The microarray **(a)** contains the probes which will hybridise the complementary labelled samples **(b)**. After washing off the non-specific bonding sequences, the strength of the signal of a spot will be proportional to the amount of sample binding to the probes on that spot*

for each sample. An additional Chip Description File (the CDF file) summarises the information for each probe cell on the chip.

The preprocessing of the CEL file is accomplished in three subsequent steps:

- Background correction (adjust for random noise)
- Normalisation (calibrate measurements of different arrays)
- Summarisation (summarise the PM/MM levels for each probeset to a single expression value)

A number of available tools perform this analysis in an automated fashion requiring minimal user input. The most significant difference between the tools resides in the normalisation procedure used. Some methods, such as MAS 5.0, the default measure available from Affymetrix, and dChip (Li and Wong, 2001), are based on PM-MM. In contrast, another set of methods base the normalisation on PM values only. This is the case of robust multi-array average (RMA) (Irizarry, Hobbs, Collin, Beazer-Barclay, Antonellis, Scherf, and Speed, 2003) and GCRMA (Wu, Irizarry, Gentleman, Murillo, and Spencer, 2004). The choice of normalisation procedure is guided by the microarray platform and array design, the experimental design, and the underlying biological assumptions. The R package *affycomp* (Cope, Irizarry, Jaffee, Wu, and Speed, 2004) facilitates the comparison of expression measures and the selection of methods.

RMA is one of the most widely used methods. The RMA background normalisation method only considers PM probe intensities as the sum of signal and noise. The normalisation on the PM probe intensities is carried out by quantile normalization, and the summarisation of the values into expression values is done using the median polish method. The implementation of the RMA

method is included in the *affy* R package of the Bioconductor project (Gentleman, Carey, Bates, Bolstad, Dettling, Dudoit, Ellis, Gautier, Ge, Gentry, *et al.*, 2004).

In Chapter 5 we will describe the microarray datasets in which part of the present thesis is based. Additionally, we will discuss the results of the RMA analysis in some depth. The high-level analysis discussed in Chapter 6 uses the microarray expression values normalised and summarised using RMA as a starting point.

2.7.2 High-level analysis

Following the summarisation step, the intensity values of the probesets in the array have been translated into single gene expression values. As mentioned earlier, this often represents the starting point for further high-level analyses concerned with extracting knowledge about the underlying biological processes. These analyses are often based on the identification of differentially expressed genes. While there exist several tools that perform this function, LIMMA (Smyth, 2005) is one of the most widely used. Results of this algorithm with an microarray dataset are shown in Chapter 5.

The LIMMA analysis takes a linear modelling approach to handle the experimental design, fitting a linear model to the expression data for each gene. The output is a set of log_2 fold change values which indicate the degree of change between the two samples. It uses a moderated t-test to estimate the p-values and calculates the false discovery rate (FDR). Both measures take into account multiple testing bias (an indication of the frequency of false positives among the significant hypotheses). The implementation of the LIMMA analysis can be found as an R package within de Bioconductor project (Smyth, 2005; Gentleman *et al.*, 2004).

Differential expression analysis can be used as a starting point for further studies, since it allows to rank the genes according to their putative relevance in the biological processes linked with the different conditions of the samples studied. In this regard, differential expression analysis can be seen as a middle-level analysis. A rather large number of methods exist to study the gene expression matrix obtained from microarrays. In general terms, the strategies aim to compare the expression profiles either in rows or columns of the expression matrix, although both methods can be combined (Brazma and Vilo, 2000). Commonly, the studies that compare microarrays of different conditions correspond to different types of tissues. For instance, to understand the gene expression mechanisms of a particular type of cancer, the disease and non-disease samples will be used to hybridise different arrays (or use different fluorescent dyes). The differential expression analysis will offer valuable information on the physiological differences between carcinogenic tissue and healthy tissue. These types of parallel analyses are not limited to different tissues. For example, investigations on temporal changes in gene expression can also be tackled.

The comparisons between genes are based on the similarity of their profiles. The Euclidean distance or correlation measures are often used to measure the distances, although other measures could have been used as well (e.g. rank correlation coefficient, mutual information; Smith, 2007). The data can subsequently be analysed by unsupervised methods to cluster genes and/or samples. Supervised methods are often used to build classifiers. The underlying assumption is that genes with similar expression profiles, may be co-regulated.

Other high-level analyses of microarray data include the integration of data from other sources, such as the one from function annotation databases.

2.8 Microarrays in neuroscience

The brain functions as the central processing unit in vertebrates, integrating the information collected from the environment. The complexity of the gene networks involved in the brain processes adds an additional layer of organisation that exchanges information with the highly organised synaptic networks. The study of gene expression in the brain aims to shed light on the mechanisms of brain

functioning as well as to gain a deeper understanding on the processes that lead to pathological states.

The capability of analysing a whole genome in parallel allows us to tackle the study of these complex systems. In this regard, the study of the transcriptional regulatory networks associated with mechanisms involved in learning and memory represents a step towards bridging the classic methodologies applied by neuroscientists with the molecular and systems neuroscience (Geschwind and Konopka, 2009). In fact, since the very first microarray experiments described by Schena *et al.* (1995), this technology has gained an increasingly important role in neuroscience (see Figure 2.4).

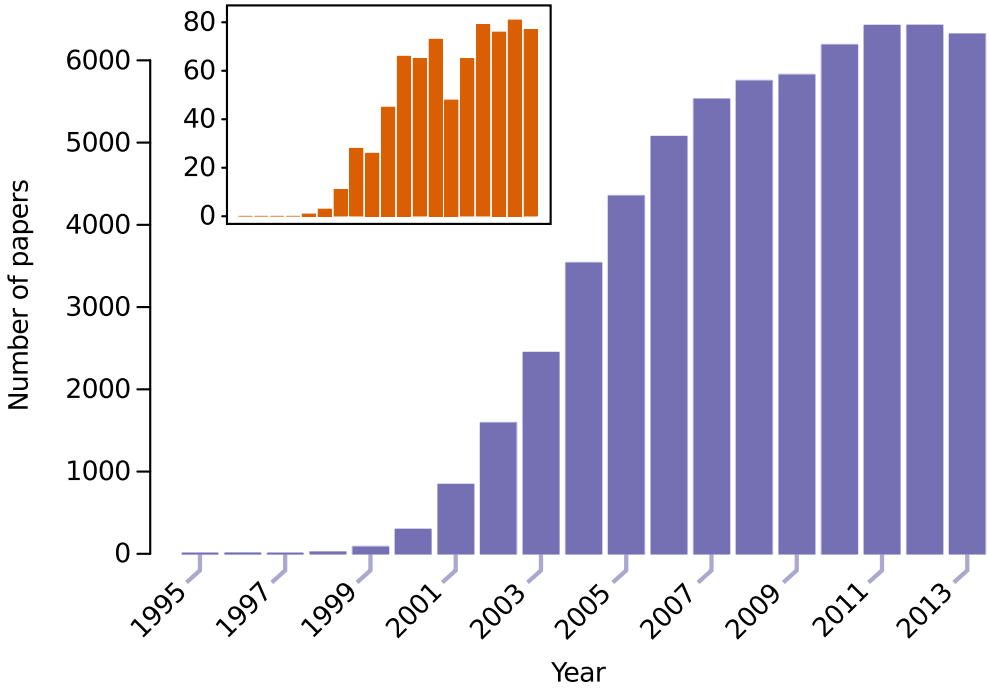

Figure 2.4: *The main plot represents the number of scientific papers returned by a PubMed database search with the word "microarray" on the title or abstract from 1995 to the current day. The orange bars in the inset plot represent the subset of those papers in the field of neuroscience*

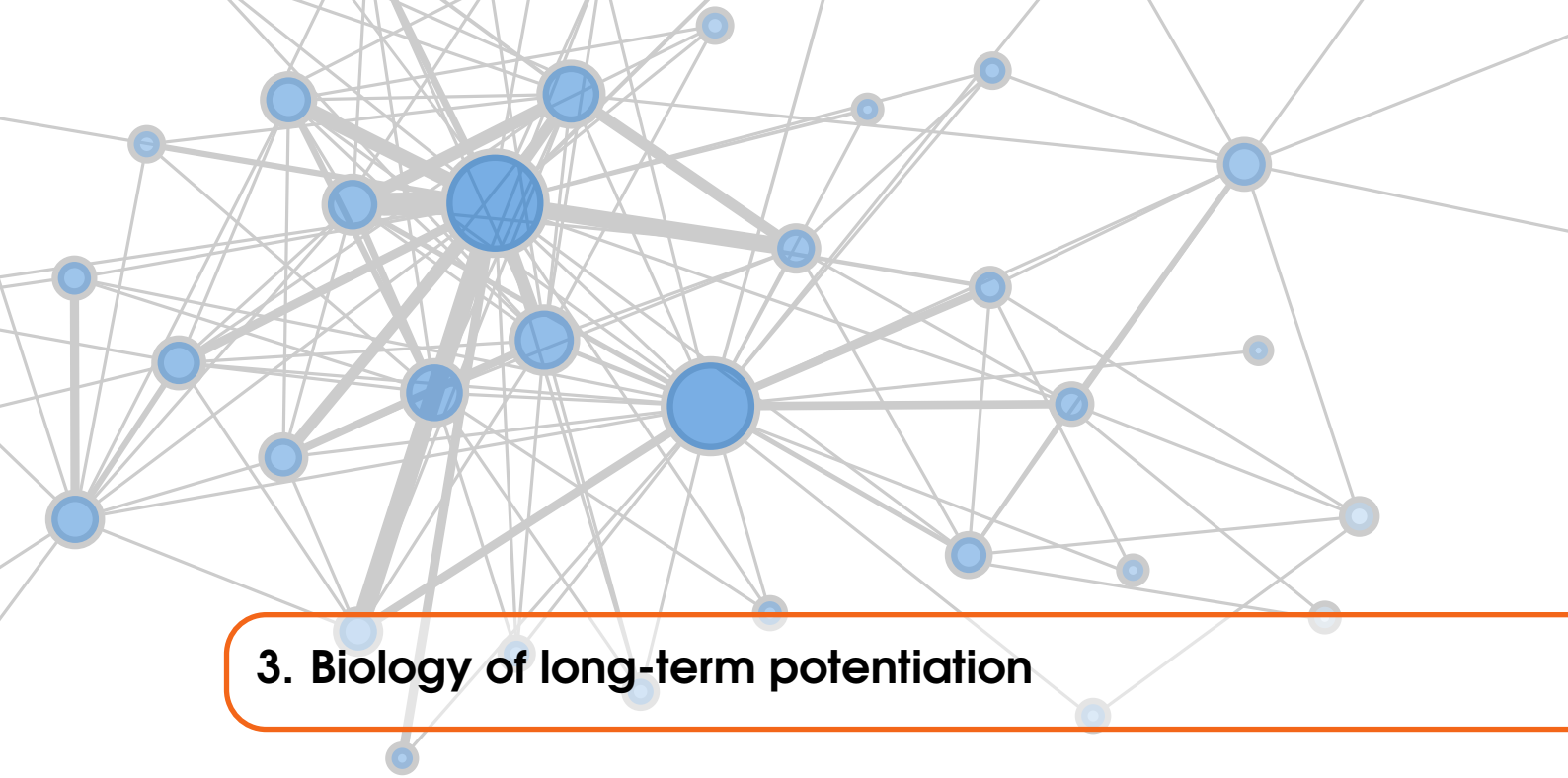

3. Biology of long-term potentiation

"For all that let me tell thee, brother Panza," said Don Quixote, "that there is no recollection which time does not put an end to, and no pain which death does not remove"

Miguel de Cervantes

3.1 The neuron

Neurons represent the unit of transmission of information in the nervous system. Information travels along their axons as electric potential in their membranes. From a morphological point of view, neurons are made of a soma (cell body), dendrites, and the axon. Brain tissue is constituted of two cell types – neurons and glial cells. There are several classes of each of these cell types, and have different functions within the nervous system. The glial cells provide physical and nutritional support to the neural cells, and in addition they can play active roles in synaptic plasticity. In particular, glial cells of the hippocampus and cerebellum have been shown to actively participate in synaptic transmission (Newman, 2003; Koob, 2009).

Although mitochondria – the cellular "powerhouses" – are found in axon terminals and dendrites, most of the metabolic processes take place in the soma. The soma accommodates the cell nucleus, which contains the genetic information of the neuron. The dendrites are protrusions of the cell membrane that receive the inputs from incoming connections from other neurons (Figure 3.1).

In the nervous system, neural cells are connected forming neural circuits – nets of interconnected neurons that allow the organism to integrate the information gathered from the environment and generate specific responses. The nervous system, in addition, allows for the storage and retrieval of information, both implicit and explicitly.

3.1.1 The resting potential

Neurons keep a gradient of electrical charges between the cytoplasm and the exterior. This resting membrane potential is around $-70mV$ (negative inside) and it is actively maintained by the cell.

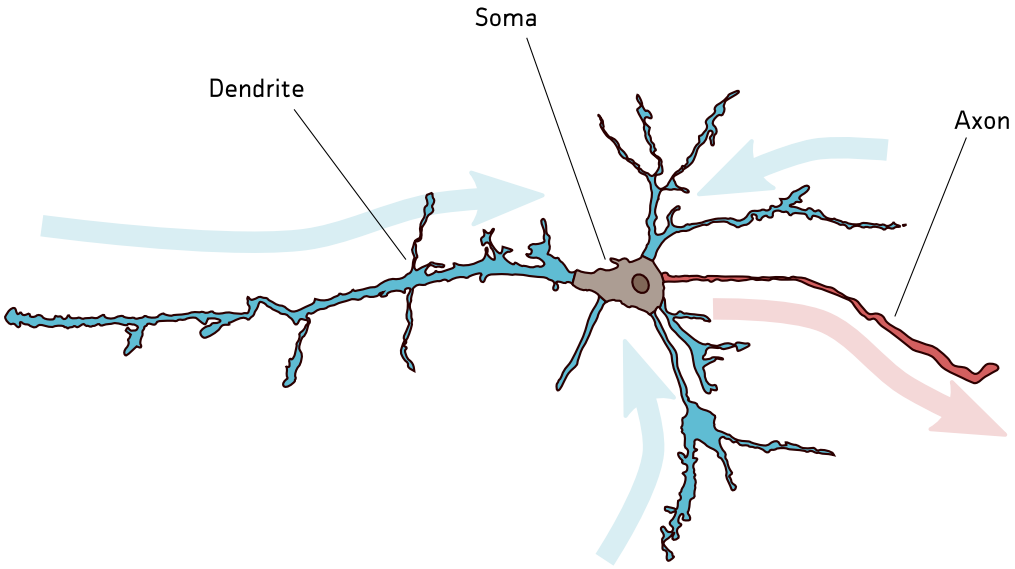

Figure 3.1: *Pyramidal neuron from the hippocampus. In blue, the tree-like structures known as dendrites carry information from other neurons. The information is then integrated eventually leading to an action potential which travels along the axon (in red) to other neurons. The arrows indicate the direction of information flow*

The resting membrane potential is the result of an equilibrium in the passive flow of ions through the membrane. Neurons are permeable to K^+, Na^+, and Cl^-, but the permeability differs for each of these ions. Protein channels that allow the flow of the ions are embedded in the membrane of the cell, and their different concentration leads to different permeabilities. The flow of ions across the membrane is dependent on two factors – the unequal concentration of the ions on each side (*chemical* driving force) and the difference in potential across the membrane (*electrical* driving force). The flow of a particular ion depends not only on the sum of the chemical and electrical driving forces, but also on the membrane permeability to that particular ion.

Given the concentration gradients in the cell, the total flow of ions across the membrane would tend to reach an equilibrium in which K^+ ions leave the cell (the concentration of K^+ is significantly higher inside the cell) and Na^+ ions enter the cell. To compensate this concentration gradient leak, neurons actively transport these ions against their concentration gradients using a special channel known as sodium-potassium pump. In contrast to the channels described previously, the sodium-potassium pump is not a passive channel and needs cellular energy in the form of ATP.

Ca^{2+} is a fundamental ion in the neurons. Its concentration is considerably inferior in the cytoplasm than in the extracellular fluid. In order to maintain its the gradient across the membrane, there are several types of channels that transport the Ca^{2+} out of the cell or hoards it in intracellular stores. Similarly, the Cl^- anion is actively transported to the extracellular fluid.

3.1.2 The action potential

The transmission of information is encoded in electrical pulses that travel throughout the length of the axons. This depolarisation is known as “action potential” and propagates along the axon without attenuation, self-regenerating until reaching the synaptic terminals. There, the axon transmits the

information to other neurons.

For the action potential to happen, the depolarisation has to reach a threshold. Small depolarising currents can increase the resting potential from $-70mV$ to that threshold, which lies around $-50mV$. The action potential differs from other graded biological responses in that it is an *all-or-none* event – once the threshold is reached, the signal is transmitted without decrement.

The action potential is the result of the presence of Na^+ and K^+ channels in the membrane, whose opening is regulated by the local potential of the membrane surrounding them. These type of channels are known as voltage-gated channels. The depolarisation of the membrane above the threshold increases the permeability to Na^+ by opening these voltage-gated channels, leading to a further depolarisation. This feedback cycle is responsible for initiating the action potential. The new membrane potential acquired after the action potential takes place is restored by the flow outwards of K^+, eventually reaching the initial charge separation. This flow is driven by voltage-gated K^+ channels, whose opening times are slower than the voltage-gated Na^+ channels.

In addition to the open and closed states, the voltage-gated Na^+ channels have an inactivated state. Following a sufficiently large depolarisation, these channels become unable to open until the membrane restores its resting potential. This three-state switch is responsible for the refractory period, which limits the frequency of action potentials (Figure 3.2).

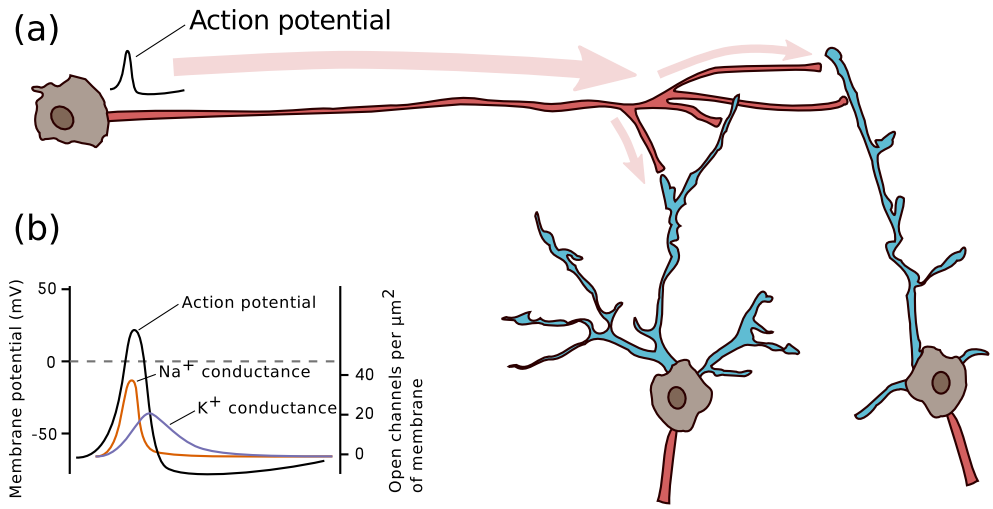

Figure 3.2: ***(a)*** *Action potential propagates along the axon reaching the synaptic terminals, where the signal is passed to postsynaptic neurons.* ***(b)*** *Temporal membrane permeability changes with the onset of the action potential. Positive feedback by the entry of Na^+ and the resulting Na^+ voltage-gated channel opening generates a fast depolarisation of the membrane. Eventually, the slow-opening voltage-gated K^+ channels increase the permeability of the membrane to K^+ restoring the resting potential* Figure **(b)** based on Hodgkin and Huxley (1952)

In addition to the channels briefly described here, there are other channels of similar properties which are permeable to other ions such as Ca^{2+} or Cl^-. There are multiple variants that bestow specific properties to the action potential in different types of neurons.

3.1.3 The chemical synapse

The information transmission between different neurons takes place in the synaptic terminals, where the action potential reaches from the presynaptic neuron and is passed over to the postsynaptic neuron. The action potential can cross directly to the other membrane (*electrical* synapse) or cross by chemical intermediates (*chemical* synapse). The electrical synapses communicate very fast, but chemical synapses are more common and have the fundamental property of *signal amplification* (Kandel *et al.*, 2000).

The chemical synapses are dependent on the release of a neurotransmitter molecule from the axonal ending of the presynaptic cell to the extracellular space between the cells. The molecule diffuses reaching specific receptors in the postsynaptic membrane. The release of neurotransmitter depends on the opening of Ca^{2+} channels in the presynaptic membrane, which in turn lead to the fusion of vesicles stored in the axon terminal and loaded with the neurotransmitter molecules. The eventual binding of the neurotransmitter to the receptors in the postsynaptic cell drives the opening of other transmembrane receptors, changing the postsynaptic membrane potential. There are two types of neurotransmitter receptors, *ionotropic* receptors and *metabotropic* receptors (Nicoll, Malenka, and Kauer, 1990). Ionotropic receptors form an ion channel pore, while metabotropic receptors act through secondary messengers, activating intracellular signalling cascades that can lead to changes in membrane permeability or other cellular effects.

Ionotropic receptors (Wisden and Seeburg, 1993) are made of several subunits that form a ion channel. The extracellular domain of the channel functions as a binding site to the neurotransmitter. Upon binding, the channel undergoes a conformational change that permits the transit of ions through its transmembrane domain. Ionotropic receptors act faster, since they combine transmitter-binding and channel functions in the same molecular entity.

Ionotropic receptors are generally subdivided into 3 superfamilies:

1. Receptors that resemble the nicotinic acetylcholine receptors
    - Glycine receptors
    - Gamma-aminobutiric acid A ($GABA_A$) receptors
    - Nicotinic acetylcholine receptors
    - Some serotonin receptors
2. Ionotropic glutamate receptors (GluR)
3. ATP-gated purine receptors

The other family of neurotransmitter receptors are known as metabotropic receptors (Traynelis, Wollmuth, McBain, Menniti, Vance, Ogden, Hansen, Yuan, Myers, and Dingledine, 2010). Their contribution to the membrane permeability to ions is indirect, through series of metabolic steps. Upon binding of the neurotransmitter in the extracellular domain, the coupled G-proteins become active and dissociate from the receptor. Activated G-proteins can directly activate transmembrane channels or activate other effector proteins which will, in turn, regulate other postsynaptic channels. The activation of metabotropic receptors can trigger complex cellular responses through the production of second-messengers, diffusible molecules able to activate other proteins.

Neurons in the central neural system receive excitatory and inhibitory inputs depending on the type of receptors located in the postsynaptic membrane. In the brain of vertebrates, presynaptic neurons that release the glutamate neurotransmitter act on neurons that carry excitatory receptors in their membranes, while neurons that release GABA or glycine act on neurons that carry receptors that cause inhibition. The information coming from a number of neurons is integrated to generate an action potential in the postsynaptic neuron.

3.1.4 The excitatory synaptic transmission

The major excitatory transmitter in the brain is L-glutamate which binds to specific ionotropic and metabotropic receptors. There are three subtypes of ionotropic receptors for glutamate:

1. α-amino-3-hydroxy-5-methyl-4-isoxazolepropionic acid (AMPA) receptor
2. N-methyl-D-aspartate (NMDA) receptor
3. Kainate

While open, all these allow the flow of Na^+ and K^+. NMDA receptors, in addition, are permeable to Ca^{2+}. Their active structure in the membrane is in the form of a tetramer, an oligomer formed from four protein subunits. Among the three types of receptors, kainate receptors are the less understood, but they may have an effect on the amount of neurotransmitter released presynaptically (Schmitz, Mellor, and Nicoll, 2001).

There are four different types of subunits of AMPA receptor (GluR1, GluR2, GluR3, and GluR4) that combine in two dimers (an odimer of GluR1 and either a dimer of GluR2, GluR3 or GluR4). The differences in the subunits determine their interactions with other proteins (Greger, Ziff, and Penn, 2007). In the case of the NMDA receptor, the tetramer is formed by two GluN1 subunits and two GluN2 subunits. There are eight variants of GluN1 and 4 of GluN2, and the different combinations confer the channel different kinetic properties (see Teng, Cai, Zhou, Zhang, Liu, Wang, Dai, Zhao, and Sun (2010) for a recent review). NMDA receptor is considered the predominant molecular device for controlling synaptic plasticity and memory function (Li and Tsien, 2009).

While the non-NMDA receptors open upon neurotransmitter binding, the NMDA receptors require both the binding of glutamate and the postsynaptic membrane depolarisation to open. The postsynaptic depolarisation when at resting potential is, hence, due mainly to the action of the AMPA receptors. The NMDA receptors act as detectors of the co-occurrence of glutamate release and postsynaptic depolarisation. When NMDA receptors open, they allow the flux of Ca^{2+} from the extracellular space to the cytoplasm. This rise in Ca^{2+} activates a set of signalling cascades that can lead to long-lasting changes in the synaptic efficacy. The ability of modulating the efficacy of synaptic transmission is involved in the formation of some forms of memory. In most neural pathways in the mammalian hippocampus, LTP is NMDA receptor-dependent (see Section 3.2.3).

3.2 Long-term potentiation

3.2.1 The discovery of long-term potentiation

The archetypical case of H.M. in the 1950s commented in Chapter 1 was influential for its contribution to the understanding of human memory organisation in the brain, pinpointing the anatomical location of explicit memories in the hippocampus. About 20 years later, in 1973, Timothy Bliss and Terje Lømo, discovered what today is considered the cellular mechanism underlying long-term memory – LTP. Their experiments demonstrated that while a single pulse of electrical stimulation to the presynaptic cells caused an excitatory postsynaptic potential (EPSP), a high-frequency train of stimuli enhanced the subsequent EPSPs to single stimuli. This effect lasted for long periods of time. Effectively, a long-lasting change in the synaptic strength was being induced by the high-frequency stimulus (HFS).

Although the discovery of LTP is placed within a scientific context where several research groups participated actively to the development of such a cellular model, Lømo has been credited as the "discoverer" of LTP. Scientific literature often refers to the seminal papers of Bliss and Lømo (1973) and Bliss and Gardner-Medwin (1973) as the keystone, although the discovery began earlier in Oslo in 1964. According to Lømo himself (Lømo, 2003), the first findings related with what

would be an intense area of research later on were presented in a meeting of the Scandinavian Physiological Society in 1966 (Lømo, 1966), and the first mention to the "possible relationship between frequency potentiation and learning processes" came in a paper prepared for a meeting in 1965 by Andersen and Lømo (1967).

It is noteworthy that the results of the refined experiments after the 1966 meeting would not have been published until 1973 and, more interestingly, that there was a "relative lack of enthusiasm expressed by most people upon hearing the results". Apparently, on Lømo's own opinion, both the scientific community and himself were overcome by the complexity of the system, and the lack of understanding of what was behind the findings (Lømo, 2003).

By the late 1970s, LTP-related research was being conducted worldwide, and in 1983 the central role of NMDA receptor was revealed by the work of Collingridge and coworkers (Collingridge, Kehl, and McLennan, 1983; Coan and Collingridge, 1985; Collingridge and Bliss, 1987). At the same time, the hippocampus was gaining attention as a crucial structure for spatial learning Morris, Garrud, Rawlins, and O'Keefe (1982); Morris (2003).

Despite the early lack of interest shown by the scientific community, the results published in 1973 in the aforementioned paper represent the first detailed description of LTP, and 40 years later it has been referenced in more than 3,000 publications. Indeed, LTP is still today the focus of intense research. The modern studies fall either into a mechanistic perspective, seeking to clarify the cellular biology of the phenomenon – or into a functional perspective, aiming to shed some light on the link between LTP and behavioural learning. With the advent of the computer era, new lines of research have ventured into the study of LTP by means of computational models (Benuskova, 2000; Benuskova and Kasabov, 2007). Many of the fundamental questions, however, remain yet unanswered.

3.2.2 Definition and properties

In a review by Malenka and Bear (2004), the LTP definition is generalised as the "long-lasting enhancement of synaptic effectiveness that follows certain types of tetanic electrical stimulation". This enhancement of the synaptic strength is measured as the percent change in the EPSPs.

Although LTP was discovered in the hippocampus – more precisely in the synapses formed from the inputs of the perforant path fibres to the granule cells of the dentate area – other structures in the brain have been shown to possess the ability to form LTP, including the cerebral cortex, cerebellum, and amygdala. This has raised the possibility that LTP may potentially occur in all excitatory synapses in the mammalian brain (Malenka and Bear, 2004). However, the best studied form of LTP in terms of the amount of experimental work has been performed in the synapses between the Schaffer collateral and commissural axons and the apical dendrites of CA1 pyramidal cells of the hippocampus – an *associative, NMDA receptor-dependent LTP* (Reymann and Frey (2007), see Section 3.2.3).

The majority of the biochemical data available comes from LTP induction in the CA1 region of the hippocampus, and is therefore considered as the prototypic form of synaptic plasticity NMDA receptor-dependant. In such context, LTP displays some properties that have been classically considered as "suggestive of an information storage device" (Martin, Grimwood, and Morris, 2000):

1. Input specificity
2. Associativity
3. Persistence

Input-specificity refers to the fact that when LTP is generated at one particular set of synapses by

repetitive activation, the corresponding increase in synaptic strength does not necessarily occur in other synapses, even in the same cell. This property may be important in terms of storage capacity.

Associativity refers to the observation that when stimulation in a set of synapses is not enough to trigger LTP, the latter can be facilitated by a strong activation of an independent set if both sets are activated simultaneously.

Persistence is the ability of LTP to last from several minutes to many months, and is this persistence that separates LTP from other short-term plasticity mechanisms.

3.2.3 Types of LTP

The input to the hippocampus comes from neurons of the entorrhinal cortex through the so-called perforant pathway, which connects with the granule cells of the dentate gyrus. The latter make synaptic contacts with the pyramidal cells of the CA3 region (the mossy fiber pathway). In turn, the axons of the pyramidal cells of the CA3 region are connected to the pyramidal cells of the CA1 region via the Schaffer collateral pathway (see Figure 3.3). The importance of each of these pathways is highlighted by the fact that damaging any of them is sufficient to produce memory disruption in humans (Zola-Morgan, Squire, and Amaral, 1986).

The dependence on the frequency of the presynaptic activity encodes the long-term changes in synaptic efficacy at excitatory glutamatergic synapses. The frequency of the local Ca^{2+} concentration at the postsynaptic spines will vary according to the presynaptic activity, and consequently distinct forms of potentiation can be triggered in the synapse. This is particularly evident in the extreme case of low-frequency stimulation, which triggers a completely different form of long-lasting change in synaptic strength known as long-term depression (LTD). While out of the scope of the present thesis, it is worth mentioning that while both LTP and LTD are triggered by increased Ca^{2+}, the distinct frequencies will be decoded to initiate the pertinent cellular and molecular changes. The cell, hence, requires a mechanism to discriminate these different temporal patterns.

The mechanism underlying the LTD/LTP decision relies on a different activation of NMDA receptors, which in turn leads to different increases in postsynaptic Ca^{2+}. A small increase in intracellular Ca^{2+} triggers LTD, while a stronger activation of NMDA receptors and the resultant rise in Ca^{2+} leads to LTP (Bear and Malenka, 1994).

The forms of LTP in the different pathways possess different cellular and molecular characteristics. Moreover, LTP seems to be a family of different processes that alter the synaptic strength in the different areas of the hippocampus. The two main classes of LTP in the hippocampus are *associative* and *nonassociative* LTP.

In the mossy fiber pathway (see Figure 3.3), an example of nonassociative LTP takes place. In this class of LTP, only AMPA receptors have a significant role in synaptic transmission – experimentally blocking NMDA receptors has no effect on the onset of LTP (Zalutsky and Nicoll, 1990). On the contrary, LTP induced in the Schaffer collateral pathway is associative, requiring activity in the postsynaptic cell to activate the NMDA receptors (Lynch, 2004; Nicoll and Malenka, 1995; Larkman and Jack, 1995). Hence, questions regarding the functional roles of LTP must be placed into very specific contexts.

It is important (and reassuring to a certain extent) to realise that despite the repertoire of long-lasting modifications and the complexity of the underlying molecular mechanisms, the synaptic changes undergone by LTP are considered to be a fundamental property of the majority of excitatory synapses in the mammalian brain (Malenka and Nicoll, 1999). A deeper understanding of a prototypic LTP will definitely help to uncover not only the common mechanisms among the different subtypes, but also point towards the differences and their functional roles in different regions of the brain. As pointed out by Malenka and Bear, “just as different neurons express different complements of ion channels to control their firing properties, neurons can vary in terms of the specific forms of LTP and LTD they express” (Malenka and Bear, 2004).

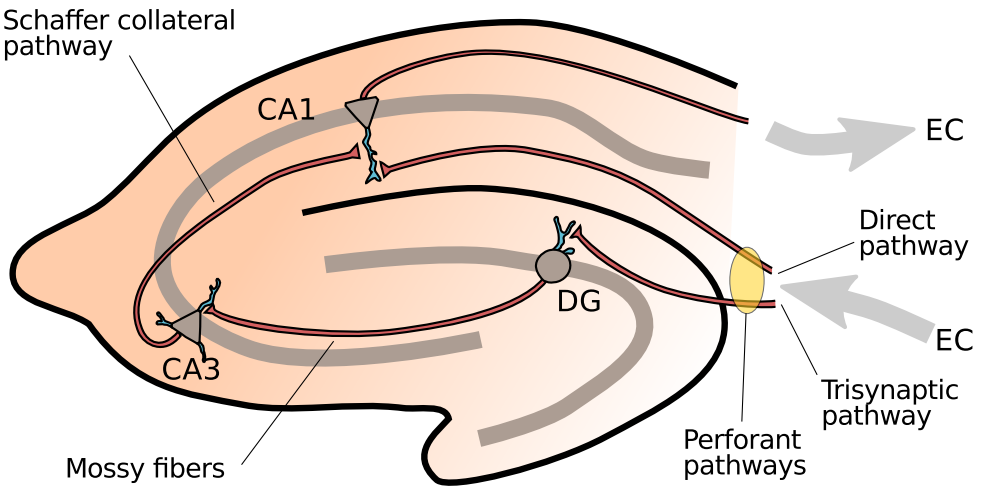

Figure 3.3: *Basic circuit of the hippocampus, composed of different subfields – DG: Dentate Gyrus, CA: Cornu Ammonis. The impulse flow arrives to the hippocampus from the entorhinal cortex (EC), which is, in turn, connected with many other parts of the cerebral cortex. The EC output arrives to the hippocampus via the perforant pathways, which project the information into the CA1 region. The direct pathway directly drives the EC excitatory impulse to the CA1 neurons whereas the trisynaptic pathway flows through the granule cells in the dentate region and the CA3 pyramidal cells to finally excite the CA1 neurons. CA1 cell project back to the EC*

3.2.4 Experimental induction

The experimental induction of LTP consists in the implantation of stimulating electrodes in the input pathway and similar recording electrodes in the postsynaptic area. The position of the post-synaptic recording electrodes should produce a maximal positive-going field EPSP (fEPSP). If the procedure is being conducted *in vivo*, the animals are given a recovery time, after which sets of baseline recordings be made (Abraham, Logan, Greenwood, and Dragunow, 2002).

The induction of LTP follows a previous baseline recording period and is triggered by the HFS. Different areas require different patterns of HFS protocols, and even in the same areas, it is possible to elicit different types of LTP by different HFS. In general terms, the stimulation needed to elicit LTP consists of a number of trains of pulses applied in sets. A train is defined as a series of pulses at a particular frequency and for a certain amount of time. As an example, the microarray data used in this thesis was originally obtained by Ryan *et al.* using 50 trains of $400Hz$ stimulation ($250\mu s$ pulse duration), 10 pulses/train, in sets of five trains $1s$ apart, with $60s$ between sets, delivered to the ipsilateral perforant pathway, which is the main excitatory input of granule cells in the dentate gyrus. This protocol was developed based on electroencephalography signals observed in the hippocampus of freely moving rats, and has a physiological meaning.

The HFS results in the induction of LTP. The recording electrodes show an increase in the efficiency of synaptic transmission together with an increase in the excitability of the cell population. Figure 3.4 shows how the HFS affects the size of the fEPSP as measured by the recording electrodes.

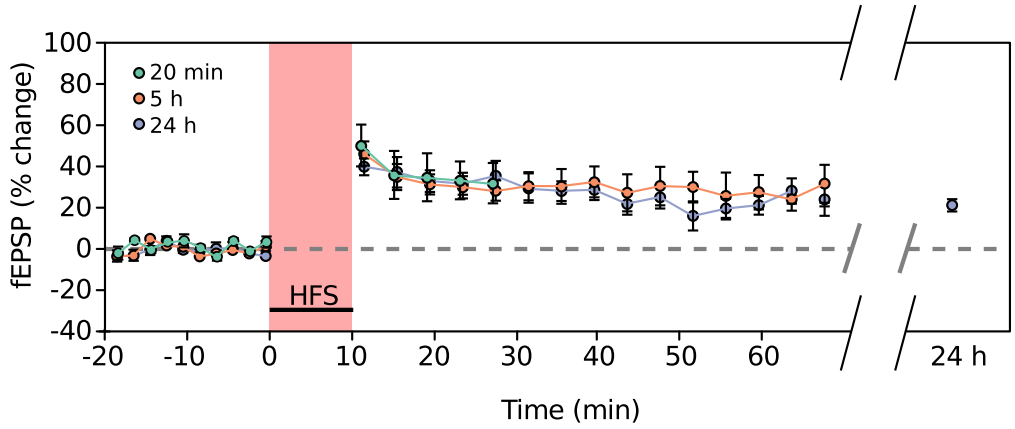

Figure 3.4: *The effect on the fEPSP of the HFS over an extended period of time. The baseline recordings prior to the stimulation (*20*m) are followed by the HFS (red shading), which lasts for* 10*m. After the LTP induction, the recording electrodes show a change in the fEPSP which lasts for more than* 24*h. The different colours in the plot represent different groups of animals according to time of RNA extraction post-LTP induction (see Chapter 2).* Adapted from Ryan *et al.* (2011) and Ryan *et al.* (2012)

3.2.5 Phases of LTP

There are at least three mechanistically and temporally distinct phases following HFS in hippocampal neurons. Short-term potentiation (STP), lasting 15-30 min, early-LTP (E-LTP), stable for up to 2-3 h, and late-LTP (L-LTP), which in some cases can last up to 6-8 h in hippocampal slices, months in vivo. While these mechanisms are initiated by the same extracellular neurotransmitter, the underlying molecular mechanisms differ. Proteins and mRNAs critical for earlier phases are likely to be pre-existing and turn over slowly. As noted from the earlier studies on LTP, the molecular species responsible for L-LTP and long-term memory must be either induced or, if constitutively expressed, only transiently accessible to modification (Goelet *et al.*, 1986).

STP is typically restricted to the first 20-30 minutes, with a gradual decay that uncovers the overlapping E-LTP. This is, however, dependent on the stimulation protocol and varies notably from experiment to experiment. The magnitude of STP depends on the frequency of the HFS, and the duration depends on the number of stimuli used during HFS and the frequency of low-frequency stimuli that are delivered following its induction, generally applied to monitor the level of synaptic plasticity during experiments. This implies that STP can be stored (Volianskis and Jensen, 2003). In a recent review (Park, Volianskis, Sanderson, Bortolotto, Jane, Zhuo, Kaang, and Collingridge, 2014), the authors speculate that STP is expressed by an alteration in the probability of transmitter release, while LTP is expressed by a postsynaptic component.

Although STP has classically been characterised as a single mechanism and sometimes even considered inconsequential, an *in vitro* study that employed a range of different NMDA receptor antagonists differing on their preferring type of NMDA receptor subunits, distinguished a total of three pharmacologically different components of synaptic potentiation – STP1, STP2, and LTP (Volianskis, Bannister, Collett, Irvine, Monaghan, Fitzjohn, Jensen, Jane, and Collingridge, 2013).

Similarly, LTP has at least two distinct components, which seem to be the result of different

stimulation patterns – single-episode or compressed HFS versus spaced HFS (Woo, Duffy, Abel, and Nguyen, 2003). These patterns elicit E-LTP and L-LTP respectively, which classically have been interpreted as temporally distinct phases. E-LTP is independent on PKA activity and protein synthesis contrarily to L-LTP, that depends on PKA activation and protein synthesis.

The inherent complexity of memory storage processes at the different levels of organisation result in a plethora of different methodologies and experimental approaches applied to the study of LTP. The extensive literature on LTP available as per today reflects these difficulties. It is well known that there are different subtypes of LTP that can be induced in the same synapses by distinct induction protocols, brain regions, or developmental stages. While modulatory molecules can play fundamental roles in some aspects of LTP, such as long-term morphological changes or processes specific to each subtype of LTP, it is of a practical and theoretical interest to pinpoint the core elements necessary and sufficient for the establishment LTP. The following sections represent a starting point for further improvement and do not preclude the possibility that other forms of LTP may differ in some of its key components or transduction mechanisms. However, as stated previously, our study is restricted to the NMDA receptor dependent LTP induced at perforant path synapses using multiple, spaced trains of stimuli and analysing molecular changes in the dentate gyrus. The following discussion is articulated around these core molecules and transduction pathways. The most studied downstream elements will also be discussed.

3.3 Molecular mechanisms of LTP

It is well accepted that E-LTP requires synaptic activation of postsynaptic NMDA receptors. Repetitive tetanic stimulation leads to the depolarisation of the postsynaptic cell and the subsequent activation of the NMDA receptor (Huang and Kandel, 1994). The mechanism underlying the triggering of the early phase requires both AMPA receptor and NMDA receptor activation.

While the depolarisation in the postsynaptic cell caused by AMPA receptors upon glutamate binding is short-lived, the summation of EPSPs will eventually lead to the dissociation of the Mg^{2+} cation blocking the NMDA receptor allowing Ca^{2+} as well as Na^{+} to enter the postsynaptic cell. This rapid rise in intracellular Ca^{2+} concentration activates the enzymes mediating E-LTP induction. It is thought that a short-lasting threshold level of Ca^{2+} must be reached to trigger LTP (Svoboda and Mainen, 1999; Malenka and Nicoll, 1999). Note, however, that whereas the increase in postsynaptic Ca^{2+} concentration is a necessary element for the induction of LTP, NMDA receptor activation can be experimentally bypassed (Kauer, Malenka, and Nicoll, 1988), and therefore may not be necessary for all forms of LTP.

L-LTP, as well as long-term memory, is dependent on changes in gene expression and protein synthesis (Nguyen, Abel, and Kandel, 1994; Abraham and Williams, 2003, 2008; Alberini, 2009). Some authors further subdivide L-LTP into two mechanistically different phases according to the dependence on new gene transcription. The first phase (some times referred to as LTP2) requires of the regulation of translation of mRNA already present at the synapses while the second (LTP3) depends both on new gene transcription and protein synthesis (Raymond, 2007; Abraham and Williams, 2008).

The new transcripts and proteins that characterise LTP3 could be targeted to the specific synapses from the nucleus by means of a synaptic "tag" generated at the potentiated synapses to maintain their specificity (Frey and Morris, 1997). The rise in intracellular Ca^{2+} activates second messenger systems that converge (via kinase activity) to phosphorylate in the nucleus a set of constitutive transcription factors such as NF-κB, CREB, Egr1, and serum response factor (SRF). The activation of constitutive transcription factors (CTFs) brings a first wave of *de novo* gene transcription consisting of effector genes and inducible transcription factors (ITFs). In turn, ITFs are responsible for a second wave of transcription (Ryan *et al.*, 2012; Abraham and Williams, 2003).

3.3.1 The CaMKII pathway and early LTP

Temporal decoding of intracellular Ca^{2+}

The concentration of Ca^{2+} in the postsynaptic cell encodes both temporal and spatial information which has to be decoded reliably. In addition to being decoded, the information contained in the transient intracellular elevation of Ca^{2+} has to be translated into a prolonged physiological response. Experimental evidence seems to indicate that CaMKII may act as the decoding molecule. CaMKII is a multifunctional kinase with a catalytic domain, an autoinhibitory domain, a variable segment, and a self-association domain. In the basal state, the protein is inactive – its catalytic domain is blocked by the autoinhibitory domain. CaMKII is a large holoenzyme comprising 12 homologous subunits associated via the self-association domain forming large multimers.

Intracellular Ca^{2+} binds to Calmodulin (CaM), a small protein that serves as an intermediate messenger. The Ca^{2+}/CaM complex is able to bind and activate transiently CaMKII subunits. A long-lasting activation of CaMKII only takes place by phosphorylation of the Thr 286 residue by neighbouring subunits via the catalytic domain. The ability to phosphorylate neighbouring subunits (autophosphorylation) represents the model by which a local transient increase in Ca^{2+} can be decoded into a longer-lasting form of molecular memory (Miller and Kennedy, 1986). In fact, once phosphorylated at Thr 286, CaMKII is independent of Ca^{2+}/CaM. The levels of Ca^{2+} and CaM, however, must reach a threshold – autophosphorylation does not occur if neighbouring subunits are not activated simultaneously (see Figure 3.5c). Several computational studies have been recently proposed to model the complex dynamic interactions of Ca^{2+}, CaM, and CaMKII (e.g. Pepke, Kinzer-Ursem, Mihalas, and Kennedy, 2010; Byrne, Putkey, Waxham, and Kubota, 2009). The computational models for postsynaptic signal transduction in LTP have been recently reviewed by Manninen, Hituri, Kotaleski, Blackwell, and Linne (2010).

Direct evidence for the requirement of CaMKII autophosphorylation in hippocampal LTP was provided by the work of Giese, Fedorov, Filipkowski, and Silva (1998). A mutation that precluded autophosphorylation was introduced in CaMKII. While the enzyme was still activated by Ca^{2+}/CaM, the inability to lock off the transient increase in Ca^{2+} prevented the transgenic mice from undergoing LTP. The Ca^{2+}-independent activation of CaMKII by autophosphorylation is stable for at least 1 hour (Fukunaga, Stoppini, Miyamoto, and Muller, 1993), during which the enzyme slowly phosphorylates other substrates. Furthermore, injecting active CaMKII enzymes into CA1 hippocampal neurons, increases the size of excitatory postsynaptic currents (EPSCs) and prevents induction of LTP by synaptic stimulation (Lledo, Hjelmstad, Mukherji, Soderling, Malenka, and Nicoll, 1995; Lisman, Yasuda, and Raghavachari, 2012). These studies seem to imply that activation of CaMKII is sufficient and necessary for LTP induction.

Spatial decoding

Consistent with a local specificity in sensing the Ca^{2+} signal, CaMKII is localised nearby the postsynaptic density (PSD), Sheng and Kim (2011), a protein-rich area attached to the postsynaptic membrane in close proximity to the presynaptic active zone. Furthermore, in hippocampal cultured neurons it has been shown that from an initial localisation at F-actin in the dendrite, CaMKII translocates to the PSD (Shen and Meyer, 1999). A number of substrates of CaMKII have been identified. In the PSD, a subunit of the NMDA receptor, GluN2B, has been shown to bind activated CaMKII (Leonard, Lim, Hemsworth, Horne, and Hell, 1999; Strack and Colbran, 1998). Accumulating evidence suggests that the CaMKII/GluN2B system is required for activation and translocation of CaMKII (Bayer, Paul De Koninck, Hell, and Schulman, 2001; Bayer, LeBel, McDonald, O'Leary, Schulman, and De Koninck, 2006), CaMKII Ca^{2+}-independent persistent activation, LTP induction (Halt, Dallapiazza, Zhou, Stein, Qian, Juntti, Wojcik, Brose, Silva, and Hell, 2012; Barria and Malinow, 2005), and LTP maintenance (Sanhueza, Fernandez-Villalobos, Stein, Kasumova, Zhang, Bayer, Otmakhov, Hell, and Lisman, 2011).

Other mechanisms outside of the CaMKII pathway contribute to the spatial decoding of the Ca^{2+}

signal. For example, the dendritic spine heads physically segregate the concentration dynamics of intracellular species (Svoboda, Tank, and Denk, 1996), although interactions between neighbouring synapses can take place (Harvey, Yasuda, Zhong, and Svoboda, 2008).

The molecular switch hypothesis

During the Ca^{2+}-independent CaMKII activated phase, the activity of phosphatases acting on the Thr 286 residue has to be suppressed. While a number of phosphatases are able to dephosphorylate CaMKII *in vitro* (Strack, Barban, Wadzinski, and Colbran, 1997), the activity of protein phosphatase 1 (PP1) has been shown to be inhibited during LTP by the phosphatase inhibitor 1 (I1, see Cohen (1989) for a review). Protein kinase A (PKA, discussed in Section 3.3.3) directly phosphorylates I1 which, in turn, inhibits the phosphatase activity of PP1 (Blitzer, Connor, Brown, Wong, Shenolikar, Iyengar, and Landau, 1998). Another phosphatase, Calcineurin (PP2B), has been directly linked to LTP (see Figure 3.5c-d). It seems that low concentrations of Ca^{2+}/CaM are enough to inhibit PP2B in hippocampal neurons after LTP induction (Wang and Kelly, 1996), preventing the phosphatase activity upon I1. The CaMKII-phosphatase coupling is consistent with a bistable switch, with low and high CaMKII activities both stable, originally proposed by Lisman (1985).

Yet, a study conducted *in vitro* found no evidence of bistability in the CaMKII-PP1 system (Bradshaw, Kubota, Meyer, and Schulman, 2003). In addition, a detailed model of CaMKII activation published by Michalski in 2013 predicted that the CaMKII system would never be bistable at resting Ca^{2+} concentrations. Specifically, the concentrations of intracellular Ca^{2+} needed for a bistable regime should lie above the observed physiological levels. Taken together, these studies call into question the role of CaMKII as the sole responsible for the biochemical switch underlying LTP and memory. Furthermore, a study by Lee, Escobedo-Lozoya, Szatmari, and Yasuda (2009) using two-photon fluorescence on single spines found that CaMKII activation is brief, and returns to baseline in about 1 min. It has been proposed that the process responsible for maintaining LTP must be downstream of CaMKII (Nicoll and Roche, 2013).

To further clutter the picture, a recent *in vitro* study published in 2014 by Urakubo, Sato, Ishii, and Kuroda (2014) demonstrated how a single holoenzyme of CaMKII can function as a molecular switch in the presence of an NMDA receptor-derived peptide. The intracellular Ca^{2+} transient was sufficient to trigger the phosphorylated ON state. In order for the system to switch from the ON state to a dephosphorylated OFF state, an increase in PP1 concentration was needed. Interestingly, reversal of LTP by phosphatases PP1 and PP2A has been documented in the literature (Kang-Park, Sarda, Jones, Moore, Shenolikar, Clark, and Wilson, 2003).

Note, however, that while the Ca^{2+} concentrations needed to reach bistability were found to be above $200nM$ (physiological levels are in the $80-150nM$ range), it is conceivable that the synergistic interplay between other proteins, perhaps in conjunction with other, less studied CaMKII phosphorylation sites (Thr 305 and Thr 306), may shift or extend the bistability phase to basal Ca^{2+} levels. The complexity of CaMKII regulation is remarkable, and a study seems to point out that phosphorylation at Thr 305 and Thr 306 may promote LTD rather than LTP (Pi, Otmakhov, Lemelin, De Koninck, and Lisman, 2010). The active involvement of other proteins would also account for the high concentrations of CaMKII observed in the PSD that cannot be accounted for solely by the binding to NMDA receptor (Petersen, Chen, Vinade, Dosemeci, Lisman, and Reese, 2003).

In the light of evidence from these studies, the molecular switch that CaMKII may constitute does not seem to be sufficient to elicit LTP. As we have emphasised, LTP is a complex process which may encompass a number of different overlapping and interrelated mechanisms acting at different levels of biological organisation. The putative binary switch that CaMKII presents provides an attractive hypothesis consistent with the robustness to noise and integrative capabilities of a molecular gating system. At different levels, however, it is conceivable that synaptic changes in strength may behave as multi-level mnemonic devices. In fact, graded storage devices can

theoretically have longer retention times, more noise tolerance, and greater storage capacity (Fusi, Drew, and Abbott, 2005; Satel, Trappenberg, and Fine, 2009).

AMPA receptor phosphorylation and trafficking

The glutamate receptor 1 (GluR1) subunit of the AMPA receptor represents another crucial substrate of CaMKII in the PSD (see Soderling and Derkach (2000) for a review and Barria, Muller, Derkach, Griffith, and Soderling (1997) for a paradigmatic study carried out by inducing LTP in region CA1 of hippocampus). Among the different phosphorylation sites in GluR1, Ser 831 is likely to be the responsible for the increase in conductance observed during E-LTP (Barria *et al.*, 1997). The Ser 831 residue is phosphorylated by CaMKII and PKC (see Section 3.3.2) and results in an increase on the average single channel conductance. However, this is only one mechanism by which AMPA receptor function is potentiated during E-LTP. The early recruitment of other AMPA receptor channels already present in the plasma membrane, together with the temporally subsequent exocytosis of AMPA receptor-enriched vehicles are the other two fundamental mechanisms known to contribute. The phosphorylation-induced increment of AMPA receptor conductance appears to be a fundamental component of LTP (Giese *et al.*, 1998).

Furthermore, the different subunits that form the AMPA receptor can play a role in the redistribution of the channels in the membrane. While the primary subtype of AMPA receptor inserted during LTP is the heteromeric GluA1/GluA2 (Adesnik and Nicoll, 2007), it has been suggested that a GluA2-lacking AMPA receptor is required for LTP maintenance. This type of AMPA receptor seems to appear during the first 10-20 min post-LTP induction (Plant, Pelkey, Bortolotto, Morita, Terashima, McBain, Collingridge, and Isaac, 2006). A study *in vivo* in rat dentate gyrus suggested that trafficking of GluA1-containing AMPA receptors takes place in the early-phase of LTP, although these studies are not conclusive (Adesnik and Nicoll, 2007).

AMPA receptor activity is also dependent on auxiliary proteins. The anchoring of the AMPA receptor at the synapse is mediated by the phosphorylation of the protein stargazin, which allows more receptors to bind to PSD-95 (Tomita, Stein, Stocker, Nicoll, and Bredt, 2005; Opazo, Labrecque, Tigaret, Frouin, Wiseman, De Koninck, and Choquet, 2010). Stargazin acts as an auxiliary subunit of most AMPA receptors influencing their conductance and kinetics – the expression of a stargazin construct unable to undergo phosphorylation prevented LTP in hippocampal neurons (Tomita *et al.*, 2005). The TARP family have been shown to have an important role in membrane insertion and lateral redistribution of AMPA receptors (see Blakely and Edwards (2012) for a review). A member of the TARP family, γ-8, appears to participate in the formation of the pool of extrasynaptic AMPA receptors. Mice lacking γ-8 show a severe defect in LTP (Rouach, Byrd, Petralia, Elias, Adesnik, Tomita, Karimzadegan, Kealey, Bredt, and Nicoll, 2005) due to the lack of extrasynaptic AMPA receptors.

CaMKII role in LTP maintenance

The increase in the number of channels by exocytosis is also mediated indirectly by CaMKII, and it is essential for the later stages of LTP. Activated CaMKII stimulates the fusion of AMPA receptor-containing vesicles with the cell membrane via the Ras-Erk1/2 pathway (Patterson, Szatmari, and Yasuda, 2010), Rab-GTPase proteins, SNARE proteins, syntaxin 4 and 13, and the motor protein myosin V (see Kennedy and Ehlers (2011) for a review, pathway represented with a black dashed arrow in Figure 3.5). These components, although not necessary for the early phase of LTP, strongly reduce the potentiation at later times (Lisman *et al.*, 2012), which suggest that during E-LTP it suffices to recruit and anchor the AMPA receptors readily available in the cell membrane. On the other hand, L-LTP relies on the exocytosis of AMPA receptor vesicles. Note that the Ras-Erk1/2 pathway is likely not to be the only one mediating the vesicle fusion (Cullen and Lockyer, 2002; Patterson *et al.*, 2010).

Nevertheless, conflicting views exist regarding the persistence of the CaMKII/NMDA receptor

complexes and the multiple roles of CaMKII in LTP maintenance (Lee *et al.*, 2009; Bayer *et al.*, 2006).

3.3.2 The PKC pathway

The induction of LTP is not only dependent on CaMKII. In 1989, Malinow, Schulman, and Tsien reported that the inhibition of either CaMKII or protein kinase C (PKC) blocked the induction of LTP, but had no effect on its expression after its establishment. In fact, the role of PKC in LTP was the subject of a number of earlier studies. While the exact molecular mechanisms by which PKC is activated after increases in intracellular Ca^{2+} are unclear, the information carried by its activation converges with the flux of information carried by the activated CaMKII – both molecules phosphorylate the identical site on GluR1 subunit of AMPA receptor, increasing its conductance (Mammen, Kameyama, Roche, and Huganir, 1997; Roche, O'Brien, Mammen, Bernhardt, and Huganir, 1996). This view is consistent with the fact that inhibition of both PKC and CaMKII is necessary to reverse the expression of E-LTP (Wang and Feng, 1992).

PKC may also be associated with later stages of LTP. PKMζ, an autonomously active isoform of PKC, has been proposed to be responsible for the maintenance of the initial cellular changes established following LTP induction. The kinase acts to preserve both LTP maintenance and the long-term memory trace by a continuous phosphorylation that enhances AMPA receptor (Sacktor, Osten, Valsamis, Jiang, Naik, and Sublette, 1993). PKMζ mRNA contains a long untranslated region that is crucial for the regulation of the PKMζ protein synthesis at the synapse (Hernandez, Blace, Crary, Serrano, Leitges, Libien, Weinstein, Tcherapanov, and Sacktor, 2003). The translational block is mediated possibly via microRNA, allowing stores of PKMζ mRNA that can be activated promptly following synaptic stimulation (Sacktor, 2008). A number of intracellular signalling cascades converge in the activation of the repressed mRNA, including CaMKII, PKA, and PI3K-Akt-mTOR pathways. For reviews, see Sacktor (2010) and Kwapis and Helmstetter (2014).

3.3.3 The PKA pathway

The protein kinase A (PKA) cascade is often referred to as the cAMP signalling pathway (Figure 3.5d). Activation of NMDA receptor increases cAMP levels via Ca^{2+}-sensitive adenylyl cyclases AC1 and AC8, which activate PKA by promoting the detachment of its inhibitory subunit. This process is Ca^{2+}/CaM-dependent. The activated PKA has the ability to enhance voltage-gated Ca^{2+} channel and AMPA receptor conductance, while simultaneously attenuating voltage-dependent K channel function. By this mechanism, an initial Ca^{2+} influx can be amplified (Chetkovich, Gray, Johnston, and Sweatt, 1991; Roche *et al.*, 1996). This feedback is complemented by the crosstalk between the PKA cascade and the CaMKII switch. Specifically, PKA activates I1 by phosphorylation, which will inhibit the phosphatase activity of PP1 and PP2A upon CaMKII (Blitzer, Wong, Nouranifar, Iyengar, and Landau, 1995; Blitzer *et al.*, 1998). As the dephosphorylation of I1 can be regulated by PP2B, it is probable that the antagonistic regulation of PKA and PP2B on I1 regulates the level of synaptic output (Winder, Mansuy, Osman, Moallem, and Kandel, 1998). In this scenario, the cAMP pathway can be interpreted as a gate acting on the CaMKII cascade rather than carrying the signal for LTP.

Yet, the role of PKA has been regarded as having a fundamental importance in L-LTP (Abel, Nguyen, Barad, Deuel, Kandel, and Bourtchouladze, 1997). Activated PKA translocates to the nucleus and activates CREB, which mediates the transcription of genes responsible for L-LTP maintenance (Thomas and Huganir (2004), see Section 3.3.6). While E-LTP and L-LTP have been classically regarded as temporally and mechanistically distinct phases, they may well overlap in time. In fact, the PKA- and protein synthesis-independent E-LTP can last for periods of time that overlap with L-LTP which, in the other hand, can develop quickly (Park *et al.*, 2014).

3.3.4 The Ras-Erk1/2 pathway

The Ras-Erk1/2 signalling pathway has been shown to be of crucial importance for induction and maintenance of LTP (Impey, Obrietan, and Storm, 1999), and for some types of memory (Atkins, Selcher, Petraitis, Trzaskos, and Sweatt, 1998; Blum, Moore, Adams, and Dash, 1999; Runyan, Moore, and Dash, 2004). Erk is a member of the MAPK family of protein kinases. Upon activation by an Erk kinase (MEK), Erk can phosphorylate the protein kinase Rsk2, which in turn translocates to the CREB and the SRF (Xing, Ginty, and Greenberg (1996), see Section 3.3.6 and Figure 3.5b). Erk can also dimerize and translocate to the nucleus to activate other transcription factors such as Elk-1 (Gille, Sharrocks, and Shaw, 1992), and SMAD3 (Gille, Kortenjann, Thomae, Moomaw, Slaughter, Cobb, and Shaw, 1995).

The activation of MEK is accomplished by another class of protein kinases, the Raf kinase family. Raf activation pathway is not clear, but seems that at least two mechanisms must converge – Ras interaction plus phosphorylation mediated by an Src kinase or PKC (Morrison and Cutler Jr, 1997).

A relevant feature of the Ras-Erk1/2 cascade is the capacity for serial amplification through the successive protein kinases, which could have an important role in the induction phase of LTP.

3.3.5 The presynaptic component

The mechanisms described so far are all located within the postsynaptic cell. A long dispute has taken place since the discovery of LTP regarding the locus of expression. Early studies showed an increase in glutamate release following LTP (Dolphin, Errington, and Bliss, 1982; Errington, Galley, and Bliss, 2003; Bliss, Errington, Laroche, and Lynch, 1987; Lynch, Errington, Clements, Bliss, Redini-Del Negro, and Laroche, 1990), but contradicting reports also exist (Lüscher, Malenka, and Nicoll, 1998; Manabe and Nicoll, 1994; Mainen, Jia, Roder, and Malinow, 1998). While the models of postsynaptic LTP expression have became widely accepted, the presynaptic component is still subject of research. A recent study reported an increase in the reliability of transmitter release in active synapses (Enoki, Hu, Hamilton, and Fine, 2009). The authors hypothesised that the pre- and postsynaptic components of LTP are differentially regulated during development – immature synapses (deficient in AMPA receptors) recruit AMPA receptors upon potentiation as the brain matures via the post-synaptic mechanism, while already matured synapses express subsequent plasticity via presynaptic changes in transmitter release probability.

3.3.6 Gene expression in LTP

Signalling crosstalk between synapses and nucleus

We have so far discussed the molecular effectors and processes underlying LTP induction. Consolidation and maintenance of LTP, however, may actually require additional molecular mechanisms that involve new mRNA and protein synthesis (Kandel, 2001; Bito, Deisseroth, and Tsien, 1997; Morgan and Curran, 1989; Okuno, 2011). The crosstalk between the nucleus and the active synapse is believed to involve a *tagging* of the activated synapse. The "synaptic tagging and capture" hypothesis (Frey and Morris, 1997) argues that activated synapses are marked with a long-lasting *tag* to direct the delivery of the new synthesized proteins towards them (for a recent review, see Redondo and Morris, 2010).

The cAMP-responsive element

Another Ca^{2+}/CaM-dependent protein kinase, CaMKIV, has been shown to be involved in LTP. In contrast to CaMKII, CaMKIV is prominently located in the nucleus, where it can be activated upon phosphorylation by CaMKK. Activated CaMKIV is capable of phosphorylating CREB at Ser 133, which leads to the recruitment of an additional protein, the CREB binding protein (CBP). The CREB/CBP complex is ultimately responsible for the cAMP-responsive element (CRE)-dependent

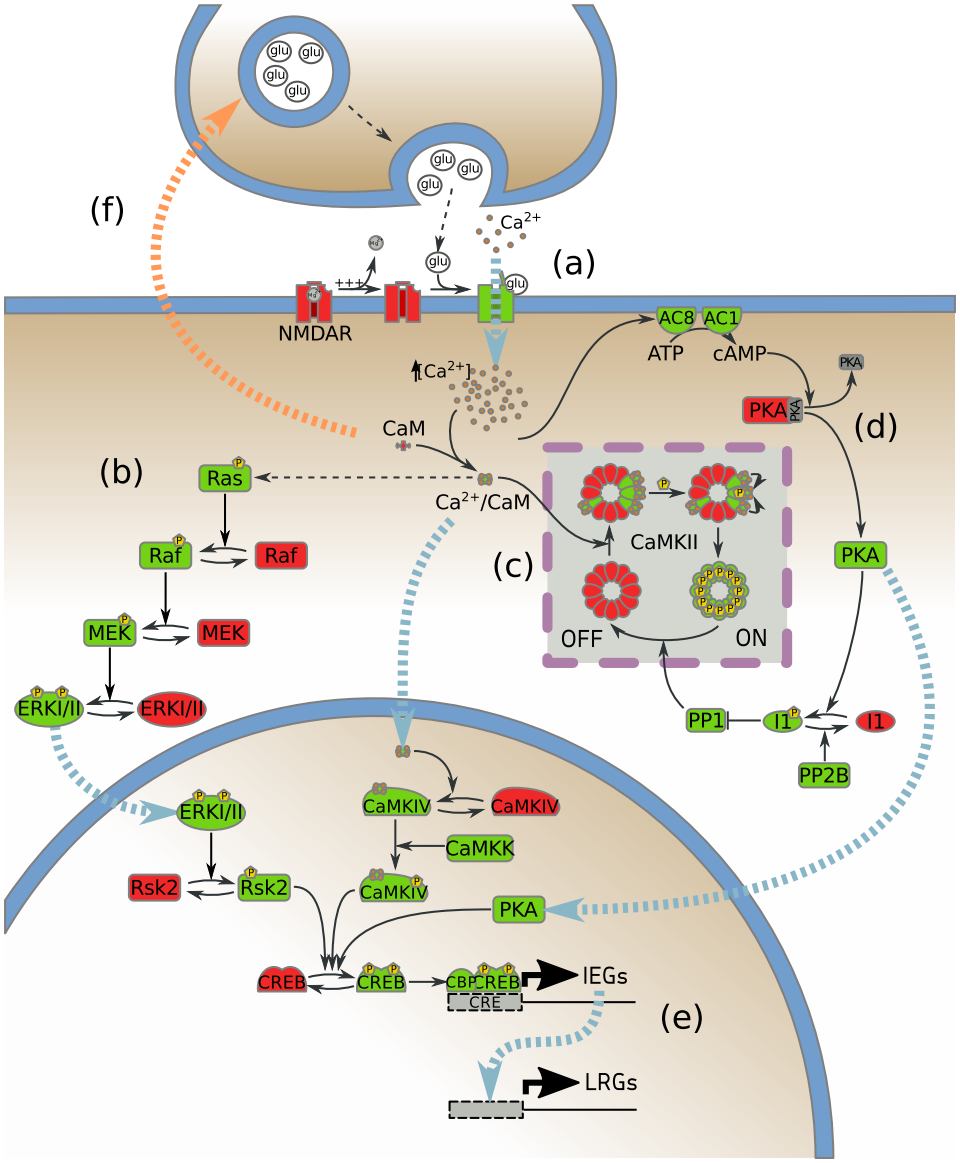

Figure 3.5: ***(a)*** *Co-occurrence of membrane depolarisation and glutamate binding opens NMDA receptors. The intracellular raise in Ca^{2+} is sensed by at least three pathways. The Ras-Erk1/2 pathway* ***(b)****; the CaMKII molecular switch* ***(c)****; the PKA pathway* ***(d)****. The pathways converge (including CaMKIV) in the activation of CREB* ***(e)****. A "retrograde messenger" travels to the presynaptic cell leading to an increase in the presynaptic response to subsequent stimuli* ***(f)***

gene expression (Braun and Schulman, 1995; Bito, Deisseroth, and Tsien, 1996). It has been demonstrated that CBP activity is, in addition, positively regulated directly by CaMKIV (Chawla, Hardingham, Quinn, and Bading, 1998). It appears that the main role for CaMKIV consists in activating CPB while the Ras-Erk1/2 pathway is responsible for ensuring a prolonged CREB

phosphorylation (Impey, Fong, Wang, Cardinaux, Fass, Obrietan, Wayman, Storm, Soderling, and Goodman, 2002).

Another pathway that has been studied in reference to CREB activation is triggered by a type of membrane channels called voltage-dependent Ca^{2+} channels (VDCC). A particular class, the L-type VDCC, has been shown to participate actively in some forms of LTP (Grover and Teyler, 1990; Morgan and Teyler, 1999). In fact, the L-type VDCC-mediated Ca^{2+} increase is likely to be a trigger for CRE-mediated transcription (Bading, Ginty, and Greenberg, 1993).

The downstream CRE-regulated genes are initiators and modulators of long-term structural and functional changes elicited by LTP and memory (Deisseroth, Bito, and Tsien, 1996; Bourtchuladze, Frenguelli, Blendy, Cioffi, Schutz, and Silva, 1994; Bito *et al.*, 1997; Okuno, 2011). Other signalling cascades, such as the PKA pathway and the Ras-Erk1/2 pathway may converge in CREB phosphorylation (Flavell and Greenberg, 2008). While the phosphorylation of CREB by the Ras-Erk1/2 cascade seems to work at a slower time scale, its role in LTP-induced gene expression is still unclear.

A large number of target genes for CREB have been proposed, and CREs exist in the promoter regions of c-Fos, BDNF, Egr1, homer1a/vesl1s, cpg15, and Arc (Benito, Valor, Jimenez-Minchan, Huber, and Barco, 2011). The regulation of these genes will be discussed in Section 3.3.6.

NFκB

NFκB is a CTF ubiquitously expressed with a strong presence in the brain. There are a total of seven members in the Rel-NFκB family – p50, p52, p65 (RelA), p100, p105, RelA, c-Rel, and RelB. They form homo- or heterodimers, and the prototypical dimer in the nervous system is p50/p65 (May and Ghosh, 1997). NFκB is localised in the cytoplasm bound to an inhibitor protein, IκB. Upon stimulation, the phosphorylation of IκB by the IκB kinase (IKK) leads to its ubiquitination and subsequent degradation by the proteasomal machinery, exposing the DNA binding site of NFκB. Following translocation to the nucleus, the active dimer is able to promote transcription of its target genes (Karin and Ben-Neriah, 2000). Neuronal stimulation may activate NFκB through several signalling cascades, including PI3K-Akt-mTOR, PKC and CaMKII (Lilienbaum and Israël, 2003; Rojo, Salinas, Martín, Perona, and Cuadrado, 2004).

Freudenthal, Romano, and Routtenberg (2004) documented the activation of NFκB during LTP in the mouse hippocampus. An increment in p50 has also been observed (Meberg, Kinney, Valcourt, and Routtenberg, 1996). In addition, Albensi and Mattson (2000) showed that a DNA decoy containing the consensus sequence recognised by NFκB reduced the magnitude of LTP. In particular, c-Rel has been shown to be necessary for LTP *in vitro* and for hippocampus-dependent memory formation *in vivo* (Ahn, Hernandez, Levenson, Lubin, Liou, and Sweatt, 2008).

In addition to the transcription factor activity following translocation to the nucleus, NFκB may act locally at the synapse Salles, Romano, and Freudenthal (2014). In this regard, the fruitfly homologous gene, Dorsal, was shown to regulate glutamate receptor density in an transcriptionally independent way (Heckscher, Fetter, Marek, Albin, and Davis, 2007).

The serum response element

The serum response element (SRE) is the binding site for another inducible transcription factor activated by phosphorylation – SRF. While SRF and CREB may jointly contribute to some neuronal functions (such as the control of Arc expression), the functions of the SRF-induced immediate early genes (IEGs) seems to be restricted to plasticity-associated structural changes in neuronal connectivities via the control of actin dynamics (Knöll and Nordheim, 2009). A gene profiling study using transfected hippocampal cultures indicated that the effect of overexpression of SRF only had effect on around 200 transcripts, while CREB affected up to 10% of the transcriptome (around 30,000 transcripts, Benito *et al.*, 2011).

Within the SRE, an additional binding site to accommodate a ternary complex factor (TCF),

a family of proteins with an Ets domain such as Sap-1, Sap-2, and Elk-1 (Price, Rogers, and Treisman, 1995). These proteins are capable of binding the SRE/SRF complex. The Ras-Erk1/2 pathway mediates the activation of the SRE pathway, initiated by the Ca^{2+} transient (Hardingham, Arnold, and Bading, 2001).

Immediate early genes

CREB and SRF are CTFs – the protein is present regardless of the activation state of the neuron, and its transcription factor activity is switched on upon phosphorylation. Other CTFs such as CREM and ATF-2, have unclear functional roles in LTP (Herdegen and Leah, 1998). Together with the activation of CTFs, a wave of newly transcribed genes are synthesised by the transcriptional machinery following LTP induction. These so-called IEGs can be ITFs, which will in turn regulate a second wave of gene transcription (delayed response genes). Transcription of IEGs requires only pre-existing transcription factors and is independent on *de novo* protein synthesis (Abraham and Williams, 2008). Among the IEGs, some do not act as transcription factors and exhibit other structural or functional roles associated wit the synaptic changes necessary for LTP (Abraham and Williams, 2003, 2008)

The characterisation and isolation of IEGs started as early as in 1987 with the description of a rapid induction of c-Fos following stimulation (Morgan, Cohen, Hempstead, and Curran, 1987). A number of successive studies have succeeded at isolating other IEGs with the aim of defining central genes involved in learning and memory.

c-Fos is a proto-oncogene, part of the Fos family of transcription factors. Together with c-jun it forms an heterodimer (AP-1) which binds DNA at AP-1 specific sites to regulate transcription of other genes (Chiu, Boyle, Meek, Smeal, Hunter, and Karin, 1988). It has been used as a marker of neural activity and mutant mice with a disrupted c-Fos results in an impairment of hippocampal LTP (Fleischmann, Hvalby, Jensen, Strekalova, Zacher, Layer, Kvello, Reschke, Spanagel, Sprengel, *et al.*, 2003). The c-Fos gene has a simple proximal promoter sequence which contains a CRE and an SRE (Robertson, Kerppola, Vendrell, Luk, Smeyne, Bocchiaro, Morgan, and Curran, 1995).

The brain-derived neurotrophic factor (BDNF) is a secreted protein member of the neurotrophin family of growth factors involved in neural survival and growth. In addition, BDNF seems to play a fundamental role in the maintenance of LTP and its synaptic specificity (Barco, Patterson, Alarcon, Gromova, Mata-Roig, Morozov, and Kandel, 2005; Panja and Bramham, 2014). It contains a number of different promoters with distinct activity dependencies including CRE and SRE (Greer and Greenberg, 2008).

Arc/Arg3.1 is probably the most studied ITF in neurons. Its expression pattern correlates with neuronal activity (Lyford, Yamagata, Kaufmann, Barnes, Sanders, Copeland, Gilbert, Jenkins, Lanahan, and Worley, 1995; Link, Konietzko, Kauselmann, Krug, Schwanke, Frey, and Kuhl, 1995), and its disruption impairs the maintenance of LTP without affecting the induction phase (Guzowski, Lyford, Stevenson, Houston, McGaugh, Worley, and Barnes, 2000; Plath, Ohana, Dammermann, Errington, Schmitz, Gross, Mao, Engelsberg, Mahlke, Welzl, *et al.*, 2006). Arc mRNA moves to the activated dendrites after induction by synaptic activation at a rate of $300\mu m/h$ (Wallace, Lyford, Worley, and Steward, 1998). The means by which Arc mRNA is recruited selectively to the activated synapses was attributed to the synaptic tagging and capture hypothesis. In this regard, a study of Steward, Wallace, Lyford, and Worley (1998) suggested that the selective localisation of newly synthesised Arc mRNA was not caused by a general reorganisation of the dendritic cytoplasm or cytoskeleton nor by selective degradation of mRNA in non-activated synapses, but rather by the presence of some "tag" generated following synaptic activation that recognises a signal in the mRNA molecule itself. Contrarily to this belief, however, a study has shown that Arc targets inactive synapses, by interacting with an inactive, CaM-unbound form of CaMKII (Okuno, Akashi, Ishii, Yagishita-Kyo, Suzuki, Nonaka, Kawashima, Fujii, Takemoto-Kimura, Abe, *et al.*, 2012). This study suggests that the localisation of Arc is inverse to the activated synapses, observation

consistent with the results published earlier by Shepherd, Rumbaugh, Wu, Chowdhury, Plath, Kuhl, Huganir, and Worley (2006). They showed that in the absence of Arc, AMPA receptors endocytosis is low, leading to a shifted equilibrium towards AMPA receptor membrane insertion whereas on the contrary, high levels of Arc promote AMPA receptors endocytosis. Sustained Arc expression acts by counteracting saturation of synaptic strength.

The Arc promoter contains a region named synaptic activity-responsive element (SARE) (Inoue, Yagishita-Kyo, Nonaka, Kawashima, Okuno, and Bito, 2010), which requires the simultaneous binding of CREB, SRF and MEF2. Both CaMK- and Ras-Erk1/2-dependent pathways are involved in SARE activation(Kawashima, Okuno, Nonaka, Adachi-Morishima, Kyo, Okamura, Takemoto-Kimura, Worley, and Bito, 2009). In the promoter, there are also SREs and AP-1 (the binding motif for Fos/Jun complex) sites (Waltereit, Dammermann, Wulff, Scafidi, Staubli, Kauselmann, Bundman, and Kuhl, 2001).

The early growth response protein 1 (Egr1, also known as zif268, krox24, and NGFI-A), contains a zinc finger domain and is coregulated with c-Fos during some cellular processes (Sukhatme, Cao, Chang, Tsai-Morris, Stamenkovich, Ferreira, Cohen, Edwards, Shows, Curran, *et al.*, 1988). Egr1 is an ITF, and only low levels of protein are detected in the absence of a stimulus. Activation of NMDA receptor converges on the phosphorylation of CREB and Elk-1, inducing Egr1 transcription. Raise in Egr1 protein has been linked with learning and memory. Its role as a signalling molecule downstream from the NMDA receptor in the hippocampal synaptic plasticity has been documented in a number of studies (Cole, Saffen, Baraban, and Worley, 1989; Wisden, Errington, Williams, Dunnett, Waters, Hitchcock, Evan, Bliss, and Hunt, 1990; Wei, Xu, Qu, Milbrandt, and Zhuo, 2000). In particular, the disruption of the cyclic AMP response element (CRE) in the promoter region of the Egr1 gene leads to impairment of *in vivo* dentate gyrus L-LTP (Jones, Errington, French, Fine, Bliss, Garel, Charnay, Bozon, Laroche, and Davis, 2001). For a review, see Thiel, Mayer, Müller, Stefano, and Rössler (2010).

Other members of the Egr family have been identified – Egr2, Egr3, and Egr4. In neurons, these Egr proteins are expressed following synaptic activity and have been associated with LTP (Murphy, Worley, and Baraban, 1991; O'Donovan, Tourtellotte, Millbrandt, and Baraban, 1999; Ryan *et al.*, 2011).

Table 3.3.6 reports the most studied IEGs in the literature.

Table 3.1: *List of the some of the most studied IEGs. Note that the temporal expression of the genes reported in the Table do not always fulfil the definition of IEGs since their expression falls within the first 2 h post-LTP induction. IEGs are typically induced within 15-45 minutes of the stimulus, returning to basal levels in few hours*

Category	Gene	Structure/function	References
Transcription factors	c-Fos	Component of AP-1	Greenberg *et al.*, 1983; Morgan *et al.*, 1987
	fosB	Component of AP-1	Hope *et al.*, 1992; Dragunow *et al.*, 1992
	c-Jun	Component of AP-1	Saffen *et al.*, 1988; Cole *et al.*, 1990
	Jun-B	Component of AP-1	Saffen *et al.*, 1988; Cole *et al.*, 1990; Demmer *et al.*, 1993
	Jun-D	Component of AP-1	Demmer *et al.*, 1993
	Egr1	Zinc finger	Cole *et al.*, 1989; Worley *et al.*, 1993
	Egr2	Zinc finger	Bhat *et al.*, 1992; Williams *et al.*, 1995
	Egr3	Zinc finger	Yamagata *et al.*, 1994; Li *et al.*, 2005

Continued on next page

Table 3.1 – *Continued from previous page*

Category	Gene	Structure/function	References
	Egr4	Zinc finger	Coba *et al.*, 2008
	RNF39	Zinc finger	Matsuo *et al.*, 2001
	bmi1	Zinc finger	Haavik *et al.*, 2007; Alkema *et al.*, 1993
	NR4A1	Orphan hormone receptor	Watson *et al.*, 1989; Wisden *et al.*, 1990
	Etv5	Ets-related molecule	Haavik *et al.*, 2007; Monte *et al.*, 1994
Postsynaptic proteins	Arc	Regulator of AMPA receptor trafficking	Lyford *et al.*, 1995; Link *et al.*, 1995
	Homer1	Inducible form of EVH proteins	Brakeman *et al.*, 1997; Kato *et al.*, 1997
Intracellular signalling	Rheb	Ras homolog protein	Yamagata *et al.*, 1994
	RSG2	Regulator of G-prot signalling	Ingi *et al.*, 1998
	Plk2	Polo-like kinase	Kauselmann *et al.*, 1999
	Cox-2	Inducible cyclooxygenase	Yamagata *et al.*, 1993
	Timp2	Metallopeptidase inhibitor	Chaillan *et al.*, 2006
	prickle 1	Implicated in tissue polarity	Haavik *et al.*, 2007; De *et al.*, 1992
	baiap2	Implicated in neuronal growth	Haavik *et al.*, 2007; Oda *et al.*, 1999
	BAD2	MAPK phosphatase	Qian *et al.*, 1994
Secretory factors	BDNF	Member of neurotrophin family	Hughes *et al.*, 1993; Lauterborn *et al.*, 1996
	ActivinβA	Member of TGF-β superfamily	Andreasson *et al.*, 1995; Inokuchi *et al.*, 1996
	Narp	Presynaptically released	Tsui *et al.*, 1996
	tPA	Extracellular serine protease	Qian *et al.*, 1993
Membrane proteins	Arcadlin	Protocadherin family protein	Yamagata *et al.*, 1999
	neuritin	GPI-anchored protein	Nedivi *et al.*, 1993; Naeve *et al.*, 1997
	Grm6	Glutamate receptor	Riedel *et al.*, 1996
	Syt4	Synaptotagmin	Lynch *et al.*, 1994
	scn1b	Sodium channel	Haavik *et al.*, 2007; Tseng *et al.*, 1996
	NR2A, NR2B	NMDA receptor subunits	Williams *et al.*, 1998
Immunity-linked genes	cd74	Immunity-like processes	Haavik *et al.*, 2007
	rt1-Da	Immunity-like processes	Haavik *et al.*, 2007
	c3	Immunity-like processes	Haavik *et al.*, 2007
	nptxr	Immunity-like processes	Haavik *et al.*, 2007

Late response genes

A second wave of transcription is believed to occur following the IEGs. This set of genes are typically induced with a slower time course (2-3 h after the stimulus). While some late-response genes are transcriptions factors, most of them function as effector proteins and carry a wide spectrum of functions, including intracellular signalling, cell adhesion, cytoskeleton and cellular scaffolding regulation, secretory factors and membrane channels Hong, Li, Becker, Dawson, and Dawson (2004); Davies (2004).

While several efforts have been made towards defining a wider picture of the biochemical networks underlying the maintenance of LTP (Lee, Cohen, Becker, and Fields, 2005; Park, Gong, Stuart, and Tang, 2006; Håvik, Røkke, Dagyte, Stavrum, Bramham, and Steen, 2007a; Valor and Barco, 2010; Ryan *et al.*, 2011), it is unclear how IEGs and late response genes (LRGs) coordinate in order to lead to the persistence of LTP.

The work by Ryan *et al.* (2012) represents one of the most recent approach towards understanding the role of the new gene transcription in LTP maintenance. They identified a set of differentially expressed genes whose interactions served to identify biologically relevant networks and pathways related with LTP. Genes identified as major hubs in the LTP-regulated gene networks confirmed

previous findings regarding major key regulators. In addition, using databases of cellular pathways with the most differentially expressed genes allowed to pinpoint other molecular species that may play central roles during LTP without showing a significant alteration in their expression levels (e.g. becoming active by phosphorylation), such as the CTF NFκB.

These results, taken together with previous knowledge, stress the importance of plasticity-associated gene transcription in LTP. Interestingly, some of the overrepresented functions across the LTP-related genes are development, proliferation and neurogenesis, suggesting that new gene transcription may have an active role in the morphological restructuring of the synapses following LTP. Note that these reported genes have been linked to long-term memory, specially the CREB family and its associated pathway, AP-1, Egr1, and NFκB (for a review, see Alberini, 2009).

It is worth commenting that despite the evidence of a protein-dependent phase in LTP maintenance, other lines of research have shown that LTP can be maintained in the absence of protein synthesis (e.g. Pang, Teng, Zaitsev, Woo, Sakata, Zhen, Teng, Yung, Hempstead, and Lu, 2004; Fonseca, Nägerl, and Bonhoeffer, 2006). While it is now clear that it is possible to maintain LTP in the absence of protein synthesis using particular induction protocols (BNDF-LTP, avoiding test pulses, inhibiting proteasome degradation; Abraham and Williams, 2008) these results do not rule out the requirement for protein synthesis *in vivo*. These studies, however, suggest that there may be a stimulation-dependent depotentiation caused by protein degradation, which raises the possibility that the role of *de novo* synthesised proteins is to replenish the protein pools at the synapses to avoid an LTP decay due to protein turnover.

On the other hand, *de novo* gene expression has been shown to be involved in L-LTP consolidation and maintenance, and constitutes a distinct phase of L-LTP. Gene expression following LTP induction is thought to mediate the structural remodelling of the stimulated synapses by neural growth of new dendritic spines and enlargement of pre-existing (Matsuzaki, Honkura, Ellis-Davies, and Kasai, 2004; Krucker, Siggins, and Halpain, 2000; Bramham, 2008). However, the integrated genomic response elicited by LTP is far from being well understood.

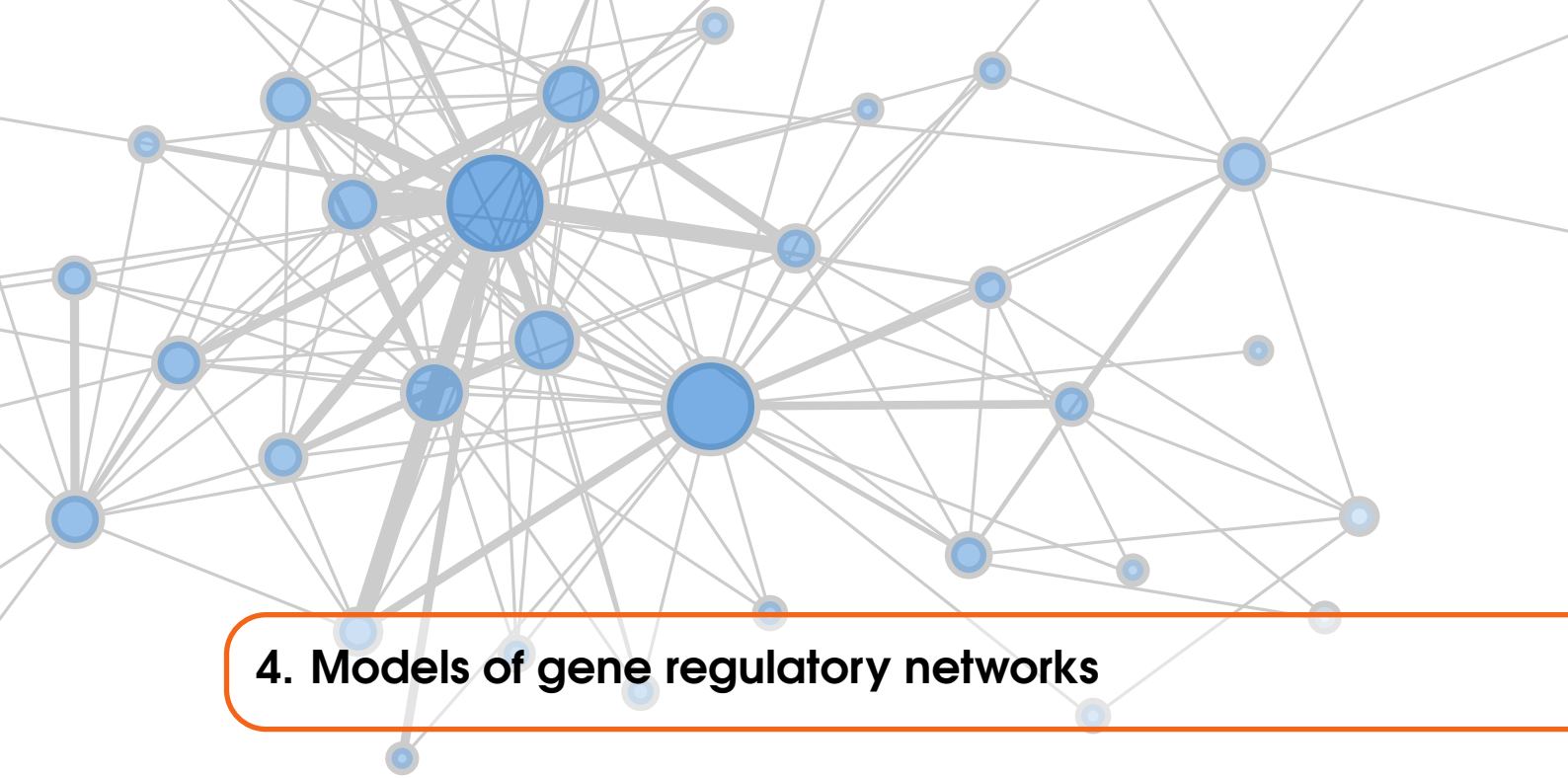

4. Models of gene regulatory networks

It is hard enough to remember my opinions, without also remembering my reasons for them!

Friedrich Nietzsche

4.1 Introduction

Biological phenomena are inherently complex and difficult to study, and the application of mathematical and computational tools are strongly limited to a certain spatio-temporal scale. In contrast, biological systems have the capacity to receive signals from a surprisingly broad spatio-temporal range and process them in a highly reliable manner. The unifying principles, however, seem to be difficult to comprehend and their predictive ability limited to the available computational power.

Living cells are equipped with a robust and yet plastic analog system which equips them with the ability to respond to the environmental inputs. In order to sense and respond to this changing environment, organisms implement networks of interacting elements capable of integrating and processing information in an interdependent manner. Despite the complexity of the underlying networks, some aspects of the cellular behaviour are of apparent Boolean nature, namely, the cellular output represents a switch. A stereotypical example is the case of the cell cycle – there are several checkpoints in which the cell senses the critical variables (e.g. DNA damage) and decides whether to proceed to the next cell cycle phase. The decision of transitioning to a subsequent phase is controlled by a biochemical switch (Santos and Ferrell, 2008). Cell differentiation and apoptosis are other examples of multi-component switches that generate robust (and potentially irreversible) transitions (Siegal-Gaskins, Mejia-Guerra, Smith, and Grotewold, 2011).

An operative definition of a biological network represents the molecules as nodes and their interactions as edges. Ideally, a network representation of a biological system aims to capture its essential characteristics. Within the cell, there are a number of possible interactions between different types of molecules (e.g. protein-protein, protein-DNA, RNA-RNA, protein-metabolite interactions) and the information can flow without direct interactions (transcription from DNA to RNA and translation from RNA to protein). In addition, the interactions between the molecules can

have different strengths. Despite the complexity that these models can entail, biological networks can often be simplified depending on the analysis undertaken. Furthermore, the network description allows the application of graph theory formalities, a well developed field of mathematics (Strogatz, 2001).

While few general formalisms and methods to study the structure and dynamics of cellular signalling and regulatory networks have been proposed (see for example Klamt, Saez-Rodriguez, Lindquist, Simeoni, and Gilles (2006)) structural analysis of networks is a well-established field. Signal transduction research is still in its first stages, and its standards are still being settled (Saez-Rodriguez, Alexopoulos, and Stolovitzky, 2011).

The validity of network modelling arises from the assumption that digital computed steady states correspond to the actual analog steady states of the cellular circuitry. When constructing a dynamical mathematical model, the choice of variable types is one aspect, the second being the character of their dynamics in time. A prominent feature of molecular concentration changes is their often rapid change, when compared with the typical metastable character in between changes.

Computational models for regulatory network analysis fall into three broad categories (Karlebach and Shamir, 2008). In a first class of *continuous models*, explicit molecular concentrations are considered. These kind of models are generally used to understand behaviours that depend on fine time and space scales.

The second main class of models are the *logical models*, generally used to study networks qualitatively to understand their functionality under different conditions. Despite not being able to explain quantitative questions, they became very useful owing to their flexibility and simplicity.

A third class of models study the influence of noise at a single-molecule level, explaining the relationship between stochasticity and gene regulation.

In this chapter we overview some of the main logic-based computational methods in gene regulatory networks. Methods applied in this thesis will be covered in particular detail – random Boolean networks (Section 4.2.1) and weight matrices dynamics (Section 4.2.3).

4.2 Logic-based models

Logic-based network modelling was introduced in 1973 in the papers of Kauffman and Thomas (Glass and Kauffman, 1973; Thomas, 1973), and it represents the simplest modelling methodology. In these models, the state of each element in the network (genes, RNA, and/or proteins) is represented at any time as a discrete value. The update of these values follows a set of rules and takes place in discrete time steps. The simplicity of this methodology allows the study of networks when only qualitative data is available. Extensive reviews can be found in Watterson, Marshall, and Ghazal (2008); Morris, Saez-Rodriguez, Sorger, and Lauffenburger (2010).

4.2.1 Boolean models

Boolean regulatory networks (Glass and Kauffman, 1973) are a particular case of logical models in which the states of the components of the network can only attain two levels (active/inactive, or overexpressed/underexpressed). In a Boolean network, there are N components (nodes) connected by a set of E edges, which represent biological interactions that modulate their expression. The values that each of the N nodes can take at any time are only two, $x_i(t) \in \{0,1\}$. The rules by which these states are updated during the subsequent time steps are defined by a set of N Boolean functions $B_1,...,B_N$. Note that each B_i function has k_i number of inputs, corresponding to the in-degree of the node i, and an output whose value is defined by the combination of the input values (truth table, for an example see Table 4.1). The input values correspond to the values $x_{i1},...,x_{ik_i}$ of the genes connected to that node. Hence, a bit vector $x(t) = (x_i,..,x_N)$ defines the state of the

Table 4.1: *Example of two Boolean functions with three arguments. B_{rnd} is a fully random function, whereas B_{can} is a canalizing function. In the latter the output is canalized on the input x_1: whenever its input value is $x_1 = 1$, the output of the function is always the same (0) regardless of the values of the other inputs. This particular rule it is also said to be nested, since the non-canalising value of x_1 is in turn canalized on the input $x_2 = 1$. This means that if $x_1 = 0$ and $x_2 = 1$, the output is independent of the value of x_3*

x_1	x_2	x_3	$B_{rnd}(x_1,x_2,x_3)$	$B_{can}(x_1,x_2,x_3)$
1	1	1	0	0
1	1	0	1	0
1	0	1	1	0
1	0	0	0	0
0	1	1	1	1
0	1	0	0	1
0	0	1	1	1
0	0	0	1	0

network at a particular time step and the update at $t+1$ of each i-th gene is calculated according to

$$x_i(t+1) = B_i(x_{i1}(t), ..., x_{ik_i}). \tag{4.1}$$

Figure 4.1 depicts a simple network of $N = 3$.

In a Boolean dynamic model, the values of $x(t)$ can be updated synchronously based on the vector at time $t-1$ and according to the Boolean rules. Hence, given an initialised vector at $t = 0$ and the set of truth tables, this type of dynamics are deterministic. The set of rules B will stay the same over time during the simulation, whereas the state vector $x(t)$ will evolve. The finite number of states, 2^N, and the deterministic nature of the synchronous update scheme implies that a state will be inevitably revisited. Alternative asynchronous updating schemes are sometimes used. In those updating schemes, the values of the inputs for the Boolean rules can be current, $x(t)$, or prior, $x(t-1)$. The main asynchronous algorithms are the random order asynchronous (Chaves, Albert, and Sontag, 2005), the general asynchronous (Harvey and Bossomaier, 1997) and the deterministic asynchronous (Chaves, Sontag, and Albert, 2006) update methods. A comparative study on the dynamic behaviour of synchronous and asynchronous updating schemes can be found in Saadatpour, Albert, and Albert (2010).

The complete state space is described by all the potential values of the vector V. The possible trajectories can be represented by a state transition graph in which the nodes represent the states of the system (values of $V(t) = (x_i, .., x_N)$), and the edges represent the allowed transitions among states based on the set of Boolean rules and the updating scheme (see Figure 4.1d). Eventually, the updates of the state vector V will converge into a steady state or a set of recurrent states. These states are known as attractors. Any initial value for the state vector that leads to a particular attractor is part of its basin of attraction. In the toy example shown in Figure 4.1, there are two basins of attraction in the state space. Coincidentally, these basins of attraction are made up with the same states than their corresponding attractors. This is not always the case, and often the states that make up a basin of attraction include other states aside from the attractor itself. In the asynchronous models, each state in the transition graph can have several successors, and hence the basins of attraction for different attractors may overlap. This is never the case for synchronous deterministic update schemes, where each node in the transition graph has one and only one successor.

An important measure in Boolean networks quantifies how distant two states are in the state space. Between any two states x^A and x^B, the normalised number of genes whose values differ between them is known as Hamming distance. It is defined as

$$h(x^A, x^B) = \frac{1}{N} \sum_{i=1}^{N} (x_i^A - x_i^B)^2. \tag{4.2}$$

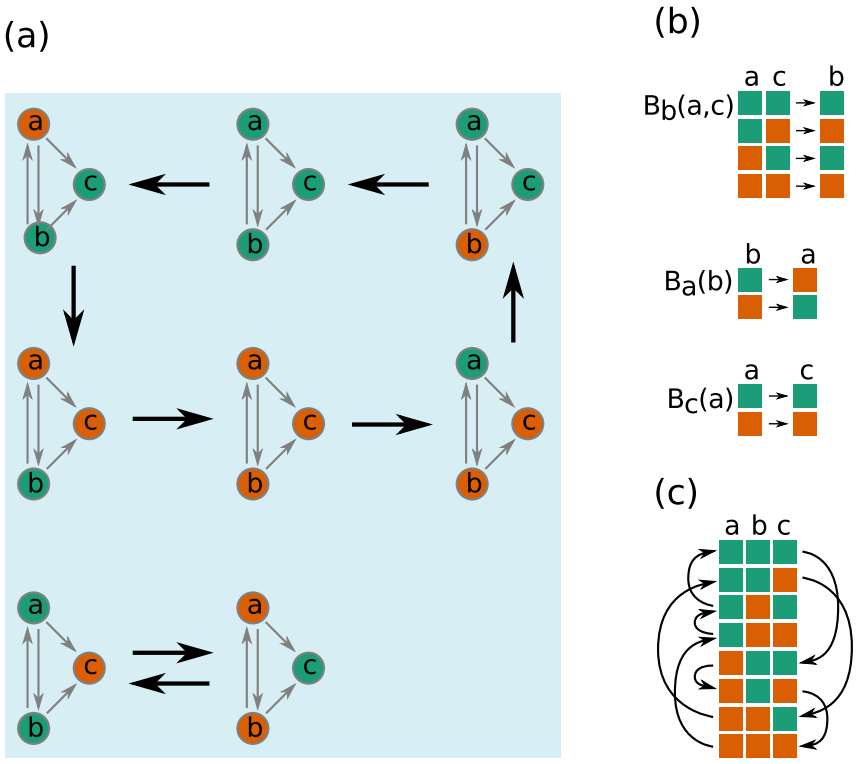

Figure 4.1: *Boolean network of $N = 3$.* ***(a)*** *The transitions between the 8 possible states are represented. The Boolean values for the nodes correspond to the two different colours (green and orange). Gray arrows represent biological interactions that influence protein expression, black arrows represent transitions from a time step to the next.* ***(b)*** *The set of Boolean rules B are fully described. The rules determine the values that each of the nodes will have in the following time step.* ***(c)*** *A complete representation of the state space is depicted, including all the transitions as shown in a. The state space is characterised by two attractors, which in this minimal example overlap entirely with their respective basins of attraction.* Based on Karlebach and Shamir (2008)

Whereas the choice of the set of Boolean functions B can be guided by experimental evidence, often the available data does not suffice to model the truth tables. A methodology used to overcome this limitation is known as random Boolean networks (RBNs) (Kauffman, 1969b). The Boolean function $B_i(x_{i1}, \ldots, X_{ik})$ of k_i inputs is randomly chosen from the collection of all possible Boolean functions (Kauffman, 1993). RBN models often include a bias p for the fraction of output values

that are 1, $p = P(B_i = 1)$, in the Boolean functions. To generate these functions suffices to flip a p-biased coin 2_i^k times. Additionally, in the original formulation networks were constructed with a constant in-degree $k_i = \overline{k}$ for each node. Many other alternatives have been studied, mostly consisting in random sampling from various distributions with a $\overline{k}$ mean. Notice that the bias p does not, however, preclude *per se* any local structure in the function (for broad overviews of RBNs, see Drossel, 2008; Kauffman, 1993).

Phase transitions in Boolean models

A fundamental work in RBN modelling was performed by Derrida and Stauffer (1986), who introduced the concept of *phase transition* for Boolean networks based on the Hamming distance evolution. They studied the time evolution of the state vector x in the limit $N \to \infty$ with different initial conditions, $x^A(t=0)$ $x^B(t=0)$, comparing their Hamming distance with the Hamming distance between $x^A(t \to \infty)$ and $x^B(t \to \infty)$ (we denote with H an averaged h, Equation 4.2, over a large number of initial conditions for $x^A(t=0)$ and $x^B(t=0)$). They noted the existence of two possible phases for different values of the average in-degree $\overline{k}$. The first corresponding to $\overline{k} \leq 2$, with $H(t \to \infty) = 0$ (ordered regime), and the second corresponding to $\overline{k} > 2$, with $H(t \to \infty) \neq 0$ (chaotic regime).

The initial states $x^A(t=0)$ $x^B(t=0)$ can be thought as the result of a final $H(t \to \infty) = 0$ (ordered regime) or, on the contrary, propagate across the network (chaotic regime).

The results of the temporal evolution of the Hamming distance studied in the seminal work of Derrida and Stauffer correspond to a mean-field theory approach, and hence do not necessarily hold for real biological networks, that are far from being statistically equivalent (Aldana, 2003). However, a work by Balleza, Alvarez-Buylla, Chaos, Kauffman, Shmulevich, and Aldana published in 2008 demonstrated that the phase transitions observed under the mean-field theory are equivalent those observed in networks of realistic topologies constructed with the same statistical properties than real biological networks.

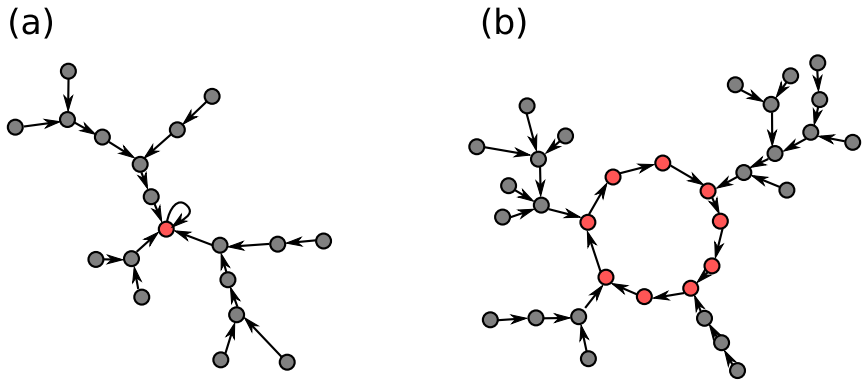

Figure 4.2: *Types of attractors in random Boolean models. Each node corresponds to a particular state of the system. Two basins of attraction are represented in the figure,* ***(a)*** *is a fixed point attractor, which corresponds to a cycle of period 1, and* ***(b)*** *is a cycle attractor of period 10. Arrows show the direction of the dynamics as in Figure 4.1d.* Adapted from Aldana *et al.* (2003)

Derrida plots

In order to visually represent the average effect of perturbations in a particular network, we can plot $H(0)$ (size of the perturbation at the beginning of the parallel runs, x-axis) against $H(\tau)$ (y-axis), where τ is a small number of discrete steps. Plotting different values of $H(0)$ (sampling different perturbation sizes) results in a Derrida plot, a popular tool used in RBNs (Derrida and Weisbuch, 1986). While some network architectures tend to absorb small perturbations and the final Hamming distances $H(\tau)$ are on average smaller than the initial perturbation, some topologies tend to amplify them – few genes with different values of expression lead to dramatically different network states. Crucially, in the Derrida plots these different behaviours fall in the opposite halves of the plot, with robust architectures represented by curves underneath the diagonal, $H(0) > H(\tau)$, and sensitive architectures above, $H(0) < H(\tau)$ (Fox and Hill, 2001), and a network whose Derrida mapping appears tangent to the diagonal is said to exhibit criticality. Note that choosing small integer values for τ (shorter dynamics) captures the effects of the network's local geometry, while larger values reflect the general characteristics of the structure of the network, since information has more time to spread across the network (Aldana *et al.*, 2003). In practice, the slope for the small $H(0)$ region reveals the average outcome of a small perturbation. Curves below the diagonal indicate a tendency towards stability (ordered regime) whereas curves above imply instability (chaotic regime). The diagonal $H(0) = H(\tau)$ represents the transition from order to chaos (see Figure 4.3).

To construct the Derrida plots, a large number of Boolean rules are constructed (for a given network topology) and for each set of randomly generated rules a large number of parallel simulations are run with random initial values, uniformly sampling different values of $H(0)$.

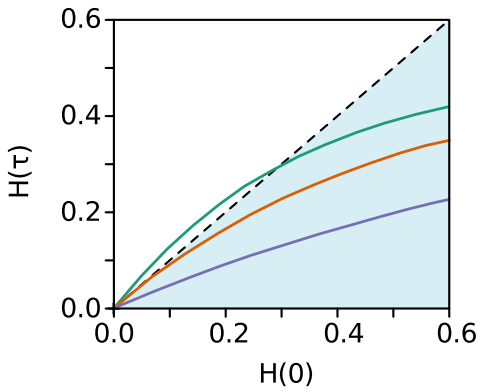

Figure 4.3: *Derrida plots of random Boolean networks with a Poisson distribution of in-degree. The different curves correspond to the plot of $H(0)$ vs $H(\tau)$ for networks which operate in different dynamic phases. Ordered, critical, and chaotic regimes are represented by blue, orange, and green colours respectively. The shaded area under the diagonal corresponds to the ordered regime. Networks exhibiting criticality appear as tangent to the diagonal, which represents the transition between the chaotic and ordered phases.* Adapted from Balleza *et al.* (2008)

Network sensitivity

The tangent to the Derrida mapping at $H(t) = 0$ represents the average sensitivity S of a Boolean network. The sensitivity S of a RBN is heavily dependent both on the bias p (Derrida and Pomeau,

1986) as well as on the average in-degree of the network $\overline{k}$ (Luque and Solé, 1997; Aldana and Cluzel, 2003). In the original formulation (Kauffman, 1969b) the phase transition is governed by

$$\overline{k}_c = \frac{1}{2p(1-p)}, \tag{4.3}$$

where $\overline{k}_c$ is the critical average in-degree.

If the bias is set to $p = 0.5$, the critical in-degree is $\overline{k}_c = 2$, with larger values corresponding to chaotic behaviour (higher sensitivity) and smaller values leading to ordered behaviour (lower sensitivity). Likewise, heavily biased Boolean functions (values of p away from 0.5) lead to ordered dynamics. These characteristics are observed in cases where the in-degree is randomly chosen from a Poissonian or from a power-law distribution (Barabási and Albert, 1999; Aldana and Cluzel, 2003; Aldana-Gonzalez, Coppersmith, and Kadanoff, 2002).

Robustness and adaptability in the critical regime

Networks with dynamic stability are by definition more robust to small perturbations. When a Derrida mapping falls under the diagonal, perturbations tend to die out with time instead of propagating through the system. It is expected from complex biological networks a certain level of stability against environmental perturbations. Some classically studied mechanisms such as gene redundancy and epistasis (Sanjuán, Moya, and Elena, 2004; Moore, 2005) suggest that the dynamical properties of biological networks are restricted to small sets of genes. However, other studies point in the direction of a "distributed robustness" scenario. All the regulatory interactions among genes play a role in the dynamical characterisation of the network (Shmulevich, Kauffman, and Aldana, 2005; Wagner, 2005).

More specifically, it has been pointed out by Kauffman and others that biological systems may lay in a dynamical region close to the border between order and chaos, often referred to as the "critical" zone (Langton *et al.*, 1992; Graudenzi, Serra, Villani, Damiani, Colacci, and Kauffman, 2011). Some studies, in fact, suggest that the optimal trade-off between robustness and readiness to change under certain conditions (evolvability) is found in the critical zone of the space of parameters (e.g. Kauffman, 1995; Shmulevich *et al.*, 2005). In addition, the information flow though the networks that are in a critical regime is optimal (Ribeiro, Kauffman, Lloyd-Price, Samuelsson, and Socolar, 2008). The capacity of complex dynamical systems to respond without reaching saturation to broad dynamic ranges of external stimuli requires a collective integration of the incoming information. This emergent property is maximised in the critical regime (Kinouchi and Copelli, 2006) and is the consequence of long-range correlations that arise in the critical point (Balleza *et al.*, 2008). This kind of responses show a remarkable sensitivity.

In addition to what we pointed out earlier in reference to the "distributed" nature of robustness across a large number of genes interacting within a network, it is likely that robustness is manifested at different levels, likewise, in a distributed fashion – from the physicochemical structural properties of macromolecules to the higher levels of multicellular organization and ecosystems.

While some biological systems are designed to elicit a graded response to an input, other systems show behaviours that resemble multistable transitions. These systems can range from relatively simple switch-like responses to more complex multistable switches (e.g. Ferrell and Machleder, 1998; Pomerening, Sontag, and Ferrell, 2003; Yao, Tan, West, Nevins, and You, 2011). The complex environmental signals integrated by the living systems generate responses at the different levels of their biological organisation, with these responses being interdependent. The interpretation of any result obtained requires, thus, a critical scrutiny.

Relevance of Boolean modelling to biological problems

During LTP, the cell state needs to transit from a stable point to another stable point. If this assumption holds for the gene expression profile, LTP induction can be seen as the perturbation

needed to push the gene expression equilibrium of the neuron to the post-LTP attractor. The discrimination of this perturbation from the environmental noise is of a fundamental importance and represents the global objective of the present thesis. In this regard, gene regulatory network analysis can help to better understanding the mechanisms of gene expression underlying LTP maintenance and consolidation, as well as generating experimentally testable hypotheses regarding (a) intermediate phases and (b) effects of gene knock-outs and mutations.

The relevance of network analysis and particularly the Boolean modelling approach, has been put forward by a number of studies that show that the Boolean approach captures the main dynamical features of gene regulatory networks (see for example Bornholdt, 2005; Espinosa-Soto, Padilla-Longoria, and Alvarez-Buylla, 2004; Davidich and Bornholdt, 2008; Serra, Villani, Barbieri, Kauffman, and Colacci, 2010; Rämö, Kesseli, and Yli-Harja, 2006; Christensen, Oliveira, and Nielsen, 2009; Thakar, Pilione, Kirimanjeswara, Harvill, and Albert, 2007; Saez-Rodriguez, Simeoni, Lindquist, Hemenway, Bommhardt, Arndt, Haus, Weismantel, Gilles, Klamt, *et al.*, 2007). At the same time, the inherent simplicity of the models allows to analyse complex behaviours in large-scale systems that would be otherwise inconceivable to tackle with the incomplete qualitative data available.

4.2.2 Other logic-based models

Probabilistic Boolean networks

Experimental data is very often insufficient to fully describe the regulatory functions of a biological network. An approach proposed by Shmulevich, Dougherty, Kim, and Zhang (2002) consists in allowing each node of the network to have a number of regulatory functions. Each function will have a probability based on the available experimental data. Among the possible functions, one is chosen randomly at each step according to its probability.

Petri nets

Petri nets (Petri, 1966) represent another type of stochastic model in which the nodes can be "places" (biological species) or "transitions" (regulation functions). The places have discrete values, which represent the number of "tokens". In Petri nets, the input places are connected to transitions, and these are in turn connected to output places. At any time step, every transition can be fired if their input places have enough "tokens" (a fired transition will reduce the number of tokens in each of its input places and increase the number of tokens in each of its output places).

Multi-logic models

The MetaReg model developed by Gat-Viks, Tanay, and Shamir (2004) is a logic-based model with the entities of the network not being restricted to Boolean values. Regulation functions are also discrete. A probabilistic version also exists (Gat-Viks, Tanay, Raijman, and Shamir, 2006) and it has been implemented in the MetaReg software (Ulitsky, Gat-Viks, and Shamir, 2008). By predicting the steady states after constructing the biological model, the methodology allows to predict component values under any experimental treatment. If there are discrepancies between the predictions and the experimental results, these can be used to automatically refine the model.

Another multi-valued logic model was proposed by Huang and Hahn (2009) and applied to infer networks based on experimental data (Morris, Saez-Rodriguez, Clarke, Sorger, and Lauffenburger, 2011).

4.2.3 Continuous and single-molecule models

In contrast to the models described so far, the class of continuous models do not discretise the expression values. While from a theoretical standpoint real-valued models are more accurate at representing experimental data, it has been pointed out that they exhibit similar dynamical properties under very general conditions (Chaves *et al.*, 2006). We will briefly review the different continuous

models with particular depth in the case of the weight matrices methodology, which is applied to characterise the dynamical properties of an LTP-related network in Chapter 7.

Linear models: weight matrices dynamics

An advantage of linear models is that they can be used to gain understanding of a qualitative nature without requiring extensive knowledge on the regulatory mechanisms. In this class of models, each regulatory function corresponds to a weighted linear sum of the inputs for each of the network units.

The simple model proposed by Weaver and coworkers (Weaver, Workman, and Stormo, 1999) (also referred to as *TReMM*, Transcription Regulation Modelled with Matrices) represents a compromise between the simplifying assumptions about biological systems of the Boolean networks, and the detailed models described by ordinary differential equations. The number of samples required to successfully model with continuous data are so large that continuous time models could only be based on theoretical data.

The gene expression state of a network is represented by a vector $u(t)$, where u_i corresponds to the expression level of the i-th gene. The regulatory interactions between genes are modelled with a weight matrix, W so that the effect of gene j on gene i is the expression level of j, $u(t)$ times its regulatory influence on i, $w_{i,j}$. This regulatory influence can be either activating ($w_{i,j} > 0$), or repressing ($w_{i,j} < 0$). The values of $w_{i,j} = 0$ correspond to the lack of experimental evidence for the effect of gene j on gene i. Put differently, only the nodes connected in Figure 7.2 have non-zero values of w.

The total regulatory input to i, $r_i(t)$, is calculated by adding all the genes which interact with it:

$$r_i(t) = \sum_j w_{i,j} u_j(t). \tag{4.4}$$

The expression $u_i(t+1)$ of a gene i to the regulatory input $r_i(t)$ is "squashed" with a sigmoidal function,

$$u_i(t+1) = \frac{m_i}{1 + e^{-(\alpha_i r_i(t) + \beta_i)}}, \tag{4.5}$$

where m_i corresponds to the maximal observed expression level for the gene i, and the parameters α_i, β_i, and $w_{i,j}$ correspond to the i-th gene's intrinsic response to the regulatory inputs (or slope of the sigmoidal response function), the gene's basal expression level, and the relative weights of the interactions respectively.

The expression levels of all N genes $u_i(t)$ are updated simultaneously on each iteration. The simulations converge to a stable state of unchanging gene expression or cyclical set of gene expression states (see Figure 4.4). Such a steady state may depend on the initial conditions $u(t=0)$, according to the gene expression landscape for the network studied.

For a given network the parameter space for α, β, and W is evenly explored by a sufficiently large number of random trials. This procedure characterises the network and results in an average frequency of bistable outputs (P_B, see section 7.2.3) which should be free of the bias introduced by the choice of an arbitrary set of parameters.

The *TReMM* methodology has the advantage of representing gene regulation with a considerable degree of complexity while still being computationally tractable for the networks' sizes studied. In this modelling methodology, the expression levels are updated simultaneously. The state of the cell at a certain time is represented by a vector $u_i(t)$ which contains the absolute values of every gene i in the system.

The regulatory interactions between the genes are modelled with a weight. This regulatory input is then squashed with a sigmoidal function in order to model the response between maximal

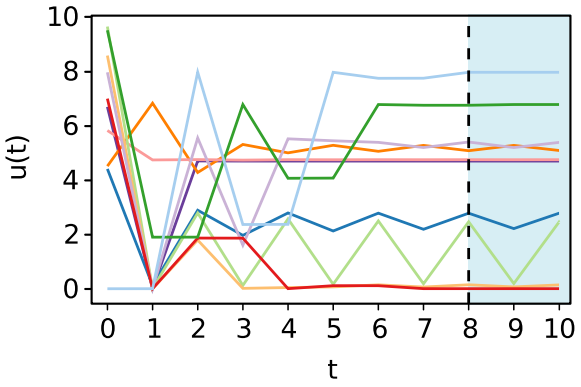

Figure 4.4: *Dynamics using weight matrices of a set of 11 genes from an LTP gene regulatory network reaching an oscillatory steady state at $t = 8$. The vertical axis represents the level of gene expression $u(t)$, the horizontal axis represents time*

repression / maximal expression,

$$x_i(t+1) = \frac{1}{1+e^{-(\alpha_i r_i(t)+\beta_i)}}, \tag{4.6}$$

where α_i and β_i are parameters to adjust the dose-response function. The positive parameter α_i makes the response curve more steeply sloped as it approaches infinity, while β_i corresponds to the curve's y-intercept, where the positive and negative regulatory inputs are equal (gene's basal level of expression).

Multiplying the normalised response x_i by the maximum of the expression for a given gene, we can compute the absolute expression value

$$u_i(t+1) = \frac{m_i}{1+e^{-\left(\alpha_i \sum w_{i,j} u_j(t)+\beta_i\right)}}, \tag{4.7}$$

where m_i is the maximal expression of the gene i, and corresponds to the maximal expression observed in any of the arrays for that given gene.

By computing the dynamics using any values to initialise $u_i(t=0)$, the system eventually reaches a steady state, namely, a state where the expressions of the genes do not change over time. The steady state can correspond to a fixed point or to limit cycle although in some cases, the dynamics could lead to chaotic behaviours.

While this approach has been used to predict the genetic pathways underlying observed expression data (Weaver *et al.*, 1999; Morris *et al.*, 2011; Saez-Rodriguez, Alexopoulos, Epperlein, Samaga, Lauffenburger, Klamt, and Sorger, 2009), it has not been proven to be valid to interpolate or extrapolate expression data points. In fact, despite the common assumption that the trajectories *in silico* would lead to a steady state with a corresponding real cellular steady state, it does not necessarily imply that the modelled trajectories exactly mimic the ones actually underlying the cellular processes.

4.2.4 Other continuous models

Other models that allow for a finer detail than linear models have been proposed. In the model of Nachman, Regev, and Friedman (2004), genes are determined by real-valued, non-linear regulation

functions that take the Michaelis-Menten form, together with mRNA decay rates. A number of similar approaches have been proposed (see for example Segal, Raveh-Sadka, Schroeder, Unnerstall, and Gaul, 2008).

Michaelis-Menten functions are used in another main class of continuous models which describe gene regulation based on ordinary differential equations. The changes in the values of the components of the network are described based on the levels of the other interacting units instantaneously. Analytical solutions other than Michaelis-Menten have been used, but larger networks usually require a numerical approach. An overview of this methodology is out of the scope of this thesis, a good review can be found in Klipp, Herwig, Kowald, Wierling, and Lehrach (2008).

Even more refined methods exist for the description of biological networks, which aim to integrate regulation and metabolism. These are generally grouped in the flux balance analysis (Palsson, 2006; Kauffman, Prakash, and Edwards, 2003).

Finally, another class of methods operate at the single-molecule level. These methods are useful when the number of molecules is small, and they incorporate the stochastic nature of regulation in the model. A review can be found in Gillespie (2007).

4.3 LTP in the context of functional genomics

A fundamental feature of most biological systems is that they exhibit non-linear behaviours and hence they are inherently difficult to analyse. However, an increasingly large amount of data available from genome sequencing projects and other -omic technologies allow for systematic analyses of gene expression. Both explanatory and predictive methods of gene regulatory networks have been proposed with success (Hasty, McMillen, Isaacs, Collins, *et al.*, 2001). However, these efforts have generally aimed at describing simple systems which can be closely linked with experiments (for a brief review see Hasty *et al.*, 2001).

Regulatory networks are quantified by the concentrations of the constitutive gene products. The system will be in a *fixed point* if small perturbations to this steady state are followed by an exponential return to the equilibrium. Ideally, a long-lasting response of a cell to a given input, requires the transcriptional machinery to transit from one steady state to another. The existence of more than one stable fixed point raises the possibility of a switch-like behaviour. In order to drive the cell from one state to another, a sufficiently large perturbation is needed.

LTP relies on gene transcription for its long-term persistence, and this stage is thought to be necessary for the acquisition of long-term memory (Nguyen *et al.*, 1994; Abraham and Williams, 2003, 2008; Alberini, 2009). The gene regulatory network is driven from a pre-LTP state to a post-LTP state by signalling cascades following the calcium influx. This transition is believed to involve post-translational modifications, local protein synthesis, translational regulation, transcription and epigenetic changes. In addition, the LTP decay has been suggested to be a consequence of activity-dependent mechanisms (Villarreal, Do, Haddad, and Derrick, 2002), which supports a driven multistable system view. There are indeed a number of other studies that point towards the possibility that the plasticity in the hippocampus in living animals may not be very persistent (Abraham and Williams, 2003), and that long-term memories are gradually reorganised so that its storage becomes independent of the hippocampal region and distributed instead in the cortex (Squire and Alvarez, 1995; McClelland, McNaughton, and O'Reilly, 1995).

4.4 Justification for the choice of models

A number of studies suggest that the architecture of biological networks may be playing a fundamental role in the stability of cellular states (Albert, Jeong, and Barabási, 2000; Jeong, Mason,

Barabási, and Oltvai, 2001; Milo, Shen-Orr, Itzkovitz, Kashtan, Chklovskii, and Alon, 2002) and hence be under evolutionary pressures (Li, Long, Lu, Ouyang, and Tang, 2004).

To characterize the topological properties of the networks involved in LTP (see Section 5.5) we have chosen logic-based models – dynamics with weight matrices (results in Chapter 7) and random Boolean networks (results outlined in Chapter 8). The choice of these models was guided by (1) the lack of any information on the rules for the interactions, which made unnecessary the use of complex continuous models, and (2) the relatively small sampling space of logic-based discrete models. Note that while discrete logic-based models for gene regulation may oversimplify the complexity underlying biological interactions, they do show remarkably rich dynamical behaviours and have a demonstrated biological significance (see e.g. Huang and Ingber, 2000; Huang, 2001; Albert and Othmer, 2003; Shmulevich *et al.*, 2005; Serra, Villani, Graudenzi, and Kauffman, 2006). The attractors postulated to represent different cell states represent in this particular study the accessible pre- and post-LTP cell states in terms of gene expression.

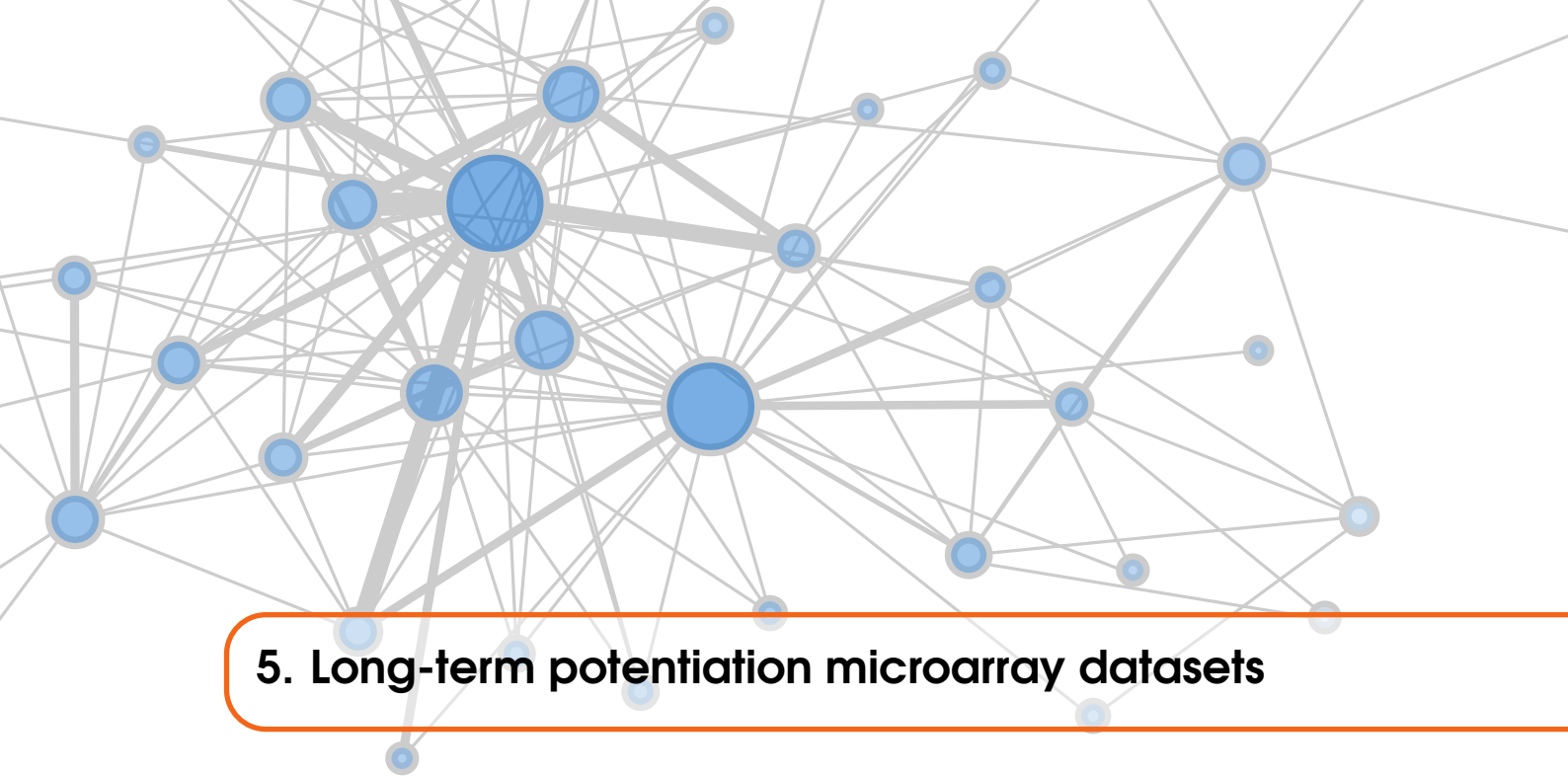

5. Long-term potentiation microarray datasets

She said the root of man's problems is memory. Without a past every day would be a new beginning

Ashes of time, Wong Kar-wai

5.1 Introduction

The microarray datasets used throughout this thesis were kindly provided as CEL files by the group of Joanna Williams at the Department of Anatomy of the University of Otago. The dataset consists of 30 Affymetrix GeneChip Rat 230.2 (TM) used and described in a series of two papers published in 2011 and 2012 (Ryan *et al.*, 2011, 2012). We describe in this Chapter the replication of the results published in the aforementioned papers. Whereas the results presented in this chapter do not represent novel unpublished data, the aim is twofold – first, the datasets serve as a case study to describe the initial high-level analysis of microarray datasets and in addition, they represent the starting point to further explore the data using co-expression analysis (see Chapter 6) and compare the results. Additionally, the gene regulatory networks used in Chapters 7 and 8 are introduced here (see Section 5.5). Hence, the present chapter should be considered as a methodological introduction for the following chapters.

5.2 Microarray experiments

The experimental procedure to obtain the microarray image data is described in the original papers. For the scope of this thesis, the replication of the microarray analysis was only carried out using the CEL files as a starting point. The resulting normalised data was used in Chapter 6 to conduct the co-expression analysis.

We normalised the microarray data using the robust multi-array average (RMA) algorithm, implemented in the *affy* package of *Bioconductor*, a free, open source and open development software project for the analysis of genomic data (Irizarry *et al.*, 2003). *Bioconductor* is based on the R programming language (R Core Team, 2013), also free and open source.

The RMA normalisation consists of three steps:

1. Background correction by convolution
   Separates probe-level signal from background signal (optical noise and non-specific binding). The probe-level model is fitted using PM intensity values only

2. Quantile normalisation
   Forces all arrays to have the same quantiles

3. Summarisation by median polish
   A robust measure of "centre", using probe-level background-corrected and quantile-normalized intensities

Figure 5.1 shows the probe-level intensities before and after the normalisation by the RMA method. The output is a matrix of expression levels. Expression data from the arrays is represented as a data matrix with rows corresponding to probes and columns to arrays.

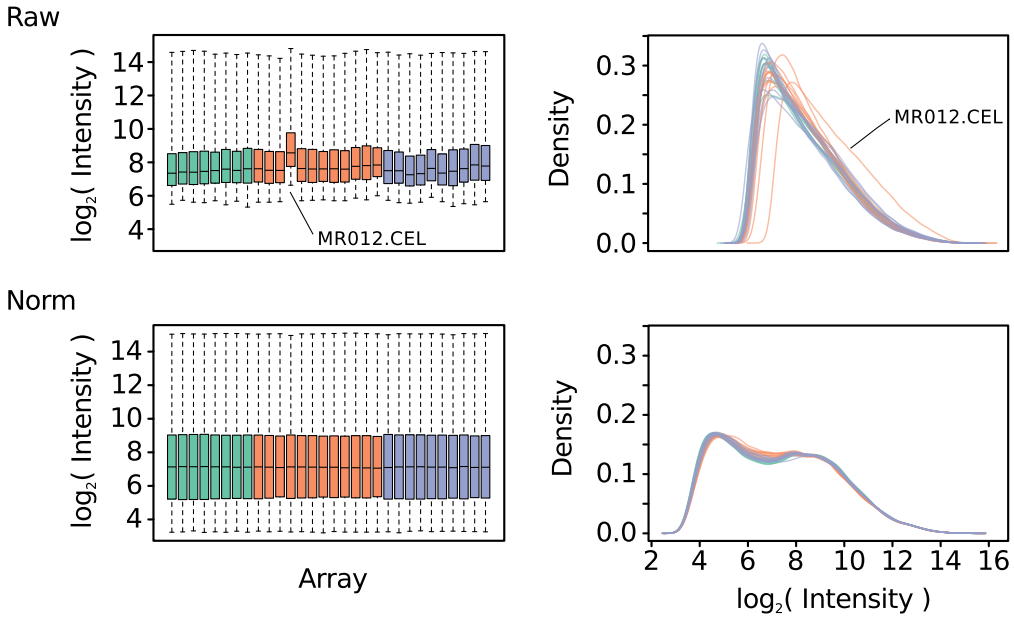

Figure 5.1: *Top-left panel shows the box plot of PM values of the raw data for each of the 30 arrays. In the top-right panel represents the density of the PM probe intensities. In the bottom panels, the same representations after RMA normalisations are represented*

5.3 Experimental design

The data consists of 30 arrays hybridised with the stimulated (S) and unstimulated (U) hemispheres of 15 rats. The animals were euthanised at different times following LTP induction (20 min, 5 h, and 24 h). These three different groups consisted of $N = 4$, $N = 6$, $N = 5$ respectively. For details see Ryan *et al.* (2011) and Ryan *et al.* (2012). The factorial design matrix is represented

Table 5.1: *List of the time course microarrays.*

Array	Time	LTP	Array	Time	LTP	Array	Time	LTP
1	20 min	S	9	5 h	S	21	24 h	S
2	20 min	U	10	5 h	U	22	24 h	U
3	20 min	S	11	5 h	S	23	24 h	S
4	20 min	U	12	5 h	U	24	24 h	U
5	20 min	S	13	5 h	S	25	24 h	S
6	20 min	U	14	5 h	U	26	24 h	U
7	20 min	S	15	5 h	S	27	24 h	S
8	20 min	U	16	5 h	U	28	24 h	U
			17	5 h	S	29	24 h	S
			18	5 h	U	30	24 h	U
			19	5 h	S			
			20	5 h	U			

in Table 5.1. The questions that can be addressed with a differential expression analysis are 1) which genes respond to LTP induction, and 2) which of those genes respond at the different times following LTP-induction. We fitted a linear model with a coefficient for each of the six factor combinations:

1. 20 min – S *vs* 20 min – U
2. 5 h – S *vs* 5 h – U
3. 24 h –S *vs* 24 h – U

For additional methodological details, see Methods section in Ryan *et al.* (2011).

5.4 Differential gene expression

A quick visual identification of genes that are significantly dysregulated can be accomplished by plotting the log-fold changes versus log-odds of differential expression (volcano plots). These plots combine a measure of statistical significance with the magnitude of the change. The volcano plots for the three time points are shown in Figure 5.2, where the outliers are also labelled.

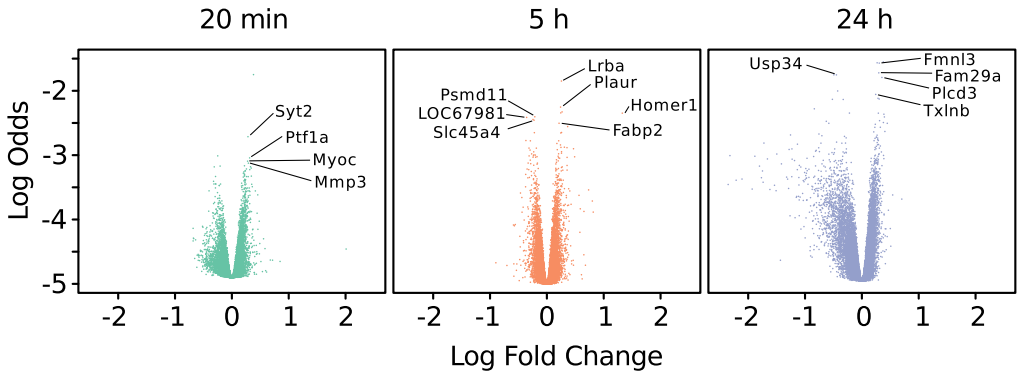

Figure 5.2: *The volcano plots in the figure represent the log-fold changes versus log-odds of differential expression for each of the time points*

Table 5.2: *Lists of differentially expressed genes with known transcripts for each of the times post-LTP induction. The genes with* $-0.15 > ln(FC) > 0.15$ *are ranked according to their p-value. Only the top 20 genes of each time point are shown. A more comprehensive list can be consulted in the Appendix A.1. Genes in red cells were significantly over expressed in the LTP-induced hemisphere, genes in green cells were significantly under expressed. FC: Fold Change*

20 min			**5 h**			**24 h**		
Gene	*ln*(FC)	p-value	Gene	*ln*(FC)	p-value	Gene	*ln*(FC)	p-value
Syt2	0.283	1.50E-03	Plaur	0.241	1.40E-03	Fmnl3	0.306	1.51E-04
Ptf1a	0.312	3.74E-03	Homer1	0.133	1.73E-03	Fam29a	0.298	2.24E-04
Myoc	0.277	4.30E-03	Psmd11	–0.212	1.96E-03	Usp34	–0.448	2.43E-04
Mmp3	0.290	4.67E-03	Slc45a4	–0.226	2.20E-03	Plcd3	0.353	2.70E-04
Fzd5	0.236	6.41E-03	Fabp2	0.214	2.44E-03	Txlnb	0.243	5.28E-04
Slc21a4	0.210	6.76E-03	Tgif2	0.366	2.73E-03	Rnf152	–0.519	6.41E-04
Eftud2	0.202	7.13E-03	Rhod	0.258	3.33E-03	Gfod2	0.387	1.14E-03
Pgap2	0.222	7.44E-03	Slc2a9	–0.220	3.36E-03	Kank3	0.311	1.46E-03
Prodh2	0.343	8.05E-03	Ldb3	–0.369	4.38E-03	Igsf1	–0.626	1.49E-03
Itih4	–0.287	8.18E-03	Rcsd1	0.208	4.41E-03	Chtf18	0.379	1.57E-03
Trim14	0.287	8.23E-03	Fbxl6	–0.291	4.42E-03	Igfbp5	–0.581	1.61E-03
Cmah	0.226	9.35E-03	Lingo1	0.354	5.56E-03	Mylpf	0.447	1.61E-03
Memo1	0.212	9.82E-03	Gmip	–0.296	6.02E-03	Grpr	0.324	1.87E-03
Tap1	0.249	1.12E-02	Adora2b	0.258	6.37E-03	Rab22a	0.209	2.23E-03
Sema6c	–0.281	1.12E-02	Gstcd	–0.231	6.39E-03	Enpp2	–0.126	2.50E-03
Onecut1	0.226	1.13E-02	Pttg1ip	0.257	6.68E-03	Mcm10	0.268	2.52E-03
Arid5a	0.233	1.16E-02	Dennd1c	–0.268	6.84E-03	Abca4	–0.703	2.58E-03
Fut4	–0.220	1.19E-02	Anapc1	–0.228	7.06E-03	Llgl2	–0.306	2.64E-03
Cyp3a2	0.170	1.21E-02	Osbpl9	–0.203	7.12E-03	Atxn7l4	0.279	2.99E-03
Tet3	0.359	1.25E-02	Tut1	–0.237	7.29E-03	Kdm6a	0.290	3.08E-03

The list of the top 20 differentially expressed genes for each of the groups (20 min, 5 h, 24 h after induction of LTP) are shown in Table 5.2. The cut-off for fold change (FC) was set to $-0.15 > ln(\text{FC}) > 0.15$, which corresponds to a ratio of expression of around $1 : 1.16$ between stimulated and unstimulated tissues. The genes are ranked according to their p-values. Note that only the genes with a known transcript are shown. As there are multiple probesets to a given transcript and some transcripts are only predicted, we include a more comprehensive table with all top 50 probesets per group in Appendix A.1. The number of differentially expressed genes at different times with respect to their unstimulated controls are represented in the Venn diagram of Figure 5.3.

The normalisation procedures carried out and outlined in the present chapter are necessary to the co-expression analysis performed in the following chapter. The results obtained in the differential expression analysis, on the other hand, are largely identical to the originally reported in Ryan *et al.* (2011, 2012). Minor differences are to be expected since the databases of transcript-gene mappings have been updated since the original work was published. Results are summarised in Figure 5.3 and Table 5.2.

5.5 Gene regulatory networks

The networks used in Chapter 7 and 8 were obtained from Ryan *et al.* (2011) and Ryan *et al.* (2012). They were originally identified by using the lists of differentially expressed genes as an input to *Ingenuity pathway analysis* (IPA; Ingenuity Systems, USA; `www.ingenuity.com`).

Based on the original input list of genes, the application generates a set of networks that can contain genes from the original list in addition to other genes which have a significant number of interacting partners from the list. Each network contains up to 35 genes and has an associated score which indicates the expected likelihood of not being generated by chance. The main advantage of IPA with respect to other tools of similar characteristics is the proprietary IPA knowledge base

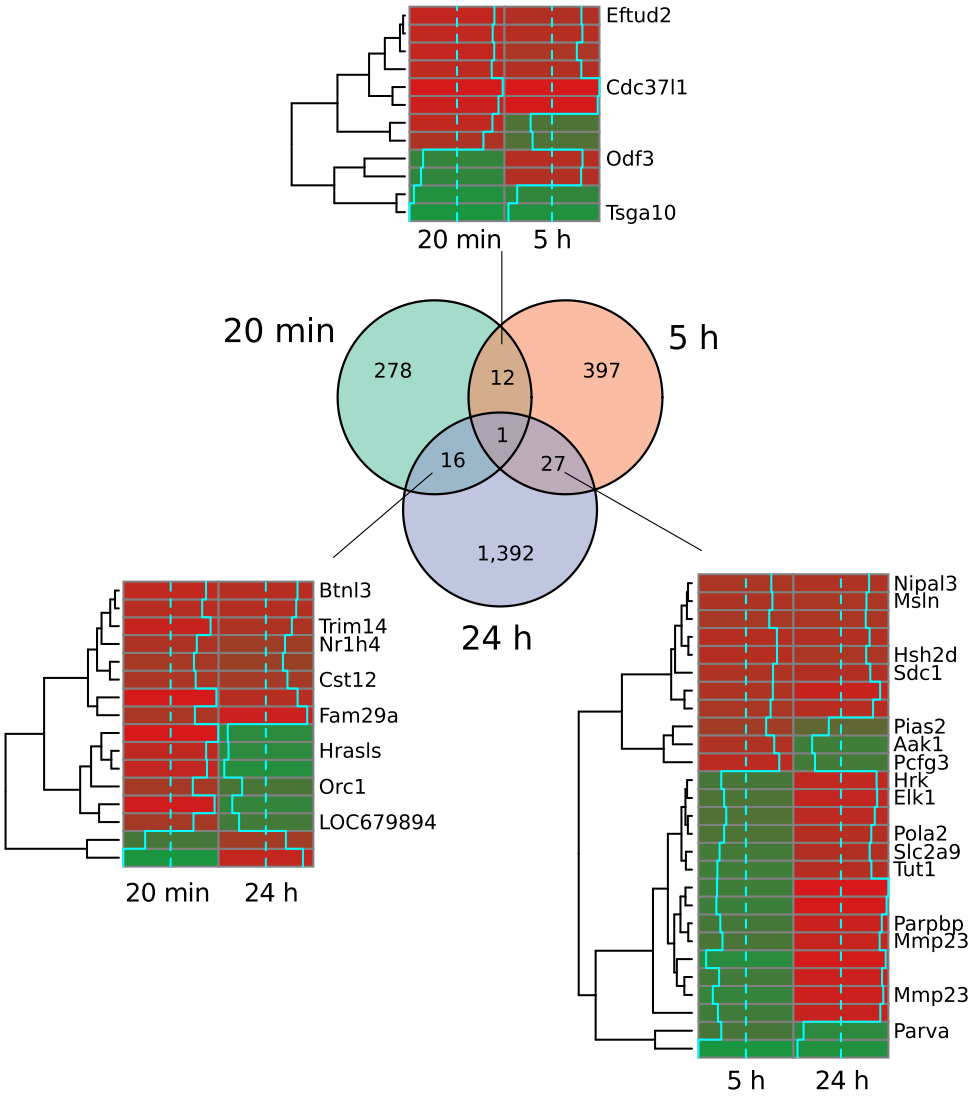

Figure 5.3: *The Venn diagram in the centre of the figure shows the number of differentially expressed genes ($p < 0.05$) at the different times post-LTP. The fraction of the genes found to be differentially expressed for more than one time points are depicted in the heatmaps. Green represents under-expression and red represents over-expression. Only one probeset shows a differential expression on every time point (1376179_at). In order to visualise all the differential expression information overlap between time points, for this figure no cut-off on fold change was used*

(IPKB), queried for the network constructions. The IPKB is a manually curated interaction database of cellular proteins sourced from literature references.

A broader discussion of these networks can be found in the original publications (Ryan *et al.*, 2011, 2012). The networks are depicted in Figure 5.4.

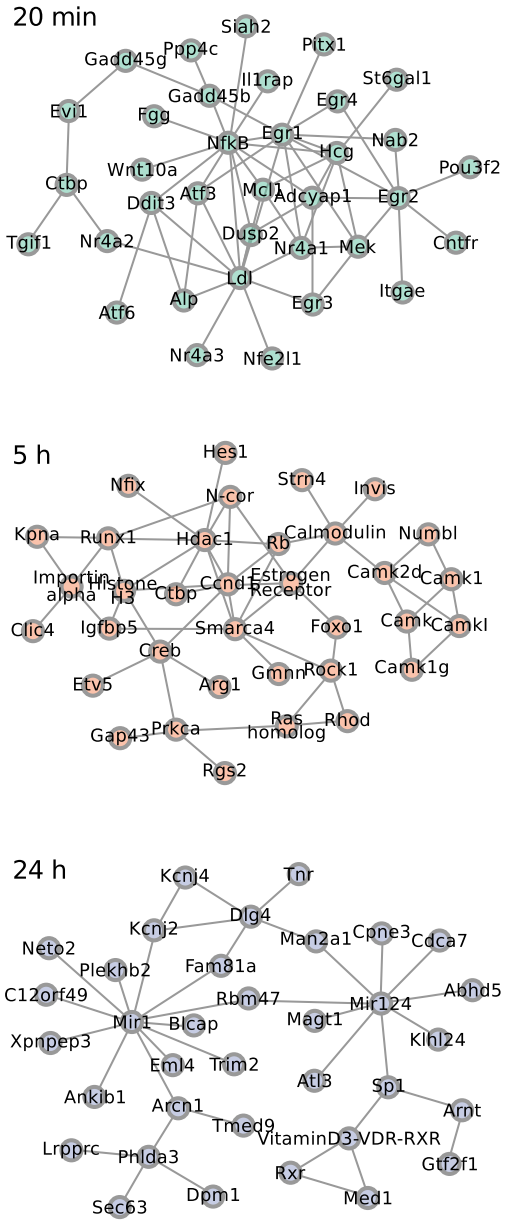

Figure 5.4: *From the LTP networks previously identified by Ryan* et al. *(2011, 2012) at different times post-LTP induction, we represent in this figure the most significant for each time point. These networks were identified using IPA software*

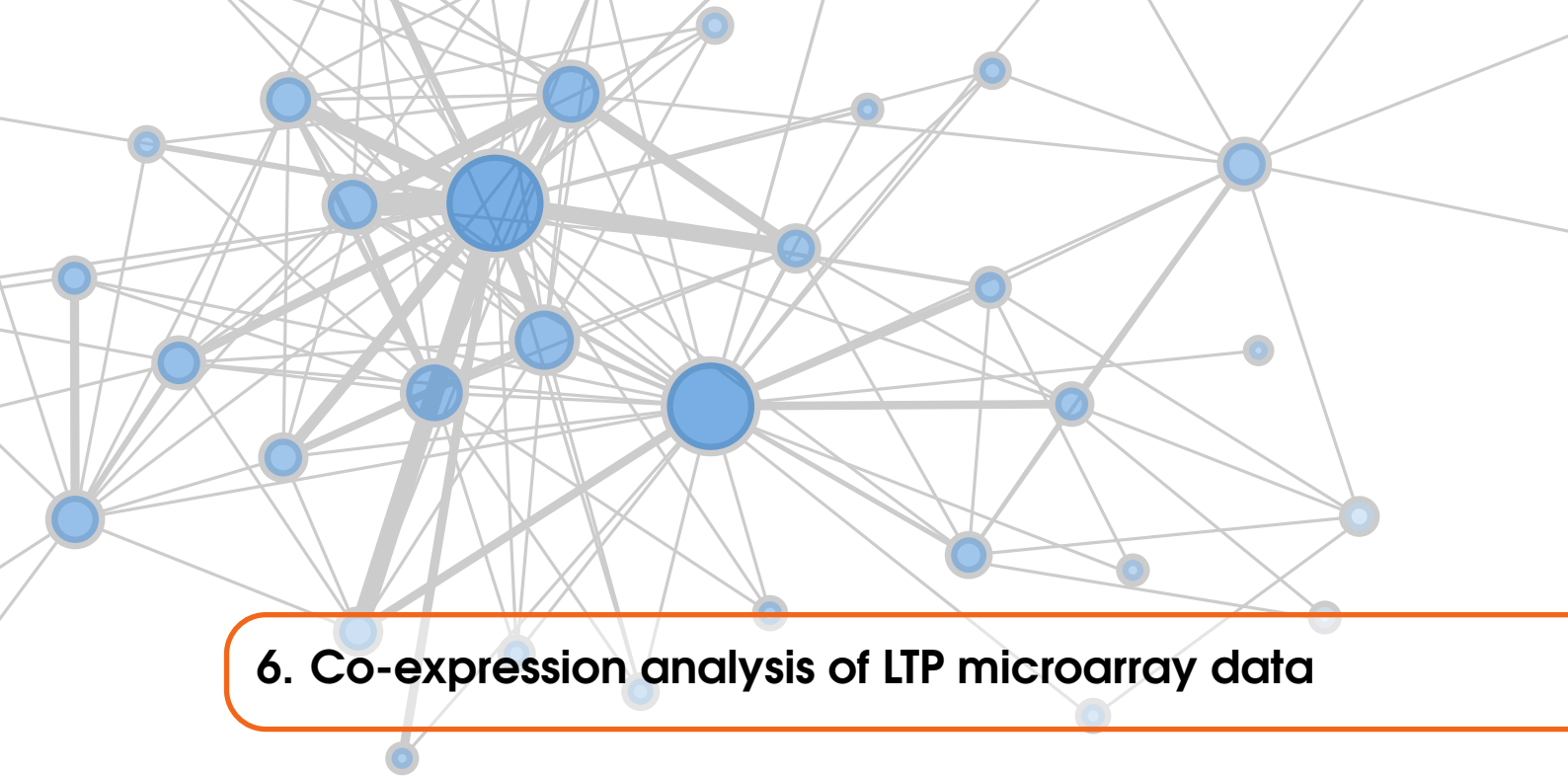

6. Co-expression analysis of LTP microarray data

There is no greater sorrow than to recall in misery the time when we were happy

Dante Alighieri

6.1 Introduction

The cellular and molecular mechanisms underlying LTP seem to be several and to operate at different scales. Currently, we know that LTP exhibits at least two mechanistically distinct phases of maintenance – a protein-synthesis independent early phase and a protein-synthesis dependent phase which lasts for longer periods.

A third biochemically distinct phase has been identified. This third phase is a translation- and transcription-dependent phase. The role of *de novo* gene transcription in the late phases of LTP has drawn considerable attention in the last decades. New gene expression seems to be of crucial importance in the downstream processes required to maintain late LTP. Within minutes of the high-frequency stimulus (HFS), the expression of immediate early early genes (IEGs) is induced by activated constitutive transcription factors. This wave of expression is followed by a second wave, the late response genes (LRGs; see Section 3.3.6).

The variety of functions held by the non-nuclear IEG products (or "effector IEGs") offers a glimpse of the potential complexity underlying the genomic response following LTP induction. A number of studies have aimed at unravelling this tightly coordinated response by using a range of microarray technology platforms (Lee *et al.*, 2005; Park *et al.*, 2006; Wibrand, Messaoudi, Håvik, Steenslid, Løvlie, Steen, and Bramham, 2006; Håvik *et al.*, 2007a).

In the light of its apparent complexity it becomes necessary to investigate the effects that LTP induction elicits from an integrative perspective. In order to overcome the limitations imposed by the classical differential expression analysis and also to quantify temporal network reorganization, we describe in this Chapter the analysis of the microarray data from Ryan *et al.* (2011, 2012) described in Chapter 5 using weighted gene co-expression network analysis (WGCNA Zhang, Horvath, *et al.*, 2005). By clustering the genes according to the similarity in their co-expression

patterns, we identified a set of modules of highly connected genes. This analysis allowed us to pinpoint genes of relevance based on their high intramodular connectivity. In addition, the functional enrichment in the different modules allows us to understand the cellular context in which these highly connected genes function – the degree of connectivity of a gene has been correlated with its *essentiality*. Essential genes are those genes that are critical for the survival of the organism or for the achievement of a particular cellular function, in this case, LTP (Giaever, Chu, Ni, Connelly, Riles, Veronneau, Dow, Lucau-Danila, Anderson, Andre, *et al.*, 2002).

We inspected and quantified the reconfiguration of the molecular interaction structure within these gene modules along the different phases of LTP by using two complementary measures. First, a module-centric measure which indicates the average gain or loss of intramodular connectivity with time. Secondly, we considered a gene-centric measure to take into account the changes in expression similarities between pairs of genes in time.

6.2 Methods

6.2.1 Data sets and sample clustering

Raw gene expression data was obtained from Ryan *et al.* (2011) and Ryan *et al.* (2012) and corresponds to 30 brain tissue samples from 15 adult rats. More precisely, they induced LTP on freely moving animals unilaterally so that for each animal an unstimulated hemisphere could be used as control. At different times post-LTP induction, groups of animals were anaesthetized and decapitated: 20 min, 5 h, and 24 h ($N = 4$, $N = 5$, $N = 6$ respectively). These times are representative of the different phases of LTP.

The data had been previously normalised using the *robust multichip average* package (RMA; Irizarry, Bolstad, Collin, Cope, Hobbs, and Speed, 2003). In addition, the correlation between measurements on the same subject (within-animal correlation) was estimated and considered in the model fit. The t-statistic was generated using the *LIMMA* package, which uses a standard error moderated across all genes using a simple Bayesian model (Smyth, 2005).

The moderated paired t-test between the stimulated and unstimulated pairs of samples produced three lists, one for each temporal contrast, ranking the genes according to the significance of their differential expression (p-value). For computational reasons, we restricted the network analysis to the subsets of the top genes of each of the lists according to their p-value. Namely, we merged the top 1,700 genes of each of the temporal contrasts, so that the contribution to the final list of each of the different time groups was equivalent in terms of number of genes. This intersection resulted in a set of differentially expressed genes across early and late-LTP (L-LTP) of 4,804 genes with p-values ranging from 7.7×10^{-6} to 6.7×10^{-2}.

The 30 brain samples were clustered according to the similarity in their gene expression profiles using a standard unweighted pair group method with arithmetic mean (UPGMA). The clustering dendrogram is shown in Figure 6.1. Samples tend to cluster together reflecting their belonging to the different time points. As there appear not to be outliers, every sample was kept for further analyses.

6.2.2 Construction of gene co-expression networks

The identification of modules of highly co-expressed genes for the three temporally distinct LTP-induced tissues and control was carried out using the WGCNA package (Langfelder and Horvath, 2008). The details are further reviewed in Zhang *et al.* (2005). For every pair of genes i, j the Pearson correlation is calculated and transformed into an adjacency measure with a power function, a_{ij}. We adopted a scale-free topology criterion for choosing the parameter for the adjacency function. Figure 6.2 shows the scale-free fit index as a function of the parameter p used for the power adjacency function. We chose $p = 5$ since at around that value the R^2 fit curve reaches

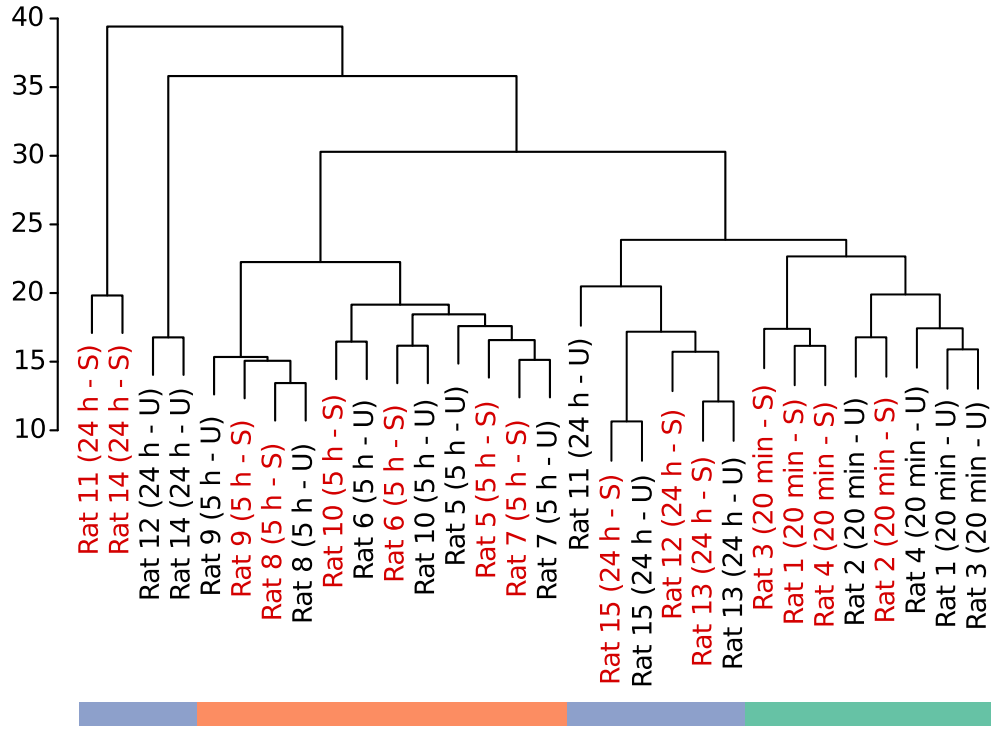

Figure 6.1: *Clustering of the 30 brain samples according to the similarity in terms of gene expression profiles. Only the 4,804 most differentially expressed genes were used to perform the clustering*

saturation for the unstimulated and 24 h co-expression networks. Higher values of the exponent may lead to networks with very few connections (Zhang *et al.*, 2005).

In order to identify modules of highly connected genes, the topological overlap (TO) (Ravasz, Somera, Mongru, Oltvai, and Barabási, 2002) is used as a similarity measure:

$$w_{ij} = \frac{l_{ij} + a_{ij}}{min\{k_i, k_j\} + 1 - a_{ij}}$$

where $l_{ij} = \sum_u a_{iu} a_{uj}$ and $k_i = \sum_u a_{iu}$ is the node connectivity and a_{ij} is the adjacency between the expression profiles of the genes i, j. In this way we obtained four undirected weighted networks constituted each by the same 4,804 nodes but whose connections would differ depending on the values of TO. The first of the networks corresponds to the unstimulated tissues (unstimulated hemispheres) and the other three to the different times after LTP induction (20 min, 5 h, and 24 h). Figure 6.5 represents these weighted networks as heatmaps.

To identify the gene co-expression modules, the TO is used as a similarity measure to perform a hierarchical clustering. The default parameters for the cluster splitting are left unchanged (for more details, refer to Zhang *et al.*, 2005). For each of the four groups we obtained specific gene co-expression modules based on their TO.

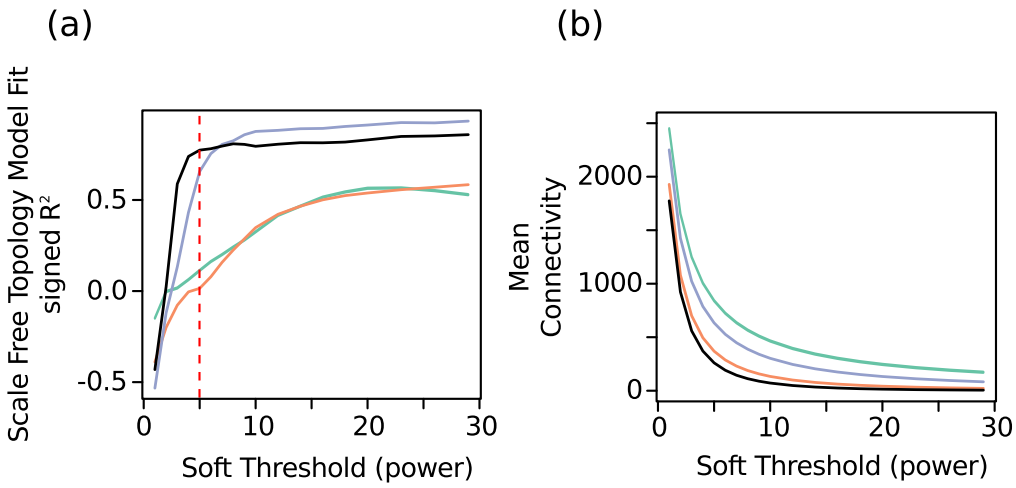

Figure 6.2: ***(a)*** *Scale-free fit index as a function of the soft-thresholding power p. The degree distributions corresponding to the red dashed lines are expanded in the panels of Figure 6.4. The R^2 fit to a scale-free distribution of the unstimulated control and the 24 h networks are both higher and saturate at lower values of p than the earlier networks (20 min and 5 h data). The latter reach a saturation only of around $R^2 = 0.5$.* ***(b)*** *Mean connectivity as a function of the soft-thresholding power p*

6.2.3 Functional enrichment

The Gene Ontology (GO) project (Ashburner, Ball, Blake, Botstein, Butler, Cherry, Davis, Dolinski, Dwight, Eppig, *et al.*, 2000) is a database that unifies descriptions of gene products from different sources. It consists of three structured vocabularies describing gene products in terms of their associated biological processes, cellular components and molecular functions.

Genes belonging to the same module are likely to be related functionally. In order to detect GO terms that are associated with a significant number of genes within a given module, we used the R package *topGO* (Alexa and Rahnenfuhrer, 2010). This tool finds significant shared GO terms or parents of those GO terms, associated with the set of genes. The statistical significance was assessed through Fisher's exact test.

6.2.4 Measures of network reconfiguration

For each of the 58 modules obtained by WGCNA (9, 9, 24, and 16 modules for the control, 20 min post-LTP, 5 h post-LTP, and 24 h post-LTP respectively), we quantified the modular differential connectivity (MDC; Zhang, Gaiteri, Bodea, Wang, McElwee, Podtelezhnikov, Zhang, Xie, Tran, Dobrin, *et al.*, 2013). The MDC is a module-centric measure and corresponds to the ratio of the average connectivity for any pair of module-sharing genes at time T_1 compared to that of the same genes at time T_2

$$\mathrm{MDC}(T_1, T_2) = \frac{\sum_{i=1}^{N-1} \sum_{j=i+1}^{N} w_{ij}^{T_1}}{\sum_{i=1}^{N-1} \sum_{j=i+1}^{N} w_{ij}^{T_2}}$$

where w_{ij} is the TO between two genes i and j in a given network (see Figure 6.3). The statistical significance was assessed by a false discovery rate (FDR) based on permutation of the gene labels. This corresponds to randomly permutating the rows and columns of the TO matrix of a given module. MDC > 1 indicates enhanced co-regulation between genes, whereas MDC < 1 indicates reduced co-regulation. The MDC was calculated for each of the 58 networks for each of the 3 temporal transitions (control $\rightarrow$ 20 min, 20 min $\rightarrow$ 5 h, 5 h $\rightarrow$ 24 h).

In addition, we used a gene-centric measure to rank the pairs of genes according to the specificity of the TO value in the adjacent temporal points. We employed a measure based on Oldham, Horvath, and Geschwind (2006)

$$S_{ij}(T_1,T_2) = \frac{w_{ij}^{T_1}/\text{mean}(w^{T_1})}{w_{ij}^{T_1}/\text{mean}(w^{T_1}) + w_{ij}^{T_2}/\text{mean}(w^{T_2})}$$

For a pair of genes i,j in a given module, a high $S_{ij}(T_1,T_2)$ captures a high TO at time T_1, and a low TO at time T_2. A low $S_{ij}(T_1,T_2)$ value captures the opposite relation, while a value of 0.5 means no change in the TO for those genes.

Each gene can also be ranked according to its degree, which identifies the main hubs within a module. As the networks are weighted, the degree is calculated simply by summing over each connection weight (TO) and normalising by the size of the module.

6.3 Results

6.3.1 Structural organisation of the temporally distinct networks

It is widely accepted that biological networks tend to have connectivity distributions which approximate scale-free distributions (Jeong, Tombor, Albert, Oltvai, and Barabási, 2000). In that aspect, the four distinct co-expression networks identified in this study exhibit different network properties in relation to the fit to a scale-free topology. Figure 6.2 depicts the fit to a scale-free topology model with different values for the soft thresholding power p used for the adjacency function. Note that for higher values of p the fit reaches saturation. From a qualitative point of view, the networks seem to reach the saturation at different values of p, with the unstimulated control and the 24 h networks saturating earlier ($p \approx 5-10$) than the 20 min and 5 h networks ($p \approx 20$). In addition, the saturation value of the scale-free fit coefficient is higher for the control and 24 h than for the 20 min and 5 h networks.

A closer inspection to the scale-free model fit in Figure 6.4 reveals that in fact, at sufficiently high values of p, both the unstimulated control and the 24 h networks fit to a scale free distribution. On the other hand, the earlier networks have few nodes with a low degree (truncated left side of the distribution). Considering that the scale-free architecture has been shown to display a high robustness against random perturbations (Albert *et al.*, 2000), and that this property seems to have been selected for in biological networks (Jeong *et al.*, 2000), it is plausible that transient topological rearrangements exhibit less stable architectures. We hypothesise that such could be the case of the earlier 20 min and 5 h networks – the homeostatic cell state acquired 24 h post-induction could have restored a scale-free architecture that is also observed in the unstimulated tissue. The intermediate networks at 20 min and 5 h post-LTP could be temporarily organised in topologies that resemble the characteristics of random networks.

As proposed by Zhang *et al.* (2005), we adopted the value of the fit as a criterion to select a power for the adjacency function. Given the above observations we opted to chose an exponent where the curve reaches saturation for the unstimulated control and the 24 h networks ($p = 5$).

For each temporal network generated after LTP-induction, we show in Table 6.1 the top hubs.

Table 6.1: *Top hubs in the co-expression networks*

20 min network

Probe ID	Gene Symbol	Gene Title
1395900_at	Chtf8	CTF8, chromosome transmission fidelity factor 8 homolog (S. cerevisiae)
1385824_at	Cep350	centrosomal protein 350
1381003_at	Ikzf2	IKAROS family zinc finger 2
1386234_at	NA	NA
1391555_at	Ncoa3	nuclear receptor coactivator 3
1388079_at	Cacng8	Ca^{2+} channel, voltage-dependent, gamma subunit 8
1388684_at	Fnbp4	formin binding protein 4
1382979_at	NA	NA
1387435_at	St8sia3	ST8 alpha-N-acetyl-neuraminide alpha-2,8-sialyltransferase 3
1387795_at	Pola2	polymerase (DNA directed), alpha 2

5 h network

Probe ID	Gene Symbol	Gene Title
1384230_at	Krtcap3	keratinocyte associated protein 3
1374827_at	Ndst2	N-deacetylase/N-sulfotransferase (heparan glucosaminyl) 2
1383540_at	NA	NA
1384860_at	Zfp84	zinc finger protein 84
1394492_at	RGD1563482	similar to hypothetical protein FLJ38663
1368005_at	Itpr3	inositol 1,4,5-triphosphate receptor, type 3
1371697_at	Pnpla2	patatin-like phospholipase domain containing 2
1368229_at	Sip1	survival of motor neuron protein interacting protein 1
1385928_at	Smad6	SMAD family member 6
1368321_at	Egr1	early growth response 1

24 h network

Probe ID	Gene Symbol	Gene Title
1369067_at	Nr4a3	nuclear receptor subfamily 4, group A, member 3
1369398_at	Naaladl1	N-acetylated alpha-linked acidic dipeptidase-like 1
1369255_at	Il1r1	interleukin 1 receptor, type I
1384999_at	Lce1d	late cornified envelope 1D
1371003_at	Map1b	microtubule-associated protein 1B
1369237_at	Slc6a7	solute carrier family 6 (neurotransmitter transporter, L-proline), member 7
1380864_at	NA	NA
1397942_at	Cdc37l1	cell division cycle 37 homolog (S. cerevisiae)-like 1
1370641_s_at	Cacna1i	Ca^{2+} channel, voltage-dependent, T type, alpha 1I subunit
1377276_at	Cdk5r2	cyclin-dependent kinase 5, regulatory subunit 2 (p39)

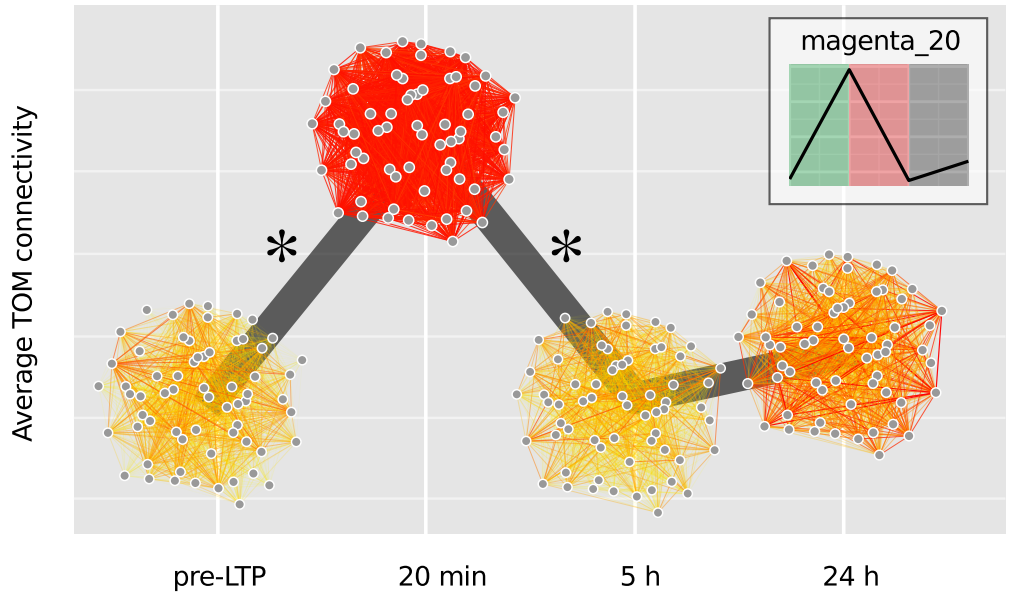

Figure 6.3: *The MDC measures the change in the average connectivity between the nodes within a module. In the example, the module* magenta_20 *is used as an example. It is constituted by a total of 64 nodes (probes in the array). The colour of the edges connecting the nodes in the networks correspond to their TO. The nodes are the same in the four networks, but their connectivity varies at different times. The* y*-axis represents the average TO of the module and the x-axis represents time. The asterisks (*) represent significant variation according to 10% FDR as described in the Methods. A simplified version of this plot is shown in the right-top corner inset for this particular module, and for each of the modules in Figure 6.7*

6.3.2 Modular functional analysis

The identification of co-expression modules within the four temporal networks consists in the selection of a height for cutting the dendrograms. This is done automatically by the WGCNA package, and results in a number of densely connected subsets of networks corresponding to the branches of the dendrogram. This procedure was conducted independently for each of the four network datasets and resulted in control, 9 modules ranging from 69 to 2327 genes; 20 min, 9 modules ranging from 64 to 1184 genes; 5 h, 24 modules ranging from 31 to 535; and 24 h, 16 modules ranging from 42 to 1164 genes). The distribution is similar in the early phase of LTP when compared to the unstimulated tissue, whereas the networks generated for the later times (5 h and 24 h) appear to be more dissociated, splitting up into more modules for the same power threshold (Figure 6.5 and Table 6.2).

The intersections between the 58 modules identified are not always empty since each temporal expression dataset was analysed independently. As larger modules in the control and 20 min samples appear to segregate into different sets of genes, we chose to keep all the modules and not to merge overlapping modules. We show in Figure 6.6 the normalised overlap between modules.

The different modules were tested for Gene Ontology (GO) term enrichment. A representative top GO term for each module is shown in Table 6.2. For a more comprehensive list, see the

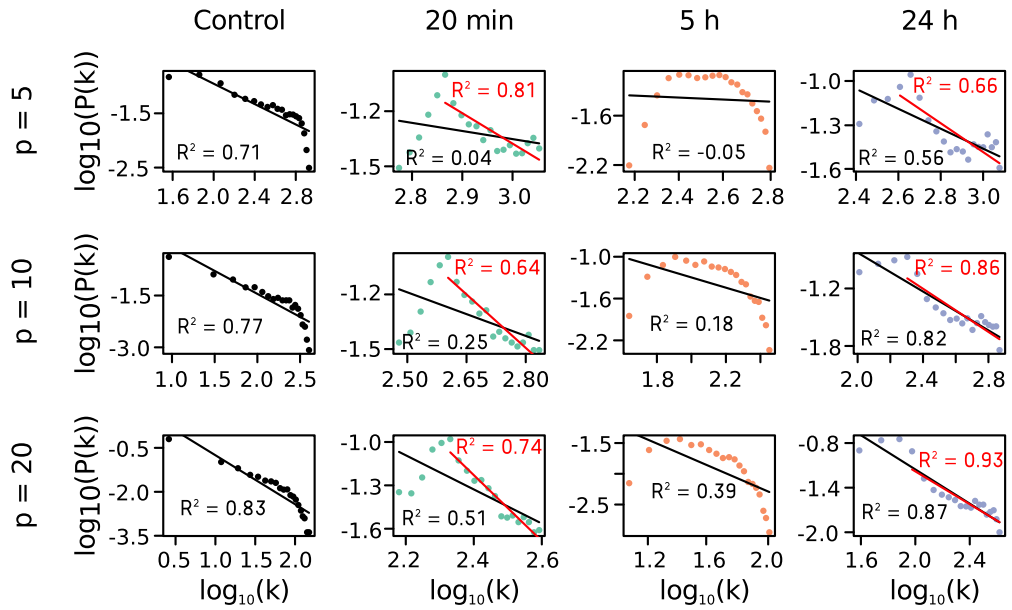

Figure 6.4: *Degree distributions of the networks using different values of p. From left to right, unstimulated control, 20 min, 5 h, and 24 h networks. From top to bottom, $p = 5$, $p = 10$, and $p = 20$. The distributions are log-transformed both in the x and y axes. The black lines represent the linear model fit. For the 20 min and 24 h networks, an additional linear model fit is shown with a red line, using only the right decrementing side of the distribution. Values of R^2 are shown for the linear model fits*

Appendix A.2.

Table 6.2: *List of modules identified by WCGNA with at least 50 genes*

Module	**Size**	**Functional category**	**Top genes by k_{TO}**
cyan_24	97	endosome transport	Nog, Thbd, Zscan10
green_U	206	cation transmembrane transport	Camk4, St6gal1, Slc31a1
black_20	329	(+) reg. of endocytosis	Arhgap27, Kdm5b, Acrv1
brown_24	459	cofactor transporter activity	Mast2, Mlst8, Fgd2
black_24	269	epitelial polarization	Cpn1, Thoc2, Pqlc3
brown_20	730	neuron part and cytoplasmic microtubule	Ddi2, Atp5i, Rab22a
red_20	455	axogenesis	Slc10a5, Tnfrsf17, Slc4a11
yellow_U	222	BRCA1-A complex	Acap2, Dr1, Alpk3
blue_20	779	leukocyte activation	Pias2, Atp6v1b2, Pdzd3
green_20	461	response to axon injury	Igha, Tp53bp1, Tal1
pink_20	78	calmodulin-dependent kinase activity	Lmo2, Pacsin1, Hmox3
yellow_20	724	transcription from RNApolI promoter	Ndst2, Kcnj12, Ptpn7
turquoise_20	1184	oxidoreductase activity	Brpf1, Tsta3, Kdelc1
blue_24	753	reg. of endocrine process	RT1-Da, Mrpl14, Ccnd1
turquoise_24	1164	neuron projection membrane	Ak3, Cacna1i, Rbm4
black_U	145	activation of prot kinase and membrane	Znf609, Cd24, Dab2
pink_24	238	fatty-acyl-CoA binding	Gtf3c6, Ak3l1, Ap2a2
yellow_24	355	proteasomal protein catabolism	Qtrt1, Sh3glb1, Hira
magenta_U	69	integrin binding	Uba6, Samd14, Atrx
pink_U	72	mitochondrial transport and apoptosis	nod3l, Rnasen, Glce

Continued on next page

Table 6.2 – *continued from previous page*

Module	Size	Functional category	Top genes by k_{TO}
green_24	281	histone demethylation	Gls, Junb, Fam135a
brown_U	691	synapse and reg. of secretion	Alox5, Kcnj4, Dhrs9
greenyellow_24	143	tau-protein kinase activity	Hspb3, Hist2h2be, Hiat1
magenta_24	212	proteasomal protein catabolism	Hectd1, Nans, Sec1
midnightblue_24	86	clathrin-coated endocytic vesicle	Reg3a, Dimt1l, Ctrc
red_24	278	septin complex	Crcp, Cc2d1a, Pdia6
purple_24	175	cAMP-mediated signaling	Epor, Xpnpep3, Fam120b
blue_U	836	dephosphorylation and DNA binding	Gabra5, Cdkn2c, Kl
blue_5H	521	amino acid biosynthesis	Scn11a, Abi3, Clec10a
lightyellow_5H	88	CNS neuron axonogenesis	C1qtnf3, Fbln1, St8sia3
black_5H	237	anion homeostasis and synapse assembly	Slc2a4, Pdzd4
cyan_5H	142	reg. of DNA methylation	Fmod, Fam135a, Ankrd6
magenta_5H	208	progesterone receptor signaling	Mrpl35, Prkd3, Cul5
green_5H	336	GTP-Rho binding and mitochondrion	Prelid2, Prl2b1, Abca8
lightgreen_5H	95	T cell migration	H3f3b, Cnih2, Trps1
yellow_5H	358	chromatin DNA binding	Arglu1, Mccc1, Tmem206
turquoise_5H	535	DNA catabolism	Crhr1, Kdm6b, F8
purple_5H	165	histone H3-K27 methylation	Fgf21, Adcy4, Klhl22
salmon_5H	151	oxidoreductase activity	Hs3st2, Hdac5, Ccdc115
tan_5H	158	MAPK import into nucleus	Asb1, Tpr, Pex5l
brown_5H	458	K^+ transport and Ras GTPase binding	Dhh, Cog7, Dgki
greenyellow_5H	162	response to Ca^{2+}	Flrt3, Cnga1, Adra1d
red_U	178	reg. of GTPase activity	Nppa, Cyp8b1, Igfbp2

6.3.3 Network structure reconfiguration

The four distinct expression profiles studied represent different cellular states following LTP induction. We have studied the transitions from the pre-LTP state represented by the unstimulated hemispheres to the different gene expression snapshots post-LTP induction. For each temporal transition, control $\rightarrow$ 20 min, 20 min $\rightarrow$ 5 h, and 5 h $\rightarrow$ 24 h, we have examined the topological changes in the 58 modules identified using WGCNA.

Firstly, the fraction of modules showing a significant increase in MDC is similar along the time samples, whereas the fraction of modules with a significant loss of connectivity increases (stacked bars plot, Figure 6.7).

The response elicited rapidly after LTP induction at the gene expression level corresponds to the transition observed between the control and the 20 min dataset in terms of MDC. Out of the 58 modules, 57 show a gain of connectivity (MDC > 1, of which 20 are significant with FDR $< 10\%$ (a more strict FDR $< 1\%$ gives still a total of 10 significant modules). This marked increase in the average TO connectivity takes place in combination with the documented enrichment in upregulated genes within the set of differentially expressed genes (Ryan *et al.*, 2011). The modules showing the highest significance (FDR $< 1\%$) in the connectivity gain during this early LTP stage display an enrichment in functions such as membrane compartment, endosome transport and endocytosis. Other functions over represented in these networks are cation transmembrane transport, CaM-dependent kinase activity and transcription from RNApolI. Only the module with the function regulation of GTPase activity seems to undergo a loss of average TO in the early genetic response following LTP.

Ryan *et al.* (2012) reported that the general upregulation of LTP genes observed at 20 min lasts for at least 5 h using differential expression analysis. We note a global loss of connectivity between the 20 min and 5 h networks (0.187 to 0.089 average TO respectively). Yet, the proportion of modules exhibiting gain/loss/conservation of connectivity is very similar (17/17/24, respectively). More interestingly, the fraction of the modules with a significant loss of MDC corresponds to modules that showed an increase in MDC in the earliest transition. Amino acid biosynthesis, central neural system neuron axonogenesis, anion homeostasis and synapse assembly are some of the

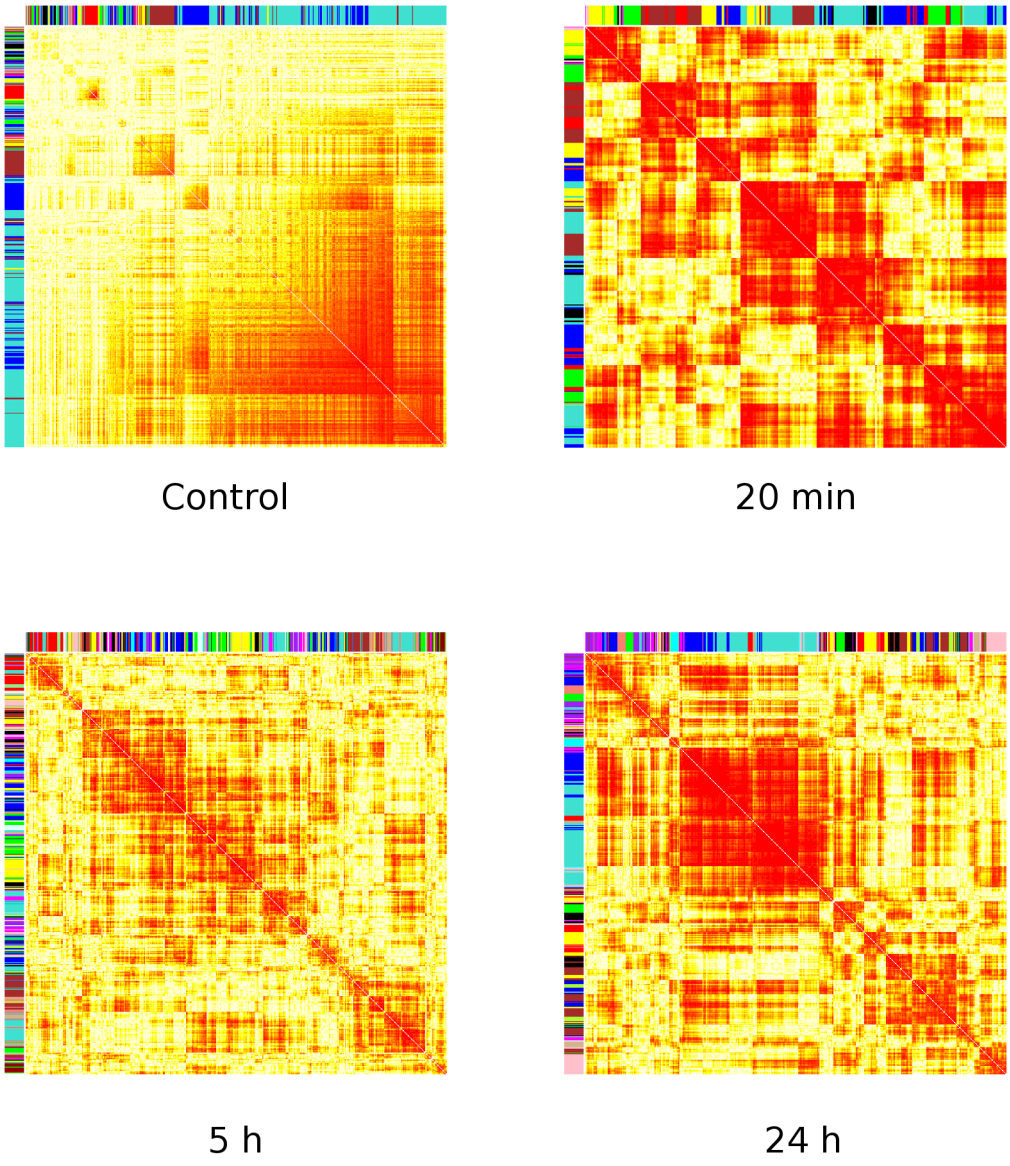

Figure 6.5: *TO matrix among genes for the time series datasets as a heatmap. The darker shade of red represents a higher TO value between the genes*

functions assigned to the modules exhibiting a significant gain of connectivity from 20 min to 5 h. Other interesting functions over-represented are regulation of DNA methylation, GTP-Rho binding, and MAPK import into nucleus.

These modules subsequently undertake a loss of connectivity in the final transition to the 24 h phase, together with the modules enriched with the functions K^+ transport, Ras GTPase binding and response to Ca^{2+}. During this last transition, a large number of networks show an increase in average TO, with ascribed functions such as neuron projection membrane, activation of protein kinase, histone demethylation, synapse, regulation of secretion, tau-protein kinase activity, protein catabolism, clathrin-coated endocytic vesicle, and cAMP-mediated signalling.

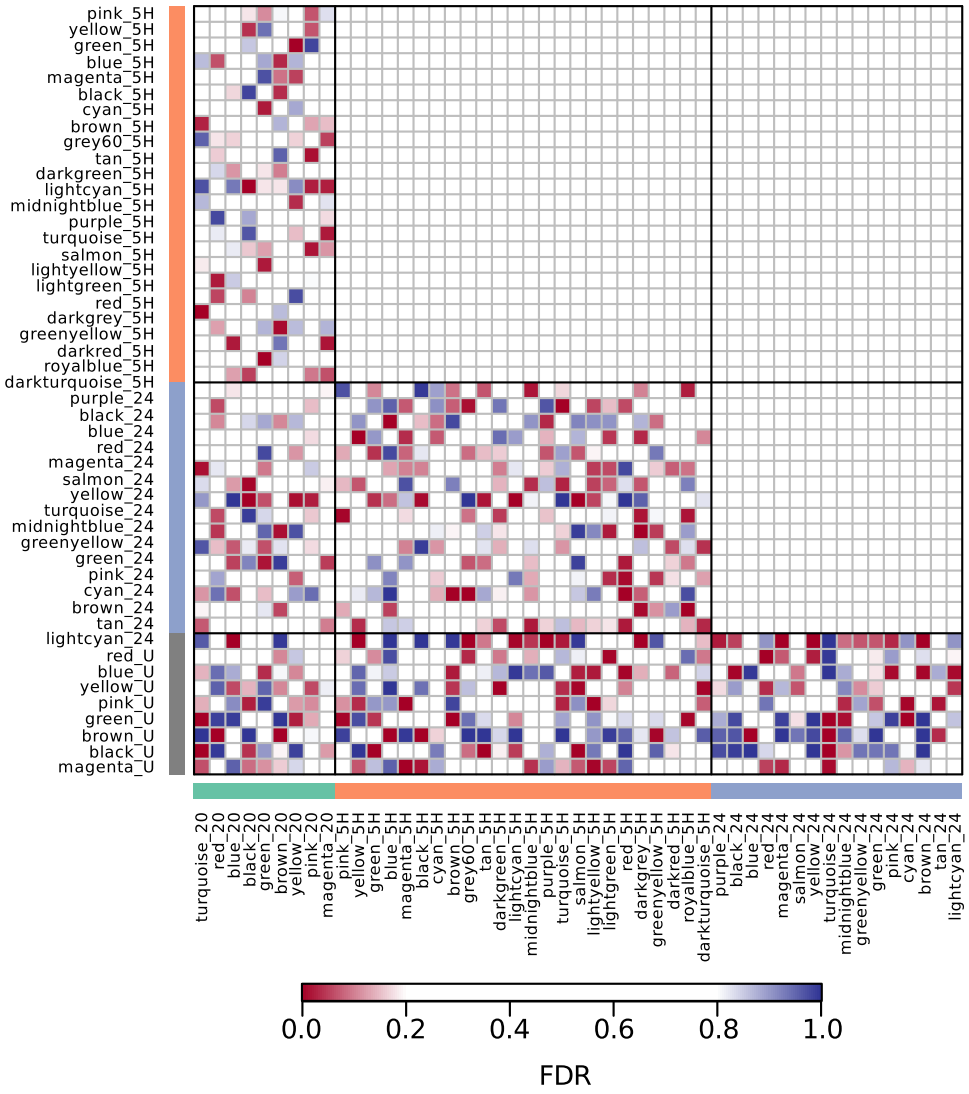

Figure 6.6: *Gene overlap between the modules generated from the different expression data corresponding to the different times post-LTP induction. The overlap was normalised by the size of the smallest module. The colour in the heatmap represents the FDR of the overlap. Red and blue represent a significant overlap and a significantly low number of genes in common respectively*

6.3.4 Overview of the time-points

20 min modules

The results of Ryan *et al.* (2012) evidenced a rapid LTP-induced increase in gene expression. We found that, in addition, the modules identified by WGCNA tend to increase their intramodular connectivity (average TO, see Section 6.2.2) – out of the 58 modules identified, only *red_U* shows a decrease in the average TO. Not surprisingly, this module corresponds to a set of genes co-expressed in the unstimulated hemispheres, with functions not specifically related with neural tissue. Out

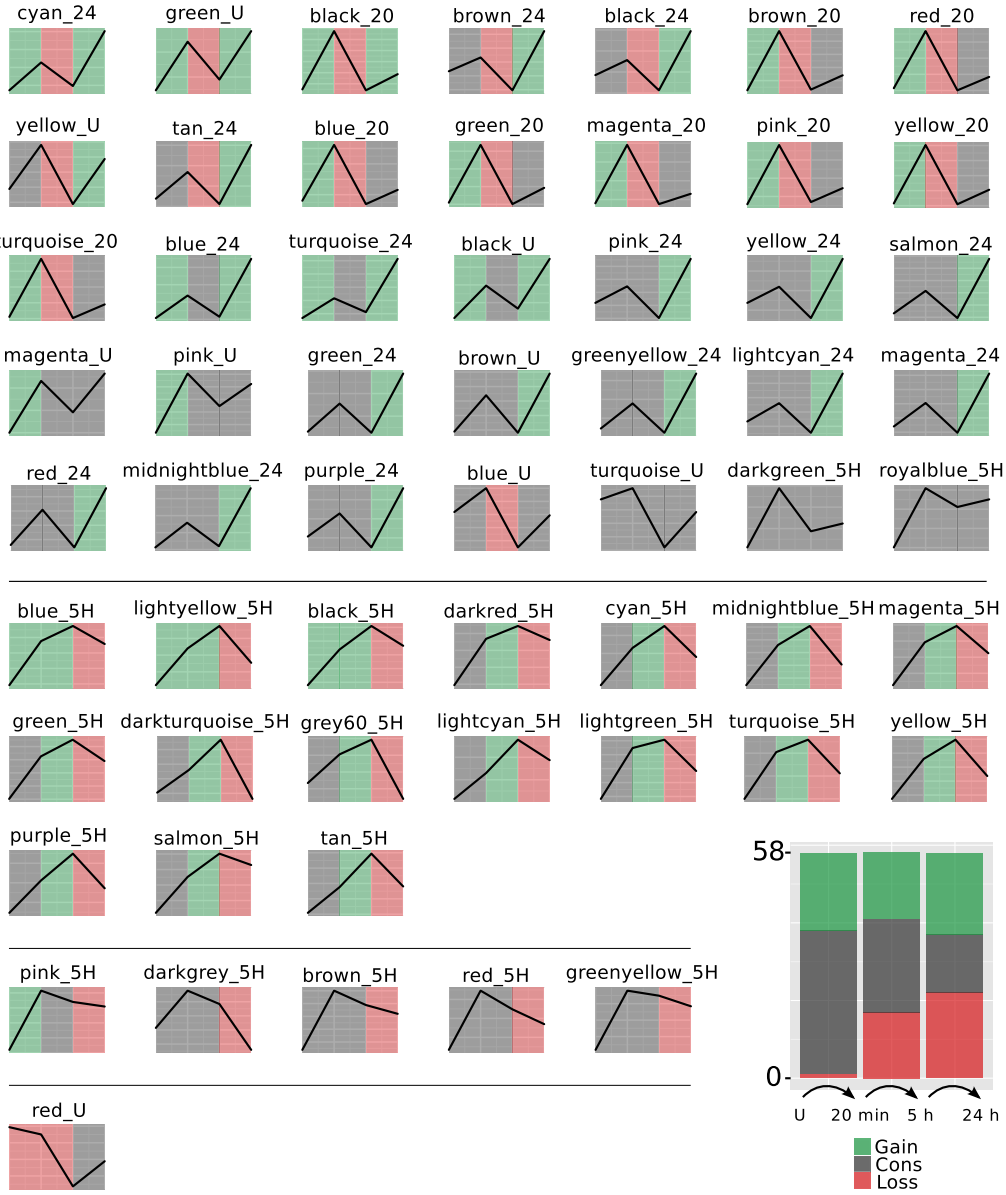

Figure 6.7: *Module reconfiguration following LTP. Each panel corresponds to one of the 58 modules identified. Time on the x-axis (control, 20 min, 5 h, and 24 h post-LTP induction) is plotted against the average TO of the module. For each transition between time points, green represents a significant gain of connectivity (MDC* > 1*; FDR* $< 10\%$*), red loss of connectivity (MDC* < 1*; FDR* $< 10\%$*), and grey conserved connectivity (FDR* $> 10\%$*). The number of modules showing each of these is represented in the bottom right panel*

of the 57 modules that show an increase in intramodular TO (MDC > 1), 20 show statistical significance (FDR $< 10\%$, see Figure 6.7).

Among the modules that show a significant gain of connectivity, it is worth noting that some

display a significant loss of connectivity 5 h post-LTP. This abrupt peak in co-expression is exhibited by the 9 modules identified in the 20 min dataset (*green_20*, *magenta_20*, *yellow_20*, *turquoise_20*, *blue_20*, *black_20*, *pink_20*, *brown_20*, *red_20*, see Figure 6.8a). These networks do not show any overlap in genes. The rapid recruitment of some clusters of co-expressed genes during the first minutes in response to the experimental HFS is in agreement with the idea of the induction of IEGs discussed in previous chapters (see Section 3.3.6).

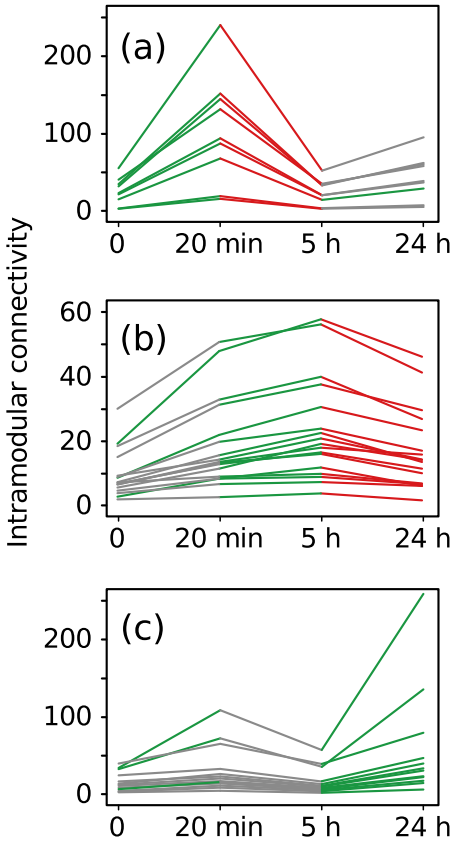

Figure 6.8: *The three main trends in modular connectivity changes across time in the co-expression modules identified is shown.* ***(a)*** *Modules identified using the 20 min data all share a similar trend – they become tightly co-regulated at 20 min to lose the connectivity at 5 h.* ***(b)*** *Modules identified at 5 h exhibit a significant decrease in TO at 24 h.* ***(c)*** *Modules identified in the 24 h data together with* black_U *and* brown_U *modules (identified using only the control data) show a significant gain in intramodular connectivity at 24 h.*
Green lines represent significant gain of intramodular connectivity (MDC > 1*, FDR* $< 10\%$*) and red lines represent significant loss of modular connectivity (MDC* > 1*, FDR* $< 10\%$*). Grey lines represent no statistical significance for the MDC*

When the top 35 genes networks are subjected to an analysis of GO term enrichment, some interesting results arise. First, the *red_20* cluster shows "long term synaptic depression" (GO:0060292)

as a significantly represented function ($p = 1.911e-03$, genes Pick1 and Plk2). The *yellow_-20* network is densely connected with "regulation of ion transmembrane transporter activity" (GO:0032412) ($p = 3.897e-04$) and "synaptic transmission" (GO:0007268) ($p = 1.821e-02$) as salient overrepresented functions. The *green_U* network shows "convergent extension involved in axis elongation" (GO:0060028) ($p = 4.913e-04$) and "positive regulation of synaptic transmission, glutamatergic" (GO:0051968)($p = 9.375e-03$) as overrepresented GO terms. Last, *black_20* contains the only two genes annotated with the function "fasciculation of motor neuron axon" (GO:0097156) in the GO database, Epha3 and Epha4 ($p = 6.881e-05$).

5 h modules

We have described a set of networks that show a significant loss of intramodular connectivity at 5 h, which is then maintained in the later 24 h dataset. The general loss of intramodular connectivity in the weighted co-expression network is evident from Figure 6.5 and parallels the onset of a general downregulation of gene expression.

A different temporal trend, however, is exhibited by a number of modules identified at 5 h – a gain in connectivity between the unstimulated control and the 20 min is followed by a subsequent significant gain at 5 h to finally lose connectivity at 24 h. And yet, these set of modules show a rather mild average TO when compared to the networks discussed in the previous section (see Figure 6.8b). These results indicate that a strong and coordinated genomic response rapidly follows LTP induction, and that there exist different phases of LTP from the perspective of the genomic response. The reason why the high co-expression levels observed at 20 min are not transferred to other networks but rather lowered is unclear. However, the experimental evidence of a critical phase in the first minutes that follow the HFS in which gene expression is necessary for L-LTP may account for these observations.

The modules identified at 5 h which show a gain of intramodular TO at 20 min and at 5 h followed by a loss of TO at 24 h are summarised in Table 6.5. Perhaps the most representative module in the 5 h dataset is the *purple_5H*, which shows the lowest gene overlap with each of the networks identified at 20 min. Furthermore, from the top 30 genes ranked according to their average TO in the full weighted co-expression network at 5 h, 6 of them belong to the module. More than half of the genes in the module are related with metabolism and biosynthetic processes ($p = 1.302e-07$), in particular transcription. Regulation of gene expression (31 out of 87 known mapped genes) is also an enriched function $p = 2.035e-04$). Interestingly, when only the top 35 genes of the network are queried for functional enrichment, the most significant GO term is "synapse maturation" ($p = 1.140e-03$). Nrxn and Shank1 are among the top 35 genes. Nrxn1 is downregulated at 5 h and encodes for Neurexin 1, a membrane protein involved in synaptic signal transmission (De Wit, Sylwestrak, O'Sullivan, Otto, Tiglio, Savas, Yates III, Comoletti, Taylor, and Ghosh, 2009). Shank1 plays a role in the structural and functional organization of the dendritic spine by recruiting Homer to the membrane at postsynaptic sites, mediating the formation of multisynapse spines (Sala, Piëch, Wilson, Passafaro, Liu, and Sheng, 2001).

The main hubs are Ythdf1 (mRNA processing), Adcy4 (a membrane-bound, CaM-insensitive adenylyl cyclase), Gnal (a G protein involved in signal transduction), Hic1 (a transcriptional repressor), Zfp84 (a zinc finger protein), and Pnpla2 (which provides free fatty acids to tissues in situations of energy depletion).

Hic1 encodes for a transcriptional repressor of the Wnt pathway discussed in Section 6.3.5, since it was also identified in the *magenta_20*. The identification of this gene as a central hub in the 5 h TO matrix stresses its central role in LTP, possibly via Sirt1 inhibition, controlled by the formation of a Hic1/Sirt1 complex which controls the transcriptional expression of Sirt1 itself (see Section 6.3.5). G2e3 encodes for a negative regulator of apoptosis (Brooks, Helton, Banerjee, Venable, Johnson, Schoeb, Kesterson, and Crawford, 2008), while Trps1 encodes for a transcriptional repressor (Kaiser, Möröy, Chang, Horsthemke, and Lüdecke, 2003).

Another network identified at 5 h shows a low gene overlap with the networks discussed previously – *darkgreen_5H*. This small network also exhibits an enrichment in positive regulation of metabolic processes ($p = 2.137e-02$).

Co-expression networks at 24 h

The weighted co-expression network at 24 h shows a further decrease in TO. While the 20 min and 5 h networks are representative of the rapid response to the HFS, at 24 h LTP has consolidated and stimulated neurons have reached a new homeostatic level.

However, a representative trend exhibited by most of the co-expression networks identified at 24 h is a gain of intramodular connectivity (see Figure 6.8c).

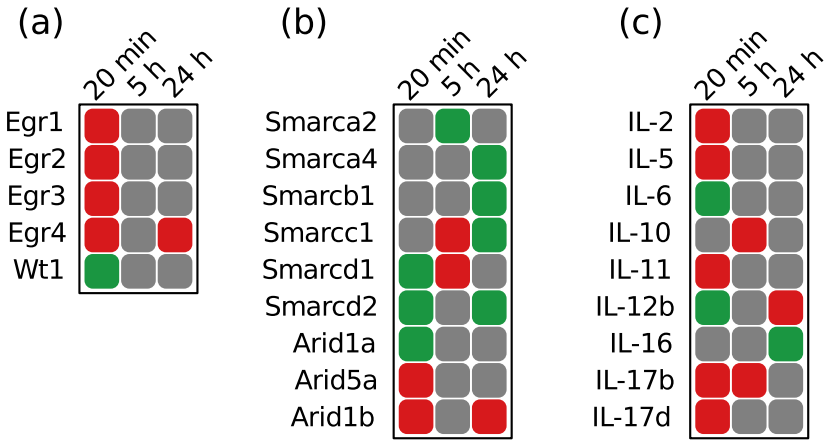

Figure 6.9: *Expression of different genes across time in relation to the unstimulated hemispheres. Red indicates overexpression, green underexpression.* ***(a)*** *Egr family,* ***(b)*** *nBAF complex subunits, and* ***(c)*** *Interleukines* ($p = 0.05$, $-0.15 > ln(FC) > 0.15$)

6.3.5 Regulation of gene expression

We have discussed in previous chapters the importance of gene expression for L-LTP. We pointed out that the late phase of LTP can be impaired if gene expression is inhibited during an short time window early after stimulation, but if the inhibition of RNA synthesis is applied later, L-LTP is not affected (Nguyen *et al.*, 1994). Hence, the changes in gene expression strictly necessary for LTP must be triggered in the early stages post-LTP induction.

Some of the top genes in the co-expression networks play roles as gene expression regulators. In the *red_20* module, the Wt1 gene encodes for a zinc finger that belongs to the Egr family of transcription factors. This family includes Egr1, Egr2, Egr3, Egr4, genes known to be involved in the early genomic response to LTP induction (see Section 3.3.6). While the Egr genes show consistent overexpression in the 20 min dataset (see Figure 6.9a), Wt1 RNA is underexpressed. This result is in agreement with its role in the brain, where it has been proposed to act as a growth suppressor by binding to and blocking/repressing the promoters of early growth-promoting genes normally activated by Egr genes (Haber, Sohn, Buckler, Pelletier, Call, and Housman, 1991).

In the *magenta_20* module, a number of transcriptional modulators are also overexpressed – Erf, Hic1, Insm2, and Tnfaip2. Erf encodes for a protein activated upon phosphorylation by Erk1/2

(Le Gallic, Sgouras, Beal, and Mavrothalassitis, 1999), a pathway involved in LTP (Section 3.3.4). According to the study of Le Gallic *et al.*, Erf may be important in the control of cellular proliferation during the G0/G1 transition in the cell cycle. The other overexpressed genes co-expressed in the *magenta_20* module, Hic1, and Insm2, are tumor suppressors, while Tnfaip2 seems to be involved in angiogenesis and development (Wales, Biel, El Deiry, Nelkin, Issa, Cavenee, Kuerbitz, and Baylin, 1995; Sarma, Wolf, Marks, Shows, and Dixit, 1992).

Homer1, an overexpressed gene which has been previously associated with LTP-related Ras signalling (Rosenblum, Futter, Voss, Erent, Skehel, French, Obosi, Jones, and Bliss, 2002) also appears in the *magenta_20* module. Nevertheless, the candidate modulators for the Ras-Erk1/2 signalling cascade appear in different networks. In the *pink_20* module, the Akirin2 gene may form a complex with Ywhab (which appears in the *red_20* network) that acts to repress transcription of Dusp1, a dual-specificity phosphatase (Komiya, Kurabe, Katagiri, Ogawa, Sugiyama, Kawasaki, and Tashiro, 2008). DUSPs are able to dephosphorylate MAPKs, and Dusp1 in particular tends to inactivate p38 (MAPK11-14), JNK (MAPK8/10), and Erk1/2 (MAPK3/1) (Owens and Keyse, 2007). Interestingly, Dusp1, 2, 5, and 6 are all upregulated in the 20 min dataset. While the role of DUSPs in LTP as modulators of the Ras-Erk1/2 pathway has been suggested previously (Ryan *et al.*, 2011), Akirin2 and Ywhab may also have a modulatory role in the pathway. In fact, while their expression is not significantly different from the controls for the 20 min dataset, they both show a significant underexpression in the 5 h dataset.

In the *turquoise_20* co-expression network, other transcription factors are overexpressed – Atf6 and Gtf3c5. Atf6 encodes for a cAMP-dependent transcription factor that may be involved in the activation of transcription by the SRF (Zhu, Johansen, and Prywes, 1997).

Gene expression, however, is not only regulated via recruitment of transcriptional activators/repressors that bind promoters and other regulatory elements. The structure of the chromatin (DNA) influences the degree of access that the transcriptional machinery has to a given gene – the protein histones form octamers that pack the chromatin (Varga-Weisz and Becker, 1998). DNA has to be exposed for transcription to take place. The changes in chromatin structure that influence gene expression have been termed *epigenetics*. The two more studied mechanisms are DNA methylation/demethylation, which involves a chemical modification of the DNA itself, catalysed by DNA methyltransferases, and post-translational modifications of the histones (acetylation, phosphorylation and methylation).

In the 20 min dataset, the tumor suppressor Hic1 is overexpressed and acts as a Sirt1 repressor (Chen, Wang, Yen, Luo, Gu, and Baylin, 2005). However, the repression of Sirt1 requires the formation of a Hic1/Sirt1 complex (Chen *et al.*, 2005). An additional gene in the same co-expression network, Bcl6, may have a role in the epigenetic control of gene expression. Bcl6 has been shown to be involved in the control of neurogenesis by epigenetic silencing (Tiberi, Van Den Ameele, Dimidschstein, Piccirilli, Gall, Herpoel, Bilheu, Bonnefont, Iacovino, Kyba, *et al.*, 2012). This mechanism involves the recruitment of Sirt1.

Other co-expressed genes are known to regulate gene expression by modifications of chromatin structure. In the *yellow_20* network, Phf21a, is a component of the BHC complex, a co-repressor complex that represses transcription of neuron-specific genes in non-neuronal cells by deacetylating and demethylating specific sites on histones (Shi, Matson, Lan, Iwase, Baba, and Shi, 2005). Accordingly, Phf21a is underexpressed in the 20 min dataset. In the *green_20* module, Cxxc1 (underexpressed) binds to demethylated regions of DNA to exhert its regulatory function.

In the *turquoise_20* module, the Arid1a gene shows significant downregulation at 20 min post-LTP. It is involved in chromatin remodelling and belongs to the neuron-specific chromatin remodelling complex (nBAF complex) (Wang, Nagl, Wilsker, Van Scoy, Pacchione, Yaciuk, Dallas, and Moran, 2004).The nBAF complex along with CREST plays a role regulating the activity of genes essential for dendrite growth and long-lasting forms of synaptic plasticity and

memory processes (Vogel-Ciernia and Wood, 2014). Also part of the same complex, Arid1b is an independent gene product that is overexpressed in one of the probes for 20 min. Different combinations of subunits in the nBAF complex are found in different tissues and cell-types. Another member of the nBAF complex, Smarcb1, appears in the *brown_20* module, and shows a modest downregulation in the 24 h dataset. In fact, this diversity in the subunit composition can target different sets of genes (Ronan, Wu, and Crabtree, 2013). The combinatorial diversity of the nBAF complex may explain the complex pattern of expression exhibited by the different subunits in the three time datasets, as depicted in Figure 6.9b.

Also in the *turquoise_20* network, the Ring1 gene encodes for a ubiquitin-protein ligase associated with the ubiquitination of the histone H2A, playing a central role in epigenetic gene regulation. It is overexpressed in the 20 min dataset (Cao, Tsukada, and Zhang, 2005). In the *black_20* module, Setdb1 encodes for a histone methyltransferase.

Gene expression modulation is also central in the co-expression modules identified 5 h post-LTP induction. However, the top genes involved in regulation of gene expression seem to be related with either epigenetic regulation of chromatin structure or with transcriptional repression. As we discussed in the previous sections, the nBAF complex seems to have a central role in regulating gene expression necessary for LTP. In two of the networks identified at 5 h (*midnightblue_5H* and *magenta_5H*), components of the nBAF complex represent top hubs, Arid1a and Smarcb1. A number of other enzymes involved in the modification of histones appear as top hubs in other networks (Kdm6b, downregulated at 5 h and encoding a histone demethylase, and Hdac5, a histone deacetylase). In the *lightgreen_5H* module, H3f3b encodes for a variant histone H3 which replaces conventional H3, while in the *darkred_5H* module, Tada3l is a component of the PCAF complex, which functions as histone acetylase in a nucleosomal context (Ogryzko, Kotani, Zhang, Schiltz, Howard, Yang, Howard, Qin, and Nakatani, 1998). Finally, Zmynd11 encodes for a zinc finger transcriptional co-repressor which binds to histone H3. Differential expression of all these genes is found at 20 min or 5 h but never at 24 h.

Alongside the identified epigenetic regulators, a large number of transcriptional repressors are identified as hubs in the 5 h modules. In particular, the *green_5H* module contains Foxn3, Morc2, and Bhlhe41, genes encoding for transcriptional repressor (Scott and Plon, 2005; Shao, Li, Zhang, Liu, Liu, Zhao, Shen, and Li, 2010; Garriga-Canut, Roopra, and Buckley, 2001) Trps1 and Tbx3 are other transcriptional repressors identified as hubs in other 5 h networks.

Gene expression has still an important role at 24 h and many of the main hubs in the networks that exhibit a gain of intramodular connectivity are involved in gene expression regulation. In particular, epigenetic regulation appears as a mayor modulator of gene expression.

In the *green_24* module, a main hub is constituted by the Junb gene, which is a well-characterised IEG in LTP (Chiu *et al.*, 1988) and exhibits an upregulation in the 20 min dataset. Junb can dimerize with the Fos family oncogenes to form the DNA-binding AP-1 heterodimer. Other transcription factors are Hdgf and Cc2d1a (transcriptional repressors), and Pbx2.

6.3.6 RNA processing and ubiquitin-proteasome pathway

From the co-expression networks identified in the 20 min dataset, the role of RNA processing is apparent. One of the main hubs in the *brown_20* network is the Tnrc4 gene (Celf3), which encodes for an RNA-binding protein involved in the regulation of mRNA alternative splicing. Perhaps important in the overlapping phases of new RNA synthesis and regulation. In particular, Celf3 activates the splicing of MAPT/Tau exon 10, whose missplicing has been shown to cause frontotemporal dementia (Wang, Gao, Wang, Lafyatis, Stamm, and Andreadis, 2004). In the same cluster, the protein encoded by Rnpc3 is also involved in mRNA splicing (Benecke, Lührmann, and Will, 2005), while Pnisr encodes for an arginine/serine-rich protein that binds to poliA in RNA (Baltz, Munschauer, Schwanhäusser, Vasile, Murakawa, Schueler, Youngs, Penfold-Brown, Drew,

Milek, *et al.*, 2012). Both are downregulated at 20 min post-LTP.

Dnajb5 encodes for an homolog of the Hsp40 chaperone, whose function consists in binding and stabilising proteins in a complex together with Hsp70, to subsequently transport them to the particular subcellular location where they are to exert their functions (Hartl, 1996). Chaperones have been shown to be localised in postsynaptic sites (Ohtsuka and Suzuki, 2000) and they have been proposed to be involved in the mechanisms that induce functionally active AMPA receptor during induction of LTP (Song, Kamboj, Xia, Dong, Liao, and Huganir, 1998). The overexpression is statistically significant in the three probes for Dnajb5 at 20 min ($p = 0.05$).

In the *red_20* module, Ccdc86 and Lgals3 also encode for proteins involved in RNA processing. The former displays overexpression in the 20 min arrays and the latter encodes for Galectin-3, a pre-mRNA splicing factor (Haudek, Spronk, Voss, Patterson, Wang, and Arnoys, 2010).

Other differentially expressed genes involved in mRNA processing are Mmaa, Zranb2, and Eftud2 (all downregulated 20 min post-LTP), Syncrip, Fam98a, Fkbp11, Pabpn1. Perhaps the best example of the genes taking part in the regulation of mRNA post-translational processing is Btg2, which is highly overexpressed. Btg2, in the *turquoise_20* network, is related to neuronal differentiation (el Ghissassi, Valsesia-Wittmann, Falette, Duriez, Walden, and Puisieux, 2002) and is considered to be necessary for neurite outgrowth (Miyata, Mori, and Tohyama, 2008).

In the top genes identified, at least 4 genes have a role in protein ubiquitination – Psmc4 and Siah2 (*black_20*, Asb14 (*blue_20*), Trim17 (*turquoise_20*), and Znrf2 (*yellow_20*). Siah2, which encodes for an E3 ubiquitin-protein ligase, shows a statistically significant pattern of overexpression in the 20 min arrays whereas Znrf2, another ubiquitin-protein ligase, shows downregulation. The latter is known to be present in presynaptic plasma membranes (Araki and Milbrandt, 2003).

An atypical E3 ubiquitin-protein ligase is encoded by the Zfp91 gene. It is indirectly involved in activating the NFκB pathway, a pathway shown to be involved in hippocampal synaptic plasticity (Albensi and Mattson, 2000; Ahn *et al.*, 2008; Jin, Jin, Jung, Lee, Lee, and Lee, 2010) and long-term memory formation (Meffert, Chang, Wiltgen, Fanselow, and Baltimore, 2003; Kaltschmidt and Kaltschmidt, 2009). Furthermore, NFκB was identified as a central regulator in the most significant network identified at 20 min by IPA (Ryan *et al.*, 2011). NFκB pathway may also be modulated by epigenetic mechanisms (Lubin, Roth, and Sweatt, 2008).

In the *magenta_5H* module, the Cul5 gene encodes for a fundamental component of a number E3 ubiquitin-protein ligase complexes, while Usp11 encodes for a protease able to remove ubiquitin from ubiquitinated proteins. Both genes are downregulated at 5 h and the latter inhibits the degradation of target proteins and plays a role in the regulation of pathways leading to NFκB activation (Yamaguchi, Kimura, Miki, and Yoshida, 2007). Trim2 and Arih1 encode for E3 ubiquitin-protein ligases (the former involved in neuroprotective functions) and are both also differentially underexpressed.

Other genes involved in proteasomal degradation are Psmd11 and Psme, encoding a subunit of a proteasome regulator and a component of the 26S proteasome, respectively. However, these two genes do not show differential expression at the earlier times but only at 24 h.

In the 24 h modules, ubiquitination is still overrepresented, with Ube2g1 up, Hectd1, and Cul3 as main hubs. The former, overexpressed at 24 h while the other two are only downregulated at 5 h.

It is also worth mentioning that Rnasen, a hub in the *pink_U* module encodes for the ribonuclease 3, which is involved in the initial step of miRNA biogenesis and significantly underexpressed at 24 h. The importance of microRNAs in neural function has been studied (Mercer, Dinger, Mariani, Kosik, Mehler, and Mattick, 2008; Im and Kenny, 2012) and it has been suggested that they play a role in the late phases, in particular in growth and neurogenesis (Ryan *et al.*, 2012).

6.3.7 Intracellular signalling

The kinase-phosphatase system

The intracellular pathways activated following LTP can also be modulated by changes in gene expression.

Identified in the top 35 *brown_20* module but not differentially expressed, Fgd2 product is capable of activating Cdc42, which in turn indirectly activates Mapk8, a c-Jun kinase (Dérijard, Hibi, Wu, Barrett, Su, Deng, Karin, Davis, *et al.*, 1994). c-Jun is one of the most studied IEG involved in LTP, part of the AP-1 complex. Activated Mapk8 is also capable of phosphorylating Elk1 (Zhang, Yang, and Sharrocks, 2007), a transcription factor involved in the co-activation of SRE-dependent gene expression upon binding to SRF (see Figure 6.10 and Section 3.3.6). Dusp1 (dual specificity protein phosphatase 1), which shows a significant upregulation in the 20 min dataset, can dephosphorylate Mapk8.

Another overexpressed dual specificity protein phosphatase, Dusp13, appears in the same co-expression module. Although it shows no phosphatase activity on Mapk8, Erk2, p38 nor Map3k5, it does exhibit a phosphatase activity-independent regulatory role in Map3k5-mediated apoptosis, preventing Map3k5 inhibition by Akt (Park, Park, Kim, Song, Park, Lee, Kim, Choi, Kim, and Cho, 2010).

The CaMKII pathway is represented in the *red_20* network by Camk2d, which encodes for the CaMKII delta subunit, the principally expressed form only in brain (Schworer, Rothblum, Thekkumkara, and Singer, 1993). The alpha subunit (Camk2a), central to the NMDA receptor-dependent LTP, is identified in the *pink_20* network. In the same module, a CaMK-kinase (Camkk1) is able to phosphorylate CaMKI, CaMKId, CaMKIg and CaMKIV (Edelman, Mitchelhill, Selbert, Anderson, Hook, Stapleton, Goldstein, Means, and Kemp, 1996). It also indirectly promotes cell survival by phosphorylating and activating Akt1, which in turn inhibits the pro-apoptotic Bcl2-antagonist of cell death (see also Section 6.3.7). In the *brown_20* module by a potent and specific inhibitor of CaMKII (Camk2n1; Chang, Mukherji, and Soderling, 2001). While it shows no significant expression changes in the 20 min dataset, it is downregulated at 5 h.

In the *brown_20* network, two phosphatases are identified among the 35 top genes – Ankrd52 (an overexpressed putative regulatory subunit of protein phosphatase 6, PP6), and Arpp19, a cAMP regulated phosphoprotein that specifically inhibits protein phosphatase 2A (PP2A) during mitosis (Irwin, Chao, Goritchenko, Horiuchi, Greengard, Nairn, and Benowitz, 2002). Arpp19 is only downregulated at 5 h post-LTP. The brain-specific isoform of the B regulatory subunit of PP2A (Ppp2r2c) is overexpressed at 20 min and part of the top 35 *black_20*. Also overexpressed is the regulatory subunit 3D of PP1 (Ppp1r3d), identified within the *blue_20* network.

Three genes encoding for subunits of phosphatases, Ppp2r5a, Ppp3r2, and Ppp1r3b, are identified in the 24 h modules. Furthermore, Ppp2r5a and Ppp3r2 are both upregulated at 24 h.

Finally, it is worth mentioning the loss of intramodular connectivity exhibited by the *brown_5H* module. One of its main hubs is CaMKIV, which plays a pivotal role in memory consolidation by phosphorylation of CREB in the nucleus (Bito *et al.*, 1996). However, the expression of the gene is not altered significantly, which suggests that its activation is mainly driven by post-translational changes (CaM-Ca^{2+} binding and phosphorylation) rather than changes in expression. It does show, however, downregulation earlier in the 5 h dataset.

The PI3K-Akt-mTOR pathway

Akt1 (also known as protein kinase B, or PKB) appears as a central gene in the *pink_20* co-expression module, although it only shows a slight overexpression at 5 h (1.6-fold change). PDGF-BB stimulates the PI3K-Akt pathway by binding to Pdgfrb (Hanai, Tokuda, Ohta, Matsushima-Nishiwaki, Takai, and Kozawa, 2006), a receptor which we identified in our *brown_20* module.

Identified in the same module as Akt1, the overexpressed Cds2 gene encodes for an enzyme that provides CDP-DAG, precursor of PI.

In the *pink_20* module we find Dgkg, a gene that encodes for a DAG kinase (DGK) gamma, upregulated at 20 min. This enzyme catalyses the conversion of DAG phosphatidic acid (PA). Both molecules constitute messengers and hence the switch among the two regulates different cellular responses (Merida, Avila-Flores, and Merino, 2008). In fact, PA can bind and stabilise the mTOR complex (Fang, Vilella-Bach, Bachmann, Flanigan, and Chen, 2001). While the gamma isoform is highly expressed in retina and brain (Sakane, Yamada, Kanoh, Yokoyama, and Tanabe, 1990), the epsilon isoform has been demonstrated to modulate LTP (de Turco, Tang, Topham, Sakane, Marcheselli, Chen, Taketomi, Prescott, and Bazan, 2001).

Finally, it is worth mentioning the possibility of formation of 2-arachidonoylglycerol (2-AG) from DAG via DAG lipase (DGL). 2-AG is an endocannabinoid present at relatively high levels in the central nervous system and interacts with cannabinoid receptors. We highlighted in Section 6.3.9 the overexpression of the endocannabinoid receptor Cnr1.

The PI3K-Akt-mTOR pathway is represented in some of the 5 h modules. Dab2, downregulated at 5 h and hub in the *lightcyan_5H*, which modulates the balance between PI3K-Akt-mediated cell survival and MAP3K5-JNK signalling pathways (Xie, Gore, Zhou, Pong, Zhang, Yu, Vessella, Min, and Hsieh, 2009). Plekha1 in the *lightyellow_5H* module binds specifically to PIP_2 (Kimber, Deak, Prescott, and Alessi, 2003).

Finally, in the *darkred_5H* network, Ip6k1 encodes for an inositol hexakisphosphate kinase overexpressed at 5 h.

NFκB and other signalling cascades

The modulation of the Ras-Erk cascade is under-represented within the top genes, but some candidates, such as Plk2 (Polo-like kinase 2, *red_20*) and Rasip1 (Ras interacting protein 1, *blue_20*) are overexpressed. The former encodes for a Ser/Thr-protein kinase known to be involved in synaptic plasticity by regulating Ras protein signalling (Lee, Lee, Rozeboom, Lee, Udagawa, Hoe, and Pak, 2011). It has also a kinase-independent activity that occludes long-term depression (LTD) via disrupting the interaction between AMPA receptor and NSF (Evers, Matta, Hoe, Zarkowsky, Lee, Isaac, and Pak, 2010).

In addition to the Ras-Erk cascade, several modulators of the transcriptional activator NFκB appear in the early co-expression networks.

In the *green_20* module, Ubfd1 is hypothesised to act as NFκB regulator (Fenner, Scannell, and Prehn, 2009), while Ncoa3 (*turquoise_20* is involved in the co-activation of the NFκB pathway via its direct interaction with the Nfkb1 subunit. It also acts as a histone acetyltransferase (Chen, Lin, Schiltz, Chakravarti, Nash, Nagy, Privalsky, Nakatani, and Evans, 1997).

Map3k3 constitutes a hub in the *midnightblue_5H* module and shows a downregulation at 5 h. It encodes for a component of a protein kinase signal transduction cascade which mediates activation of the NFκB, AP1 and DDIT3 transcriptional regulators (Ellinger-Ziegelbauer, Brown, Kelly, and Siebenlist, 1997), the former two known to be key regulators in LTP gene expression. In the *lightyellow_5H* module, the Snip gene also regulates the NFκB signalling pathway (Kim, Flanders, Reffey, Anderson, Duckett, Perkins, and Roberts, 2001), but is downregulated at 24 h.

6.3.8 Extracellular signalling and cell adhesion

In the *red_20* module, Hmox2 (heme oxygenase 2) is implicated in the production of carbon monoxide in brain, a molecule that acts as a neurotransmitter (Rotenberg and Maines, 1990). Sv2b encodes for a synaptic vesicle glycoprotein. It plays a role in the control of regulated secretion in neural cells (Janz and Südhof, 1999) and exhibits upregulation at 20 min. The phosphorylation of Svp2 modulates binding to synaptotagmin, a membrane-trafficking protein (Pyle, Schivell, Hidaka, and Bajjalieh, 2000). In the *turquoise_20* module, Gjb5, encodes for an overexpressed gap junction protein.

Two receptor tyrosine kinases of the ephrin-receptor family (EphA3 and EphA4) are identified in the *black_20* network. These receptors are involved in bidirectional signalling into neighbouring cells upon membrane-bound ephrin binding.

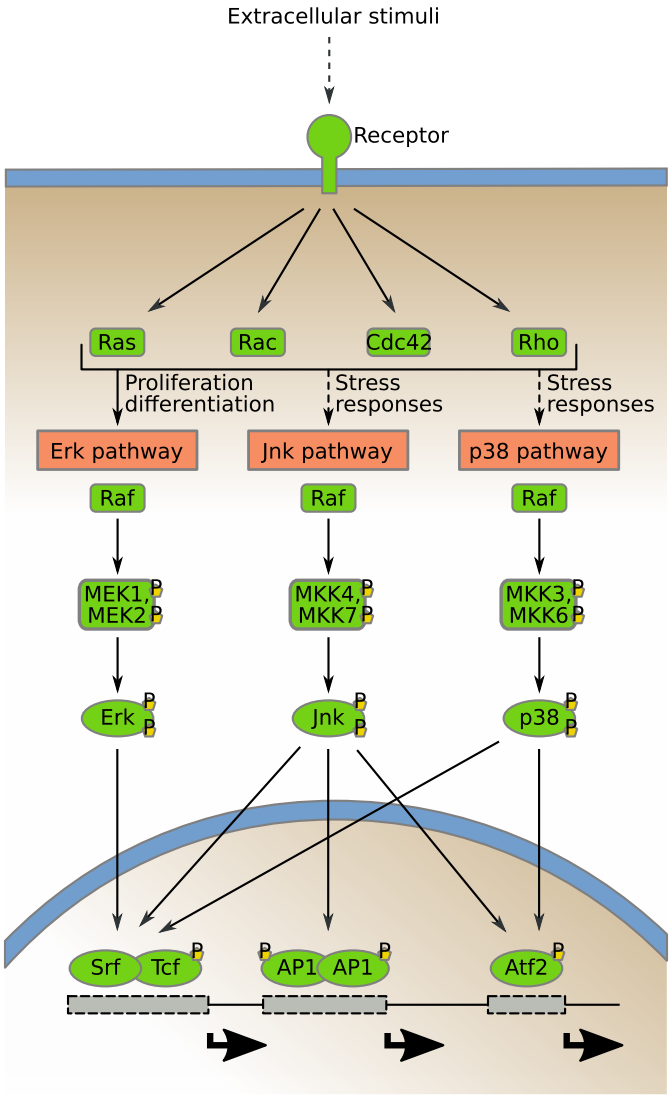

Figure 6.10: *Activation of MAPK pathways through the GTPase intermediates, leading to the expression of delayed-response genes.* Figure adapted from Liu *et al.* (2007)

Extracellular signalling is associated with cell-cell and cell-matrix adhesion. In the *magenta_20* network, the Cadm3 gene is involved in cell-cell adhesion. In the *green_20* network, Adam23, Cldn2, and Tnr are involved in cell-adhesion and interactions with different cells and matrix components. Adam23 is overexpressed, and Tnr, which encodes for Tenascin-R, has been shown to be central in LTP in mice (Saghatelyan, Dityatev, Schmidt, Schuster, Bartsch, and Schachner, 2001). In the *blue_20*, Itgb4 and Itgb7 encode for different integrin beta subunits, also involved in

cell adhesion.

Cadherin-3 (Cdh3 gene) and a cadherin-related protein (Mucdhl gene) are the main cell adhesion proteins found in the 24 h co-expression networks. The Ina gene, which encodes for a neuronal intermediate filament is also a major hub in the *green_24* module, involved in the morphogenesis of neurons (Fliegner, Ching, and Liem, 1990). Whereas both Cdh3 and Ina genes are overexpressed only at 20 min, their high TO within the networks suggest that the regulation of cell adhesion still has a central role at later stages of LTP and may be of importance for LTP maintenance.

6.3.9 Changes in membrane composition, endocytosis and exocytosis

Gene expression changes can have an effect on membrane composition via synthesis of proteins that regulate membrane channels trafficking, or by the expression of genes that encode for channel subunits.

Synthesis of new channel subunits

In the *brown_20* co-expression module Gabbr1 encodes for a subunit of the GABA receptor (see Section 3.1.3). It is worth noting that Gabbr1 expression changes significantly compared to the unstimulated control only in the 5 h dataset, in which the gene is downregulated around 15-fold.

Other genes that constitute channel subunits are identified in other co-expression modules. Cnr1, for example, encodes for the cannabinoid receptor 1, a receptor highly expressed in the hippocampus. In region CA1, the activation of these receptor leads to impairment of LTP and LTD by reducing presynaptic neurotransmitter release (Misner and Sullivan, 1999). Gpr26 (*pink_20* module) is overexpressed and encodes for an orphan receptor that stimulates adenylate cyclase and hence elevates intracellular cAMP.

In the *blue_20* module, Grm2 encodes for a G-protein coupled receptor for glutamate. Another glutamate G-protein coupled receptor appears in the *yellow_20* module, Grm6. The latter is overexpressed at 20 min. These type of receptors trigger a G-proteins signalling cascade upon glutamate binding, modulating down-stream effectors involved in synaptic plasticity (Devi, Markandeya, Maddodi, Dhingra, Vardi, Balijepalli, and Setaluri, 2013). Slc6a11 encodes for the sodium- and chloride-dependent GABA transporter 3, which terminates the action of GABA by its high affinity sodium-dependent re-uptake into presynaptic terminals (Borden, Dhar, Smith, Branchek, Gluchowski, and Weinshank, 1993).

Also in the *yellow_20* module, Htr3b encodes for one of the several known serotonin receptors. Serotonin serves as a neurotransmitter, hormone and mitogen. Binding of serotonin to the receptor causes a fast depolarising response.

The top genes in the 5 h networks are particularly enriched in genes functionally related with changes in post-synaptic membrane composition. Of note, Adrb1 and Adrb2 are both beta-adrenergic receptor subunits. These receptors mediate the catecholamine-induced activation of adenylate cyclase through the action of G proteins, and the former is upregulated at 20 min. Other receptors are Scn11a (sodium channel), Kcnk3 (voltage-insensitive, background potassium channel, which acts as an outward rectifier), Kcna2 (voltage-sensitive potassium channel), and Gabre and Gabrr1 (GABA receptor subunit epsilon and rho-1, respectively).

In the modules identified 24 post-LTP that show an gain of intramodular TO, a number of genes encoding for membrane channels and receptors appear as top hubs. Kcnj1 and Kcnj4 both encode for inward rectifier potassium channels, involved in the potassium homeostasis. Other hub genes that encode for membrane channels are shown in Table 6.3.

Expression of channel trafficking modulators

EAAC1 is the primary neuronal glutamate transporter from the extracellular environment in brain (Lin, Orlov, Ruggiero, Dykes-Hoberg, Lee, Jackson, and Rothstein, 2001), and it has been suggested to regulate the exposure of postsynaptic ionotropic GluRs to glutamate (He, Janssen, Rothstein,

Table 6.3: *Top hubs in the co-expression networks that function as membrane channels*

Module	Gene	Channel
blue_24	Kcnj1	Inward rectifier K^+ channel
turquoise_24	Kcnj4	Inward rectifier K^+ channel
	Cacna1i	Voltage-dependent L-type Ca^{2+} channel
midnightblue_24	Cacnb1	Voltage-dependent Ca^{2+} channel
magenta_U	Grm6	Metabotropic glutamate receptor
pink_U	Neto2	Accessory subunit of neuronal kainate-sensitive glutamate receptors
lightcyan_24	Abcc9	ATP-sensitive K^+ channel

and Morrison, 2000). While EAAC1 was not identified by the co-expression analysis, Arl6ip5 (GTRAP3-18), a negative modulator of EAAC1, appears in the *brown_20* network.

As we mentioned earlier, trafficking of AMPA receptors is a central mechanism in LTP (see Section 3.3). A number of genes identified in the analysis play such a role. Pick1 (*red_20*) is an adapter protein that may be involved in clustering of various receptors and is involved in the regulation of AMPA receptor trafficking. Via interaction with Arp2/3 complex, it has a role in cytoskeletal remodelling shown to regulate synaptic plasticity in excitatory synapses (Hanley and Henley, 2005; Rocca, Martin, Jenkins, and Hanley, 2008). Interestingly, the Arp2/3 complex appears in the *pink_20* module (see Section 6.3.10).

In the *black_20* module, Hip1 is involved in the regulation of AMPA receptor trafficking in the in an NMDA-dependent manner (Metzler, Li, Gan, Georgiou, Gutekunst, Wang, Torre, Devon, Oh, Legendre-Guillemin, *et al.*, 2003). Rab12 and Rab8b encode for small Rab GTPases, key regulators of intracellular membrane trafficking.

Cnih2 (in the *yellow_20* module) gene encodes for a cornichon, a protein involved in the modulation of AMPA receptor trafficking and gating properties. In the same network and in the *turquoise_20* network, two transmembrane AMPAR regulatory proteins (TARPs) are identified in the top 35 genes, Cacng4 and Cacng8, respectively. They encode for the voltage-dependent calcium channel gamma-4 and gamma-8 subunits respectively (Milstein, Zhou, Karimzadegan, Bredt, and Nicoll, 2007).

Other central genes in the co-expression networks modulate the pathways leading to changes in the protein characteristics following LTP at 5 h. Clathrin-mediated exocytosis has been demonstrated to be required for some forms of LTP (Wang and Linden, 2000), and Ap2b1 in the *black_5H* network encodes for a component of the adaptor protein complex 2 (AP-2), which regulates protein transport via clathrin-transport vesicles (Owen, Collins, and Evans, 2004). In the *lightgreen_5H* module, Cnih2 encodes for the protein cornichon homolog 2, identified also in the *yellow_20* module as a 20 min hub and involved in the regulation of trafficking and gating properties of AMPA receptors but only differentially upregulated at 5 h. Another gene that appears as a hub in a 20 min module and a 5 h module (*salmon_5H*) is Arl6ip5, which regulates intracellular concentrations of taurine and glutamate and downregulated at 5 h (see Section 6.3.9).

Finally, in the *lightcyan_5H*, Homer2 appears as a top hub although it is only overexpressed in the 20 min dataset. Homer2 protein binds Shank1, a hub in the *purple_5H* network and previously described (see Section 6.3.4). The different Homer proteins (Homer1 and Homer3), despite not representing important hubs in the co-expression networks, do show a significant overexpression at different times (Homer1 at 20 min and 24 h, Homer3 at 5 h). Consistently, the different Homer proteins are known to be differentially regulated and may play important roles in the maintenance of the synaptic plasticity. In the hippocampus, for example, Homer1 and Homer2 are mainly localized in the CA1 region and CA1-CA2 region, respectively, whereas Homer3 is concentrated in the CA2-CA3 regions (Shiraishi-Yamaguchi and Furuichi, 2007).

Putative modulators of membrane composition with a role at 24 h may involve Dlg4, which interacts with the cytoplasmic tail of NMDA receptor subunits, required for synaptic plasticity associated with NMDA receptor signalling. Furthermore, overexpression or depletion of the Dlg4 gene changes the ratio of excitatory to inhibitory synapses in hippocampal neurons (Prange, Wong, Gerrow, Wang, and El-Husseini, 2004). Ap2a2 in the *pink_24* module encodes for the alpha-2 subunit of the AP-2 complex, involved in protein transport. The beta subunit, Ap2b1 was found as hub in the *black_5H* network.

6.3.10 Neuronal structural changes via cytoskeletal remodelling

A number of genes identified in the co-expression networks have roles in the structural reorganisation of the cytoskeleton. Table 6.4 summarises these findings.

Table 6.4: *List of genes identified in the top 35 genes of the WGCNA modules recruited 20 min post-LTP involved in cytoskeletal remodelling*

Module	Gene	Encoded protein	Function	Refs.
brown_20	Diaph3	Protein diaphanous homolog 3	Recruits profilin to the membrane and promotes actin polymerisation	(1)
	Sema6a	Semaphorin-6A	Promotes reorganization of the actin cytoskeleton. Plays a role in axon guidance in the developing CNS	(2)
	Tnn	Tenascin-N	Involved in neurite outgrowth and cell migration in hippocampal explants in mouse. OVEREXPRESSED	(3)
red_20	Fmnl1	Formin-like protein 1	Involved in the regulation of cell morphology and cytoskeletal organization. Required in the cortical actin filament dynamics and cell shape	(4)
	Parvb	Beta-parvin	Participates in the reorganization of the actin cytoskeleton	(5)
	Snip	SRC kinase signalling inhibitor 1	Regulates dendritic spine morphology. Involved in calcium-dependent exocytosis	(6)
magenta_20	Actr10	Actin-related protein 10		
yellow_20	Wasl	Neural Wiskott-Aldrich syndrome protein	Regulates actin polymerization by stimulating the actin-nucleating activity of the Arp2/3 complex. UNDEREXPRESSED	(7)
green_20	Add3	Gamma-adducin	Membrane-cytoskeleton-associated protein that promotes assembly of spectrin-actin network	(8)
	Col6a1	Collagen		
	Sfrp5	Secreted frizzled-related protein 5	Involved in axis elongation in the retina	(9)
pink_20	Arpc3	Actin-related protein 2/3 complex subunit 3	Component of the Arp2/3 complex, which is involved in regulation of actin polymerization. Mediates the formation of branched actin networks. (See also Pick1 in 6.3.9)	(10)
	Krt18	Keratin type I	Plays a role in filament reorganisation	(11)
	Plekho1	Pleckstrin homology domain-containing family O member 1	Involved in actin regulation. May inhibit Akt1 upon binding	(12)
	Pacsin1	Syndapin-1	Plays a role in the reorganization of the actin cytoskeleton and in neuron morphogenesis, also involved in neurite formation, neurite branching and the regulation of neurite length	(13)
black_20	Sgcg	Gamma-sarcoglycan	Cytoskeleton component that forms a link between the F-actin cytoskeleton and the extracellular matrix. Muscle specific. OVEREXPRESSED	(14)

(1) Tominaga et al.*, 2000; (2) Janssen* et al.*, 2010; (3) Neidhardt* et al.*, 2003; (4) Bai* et al.*, 2011; (5) Yamaji* et al.*, 2004; (6) Jaworski* et al.*, 2009; (7) Zhang* et al.*, 2009; (8) Gardner* et al.*, 1987; (9) Chang* et al.*, 1999; (10) Welch* et al.*, 1997; (11) Caulin* et al.*, 1997; (12) Canton* et al.*, 2005; (13) Dharmalingam* et al.*, 2009; (14) Chan* et al.*, 1998;*

Actin polymerisation represents the major cytoskeletal remodelling cellular system in the 24 h modules, with cardiac muscle actin standing as a hub in the *magenta_U* module. Hspb3 and Enah are both involved in actin polymerisation, the former being an inhibitor, both only overexpressed at

20 min. Other cytoskeletal modulators are Map1b, involved in the tyrosination of alpha-tubulin in neuronal microtubules, and Sept3, a GTPase filament-forming specific of neural tissue.

6.3.11 Neurogenesis and cell death

Although a number of genes with putative roles in cell-cycle appear in the early co-expression networks, perhaps the most representative is Pola2, the gene encoding for the DNA polymerase alpha subunit B. It is overexpressed and central to the *turquoise_20* module.

In the *brown_20* module, Eps15 encodes for an epidermal growth factor receptor substrate involved in cell growth regulation. In the *red_20* network, Ddr2 is underexpressed at 20 min and encodes for a cell surface receptor for fibrillar collagen and regulates cell differentiation, remodelling of the extracellular matrix, cell migration and cell proliferation. In the *pink_20* module, Bcl2l14 encodes for a Blc2-like protein involved in apoptosis. Bcl2 is inhibited by Akt1, also present in the module and discussed previously (Section 6.3.7).

The long form of the GTPase PIKE-L, which activates nuclear PI3K, interacts with Homer1c and Homer2a together with mGluR1a/5 to form an mGluR1a/5-Homer-PIKE-L complex which leads the activation of PI3K and the prevention of neuronal apoptosis (Rong, Ahn, Huang, Nagata, Kalman, Kapp, Tu, Worley, Snyder, and Ye, 2003). In the *black_5H* and *darkred_5H* modules respectively, the Aven and Dapk2 genes encode for regulators of apoptosis and are both overexpressed at 5 h. Aven protects against apoptosis and Dapk2 is involved in cell survival, apoptosis, and autophagy (Kawai, Nomura, Hoshino, Copeland, Gilbert, Jenkins, and Akira, 1999; Chau, Cheng, Kerr, and Hardwick, 2000).

The Cdk5r2 gene encodes for a neural Cdc2-like kinase involved in cell cycle and another hub, Rif1, functions as a cell cycle check point in humans (Silverman, Takai, Buonomo, Eisenhaber, and de Lange, 2004). On the other hand, the Plekhg2 gene and Arhgef7 are involved in the regulation of apoptosis. The former encodes for a pleckstrin homology domain-containing protein – other proteins with the same domain were identified in other networks and discussed previously (see Sections 6.3.10 and 6.3.7). In the *brown_U* module, Robo1 is involved in axon guidance, while Ptk2, in the *greenyellow_24*, regulates axon growth and neuronal cell migration, axon branching and synapse formation and is involved in a plethora of cellular functions related with LTP (Burgaya and Girault, 1996).

6.3.12 Immunity-related genes

Genes involved in the modulation of T-cell-mediated immunity are Cd8b, a T-cell surface glycoprotein involved in the regulation of immune response (*pink_24* module), Ctla4, a inhibitory receptor acting as a major negative regulator of T-cell responses (Prange *et al.*, 2004) (*midnightblue_24*) and is overexpressed at 20 min. Ptpn22, which encodes for a negative regulator of T-cell receptor signalling (*purple_24*) is overexpressed at 5 h.

Other immunity-related genes are Cst7 (Cystatin-F) (20 min), Itgb7 (Integrin beta-7) (20 min) and Il5 (Interleukin-5) (20 min). Interestingly, these genes are differentially expressed at 20 min.

Furthermore, a number of Interleukins have been related with LTP (IL-1b, Cunningham, Murray, O'Neill, Lynch, and O'Connor (1996); IL-2, Tancredi, Zona, Velotti, Eusebi, and Santoni (1990); IL-6, Bellinger, Madamba, Campbell, and Siggins (1995); IL-10,Kelly, Lynch, Vereker, Nolan, Queenan, Whittaker, O'Neill, and Lynch (2001); IL-18, Curran and O'Connor (2001)) and they show a significant upregulation especially in the earliest time-point (20 min, see Figure 6.9b).

6.4 Discussion

We reanalysed the microarray data in the differential expression analysis presented in Chapter 5, which served as a starting point to our study. Our results are largely identical to the originally

reported in Ryan *et al.* (2011, 2012), with expected minor differences caused by the updated databases of transcript-gene mappings, together with the cut-offs used in the lists of overexpressed genes.

Compared to traditional differential expression analysis, co-expression is less error-prone for genes with a large expression variation. Perhaps more importantly, genes which are not detected by differential expression can (potentially) be detected by this type of analysis if they activate other genes which change enough to be detected. Arguably, a pair of genes with a high value of co-expression are likely to be forming complexes, pathways, or participate in the same cellular circuits (Eisen, Spellman, Brown, and Botstein, 1998).

We found that the rapid increase in gene expression observed by differential expression analysis is complemented by the increase in intramodular connectivity (average TO, see Section 6.3). Note that out of the 58 modules identified, only one exhibits a significant decrease in average TO from the control to the 20 min time point, while a total of 20 show a significant increase. This suggests that the rapid genomic response that follows LTP induction does not only involve a marked upregulation of gene expression, but also a tight coordination of the components that ultimately allow the transition to a new homeostatic cellular state.

The transitional 5 h dataset shows a loss of intramodular connectivity that parallels the onset of a general downregulation of gene expression, similar to the 24 h co-expression network. We believe that the early phase following stimulation is critical in the onset of the genomic changes that are known to be essential for L-LTP. A fundamental fraction of the genes that are transcribed rapidly after LTP induction may be of crucial importance at later times (Nguyen *et al.*, 1994).

6.4.1 LTP-induced transcription

A large number of transcriptional modulators appear as hubs in the 20 min co-expression modules, described in more detail in Section 6.3.5. Our results stress the importance of the Egr family, been previously reported to be expressed following LTP induction (see Section 3.3.6 and Figure 6.9). In addition to these expected results, we find that the Wt1 gene, a member of the same family, appears as a key regulator in the co-expression network at 20 min. This observation, together with the its role as a repressor of the other Egr family members (Haber *et al.*, 1991) suggests that it may play an important role in regulating Egr gene expression after LTP.

The Homer family is implicated in LTP though its association with the Ras-Erk1/2 pathway (see Section 3.3.4). Homer1 is overexpressed at 20 min and 24 h and has been extensively studied as an IEG. Likewise, Homer2 is overexpressed at 20 min whereas Homer3 is overexpressed at 5 h. It is known that these genes are differentially concentrated in different hippocampal regions (Shiraishi-Yamaguchi and Furuichi, 2007). Hence, it is conceivable that they may play important roles at different times after LTP induction. Note, however, that only Homer2 appears as a hub in a co-expression module. Another important hub is Shank1, whose protein recruits Homer to the membrane at the postsynaptic sites (Sala *et al.*, 2001). These findings are in agreement with the role of Homer1 as an IEG and further suggest that other members of the Homer family may be modulating gene expression at other times after induction, possibly even participating in LTP consolidation and maintenance.

The co-expression analysis also highlight the importance of the constitutive transcription factor NFκB, whose activity can be modulated in a transcription-independent manner. Its central role in LTP has been described elsewhere and discussed in previous sections (see Freudenthal *et al.* (2004); Meberg *et al.* (1996), and Sections 3.3.6 and 6.3.7). In particular, our results suggest that ubiquitin signalling may be of particular importance in the NFκB pathway during LTP. Within the top genes co-expressed at 20 min, the Zfp91 and the Siah2 genes encode for E3 ubiquitin-protein ligases indirectly involved in activating the NFκB pathway. In a later co-expression network identified at 5 h, the genes Cul5 and Usp11, which encode for components of the ubiquitin/protease system are

both underexpressed. The latter regulates pathways leading to the activation of NFκB.

Other highly co-expressed genes may be regulating the pathway via direct or indirect interaction with NFκB or its inhibitor IκB at different times post- induction, although mainly in the first time point – e.g. Ubfd1, Ncoa3, Map3k3. The Snip gene, appears as a hub at 24 h, which suggests that the modulation of the NFκB pathway may not be restricted to a short time frame following HFS, consistent with learning-related NFκB activity in the nucleus, which shows a peak immediately after training and a second peak between 6 and 12 h after training (Freudenthal and Romano, 2000), both necessary for memory consolidation (Merlo, Freudenthal, and Romano, 2002).

6.4.2 Epigenetic control of gene expression

The modification of chromatin structure arises as a fundamental mean of gene expression regulation – we find that a substantial number of highly co-expressed enzymes is involved in epigenetic control, DNA methylation/demethylation and post-translational modifications of histones.

The inhibition of DNA methyltransferases, has been shown to prevent LTP induction *in vitro* and to affect the methylation levels in the promoters of Reelin and Bdnf in the hippocampus (Levenson, Roth, Lubin, Miller, Huang, Desai, Malone, and Sweatt, 2006). *In vivo*, it has been shown that hippocampus-dependent learning can trigger changes in the methylation levels at the Reelin, PP1, and Bndf gene promoters. These changes were transient and normal levels were observed at 24 h after training (Miller and Sweatt, 2007; Lubin *et al.*, 2008). Furthermore, mice with a conditional knockdown of Dnmt1 and Dnmt3a, two DNA methyltransferases, show impairment of LTP and memory formation (Feng and Fan, 2009).

Although histone acetylation seems to be less determinant for memory formation, and inhibiting the action of histone acetylases can lead to improve memory formation (Levenson *et al.*, 2006; Guan, Haggarty, Giacometti, Dannenberg, Joseph, Gao, Nieland, Zhou, Wang, Mazitschek, *et al.*, 2009). An exception may be Sirt1. In a work carried out by Michán, Li, Chou, Parrella, Ge, Long, Allard, Lewis, Miller, Xu, *et al.* (2010), the authors evidenced the crucial role of Sirt1, a histone deacetylase, in the induction of LTP. Sirt1 was able to inhibit the transcription of miR-134, a small non-coding RNA molecule (microRNA or miRNA), able to bind to CREB mRNA and inhibit its transcription. Furthermore, LTP induction in hippocampal slice cultures from Sirt1 loss-of-function mice was impaired. Similarly, overexpression of miR-134 resulted in LTP impairment. In the case of the loss-of-function mutation, LTP was restored by the knockdown of miR-134. Furthermore, a recent large-scale study by Joilin, Guévremont, Ryan, Claudianos, Cristino, Abraham, and Williams (2014) documented a generalised and rapid down-regulation of a large number of miRNAs following LTP induction.

In the light of these results, the overexpression observed in the 20 min dataset of the tumor suppressor Hic1 is difficult to interpret, since it is known to transcriptionally repress Sirt1 (Chen *et al.*, 2005). The functions of Hic1, however, are not restricted to the inhibition of Sirt1. In addition, the repression of Sirt1 requires the formation of a Hic1/Sirt1 complex, which acts on its promoter region (Chen *et al.*, 2005). Hence, downregulation of Sirt1 is directly dependent on its own protein levels, and this pathway may only represent a homeostatic mechanism to prevent overexpression of the deacetylase, which can increase cell proliferation cancer risk (Liu, Liu, and Marshall, 2009). The Bcl6 gene, an epigenetic regulator involved in the control of neurogenesis also requires the recruitment of Sirt1 (Tiberi *et al.*, 2012).

The large number of transcriptional regulators that directly affect chromatin structure that appear as hubs in the co-expression networks identified 20 min post-LTP – e.g. Phf21a, Cxxc1, Ring1, Setdb1, and members of the neuron-specific chromatin remodelling complex (nBAF) – suggest that the epigenetic regulation is central to the early stages after the induction of LTP. However, in the 5 and 24 h datasets, other members of the nBAF complex appear as highly co-expressed, together with a significant number of epigenetic regulators, suggesting that the control of gene expression

by chromatin modification may be a fundamental process throughout the different stages of LTP. It is apparent that these mechanisms do not work in isolation, but rather in conjunction with other mechanisms (Lubin, Gupta, Parrish, Grissom, and Davis, 2011).

6.4.3 Regulation of signalling pathways via changes in gene expression

Regulation of the kinase-phosphatase system

The modulation of the Ras-Erk1/2 pathway appears to happen mainly in the 20 min dataset. In addition to the discussed Homer1, some candidate modulators such as the complex formed by Ywhab and Akirin2 show a high co-expression. This complex represses the transcription of Dusp1, which is responsible for the inactivation of Erk1/2 (see Section 6.3.5). While the Dusp family has been implicated in LTP previously, our results suggest that Akirin2 and Ywhab may also have an important role despite not showing a significant overexpression in the 20 min dataset. Downstream of Erk1/2, Erf encodes for a transcription factor involved in the control of cell cycle.

Perhaps one of the most extensively studied molecular systems involved in LTP is the kinase-phosphatase system. Changes in gene expression also modulate this structure – a large number of kinases and phosphatases were identified across the different co-expression modules (see Section 6.3.7).

It is well known that PKA boosts CaMKII in the CaMK switch in the early stages of LTP (see Section 3.3.1) by phosphorylation of I1, which in turn inhibits PP1. While the CaMKII-PP1 system may not be necessary for an early-LTP molecular switch as proposed by Lisman in 1985, the crosstalk between CaM-kinases and phosphatases has a fundamental role in LTP (Allen, Hvalby, Jensen, Errington, Ramsay, Chaudhry, Bliss, Storm-Mathisen, Morris, Andersen, *et al.*, 2000; Greengard, Allen, and Nairn, 1999). However, the high co-expression and significant upregulation at 24 h of a number of genes encoding for phosphate subunits suggests that kinase-phosphatase regulation may also be relevant in the persistence of LTP.

Regulation of the Akt pathway and lipid signalling

The involvement of Akt (or PKB) in LTP in the hippocampus has been suggested to be mediated by phosphatidylinositol 3-kinase (PI3K). PI3K may be required for the expression and maintenance of L-LTP in the CA1 region of the hippocampus (Sanna, Cammalleri, Berton, Simpson, Lutjens, Bloom, and Francesconi, 2002; Karpova, Sanna, and Behnisch, 2006) through extracellular signals in a kinase-independent manner (Opazo, Watabe, Grant, and O'Dell, 2003). PI3K phosphorylates the D-3 position of the inositol ring of phosphoinositides in the plasma membrane, which converge with phosphoinisitide-dependent kinase-1 (Pdk1) to activate Akt. This convergence is also of a spatial nature, since the activated phosphoinositides are restricted to the membrane. Full activation of Akt is the result of phosphorylation by the mTOR protein kinase. PI3K activity increases in response to Ca^{2+}/CaM, binding to AMPA receptors and driving their insertion during LTP (Man, Wang, Lu, Ju, Ahmadian, Liu, D'Souza, Wong, Taghibiglou, Lu, *et al.*, 2003).

Not surprisingly, Akt1 is central to a module in the 20 min dataset, even though its differential expression is not significant (only moderately overexpressed at 5 h). Interestingly, the analyses performed by Ryan *et al.* (2011) on the same expression data did not identify Akt as an important gene in their Network 2, which contains PI3K. That same network had as a central hub the platelet-derived growth factor-binding protein homodimer (PDGF-BB), known to stimulate the pathway by binding the receptor Pdgfrb (Hanai *et al.*, 2006), which we also identified in a 20 min module. Upon ligand binding, Pdgfrb activates the Akt signalling pathway via diacylglycerol (DAG)-inositol triphosphate (IP_3) (Kashishian, Kazlauskas, and Cooper, 1992). It can also stimulate the Ras-Erk1/2 pathway (Yokote, Mori, Hansen, McGlade, Pawson, Heldin, and Claesson-Welsh, 1994) and it is involved in the activation of c-fos transcription (Kruijer, Cooper, Hunter, and Verma, 1983).

The identification in the same module of other members of the DAG-IP_3 pathway as Akt1, such as Cds2, suggests that these pathways may be acting in conjunction. The Cds2 gene, also

overexpressed, encodes for an enzyme that provides CDP-DAG, precursor of PI (PI $\xrightarrow{PI3K}$ PIP_2).

The enzymatic reactions represented in Figure 6.11 can be summarised as

$$PIP_2 \xrightarrow{PI3K} PIP_3$$

$$PIP_2 \xrightarrow{PLC} DAG + IP_3$$

In the first case, PIP_3 then activates Akt, which subsequently activates mTOR. On the other hand, the DAG-IP_3 pathway requires the action of phospholipase C (PLC) upon PIP_2. The cleavage of the transmembrane molecule frees IP_3, that diffuses in the cytoplasm acting as a second messenger. Upon binding to IP_3 receptors in the endoplasmic reticulum, more Ca^{2+} is released into the cytoplasm. There is evidence that IP_3 plays an important role in signalling in some types of synaptic plasticity (Sarkisov and Wang, 2008). In turn, DAG acts in conjunction with the raise in Ca^{2+} to activate PKC and facilitate its translocation to the membrane (Nishizuka, 1995).

Together with the identification of other components of the lipid signalling pathway at 20 min and presented in more detail in Section 6.3.7, these findings indicate that lipid signalling actively participates in the induction of LTP, further supporting the notion that PI3K gene-expression pathway may be of importance in the early stages of LTP (Sanna *et al.*, 2002).

The regulation of the PI3K-Akt-mTOR pathway by changes in gene expression may also occur at 5 h, as evidenced by the identification of the genes Dab2 and Plekha1. These components of the pathway – Dab2 is significantly downregulated at 5 h – are highly co-expressed at 5 h, suggesting that the regulation of this pathway could be coordinating LTP-related molecular events at different time scales.

6.4.4 Other overrepresented functions

The results reported in Chapter 6 highlight a number of other overrepresented functions. In the first place, it is worth commenting the importance of the regulation of the protein product for L-LTP. In particular, we find a large number of genes involved in the ubiquitin-proteasome pathway. In this respect, a study by Dong, Upadhya, Ding, Smith, and Hegde (2008) already suggested that proteasome activity obstructs the maintenance of L-LTP by interfering with transcription and translation.

The 5 h and 24 h networks are to be enriched in a higher number of genes involved in the ubiquitin-proteasome pathway compared to the earlier networks, suggesting that protein degradation via ubiquitination may be amplified following the early phase of LTP.

Several genes co-expressed at 20 min have functions related with extracellular signalling and anchoring. The ephrin-receptors identified stress the importance of bidirectional signalling.

The involvement of this trans-synaptic signalling in hippocampal synaptic plasticity has been documented in several studies. Using hippocampal slices from gene-targeted mice, the requirement of Epha4 for the early stages of LTP at the CA3-CA1 synapses has been documented. Similarly, EphB receptors are thought to be necessary in the postsynaptic membrane for the induction of mossy fiber-CA3 synapses (Contractor, Rogers, Maron, Henkemeyer, Swanson, and Heinemann, 2002). Epha5, in turn, is known to be involved in guidance of hippocampal axons during development (Klein, 2008). Genes involved in cell adhesion were also identified at different times in the co-expression networks.

Gene expression changes also influence membrane composition. The synthesis of both trans-membrane channel subunits and proteins that modulate their trafficking to the membrane is central to synaptic plasticity. Not surprisingly, a large number of genes with membrane functions were

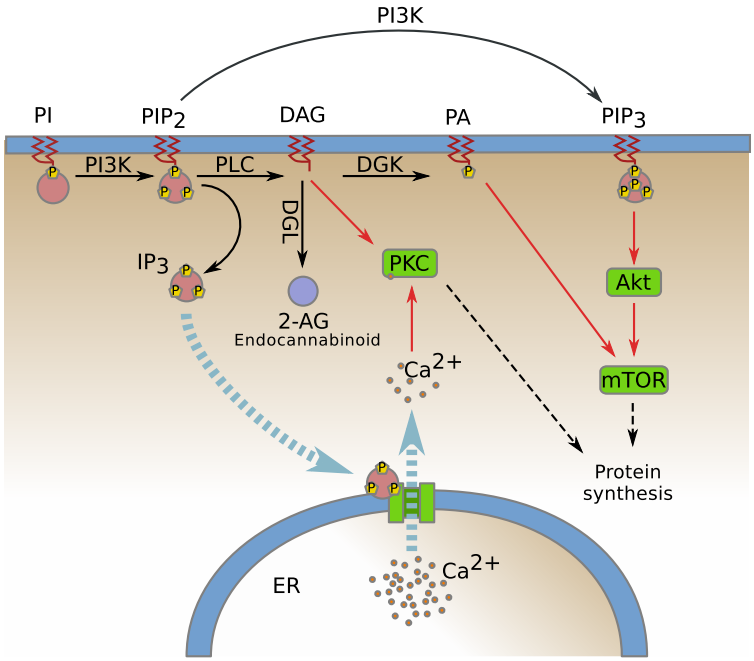

Figure 6.11: *Depicted in the figure are the different compounds involved in lipid signalling. Black arrows indicate enzymatic reaction, red arrows represent activation and blue dashed lines represent translocation*

identified in the co-expression networks. Indeed, across the three temporal datasets, a substantial number of channels and trafficking modulators appear as hubs.

For example, we found that Gabbr1, a hub in a 20 min module, was downregulated – around 15-fold compared to the control – only in the 5 h dataset. This downregulation may be directly implicated in facilitating LTP induction, as demonstrated by an experimental study carried out in hippocampal slices (Wigström and Gustafsson, 1983).

Other receptors known to be involved in LTP and identified as hubs in the co-expression analysis are cannabinoid receptors – Cnr1, a subunit highly expressed in the hippocampus whose activation leads to impairment of LTP and LTD (Misner and Sullivan, 1999) –, and receptors for glutamate coupled to G-proteins.

As we mentioned in previous sections, the trafficking of AMPA receptors is a central mechanism in LTP (see Section 3.3). Not surprisingly, we found a considerable number of gene playing this role. We want to stress the importance of cornichons, proteins involved in the modulation of AMPA receptor trafficking and gating properties. These proteins target the AMPA receptor to the synaptic membrane and regulate their rates of activation, deactivation, and desensitisation (Schwenk, Harmel, Zolles, Bildl, Kulik, Heimrich, Chisaka, Jonas, Schulte, Fakler, *et al.*, 2009). Together with transmembrane (TARPs) – also identified as highly co-expressed in the 20 min dataset – cornichons seem to have a central role in the control of AMPA receptor gating in the hippocampus (Kato, Gill, Ho, Yu, Tu, Siuda, Wang, Qian, Nisenbaum, Tomita, *et al.*, 2010).

An interesting hub identified in the analysis is the gene encoding for Reelin, which has a variety of functions related to microtubule regulation in neurons, neuronal migration, and brain

development (Rice and Curran, 2001). It also participates in the composition, recruitment and traffic of NMDA receptor subunits in the hippocampus (Qiu, Zhao, Korwek, and Weeber, 2006), in the generation of dendrites, and in the formation of dendritic spines (Niu, Yabut, and D'Arcangelo, 2008). A study carried out by Weeber, Beffert, Jones, Christian, Förster, Sweatt, and Herz (2002) showed that LTP can be augmented in mice hippocampal slices by perfusing Reelin, whereas this effect is abolished in very low density lipoprotein receptor (VLDLR) and apolipoprotein E receptor (apoER) knockout mice. Both are receptors for apolipoprotein E. The modulatory effect of Reelin on LTP is hence likely to be dependent on both there receptors. This regulation may be related with the recruitment of NMDA receptor subunits. Interestingly there is no significant overexpression of the gene in any of the datasets and this gene was not identified with the classical differential expression analysis with the exception of a 1.75 : 1 ratio of underexpression in the 5 h dataset.

Neuronal structural changes are known to follow LTP induction. For example, the dendritic spines show morphological changes following the stimulation patterns that elicit LTP. The changes in morphology are associated with the polymerization of actin (Fischer, Kaech, Knutti, and Matus, 1998; Muller, Toni, and Buchs, 2000). The enlargement of spine heads follows closely the pharmacology, amplitude, time course, and spatial localisation with synaptic potentiation, and this effect is observed soon after potentiation (Matsuzaki *et al.*, 2004). The formation of new spines and the budding of dendritic filopodia are also modulated by synaptic activity (Ziv and Smith, 1996). However, new filopodia or spines require longer times, at least 20 min after the induction of LTP Maletic-Savatic, Malinow, and Svoboda (1999); Engert and Bonhoeffer (1999).

The actin cytoskeleton is particularly rich in dendritic spines (Matus, 2000). The role of actin in LTP seems to be central, as demonstrated by the impairment of LTP that actin inhibitors cause (Kim and Lisman, 1999; Krucker *et al.*, 2000). The inhibition of actin depolymerisation may be the process underlying the changes in the actin cytoskeleton caused by LTP *in vivo* (Fukazawa, Saitoh, Ozawa, Ohta, Mizuno, and Inokuchi, 2003). Changes in actin polymerisation stand as the main cytoskeletal remodelling mechanism later in the 24 h modules.

We have pointed out that changes in cell morphology play a fundamental role in LTP *in vivo*. However, morphological changes in the existing synapses are not the only macroscopic changes that occur following LTP induction. The creation of new synapses and neurogenesis are processes linked to LTP and long-term memory (Snyder, Hong, McDonald, and Wojtowicz, 2005; Bruel-Jungerman, Davis, Rampon, and Laroche, 2006). In fact, the hippocampal region in particular is known to produce new neurons in adults, a process driven by learning processes (see for example Dayer, Ford, Cleaver, Yassaee, and Cameron, 2003; Gould, Beylin, Tanapat, Reeves, and Shors, 1999; Shors, Miesegaes, Beylin, Zhao, Rydel, and Gould, 2001; Raber, Rola, LeFevour, Morhardt, Curley, Mizumatsu, VandenBerg, and Fike, 2004).

We briefly discussed the role of the protein Reelin, involved in AMPA receptor trafficking and spine formation 6.3.9. Interestingly, Reelin seems to be involved in the regulation of postnatal neurogenesis (Pujadas, Gruart, Bosch, Delgado, Teixeira, Rossi, de Lecea, Martínez, Delgado-García, and Soriano, 2010). Perhaps the most representative gene involved in cell-cycle, however, encodes for a DNA polymerase subunit. It is overexpressed and central to a 20 min co-expression module. The number of genes involved in regulation of neurogenesis suggests that neuronal proliferation has an important role in hippocampal LTP as suggested by other previous studies (Ryan *et al.*, 2011; Bruel-Jungerman *et al.*, 2006).

Finally, our findings also support the observation that immune response genes are implicated in LTP (Håvik *et al.*, 2007a). In particular, we identified immunity-related genes as hubs of some of the modules that exhibit a gain in intramodular connectivity at 24 h.

In conclusion, we suggest that the stabilisation of LTP requires the control of multiple cellular systems which act in coordination. Although these are not restricted to gene expression changes, we argue that the genomic response plays a fundamental role in L-LTP. Indeed, we speculate that

the partial overlap in time and space exhibited by these mechanisms confers an increased stability by redundancy to the observed cellular changes following LTP, which is a central discussion in the present thesis. This interpretation justifies the different experimental results on necessity and sufficiency of the key molecular species involved in LTP found across the literature (see Section 3.3). The stability of the molecular networks will be further discussed in the following sections.

6.5 Concluding remarks

The analyses outlined in the present chapter suggest that the rapid genomic response that follows LTP does not only involve a marked upregulation of gene expression, but also a tight coordination of its components. The early phase following stimulation must be critical in the onset of LTP, consistent with the notion that a fraction of the genes transcribed rapidly after LTP induction are of crucial importance at later times (Nguyen *et al.*, 1994).

In addition, it is apparent that the stabilisation of LTP requires the control of multiple cellular systems. These include the regulation of gene expression (in particular epigenetic regulation), changes in the LTP-related signalling pathways, changes in membrane composition, and structural changes at the neuronal level via cytoskeleton remodelling. While some of the findings reported in the present chapter support previous reports in the literature, it is worth stressing that a number of genes and pathways have not been previously reported to be central to LTP. In particular,

- Wt1, a repressor of the Egr gene family
- Different members of the Homer gene family may be playing roles at later stages of LTP
- nBAF complex regulation
- Akirin2 and Ywhab, modulating the Ras-Erk1/2 pathway
- Protein degradation by ubiquitination, in particular in the NFκB pathway
- Activatino of NFκB immediately following LTP induction and then again 24 h post-LTP
- Lipid signalling
- Cadherin and its role in morphogenesis at 24 h post-LTP

Table 6.5: *Gene modules identified at 5 h with gain of TO at 20 min and 5 h and a subsequent loss at 24 h*

Module	Top 5 genes	Protein	Function
blue_5H (cellular amino acid biosynthetic process)	Scn11a	Sodium channel protein type 11 subunit alpha	Mediates voltage-dependent sodium ion permeability of excitable membranes
	Abi3	ABI gene family member 3	In vitro, reduces cell motility
	Clec10a	C-type lectin domain family 10 member A	Probable role in regulating adaptive and innate immune responses
	Atp2a1	Sarcoplasmic/endoplasmic reticulum calcium ATPase 1	Unknown
	Cdkn2aipnl	CDKN2AIP N-terminal-like protein	Catalyses the hydrolysis of ATP coupled with the translocation of calcium from the cytosol to the sarcoplasmic reticulum

Continued on next page

Table 6.5 – *continued from previous page*

Module	Gene	Protein	Function
lightyellow_5H (CNS neuron axogenesis)	C1qtnf3	C1qtnf3 protein	Positive regulation of Erk1/2 and Akt cascades
	Fbln1	Fibulin-1	Role in cell adhesion and migration. Could play a significant role in modulating the neurotrophic activities of APP, particularly soluble APP
	St8sia3	Alpha-2,8-sialyltransferase	Protein glycosylation
	Havcr1	Hepatitis A virus cellular receptor 1 homolog	Unknown
	Anks1b	Ankyrin repeat and sterile alpha motif domain-containing protein 1B	May participate in the regulation of nucleoplasmic coilin protein interactions in neuronal and transformed cells. Overexpression can down-regulate APP processing
black_5H (anion homeostasis, synapse assembly)	Ap2b1	AP-2 complex subunit beta	Involved in protein transport via transport vesicles
	Slc2a4	Glucose transporter type 4	Insulin-regulated facilitative glucose transporter
	Pdzd4	Protein Pdzd4	PDZ domain containing protein
	Aven	Cell death regulator Aven homolog	May protect against apoptosis
	Agtpbp1	Agtpbp1 protein	In mice deglutamylates target proteins. Accumulation of tubulin polyglutamylation causes neurodegeneration
darkred_5H (chondroitin sulfate metabolic process)	Dcaf4	Protein Dcaf4	May function as a substrate receptor for CUL4-DDB1 E3 ubiquitin-protein ligase complex
	Pgp	Protein Pgp	Unknown
	Kras	GTPase KRas	Oncogene Ras protein with GTPase activity
	Dapk2	Death-associated kinase 2	Ca^{2+}/CaM-dependent kinase. Involved in cell survival and apoptosis
	Ip6k1	Inositol hexakisphosphate kinase 1	Enzyme involved in conversion of inositol phosphates
cyan_5H (regulation of DNA methylation)	Fmod	Fibromodulin	May have a primary role in collagen fibrillogenesis
	Fam135a	Protein Fam135a	Unknown
	Ankrd6	Similar to Diversin protein	Positive regulator of JNK cascade
	Fndc3c1	Protein Fndc3c1	Unknown
	Tardbp	Protein Tardbp	Similar to DNA TAR binding protein 43 and DNA binding
midnightblue_5H (chaperone mediated protein folding)	Myoz2	Myozenin-2	Plays an important role in the modulation of calcineurin signalling
	Itsn2	Intersectin-2	Regulates endocytic membrane traffic
	Zfp324	Protein Zfp324	Zinc finger containing protein
	Cenpq	Centromere protein Q	Involved in mitotic progression and chromosome segregation
	Arih1	E3 ubiquitin-protein ligase ARIH1	E3 ubiquitin-protein ligase, which catalyses polyubiquitination of target proteins
magenta_5H (progesterone receptor signalling pathway)	Mrpl35	Mitochondrial ribosomal protein L35	Ribosomal protein
	Prkd3	Serine/threonine-protein kinase D3	Converts transient DAG signals into prolonged physiological effects, downstream of PKC
	Cul5	Cullin-5	Core component of multiple E3 ubiquitin-protein ligase complexes
	Pqcp	Interferon regulatory factor 2-binding protein-like	Zinc finger containing protein
	Smarcb1	SWI/SNF-related matrix-associated actin-dependent regulator of chromatin subfamily B member 1	Core component of the BAF complex
green_5H (regulation of amino acid transport)	Prelid2	PRELI domain-containing protein 2	Phospholipid transport
	Prl2b1	Prolactin-2B1	May act as a hormone
	Abca8	ATP-binding cassette sub-family A member 8	Lipophilic drug transporter

Continued on next page

Table 6.5 – *continued from previous page*

Module	Gene	Protein	Function
	Foxn3	Checkpoint suppressor 1	Transcriptional repressor. May be involved in DNA damage-inducible cell cycle arrests
	Morc2	MORC family CW-type zinc finger protein 2	Involved in lipogenesis
darkturquoise_5H (negative regulation of protein autophosphorylation)	Atad2	ATPase family AAA domain-containing protein 2	May be required for histone hyperacetylation
	Jun	Transcription factor AP-1	Increases gene expression upon cAMP signaling pathway stimulation
	Ing3	Inhibitor of growth protein 3	Component of the NuA4 histone acetyltransferase complex
	Rbm8a	RNA-binding protein 8A	Core component of the splicing-dependent multiprotein exon junction complex
	Fkbp15	FK506-binding protein 15	May be involved in the cytoskeletal organization of neuronal growth cones
grey60_5H (regulation of branching involved in salivary gland morphogenesis)	Egln1	Egl nine homolog 1	Cellular oxygen sensor
	Gabre	GABA(A) receptor subunit epsilon	Major inhibitory neurotransmitter in the vertebrate brain
	Btbd16	BTB/POZ domain-containing protein 16	Unknown
	Ifi30	Gamma-interferon-inducible lysosomal thiol reductase	Lysosomal thiol reductase
	Tsen54	tRNA-splicing endonuclease subunit Sen54	Subunit of the tRNA-splicing endonuclease complex
lightcyan_5H (pyrimidine nucleotide metabolic process)	Adrb1	Beta-1 adrenergic receptor	Receptor that binds epinephrine and norepinephrine
	Dab2	Disabled homolog 2-interacting protein	Involved in PI3K-Akt and Map3k5-JNK signaling pathways
	Rhbdl3	Rhomboid-related protein 3	May be involved in regulated intramembrane proteolysis and the subsequent release of functional polypeptides
	Cyp11b1	Cytochrome P450 11B1, mitochondrial	Forms corticosterone
	Rprml	Reprimo-like protein	Unknown
lightgreen_5H (regulation of T-cell migration)	H3f3b	Histone H3.3	Variant histone H3
	Cnih2	Protein cornichon homolog 2	Regulates the trafficking and gating properties of AMPA receptors
	Trps1	Zinc finger transcription factor Trps1	Transcriptional repressor
	Tnfaip2	Tumor necrosis factor alpha-induced protein 2	May play a role as a mediator of inflammation and angiogenesis
	Fam46a	Protein Fam46a	RNA binding
turquoise_5H (DNA catabolic process)	Crhr1	Corticotropin-releasing factor receptor 1	G-protein coupled receptor. Promotes the activation of adenylate cyclase, leading to increased intracellular cAMP levels
	Kdm6b	Lysine-specific demethylase 6B	Histone demethylase
	F8	Coagulation factor VIII	Blood coagulation
	Rad52	DNA repair protein RAD52 homolog	DNA repair
	Exoc8	Exocyst complex component 8	Involved in the docking of exocytic vesicles with fusion sites on the plasma membrane
yellow_5H (positive regulation of response to interferon-gamma)	Arglu1	Arginine and glutamate-rich protein 1	Unknown
	Mccc1	Methylcrotonoyl-CoA carboxylase subunit alpha, mitochondrial	Amino acid degradation

Continued on next page

Table 6.5 – *continued from previous page*

Module	Gene	Protein	Function
	Tmem206	Transmembrane protein 206	Unknown
	Ypel4	Protein yippee-like 4	Unknown
	Tiparp	TCDD-inducible polyA polymerase	Formation of polyA chains
purple_5H (histone H3-K27 methylation)	Fgf21	Fibroblast growth factor 21	Stimulates glucose uptake in differentiated adipocytes
	Adcy4	Adenylate cyclase type 4	Membrane-bound, CaM-insensitive adenylyl cyclase
	Klhl22	Kelch-like protein 22	Substrate-specific adapter of a BCR (BTB-CUL3-RBX1) E3 ubiquitin ligase complex
	Gnal	Guanine nucleotide-binding protein G(olf) subunit alpha	Involved in various transmembrane signaling systems
	Kcnj12	ATP-sensitive inward rectifier potassium channel 12	Inward rectifying potassium channel activated by PI2P and that probably participates in controlling the resting membrane potential
salmon_5H (positive regulation of vasoconstriction)	Hs3st2	Heparan sulfate glucosamine 3-O-sulfotransferase 2	Sulfotransferase
	Hdac5	Histone deacetylase 5	Deacetylation of lysine residues on core histones
	Ccdc115	Coiled-coil domain-containing protein 115	Unknown
	Gabrr1	GABA(A) receptor subunit rho-1	Major inhibitory neurotransmitter in the vertebrate brain
	Arl6ip5	PRA1 family protein 3	Regulates intracellular concentrations of glutamate. Negatively modulates SLC1A1/EAAC1 glutamate transport activity
tan_5H (cellular response to heat)	Asb1	Ankyrin repeat and SOCS box protein 1	Involved in protein ubiquitination
	Tpr	Nucleoprotein TPR	Component of the nuclear pore complex
	Pex5l	PEX5-related protein	Accessory subunit of hyperpolarization-activated cyclic nucleotide-gated channels
	Pank4	Pantothenate kinase 4	Plays a role in the physiological regulation of the intracellular coenzyme A concentration
	Znf609	Zinc finger protein 609	Unknown

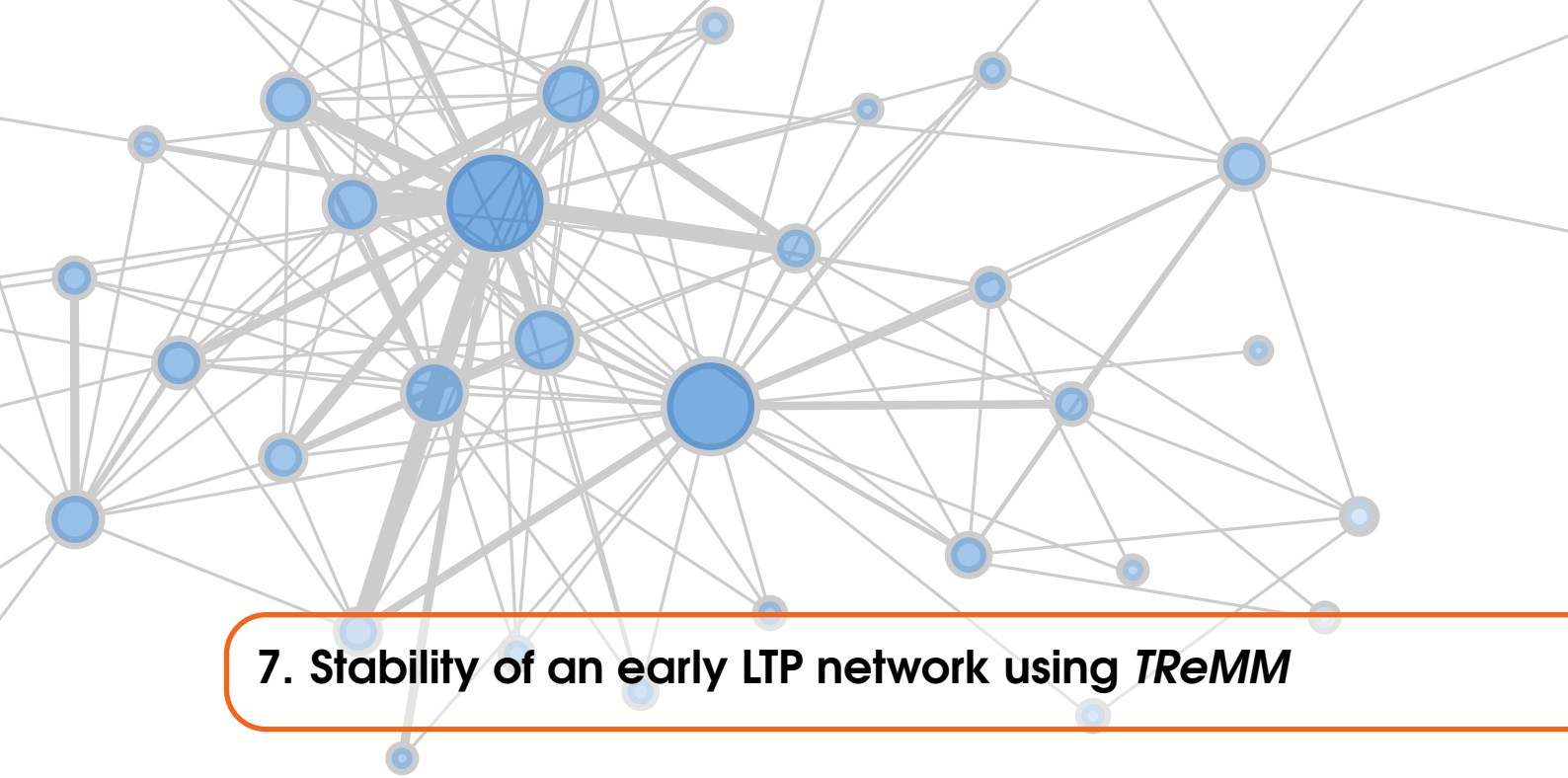

7. Stability of an early LTP network using *TReMM*

When nothing else subsists from the past, after the people are dead, after the things are broken and scattered... the smell and taste of things remain poised a long time, like souls... bearing resiliently, on tiny and almost impalpable drops of their essence, the immense edifice of memory

Marcel Proust

7.1 Introduction

Memory processes in the brain are dependent on the capacity of neurons to undergo long-lasting enhancement of synaptic effectiveness. LTP is one of such mechanisms, providing a cellular model of associative, specific, and long-lasting storage.

Although LTP is generally divided into three phases over time only the intermediate- and late-phases (often referred as LTP2 and LTP3 respectively), seem to be dependent on protein synthesis when induced in vivo at perforant path synapses. As well as long-term memory, late-LTP (L-LTP) is dependent on both changes in gene expression and protein synthesis (Nguyen *et al.*, 1994; Abraham and Williams, 2003, 2008; Alberini, 2009).

The new transcripts and proteins that characterise the L-LTP could be targeted to the specific synapses from the nucleus by means of a synaptic "tag" generated at the potentiated synapses (Frey and Morris, 1997). A first wave of transcription brought about by the activated constitutive transcription factors (TFs) would consist of effector genes and inducible TFs which, in turn, would be responsible for a second wave of transcription (Ryan *et al.*, 2011; Abraham and Williams, 2003).

Although several genes have been identified to belong to some of those categories (see Abraham and Williams, 2008, 2003; Lynch, 2004) it is unclear how do they coordinate in order to lead to the persistence of LTP. Several efforts have been taken towards defining a wider picture of the biochemical networks underlying the maintenance of LTP (Lee *et al.*, 2005; Park *et al.*, 2006; Håvik *et al.*, 2007a; Valor and Barco, 2010; Ryan *et al.*, 2011). One of the pathways leading to *de novo* gene expression is triggered by the activation by phosphorylation of cAMP response element-binding protein (CREB) by the phosphorylated calcium- and cAMP-dependent kinase.

CREB functions as a hub in the gene regulation. Its phosphorylation can be driven by a plethora of different kinases (Schulz, Siemer, Krug, and Höllt, 1999) and in turn, its activation leads to the expression of transcriptionally linked genes.

Once phosphorylated, CREB acts as a TF stimulating the expression of other TFs and other effector genes by binding to the promoter CRE region. The transcriptional response will constitute a first wave of gene expression. Other TFs which are constitutively expressed may also become active following LTP induction.

The first wave of *de novo* transcription brought about by the LTP-activated TFs consists of activity-induced TFs, structural proteins, signal transduction proteins, growth factors, and enzymes. These set of genes have been referred to as immediate-early genes (IEGs). These TFs are believed to drive the expression of delayed effector genes (see Section 3.3.6 and Abraham and Williams (2003, 2008); Miyashita, Kubik, Lewandowski, and Guzowski (2008); Tischmeyer and Grimm (1999) for comprehensive reviews).

Several studies have more recently covered the gene expression activation with studies of coregulation based on microarrays (see for example Park *et al.*, 2006; Ryan *et al.*, 2011), identifying sets of differentially expressed genes after the induction of LTP. It appears that the expression state of the LTP-related transcriptional regulatory network (LTP-GRN) shifts from a resting state (pre-LTP state) to a post-LTP state, where LTP has been induced via experimental high frequency stimulus. These expression states have been measured experimentally using high density arrays by Ryan *et al.* (2011). They identified a set of differentially expressed genes whose interactions served to identify biologically relevant networks and pathways related with LTP. Their network analyses suggest that some genes may play central roles during LTP induction without showing a significant alteration in their expression levels (such is the case of NF-κB). Other genes identified by the IPA software as major hubs in LTP-regulated gene expression networks were SRF, Egr1 and CREB. Erk also appears as a central hub in the network and its activity seems regulated by the phosphatase activity of DUSPs, which in turn appear to have a coordinated upregulation. In addition, DUSP and Egr families regulate the Ras-Erk1 signalling pathway, which is known to have an essential role in LTP.

In the present chapter, we analyse the most significant network published in Ryan *et al.* (2011) to investigate its topological properties from a dynamical perspective. We model the transcription regulation through weight matrices, and we show that the particular topology of the LTP-GRN is more likely to hold bistability when compared to random networks. On a similar perspective, we classify the LTP-related genes according to their relevance to the bistable output of the network.

7.2 Methods

7.2.1 Weight matrices dynamics

Continuous models based on differential equations entail a main disadvantage compared to discrete-time models. Despite experimental evidence can be gathered regarding the networks' topology (the *who* interacts with *who*), there is a lack of quantitative information relative to the biochemical parameters underlying gene interactions (the *how* the interacting partners interact). In other words, the strength of the interactions between genes and proteins are difficult to measure. On the other hand, the widely-used Boolean models for gene regulation might oversimplify the complexity underlying biological interactions.

For this study, we have adopted the *TReMM* algorithm (Transcription Regulation Modelled with Matrices) described by Weaver et al. (Weaver *et al.*, 1999). The *TReMM* methodology characterises the gene expression values from a state of maximal expression to a state of minimal repression. These intervals are gene-specific, and during a simulation a gene can take any continuous value in the range defined by its maximal and minimal expression. The details of the methodology are

described in detail in Section 4.2.3.

In particular, we are interested in the existence of such a landscape for the LTP-GRN, where these attractors would represent the pre- and post-LTP cell states, potentially accessible from different initial conditions. Those initial conditions could be specified by the cell's environment.

7.2.2 LTP-GRN and gene expression data

For this study we have chosen the highest scoring LTP-GRN published in Ryan *et al.* (2011), constituted by a total of 35 genes (see Figure 7.2), which was constructed using the IPA software and is based on biological information sourced from literature references (see Section 5.5).

The initial conditions for the time course experiments, $u(t=0)$, as well as the maximal expression levels m were obtained from real expression data. In the original experiments the animals were stimulated unilaterally so that the unstimulated hemisphere could serve as a within-animal control Ryan *et al.* (2011, 2012). We used the values of the microarrays hybridized with the RNA from the stimulated hemisphere as post-LTP state, and the unstimulated hemisphere values as the pre-LTP state.

7.2.3 Frequency of bistable outputs P_B

We define as *bistable* a network dynamic simulation which converges onto two different stable terminal states when initialised with different expression values. In this study, we have set those starting expression values according to the LTP-induced microarray data and the control microarray data, namely, running for each network and each set of α, β, and W parameters two parallel dynamics representing pre- and post-LTP conditions respectively. The presence of two different attractors in the gene expression state space each relatively closer to either the pre- or the post-LTP initial conditions, will lead to two different terminal states. These cases are referred to as *bistable outputs*. We have chosen the experimental expression values obtained by Ryan *et al.* since they represent real estimates of the gene expression levels.

By sampling the space of parameters and testing whether the output states of the pre- and post-LTP parallel dynamics reach different points in the N-dimensional space, we calculate the *frequency of bistable outputs* or P_B, which characterises the network's expression state space around the pre- and post-LTP initial conditions. In this work, we have randomly sampled the space of parameters by 10,000 trials with $w_{i,j} \in [-1,+1]$, $\beta_i \in [-1,+1]$, and $\alpha \in (0,+3]$.

The value of P_B is free of the bias which arbitrary parameters would introduce, and serves as a descriptor of how a particular topology is likely to show a sensitivity to the realistic initial conditions observed in the in vivo experiments. Put differently, the attractors in the gene expression states space represent stable phenotypes, while W represents the neuron's genotype.

7.2.4 Random and knock-out networks

In order to characterise the LTP-GRN, we have constructed a total of 100 random networks by preserving the same number of nodes and edges as in the LTP-GRN and without assuming any fixed degree distribution. These networks have been characterised in terms of their P_B, and the values are represented in Figure 7.1.

Similarly, we have calculated the P_B for the 35 networks resulting from the knock-out of each gene in the LTP-GRN network. Some of these knock-out networks show an inferior propensity to bistability (a lower P_B), meaning that the removed gene has a key role in the capacity of the LTP-GRN to reach bistable outputs. The P_B values for the removal of each gene are represented in Figure 7.2, where a darker shade of red means higher influence in the network's bistability propensity.

7.3 Results

7.3.1 LTP-GRN bistable frequency

The frequency of bistable outputs for the LTP-GRN ($P_B = 0.086$) is in sharp contrast with the frequencies obtained for the random networks with the same number of nodes and edges (Figure 7.1, avg. $P_B = 0.031$). Furthermore, the value of the P_B for the LTP-GRN is higher than any of the random networks. Assuming normality for the distribution of P_B in the random networks' population, ($p = 0.019$, Shapiro-Wilk test), the probability of a random network with a higher P_B than the LTP-GRN is extremely low ($P < 3.65 \times 10^{-07}$).

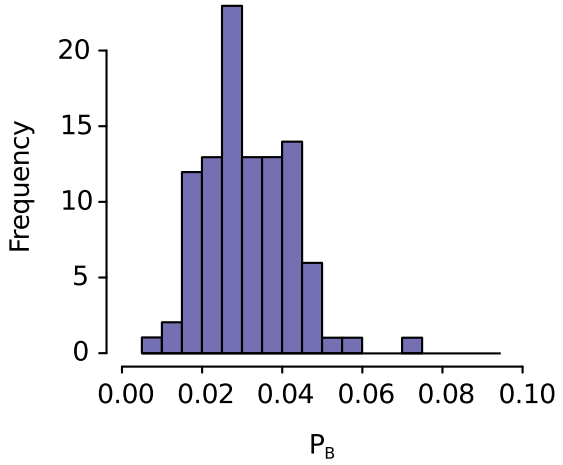

Figure 7.1: *Distribution of 100 random networks according to their bistable output frequencies P_B (10,000 simulations for each network in the parameter space). The P_B distribution for the random networks has $\mu = 0.031$ and $\sigma = 0.011$. The LTP-related network shows a much higher $P_B = 0.086$, which lies about 5 standard deviations away from the mean assuming normality for the random network distribution*

7.3.2 Knock-out effects

For each i-th gene of the $N = 35$ genes in the LTP-GRN, an independent set of knock-out runs were performed. In these runs, the ith gene of the network was removed and not considered in the simulations, setting the ith row and column of W to zero. The resulting 35 networks with $N = 34$ were characterized in terms of their frequency of bistable outputs, P_B.

Figure 7.2 summarises these results by showing in a red scale the effect of removing that particular gene from the network. NF-κB has a low influence on PB, while the Egr members appear to be of a fundamental importance, which supports previous findings (Abraham *et al.*, 1993). Interestingly, the level of expression of NF-κB does not change after LTP induction (Ryan *et al.*, 2011), suggesting a regulation by post-translational modification.

7.4 Discussion

While evolution has equipped cells with a robust and plastic analog system which confers to living cells the ability to respond in a graded manner to environmental inputs, some aspects of the cellular

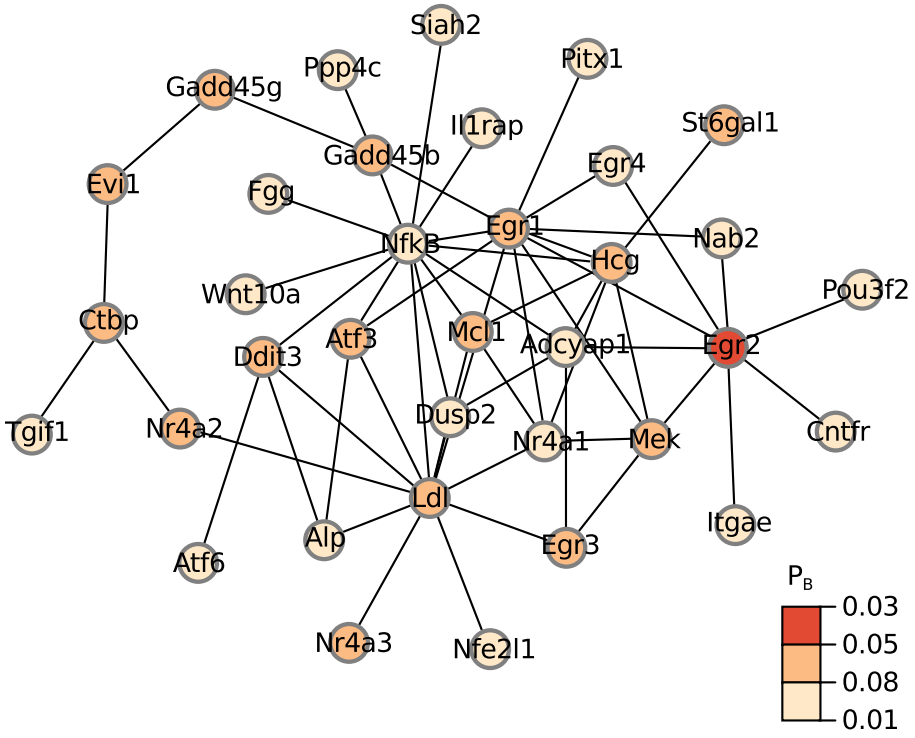

Figure 7.2: *LTP-GRN as reported in Ryan* et al. *(2011). The colours in the nodes represent the knock-out effects on the bistable output frequency of the LTP-GRN – the shade of red, indicates how the knock-out of that gene affects the ability of the network to reach bistable outputs (P_B). Darker nodes are therefore of a crucial importance for the network to show an expression landscape compatible with the two-attractor hypothesis. The Egr family seems to be of a fundamental importance for the bistable properties of the LTP-GRN. (Red nodes,* $0.01 < P_B < 0.03$*, Orange nodes,* $0.03 < P_B < 0.05$*, Light orange nodes,* $0.05 < P_B < 0.08$*)*

behaviour are of a Boolean nature – this is the case of cell cycle checkpoints, cell-fate transitions, and apoptosis to name a few. Likewise, LTP as a long-lasting phenotypic phenomenon represents one such Boolean characteristic, and its maintenance relies on gene expression.

Back in 1969, Stuart Kauffman proposed that cell types are attractors in the gene expression state space (Kauffman, 1969a). Similarly, our hypothesis extends this idea to the phenotypic pre- and post-LTP neuronal states. High-frequency stimulus would drive the state of a neuron from one gene expression attractor to another *in vivo*.

From such a perspective, we have classified in the study described in the present chapter the LTP-related genes according to their relevance to the bistable dynamic output of the network. It is noteworthy how the Egr family stands out in Figure 7.2 and in the results of the co-expression analysis. Their role in LTP has been already documented (Abraham *et al.*, 1993; Williams, Dragunow, Lawlor, Mason, Abraham, Leah, Bravo, Demmer, and Tate, 1995; Jones *et al.*, 2001), and the results presented here further stress their importance in the dynamic context of the other genes. In particular, Egr2 appears to be the most determinant gene for the network to show

bistability in the weight matrices dynamics (Section 7.3.1). Note however that this ranking only represents the relative importance of the genes for bistable behaviour. For example, NFκB shows a relatively low influence on the network's P_B, while it is believed to be involved actively in LTP and synaptic plasticity (Freudenthal *et al.*, 2004; O'Mahony, Raber, Montano, Foehr, Han, Lu, Kwon, LeFevour, Chakraborty-Sett, and Greene, 2006). The low P_B shown by NFκB is not trivial, since it also constitutes a hub in the network, and a high dependence on it for the bistable frequency might be expected. Interestingly, NFκB does not show an altered expression level after LTP induction (Ryan *et al.*, 2011), which is consistent with its constitutive expression observed in a number of studies and the notion of its activation by phosphorylation of a bound inhibitor (see Section 3.3.6). The results of the co-expression discussed in the previous section confirm the central role of NFκB signalling in LTP.

The capacity of showing different stable points in the gene expression state space must be of a crucial importance for the gene regulatory networks involved in such step-like responses. We show that this is the case for an LTP-related gene regulatory network by using realistic expression values from microarray data.

Whether this property of the LTP-GRN extends to most biological networks or only to the networks involved in Boolean decisions remains unclear and deserves further insight. Indeed, a long-lasting cellular process such as LTP is expected to function under a changing environment. Neurons are subject to both internal and environmental noise, which compromises the stability of the gene expression states. This compromise between plasticity (two-attractors hypothesis) and robustness to noise has not been addressed in this study. The role of gene expression attractors in robustness and evolvability of biological networks, from a more general perspective, emerges as an interesting generalisation of this analysis but beyond the scope of this study.

These results were published in the proceedings of the 2012 IEEE International Joint Conference on Neural Networks (Nido, Williams, and Benuskova, 2012).

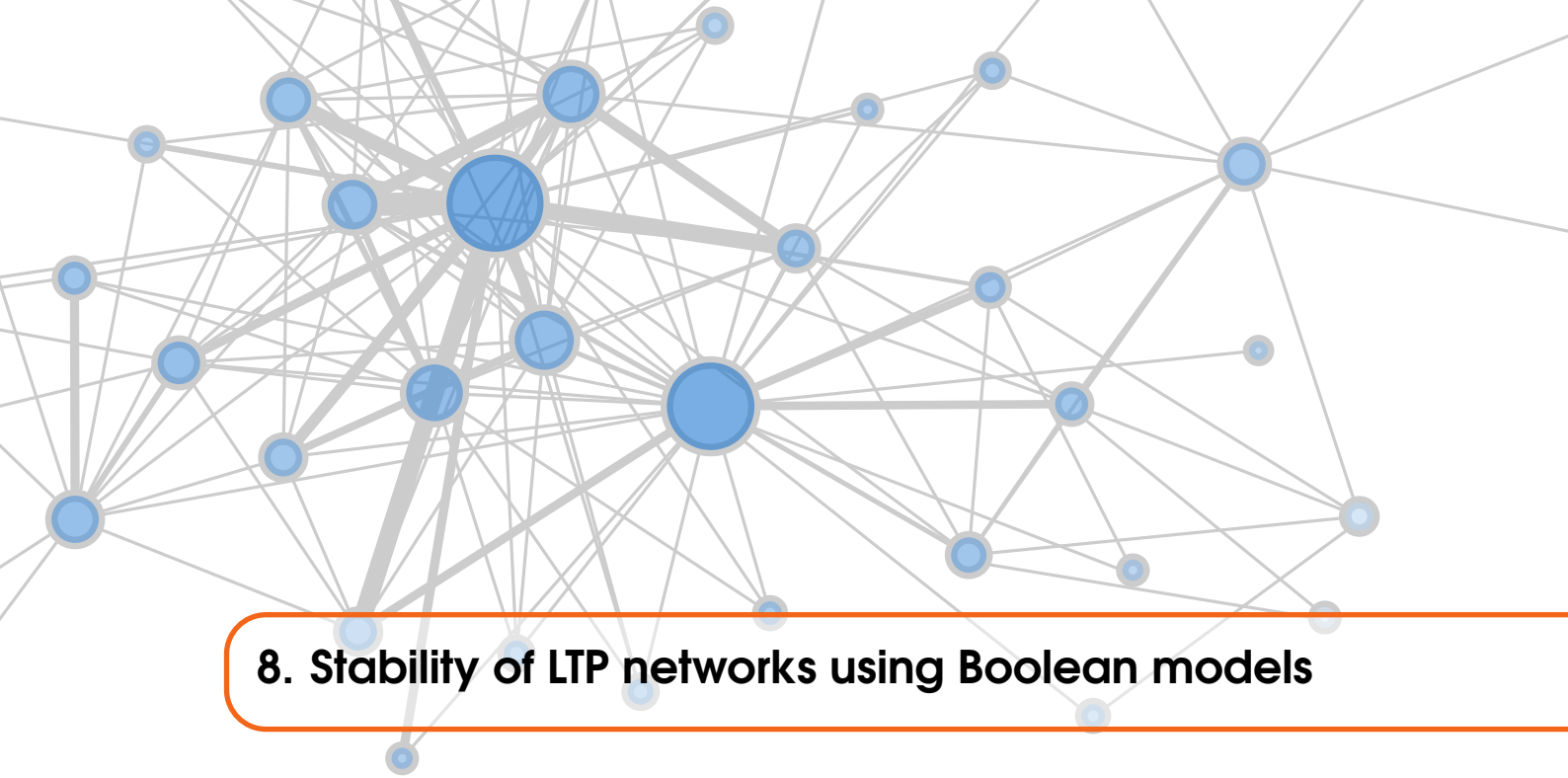

8. Stability of LTP networks using Boolean models

What matters in life is not what happens to you but what you remember and how you remember it

Gabriel García Márquez

8.1 Introduction

It has been suggested that natural genetic regulatory networks do not possess ordered dynamics, but rather lie in the so-called critical regime, the boundary between order and chaos (Balleza *et al.*, 2008). The resulting compromise between stability to small perturbations and sensitivity to specific perturbations may confer an evolutionary advantage as biological networks have to be able to discriminate background noise (robustness against unspecific changes in the environmental variables) from the meaningful signals that deserve the triggering of a specific response. Likewise, LTP as molecular mechanism that functions as a mnemonic device, must bear these central properties.

In fact, a number of studies suggest that network architecture plays an important role in the stability of cellular states (Albert *et al.*, 2000; Jeong *et al.*, 2001; Milo *et al.*, 2002) and hence be under evolutionary pressures (Li *et al.*, 2004). It can be expected that topological properties of networks differing in their functions or acting at different time scales will show different properties, tuned according to a particular compromise between robustness and plasticity. In this aspect, networks involved in early stages of a persistent mechanism are likely to be endowed with plastic properties, while networks regulated later on and responsible for the maintenance of the new homeostasis, will show a higher dynamic stability. A lack of quantitative data to date has made dynamic modelling a rather rare approach to understanding the genetic mechanisms controlling LTP maintenance.

The remarkable persistence of LTP and its highly specific nature, that is only inputs that are active during high-frequency stimulation are potentiated (Bonhoeffer, Staiger, and Aertsen, 1989), highlight LTP as a good model mechanism to study how order and chaos in gene network dynamics are tuned by living cells. By studying LTP-related networks identified at different times after LTP induction (20 min, 5 h and 24 h post-LTP) from a dynamic systems perspective, we aim to gain a

deeper understanding of the relationship between function and network structure in gene regulatory networks. In addition, the present study emphasises the key role played by new gene expression in LTP consolidation an maintenance, which is still debated.

In this chapter, we further extend the study presented in Chapter 7 by using a random Boolean network model and taking advantage of the additional gene expression data available for different times after LTP induction (5 h and 24 h, Ryan *et al.*, 2012). The goal of this work is to characterise the dynamic differences between temporally distant networks, which are regulated by the same environmental trigger. We compare the post-LTP regulated networks with random models and we use the yeast transcriptional network as a benchmark. We show that the dynamics exhibited by the latest (24 h) network are less sensitive to perturbations than the earlier networks – an effect consistent with a role in the consolidation of synaptic plasticity.

8.2 Methods

8.2.1 Random Boolean Networks

Random Boolean networks (RBN) represent one of the simplest models for gene regulatory networks. In Boolean networks, there are N nodes representing the genes which can only take *on* or *off* values at a given time, $x_i(t) \in \{0,1\}$. The values of the vector $x(t)$ are updated according to the Boolean rules $B = (f_1, ..., f_N)$ and the values of the vector $x(t-1)$ in the previous iteration. For details on the methodology, see Section 4.2.1.

In particular case of RBNs, both the set of Boolean rules B and the values of the state vector $x(t=0)$ are initialised randomly. Subsequently, $x(t)$ is updated synchronously based on the vector at $t-1$ and according to the Boolean rules. Given an initialised vector at $t=0$ and the set B of truth tables, this type of dynamics are deterministic. The set of rules B will stay the same over time during the simulation, whereas the state vector $x(t)$ will evolve until reaching an attractor. For a given network topology, a large number of simulations has to be run to properly sample random initial conditions $x(t=0)$ and B.

As described in Section 4.2.1, the dynamics of RBNs can fall in the ordered or chaotic regime, depending on their dynamic stability (Fox and Hill, 2001). For randomly connected networks with a Poisson and power-law degree distribution, it has been shown that the border between the ordered and chaotic regimes is given by $2p(1-p)K = 1$, where p denotes the bias for the fraction of output values that are 1 in the Boolean rules, $p = P(B_i = 1)$, and K the constant in-degree (Aldana-Gonzalez *et al.*, 2002; Aldana and Cluzel, 2003).

There are different strategies to study the degree of dynamical order in a Boolean network. A popular method consists in measuring the effects of small perturbations on the outcome of the simulations – two initial states that differ in a number of positions, $h(0)$ (known as Hamming distance), are evolved in parallel for τ time steps. The new Hamming distance, $h(\tau)$ is calculated. The Hamming distance h can be averaged over a large number of initial conditions and Boolean rules (denoted with $H(t)$). This methodology is very useful when combined with the Derrida plots (see Section 4.2.1). The Hamming distances in ordered networks tend to decrease on average after evolving the network in time, while the chaotic or disordered networks show the opposite behaviour, $H(\tau) > H(0)$.

8.2.2 Network topologies

The networks used in this study were sourced from the literature or generated randomly according to a set of criteria.

Ryan *et al.* (2011, 2012) carried out a series of microarray experiments at different times after LTP induction. Specifically, their analyses aimed to identify genes regulated 20 min, 5 h, and 24 h after LTP induction. For each of these groups, they provided the three highest

scoring networks according to the analysis provided by the IPA software (Ingenuity Systems, USA; `www.ingenuity.com`), making a total of 9 networks. In the present study we will analyse the highest scoring network for each time point. The 20 min network is represented in Figure 8.1a, whereas all the networks used are depicted in Figure 5.4 in Section 5.5. In addition, we have used the yeast transcriptional network as a benchmark for RBN modelling, so that our results can be readily compared to the analyses available in the literature – more specifically to the papers by Kauffman, Peterson, Samuelsson, and Troein (2003) and Karlsson and Hörnquist (2007). The results presented in those studies used the same network published in (Lee, Rinaldi, Robert, Odom, Bar-Joseph, Gerber, Hannett, Harbison, Thompson, Simon, *et al.*, 2002). We will refer to this network simply as the yeast network.

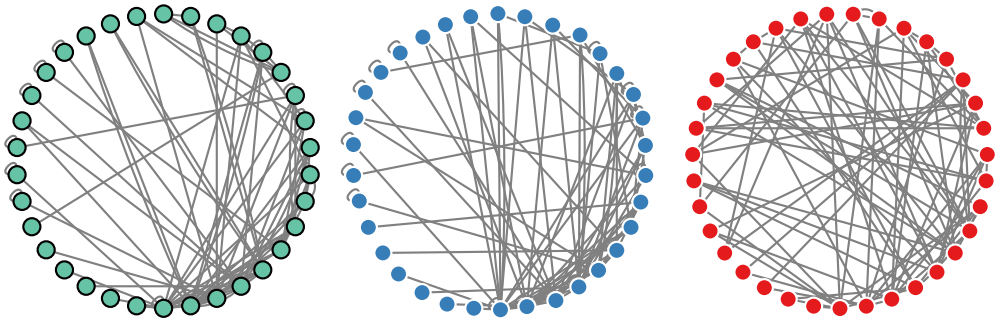

Figure 8.1: *Types of network topologies used in the study.* ***(a)*** *First of the three 20 min post LTP networks (Ryan* et al.*, 2011).* ***(b)*** *Example of a rewired network, where the edges have been swapped in order to preserve the same node degree.* ***(c)*** *Random network with the same number of nodes and edges. The in- out-degree distribution is not preserved with respect to (a). The networks are represented in a circular layout with the nodes in ascending order of degree, counter-clockwise starting from the bottom*

Although there are a number of different algorithms to compute random networks, in order to compare the dynamic properties of the LTP networks we have used two different sets of constraints to generate them. First, an ensemble of 100 random networks is generated for each of the 4 biological networks studied (20 min, 5 h, 24 h and yeast) by preserving the same number of nodes and edges. The 4 ensembles will be referred to simply as Random networks, see Figure 8.1c.

To discriminate the effects of the network's local structure from the effects of the general topology, a second type of random architecture consists of ensembles of 100 random networks where each node has the same number of in- and outgoing edges as the original biological network. To preserve these local topological properties, a randomly chosen pair of edges is swapped such that if $A \to B$ and $C \to D$, the resulting network has $A \to D$ and $C \to B$. Swapping is prevented if either $A \to D$ or $C \to B$ exist already (Kannan, Tetali, and Vempala, 1997). Within each of these 4 ensembles (referred to as Rewired networks, see Figure 8.1b for an example), each network has the same in- and out-degree distribution as the original LTP network from which they originated.

Finally, we aimed to study the effect of noise at the genetic level by generating all the 35 possible knock-out networks for each of the original LTP networks.

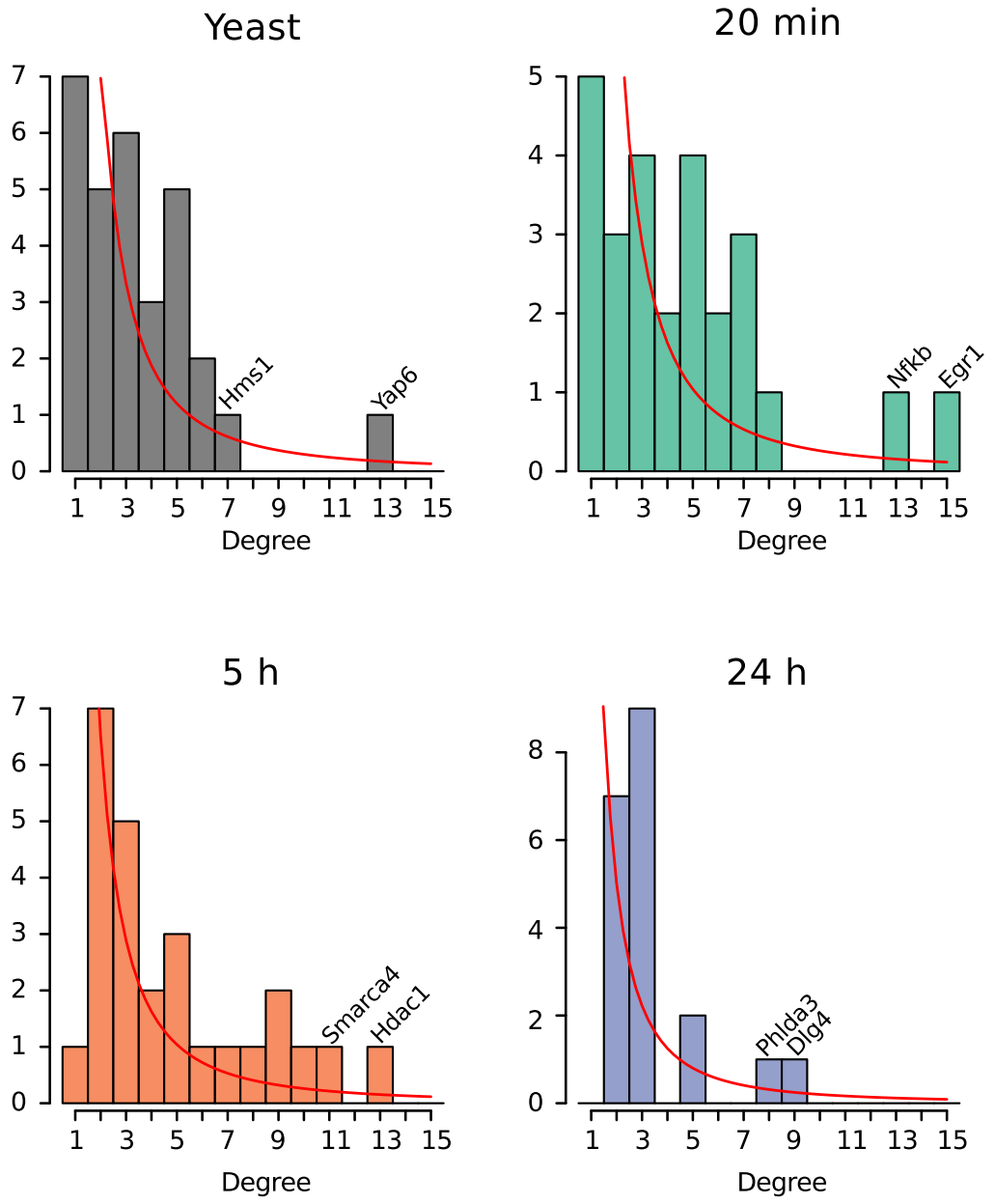

Figure 8.2: *Histograms of the degree for the LTP networks and the yeast transcriptional network*

8.3 Results

8.3.1 LTP-related networks are dynamically similar to the yeast network

To compare the effect that different topologies have on the dynamic behaviour of networks we used an RBN model. Specifically, we compared the three most significant networks derived using IPA at three time points (20 min, 5 h and 24 h) following the induction of perforant path LTP (Ryan *et al.*, 2011, 2012), with the yeast network obtained from (Lee *et al.*, 2002).

Kauffman *et al.* (2003) studied the yeast network by using a similar RBN model and showed that the yeast network was more stable around fixed points than the rewired networks. In our approach we do not assume any structure in the Boolean rules (neither canalizing nor nested functions Kauffman (see 1993); Kauffman *et al.* (see 2003) and this difference is difficult to grasp (Figure 8.3). Interestingly, when we applied the same analysis to the LTP-related networks compared to their rewired counterparts, we found this tendency towards a more ordered regime to be even more noticeable (blue lines in Figure 8.4). The dynamics fall in the chaotic regime (note that for perturbations in which a fraction of < 0.5 of the genes differ, these networks are above the diagonal, Figure 8.4) but this behaviour can be suppressed by using forcing structures in the Boolean functions (Kauffman, Peterson, Samuelsson, and Troein, 2004). For the purpose of comparing between the different time-scales networks, we opted not to assume any structure and we used a flat distribution.

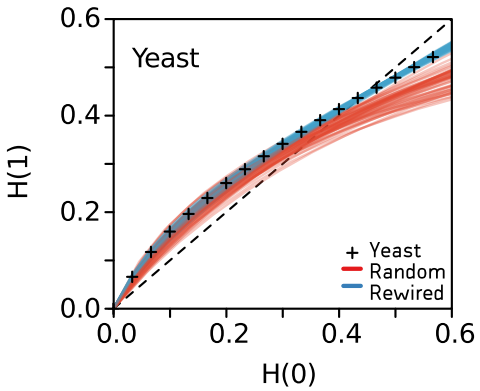

Figure 8.3: *Derrida plots for the yeast network, with* $H(0)$ vs $H(5)$. *Each point in the plot is an average over 1,000 random rule assignments for 100 random initial conditions. Hamming distances are normalised by the number of nodes*

8.3.2 Knock-out analyses

Figure 8.5 summarises the results obtained by simulating the knock-out networks. A total of 35 knock-out networks for each LTP network are represented in the figures. To highlight the effect of the degree on the dynamics shown by the original network, the knock-out networks corresponding to the removal of the top 2 genes in terms of degree are represented with different colours (red, blue) – Yeast: Yap6, Hms1; 20 min: Egr1, NFkB; 5 h: Hdac1, Smarca4; 24 h: Dlg4, Phlda3. Figure 8.6 stresses these differences by plotting the Hamming distances after 5 iterations.

8.4 Concluding remarks

The comparison of the dynamic stability between the networks obtained at different times after LTP-induction show that the regime becomes less chaotic with time after LTP induction (see Figure 8.4). In particular, the 24 h network appears to be considerably more ordered than the yeast, and ordered dynamics prevail under perturbations higher than a fraction of 0.38 genes. In contrast, the dynamic stability exhibited by the 20 min and 5 h networks is comparable to the one observed for the yeast. This observation is readily accounted for in Figure 8.7, where two states differing in

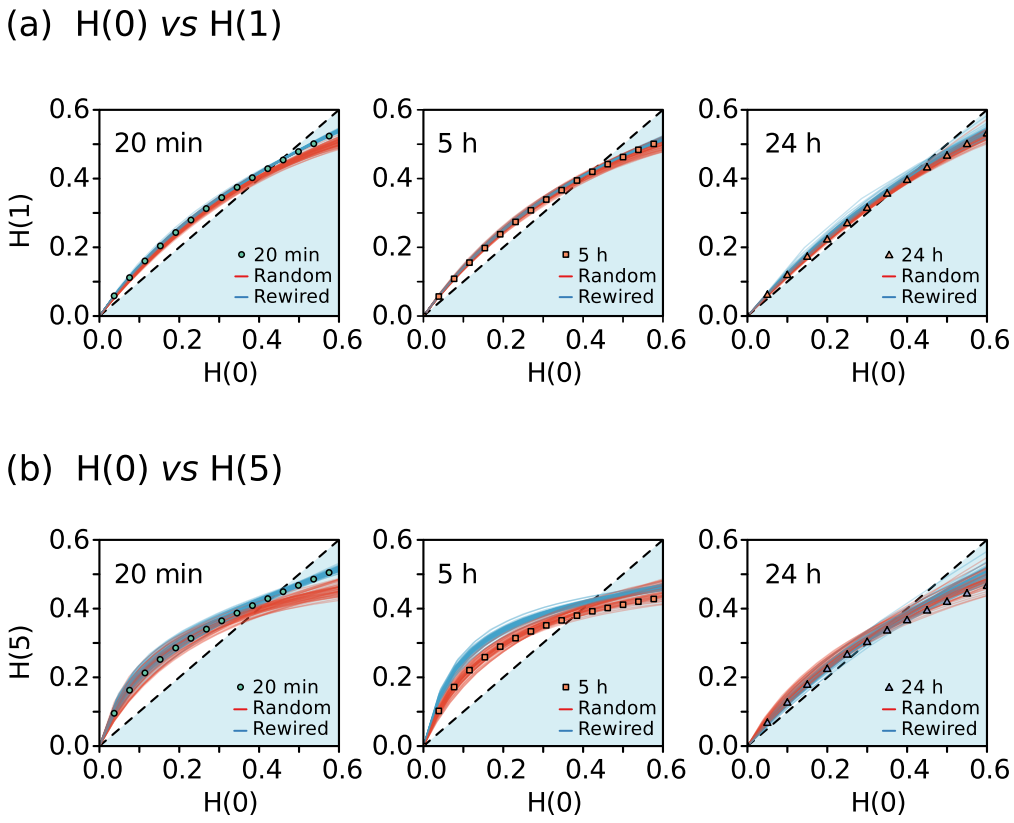

Figure 8.4: *Derrida plots for the LTP networks (from left to right: 20 min, 5 h, 24 h). Random networks for each of them are represented in red lines, Rewired networks in blue. The top plots show the $H(0)$ distance plotted against $H(1)$, while the bottom plots represent $H(0)$* vs *$H(5)$ for the same simulations. Despite showing slightly different behaviours, the curves corresponding to the real networks are above the diagonal for the same small perturbations. Contrarily to these dynamics, random Poissonian and scale-free networks dynamics have been shown to be ordered, and lie below the diagonal (Aldana, 2003; Aldana and Cluzel, 2003). Each point in the plots is the average over 1,000 random rule assignments for 100 random initial conditions (increasing these numbers has no effect on the results). The dashed diagonal, $H(0) = H(1)$, represents the edge between order and chaos. Hamming distances are normalised by the number of nodes*

only one position are independently evolved over 5 time steps. The updated distances between the two state vectors are represented in the vertical axis. The amplification of the perturbation is clearly less pronounced than the one observed for the other networks, and the yeast network lies between the earlier networks (20 min and 5 h) and the more stable 24 h network.

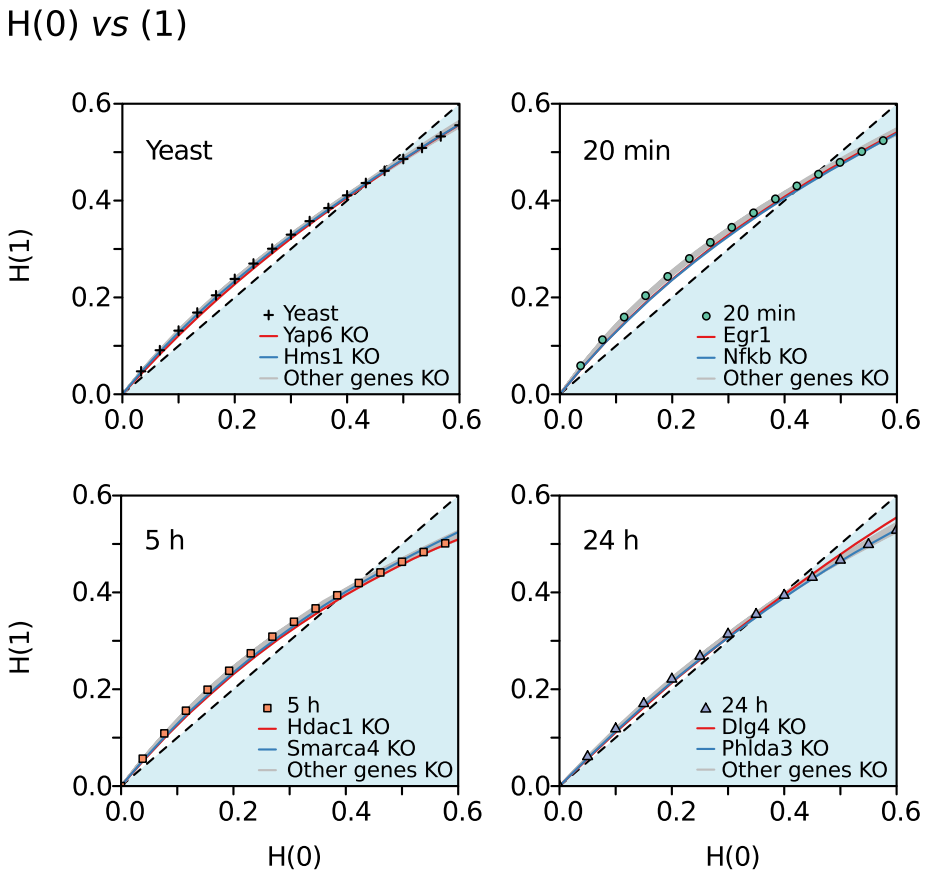

Figure 8.5: *Derrida plots for the knock-out experiments. The plots show the initial Hamming distances vs the Hamming distances after 1 iteration. Red and blue lines correspond to the knock-out of the two genes with highest degree*

8.5 Discussion

The results reported in the present chapter include dynamical characteristics of networks identified at different times post-LTP. These results reinforce the view by which the architecture of the networks is under a selective pressure. Yet, it remains unclear the contribution of the structural properties to the overall robustness of biological circuits. This tendency towards the stable regime represents only one mechanism yielding robust behaviour and does not rule out other genetic mechanisms (Wagner, 2005).

While it is clear that late-LTP is dependant on new protein synthesis, it is likely that late-LTP *in vivo* relies both on local translation of mRNA located in the synapses and on *de novo* transcription. It has been suggested that the sub-processes requiring nuclear transcription in LTP could be involved in neural maintenance, while translation would confer synaptic specificity (Vickers, Dickson, and Wyllie, 2005). Although a more detailed picture of the mechanisms that serve as a trigger for the rapid transcription of the immediate early genes (IEGs) is needed, the key regulators have been pinpointed (see Section 3.3.6 for a detailed review). Contrarily, little is known regarding the regulation of gene expression in the maintenance phase of LTP.

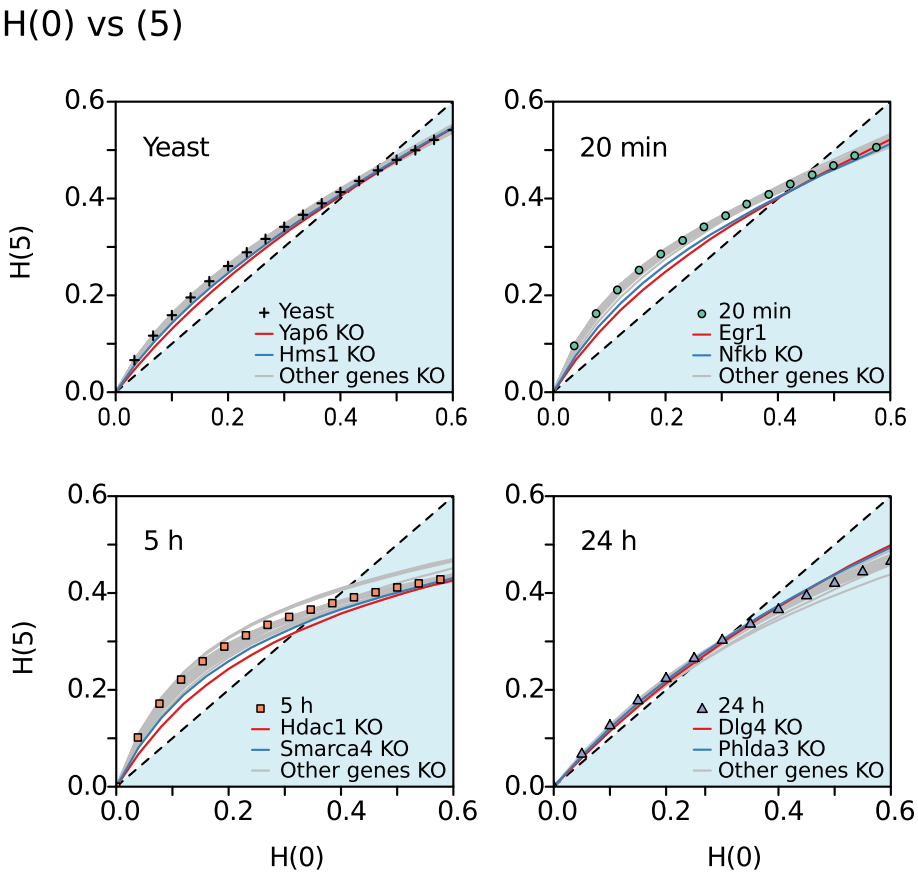

Figure 8.6: *Derrida plots for the knock-out experiments. The plots show the initial Hamming distances* vs *the Hamming distances after 5 iterations. Red and blue lines correspond to the knock-out of the two genes with highest degree*

It seems that the protein synthesis-dependent first hours of LTP are maintained by pre-existing mRNA. However, it has been noted that there is a critical temporal window after LTP induction in which a rapid nuclear response takes place (Nguyen *et al.*, 1994). This early phase is in the order of minutes, and is characterised by a rapid upregulation of gene expression which persists for at least 5 h. The network identified 20 min after induction represents these early response genes. The set of genes identified 5 h post-LTP induction are closely related to the 20 min early responding genes, as demonstrated by the expression profiles (Ryan *et al.*, 2012). The nature of this rapid transcriptional response following LTP induction suggests that the underlying mechanisms are facilitating a switch-like response. In this line, Saha, Wissink, Bailey, Zhao, Fargo, Hwang, Daigle, Fenn, Adelman, and Dudek (2011) documented recently the presence of stalled RNA polymerase II in LTP IEGs, which they interpreted as a mechanism for the rapid neuronal induction observed. However, other mechanisms may be acting jointly at different levels to complement the gene expression trigger.

The 24 h post-LTP induction represents a temporal and functionally different data set, as indicated both by the overlap in gene expression (Ryan *et al.*, 2012) as well as by the fact that mRNA-synthesis inhibitors are only effective in blocking LTP starting after about 4-6 h (Vickers

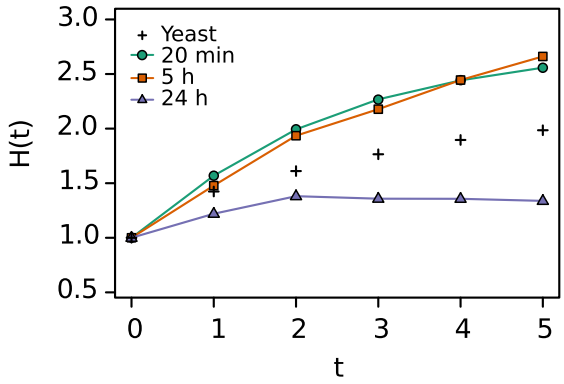

Figure 8.7: *Effect of a small perturbation, $H(0) = 1$, over 5 time steps for the LTP and yeast networks. Initial states differing only on one position are sampled during 5 subsequent time steps for each LTP network. As shown in Figure 8.1, this small difference tends to be amplified in these biological networks. The latest network appearing after LTP induction (24 h, blue), shows a less pronounced tendency to extend the perturbation. This result is consistent throughout all the initial perturbations in the chaotic regime shown in Figure 8.1*

et al., 2005). We hypothesise that if the 24 h network is representative of a new homeostatic state brought about by LTP induction, its architecture should confer an enhanced stability.

Interestingly, the temporal effect on the vulnerability of the networks discussed is mirrored by what is known about the vulnerability of LTP and memory itself. Previous studies have shown that LTP can be reversed within hours of induction, but then becomes resistant to reversal. It is of particular relevance to our studies that this resistance to reversal is dependent on new protein synthesis. Thus our new data support the conclusion that the LTP-related gene networks contribute to the stabilisation of LTP.

In light of this it is interesting to consider how on-going potential for plasticity in neural networks is maintained over time, if LTP or memories become stable. Such on-going plasticity is crucial within the central nervous system. And it is apparent that memories are at least in part labile. Interestingly, LTP does appear to remain vulnerable to reversal in some instances, for example, seemingly stable LTP in the dentate gyrus can be reversed by exposure to enriched environments up to two weeks post-induction (Abraham *et al.*, 2002). The molecules within the most significant network formed at 24 h post-LTP, and that identified as the most stable network here, relate to growth and/or neurogenesis, functions relevant to consolidation of plasticity. In contrast, the next most significant gene network contains molecules relating to histone modification and epigenetic control of gene expression, and is less stable in nature. Potentially, the vulnerability of this network to change may contribute to maintenance of on-going plasticity in the hippocampus. In summary, as persistent LTP is associated with extensive alteration in gene networks our observations suggest that, as LTP remains plastic so to will aspects of the associated genomic response.

While RBN modelling for gene networks is fraught with the disadvantages of the simplifying assumptions of the model, a number of studies have shown the validity of these simple models to study some biological properties of living systems (see for example Kauffman, 1993; Li *et al.*, 2004; Davidich and Bornholdt, 2008) as well as in other fields such as neural networks, social

networks and protein interaction networks (Aldana, 2003). In the present work we show that while LTP-related networks possess a dynamic behaviour expected from biological networks, some characteristics are specific to their sub-functions. In fact, while the networks studied are all regulated by the same cellular mechanism, the architectures seem to confer a higher stability to the latest network (24 h).

These results are in line with a model in which the rapidly induced networks following LTP induction exhibit a higher sensitivity to perturbations so that a switch-like response can be triggered in response to the signals that induce LTP in the neurons. In turn, networks associated with the late phase of LTP have to posses a more stable architecture, contributing to the homeostatic response underpinned by gene expression. Processes acting longer time scales related with the 24 h network identified by co-expression analysis and differential expression analysis are associated with growth and/or neurogenesis via microRNA epigenetic regulation.

Although analysis of the IPA generated networks has provided validated and biologically meaningful data (Ryan *et al.*, 2011, 2012; Joilin *et al.*, 2014)), some limitations are inherent to the methodology. First, potential key interactions may be excluded as the interactions of only 35 genes per network have been considered. Secondly, the architecture of each network is directly dependent upon the information contained within the IPA Knowledge base, a manually curated database, which makes these networks susceptible to false negatives. Thirdly, genes that are modestly but consistently regulated at each time point will be excluded if they do not reach the inclusion criteria at any time. Finally, the analysis is incompatible with the identification of a *control* network, allowing the characterization of a pre-LTP homeostatic state, as networks are based on differentially expressed genes. The connectivity distributions observed in the co-expressin networks further support the hypothesis that architectural properties on the LTP newtorks become more stable with time.

Taken together, our results support the idea that networks regulated at different levels possess different dynamic characteristics adjusted to their respective time frames.

The results described in this chapter have been published in the journal Frontiers in Molecular Neuroscience (Nido, Ryan, Benuskova, and Williams, 2015).

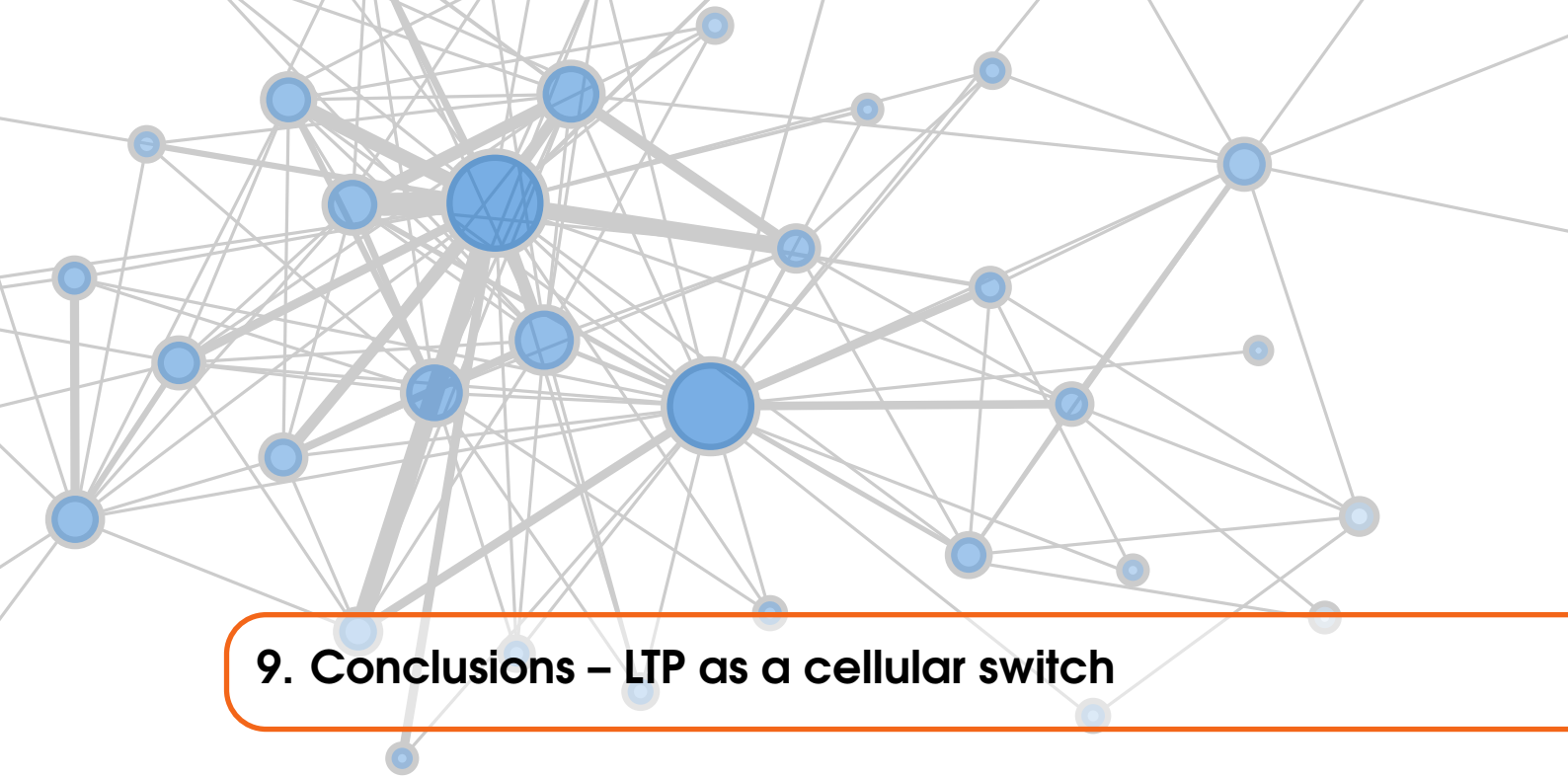

9. Conclusions – LTP as a cellular switch

Reality exists in the human mind, and nowhere else

George Orwell

As we have discussed in previous chapters, at least three distinct phases have been identified following high-frequency stimulus (HFS) required for LTP. It is unclear how these phases are interrelated, and some evidence seems to suggest that while the underlying mechanisms are distinct, they overlap in time (Park *et al.*, 2014). This should come as no surprise if we recognize that neurons capable of modifying synaptic efficacy for long periods of time are to overcome the limitations imposed by protein and mRNA half-life (in the scale of minutes or hours, Price, Guan, Burlingame, Prusiner, and Ghaemmaghami, 2010; Schwanhäusser, Busse, Li, Dittmar, Schuchhardt, Wolf, Chen, and Selbach, 2011). Protein and mRNA turnover has to be surmounted by a machinery capable of transmitting information across different levels of hierarchical associations which operate at different time scales.

The interplay between mechanisms acting at different levels of organisation and time scales ensures that neurons undergoing LTP can robustly perform their functions and maintain homeostasis. Gene expression changes, in particular, are known to be necessary for the maintenance of late-LTP. As gene expression is regulated at different times following the stimulation necessary to trigger LTP, we have aimed to study the characteristics of these genomic networks taking advantage of the availability of microarray data. The use of computational models has allowed us to further characterise the biological networks involved in LTP and delve deeper into the complexity of this form of synaptic plasticity.

The first integrative checkpoint of the signal elicited by HFS is represented by the putative role of CaMKII as a molecular switch. The capacity of autophosphorylation demonstrated for CaMKII may be sufficient to turn the transient change in intracellular Ca^{2+} caused by the neurotransmitter release from the presynaptic cell into a longer-lasting signal (see Section 3.3.1). This switch sets off the molecular changes needed to increase the post-synaptic sensitivity to subsequent stimuli. The local protein pools suffice to carry out these early changes. However, as we have discussed previously, protein synthesis becomes necessary to enter the longer-lasting late-LTP phase. Protein

turnover is overcome by replenishing the protein pools with newly-synthesised molecules.

In parallel, the signal is transmitted to the nucleus though molecular signalling cascades involving other proteins (PKA, PKC, CaMKIV). These signals seem to converge in the activation of inducible transcription factors that act on SRE- and CRE-containing genes and the subsequent induction of gene expression. Thus the original signal crosses over to an additional level. Furthermore, the signal driving the synaptic consolidation of LTP spreads to influence the morphology of the cell, inducing morphological changes in the stimulated synapses. These changes can be seen under the electron microscope (Yuste and Bonhoeffer, 2001).

This picture gives an idea of the different levels and complexity of the hierarchical associations involved in LTP at the cellular level. Furthermore, LTP only constitutes a model for the cellular mechanism that may underlie long-term memories, and it is becoming clear that LTP comprises rather a family of different processes by which neurons integrate and process the information to change their synaptic weights. For example, it has been argued recently that in the Schaffer collateral-commissural pathway at least three mechanistically different forms of synaptic plasticity co-exist, all NMDAR-dependent (Park *et al.*, 2014). These forms can overlap partially in time, and the combination of these processes can increase their functional utility.

The genomic component of LTP operates within a single neuron. Yet, it only represents one tier of data processing. This tier is "nested" on the another tier of computation constituted by the neural networks, ultimately responsible for the consolidation of memories and learning. This "nested" network architecture is, in reality, a highly modular network recollective of the fractal structure found in many naturally occurring structures (Song, Havlin, and Makse, 2005). Subsequent hierarchically higher levels have been described in cortical connectivity, in which the local neural circuits and columns are connected via nerve fiber projections between brain areas (Scannell, Burns, Hilgetag, O'Neil, and Young, 1999).

From this perspective, LTP represents the experimental representation of a cellular mechanism which acts at the interneuronal level by changing the strengths of the interactions (black arrows in Figure 9.1). The decision, however, is the result of the integration of the incoming information by the cellular machinery at the molecular level. Interestingly, the brain's genomic response to learning and other neuronal stimulation is not a new evolutionary trait to mammals, but rather seems to be an ancient process, as evidenced by the fact that gene expression changes have been documented, for a number of experimental organisms and tissues (Clayton, 2000).

In this context, in the present thesis we analysed general topological properties of the co-expression networks corresponding to different time points (control, 20 min, 5 h, and 24 h). Notably, these networks exhibit a different connectivity distribution (see Figures 6.2 and 6.4). Interestingly, the unstimulated control and the 24 h networks fit to a scale free distribution fairly well while on the contrary, the co-expression networks corresponding to the 20 min and 5 h datasets have a truncated distribution. As higher robustness is expected of scale free distributions (Albert *et al.*, 2000), this observation is consistent with the notion that cellular networks involved in the homeostatic states (pre- and post-LTP induction) are more stable, while transient topological rearrangements are characteristic of intermediate networks (20 min and 5 h).

Moreover, using the RBN paradigm we have shown that the network derived at 24 h exhibited an enhanced stability when compared to those derived at earlier times post-LTP. This temporal effect on the vulnerability of the networks is mirrored by what is known about the vulnerability of LTP and memory.

In summary, we have presented a view of LTP as a biological process in which a transient signal sets a new homeostatic state that is "remembered" by the cellular systems. Central to this process is the regulation by gene expression, in which the central role played by the Egr transcription factors after LTP induction was highlighted by differential expression and co-expression analyses. In addition, we found a rapid enrichment in connectivity at 20 min followed by a systematic decrease.

This observation provides a potential explanation for the down-regulation of gene expression at 24 h documented by previous studies. From a systems perspective, we have provided evidence that these networks will show less stable architecture, while networks recruited later will exhibit increased stability, consistent with the fact they are more directly related to LTP consolidation. The architecture exhibited by a control and the 24 h LTP co-expression networks fit well to a scale-free distribution, known to be robust against perturbations, whereas the earlier 20 min and 5 h networks showed truncated distributions. Moreover, using random Boolean network simulations we have shown that the network derived at 24 h exhibited an enhanced stability when compared to those derived at earlier times post-LTP. This temporal effect on the vulnerability of the networks is mirrored by what is known about the vulnerability of LTP and memory. Taken together, these results suggest that a new homeostatic state is achieved 24 h post-LTP, and defines an integrated view of the genomic response following LTP induction by which the stability of the networks regulated at different times parallel the properties observed at the synapse.

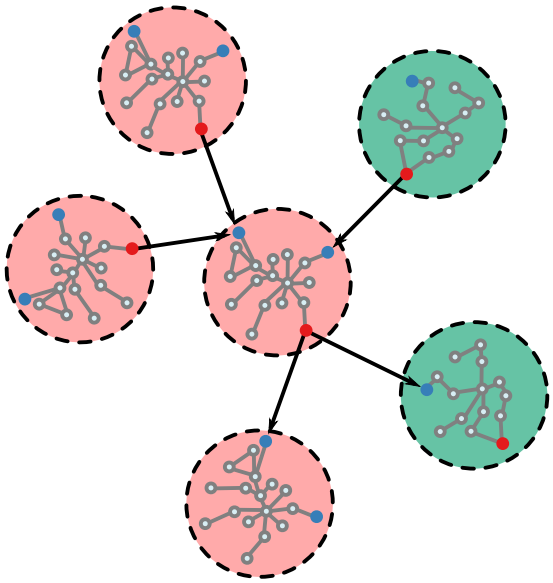

Figure 9.1: *Network representation of a two-level nested network. The molecular species (proteins, RNA, genes and other metabolites) are represented as small nodes. They are organised within a neuron (dashed circles) and they serve as a processing unit. Some nodes will act as sensors or inputs (blue nodes) of information from other neurons. The information is then processed and an output sent to other neurons (red nodes). The nested networks inside the neurons can be different according to the neuron types and regions of the brain, represented as light red and light green in the figure. In this model, LTP would act changing the weight of the connections between neurons (black arrows)*

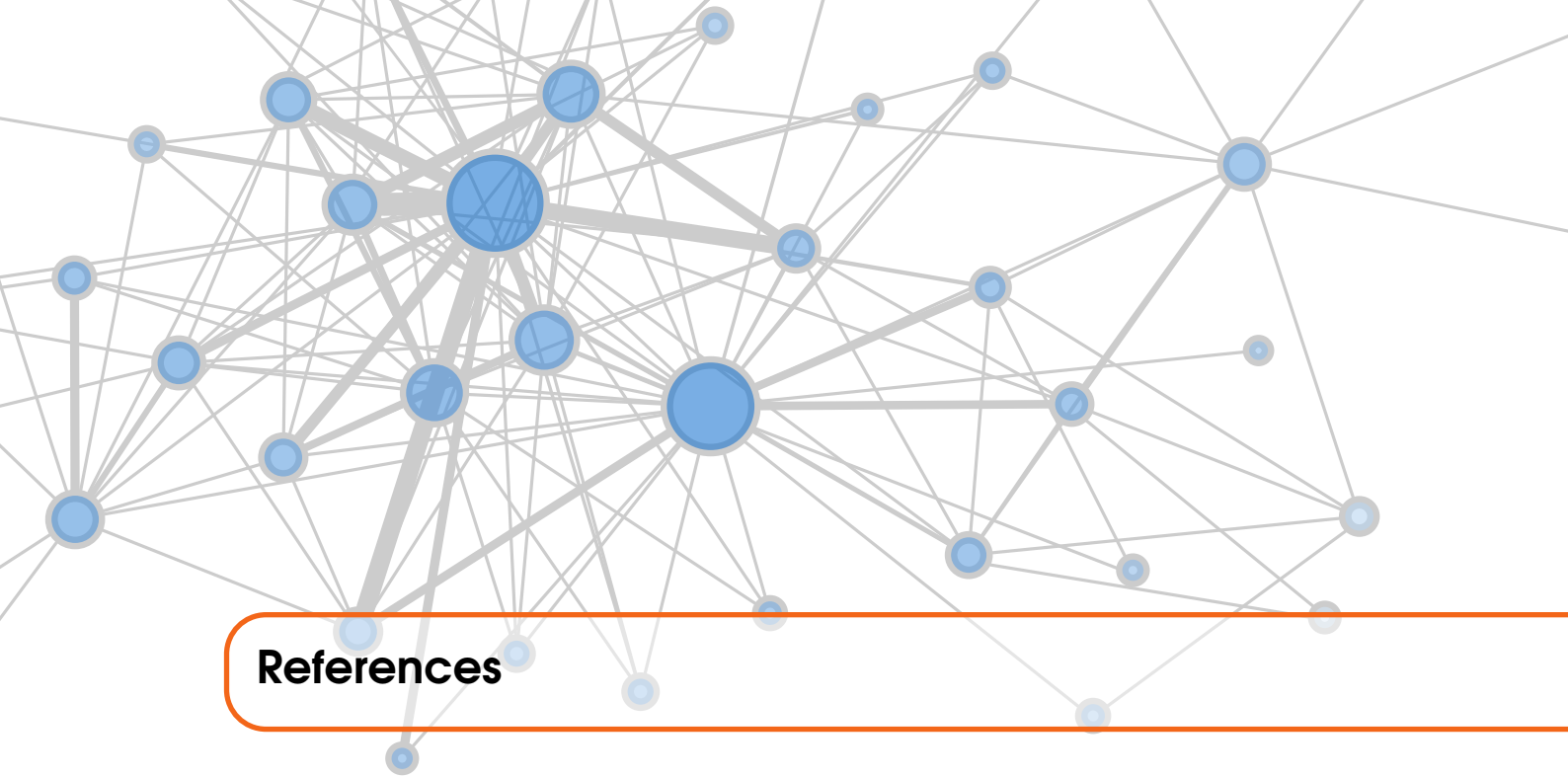

References

Abel, T., Nguyen, P. V., Barad, M., Deuel, T. A., Kandel, E. R., and Bourtchouladze, R. (1997). Genetic demonstration of a role for PKA in the late phase of LTP and in hippocampus-based long-term memory. *Cell*, *88*(5), 615–626.

Aboitiz, F., Morales, D., and Montiel, J. (2003). The evolutionary origin of the mammalian isocortex: towards an integrated developmental and functional approach. *Behavioral and Brain Sciences*, *26*(05), 535–552.

Abraham, W., Logan, B., Greenwood, J., and Dragunow, M. (2002). Induction and experience-dependent consolidation of stable long-term potentiation lasting months in the hippocampus. *The Journal of neuroscience*, *22*(21), 9626–9634.

Abraham, W., Mason, S., Demmer, J., Williams, J., Richardson, C., Tate, W., Lawlor, P., and Dragunow, M. (1993). Correlations between immediate early gene induction and the persistence of long-term potentiation. *Neuroscience*, *56*(3), 717–27.

Abraham, W. and Williams, J. (2003). Properties and mechanisms of LTP maintenance. *The Neuroscientist*, *9*(6), 463.

Abraham, W. and Williams, J. (2008). LTP maintenance and its protein synthesis-dependence. *Neurobiology of learning and memory*, *89*(3), 260–268.

Adesnik, H. and Nicoll, R. A. (2007). Conservation of glutamate receptor 2-containing AMPA receptors during long-term potentiation. *The Journal of neuroscience*, *27*(17), 4598–4602.

Ahn, H. J., Hernandez, C. M., Levenson, J. M., Lubin, F. D., Liou, H.-C., and Sweatt, J. D. (2008). c-Rel, an NF-kB family transcription factor, is required for hippocampal long-term synaptic plasticity and memory formation. *Learning & Memory*, *15*(7), 539–549.

Albensi, B. C. and Mattson, M. P. (2000). Evidence for the involvement of TNF and NF-kB in hippocampal synaptic plasticity. *Synapse*, *35*(2), 151–159.

Alberini, C. (2009). Transcription factors in long-term memory and synaptic plasticity. *Physiological reviews*, *89*(1), 121.

Albert, R., Jeong, H., and Barabási, A.-L. (2000). Error and attack tolerance of complex networks. *Nature*, *406*(6794), 378–382.

Albert, R. and Othmer, H. G. (2003). The topology of the regulatory interactions predicts the expression pattern of the segment polarity genes in Drosophila melanogaster. *Journal of theoretical biology*, *223*(1), 1–18.

Alberts, B. (2008). *Molecular Biology of the Cell: Reference edition*. Number v. 1 in Molecular Biology of the Cell: Reference Edition. Garland Science.

Aldana, M. (2003). Boolean dynamics of networks with scale-free topology. *Physica D: Nonlinear Phenomena*, *185*(1), 45–66.

Aldana, M. and Cluzel, P. (2003). A natural class of robust networks. *Proceedings of the National Academy of Sciences*, *100*(15), 8710–8714.

Aldana, M., Coppersmith, S., and Kadanoff, L. P. (2003). Boolean dynamics with random couplings. In *Perspectives and Problems in Nolinear Science*, 23–89. Springer.

Aldana-Gonzalez, M., Coppersmith, S., and Kadanoff, L. (2002). Boolean Dynamics with Random Couplings. In E. Kaplan, J. Marsden, and K. Sreenivasan (Eds.), *Perspectives and Problems in Nonlinear Science*, 23–89. Springer, New York.

Alexa, A. and Rahnenfuhrer, J. (2010). *topGO: topGO: Enrichment analysis for Gene Ontology*. R package version 2.12.0.

Alkema, M., Wiegant, J., Raap, A. K., Bems, A., and van Lohuizen, M. (1993). Characterization and chromosomal localization of the human proto-oncogene BMI-1. *Human molecular genetics*, *2*(10), 1597–1603.

Allen, P. B., Hvalby, Ø., Jensen, V., Errington, M. L., Ramsay, M., Chaudhry, F. A., Bliss, T. V., Storm-Mathisen, J., Morris, R. G., Andersen, P., *et al.* (2000). Protein phosphatase-1 regulation in the induction of long-term potentiation: heterogeneous molecular mechanisms. *The Journal of Neuroscience*, *20*(10), 3537–3543.

Andersen, P. and Lømo, T. (1967). *Control of hippocampal output by afferent volley frequency*, Volume 27 of *Progress in Brain Research*. Elsevier.

Araki, T. and Milbrandt, J. (2003). ZNRF proteins constitute a family of presynaptic E3 ubiquitin ligases. *The Journal of neuroscience*, *23*(28), 9385–9394.

Ashburner, M., Ball, C. A., Blake, J. A., Botstein, D., Butler, H., Cherry, J. M., Davis, A. P., Dolinski, K., Dwight, S. S., Eppig, J. T., *et al.* (2000). Gene Ontology: tool for the unification of biology. *Nature genetics*, *25*(1), 25–29.

Atkins, C. M., Selcher, J. C., Petraitis, J. J., Trzaskos, J. M., and Sweatt, J. D. (1998). The MAPK cascade is required for mammalian associative learning. *Nature neuroscience*, *1*(7), 602–609.

Bading, H., Ginty, D. D., and Greenberg, M. E. (1993). Regulation of gene expression in hippocampal neurons by distinct calcium signaling pathways. *Science*, *260*(5105), 181–186.

Balch, W. E., Morimoto, R. I., Dillin, A., and Kelly, J. W. (2008). Adapting proteostasis for disease intervention. *science*, *319*(5865), 916–919.

Balleza, E., Alvarez-Buylla, E. R., Chaos, A., Kauffman, S., Shmulevich, I., and Aldana, M. (2008). Critical dynamics in genetic regulatory networks: examples from four kingdoms. *PLoS One*, *3*(6), e2456.

Baltz, A. G., Munschauer, M., Schwanhäusser, B., Vasile, A., Murakawa, Y., Schueler, M., Youngs, N., Penfold-Brown, D., Drew, K., Milek, M., *et al.* (2012). The mRNA-bound proteome and its global occupancy profile on protein-coding transcripts. *Molecular cell*, *46*(5), 674–690.

Barabási, A.-L. and Albert, R. (1999). Emergence of scaling in random networks. *science*, *286*(5439), 509–512.

Barco, A., Patterson, S., Alarcon, J. M., Gromova, P., Mata-Roig, M., Morozov, A., and Kandel, E. R. (2005). Gene expression profiling of facilitated L-LTP in VP16-CREB mice reveals that BDNF is critical for the maintenance of LTP and its synaptic capture. *Neuron*, *48*(1), 123–137.

Barria, A. and Malinow, R. (2005). NMDA receptor subunit composition controls synaptic plasticity by regulating binding to CaMKII. *Neuron*, *48*(2), 289–301.

Barria, A., Muller, D., Derkach, V., Griffith, L. C., and Soderling, T. R. (1997). Regulatory phosphorylation of AMPA-type glutamate receptors by CaM-KII during long-term potentiation. *Science*, *276*(5321), 2042–2045.

Bayer, K. U., LeBel, É., McDonald, G. L., O'Leary, H., Schulman, H., and De Koninck, P. (2006). Transition from reversible to persistent binding of CaMKII to postsynaptic sites and NR2B. *The Journal of neuroscience*, *26*(4), 1164–1174.

Bayer, K.-U., Paul De Koninck, A., Hell, J. W., and Schulman, H. (2001). Interaction with the NMDA receptor locks CaMKII in an active conformation. *Nature*, *411*(6839), 801–805.

Beadle, G. W. and Tatum, E. L. (1941). Genetic control of biochemical reactions in Neurospora. *Proceedings of the National Academy of Sciences of the United States of America*, *27*(11), 499.

Bear, M. F. and Malenka, R. C. (1994). Synaptic plasticity: LTP and LTD. *Current opinion in neurobiology*, *4*(3), 389–399.

Bella, J., Eaton, M., Brodsky, B., and Berman, H. M. (1994). Crystal and molecular structure of a collagen-like peptide at 1.9 A resolution. *Science*, *266*(5182), 75–81.

Bellinger, F., Madamba, S., Campbell, I., and Siggins, G. (1995). Reduced long-term potentiation in the dentate gyrus of transgenic mice with cerebral overexpression of interleukin-6. *Neuroscience letters*, *198*(2), 95–98.

Benecke, H., Lührmann, R., and Will, C. L. (2005). The U11/U12 snRNP 65K protein acts as a molecular bridge, binding the U12 snRNA and U11-59K protein. *The EMBO journal*, *24*(17), 3057–3069.

Benito, E., Valor, L. M., Jimenez-Minchan, M., Huber, W., and Barco, A. (2011). cAMP response element-binding protein is a primary hub of activity-driven neuronal gene expression. *The Journal of Neuroscience*, *31*(50), 18237–18250.

Benuskova, L. (2000). The intra-spine electric force can drive vesicles for fusion: a theoretical model for long-term potentiation. *Neuroscience letters*, *280*(1), 17–20.

Benuskova, L. and Kasabov, N. (2007). Modeling L-LTP based on changes in concentration of pCREB transcription factor. *Neurocomputing*, *70*(10), 2035–2040.

Bhat, R. V., Worley, P. F., Cole, A. J., and Baraban, J. (1992). Activation of the zinc finger encoding gene krox-20 in adult rat brain: comparison with zif 268. *Molecular brain research*, *13*(3), 263–266.

Bito, H., Deisseroth, K., and Tsien, R. W. (1996). CREB phosphorylation and dephosphorylation: A Ca2+-and stimulus duration–dependent switch for hippocampal gene expression. *Cell*, *87*(7), 1203–1214.

Bito, H., Deisseroth, K., and Tsien, R. W. (1997). Ca2+-dependent regulation in neuronal gene expression. *Current opinion in neurobiology*, *7*(3), 419–429.

Blakely, R. D. and Edwards, R. H. (2012). Vesicular and plasma membrane transporters for neurotransmitters. *Cold Spring Harbor perspectives in biology*, *4*(2), a005595.

Bliss, T., Errington, M., Laroche, S., and Lynch, M. (1987). Increase in K+-stimulated, Ca2+-dependent release of [3 H] glutamate from rat dentate gyrus three days after induction of long-term potentiation. *Neuroscience letters*, *83*(1), 107–112.

Bliss, T. and Gardner-Medwin, A. (1973). Long-lasting potentiation of synaptic transmission in the dentate area of the unanaesthetized rabbit following stimulation of the perforant path. *The Journal of Physiology*, *232*(2), 357–374.

Bliss, T. and Lømo, T. (1973). Long-lasting potentiation of synaptic transmission in the dentate area of the anaesthetized rabbit following stimulation of the perforant path. *The Journal of Physiology*, *232*(2), 331–356.

Blitzer, R. D., Connor, J. H., Brown, G. P., Wong, T., Shenolikar, S., Iyengar, R., and Landau, E. M. (1998). Gating of CaMKII by cAMP-regulated protein phosphatase activity during LTP. *Science*, *280*(5371), 1940–1943.

Blitzer, R. D., Wong, T., Nouranifar, R., Iyengar, R., and Landau, E. M. (1995). Postsynaptic cAMP pathway gates early LTP in hippocampal CA1 region. *Neuron*, *15*(6), 1403–1414.

Blum, S., Moore, A. N., Adams, F., and Dash, P. K. (1999). A mitogen-activated protein kinase cascade in the CA1/CA2 subfield of the dorsal hippocampus is essential for long-term spatial memory. *The Journal of neuroscience*, *19*(9), 3535–3544.

Bonhoeffer, T., Staiger, V., and Aertsen, A. (1989). Synaptic plasticity in rat hippocampal slice cultures: local" Hebbian" conjunction of pre-and postsynaptic stimulation leads to distributed synaptic enhancement. *Proceedings of the National Academy of Sciences*, *86*(20), 8113–8117.

Borden, L., Dhar, T., Smith, K., Branchek, T., Gluchowski, C., and Weinshank, R. (1993). Cloning of the human homologue of the GABA transporter GAT-3 and identification of a novel inhibitor with selectivity for this site. *Receptors & channels*, *2*(3), 207–213.

Bornholdt, S. (2005). Less is more in modeling large genetic networks. *SCIENCE-NEW YORK THEN WASHINGTON-*, *310*(5747), 449.

Bourtchuladze, R., Frenguelli, B., Blendy, J., Cioffi, D., Schutz, G., and Silva, A. J. (1994). Deficient long-term memory in mice with a targeted mutation of the cAMP-responsive element-binding protein. *Cell*, *79*(1), 59–68.

Bradshaw, J. M., Kubota, Y., Meyer, T., and Schulman, H. (2003). An ultrasensitive Ca2+/calmodulin-dependent protein kinase II-protein phosphatase 1 switch facilitates specificity in postsynaptic calcium signaling. *Proceedings of the National Academy of Sciences*, *100*(18), 10512–10517.

Brakeman, P., Lanahan, A., O'Brien, R., Roche, K., Barnes, C., Huganir, R., and Worley, P. (1997). Homer: a protein that selectively binds metabotropic glutamate receptors. *Nature*, *386*, 284–288.

Bramham, C. R. (2008). Local protein synthesis, actin dynamics, and LTP consolidation. *Current opinion in neurobiology*, *18*(5), 524–531.

Bramham, C. R., Alme, M. N., Bittins, M., Kuipers, S. D., Nair, R. R., Pai, B., Panja, D., Schubert, M., Soule, J., Tiron, A., *et al.* (2010). The Arc of synaptic memory. *Experimental Brain Research*, *200*(2), 125–140.

Braun, A. P. and Schulman, H. (1995). The multifunctional calcium/calmodulin-dependent protein kinase: from form to function. *Annual review of physiology*, *57*(1), 417–445.

Brazma, A. and Vilo, J. (2000). Gene expression data analysis. *FEBS letters*, *480*(1), 17–24.

Brenner, S., Johnson, M., Bridgham, J., Golda, G., Lloyd, D. H., Johnson, D., Luo, S., McCurdy, S., Foy, M., Ewan, M., *et al.* (2000). Gene expression analysis by massively parallel signature sequencing (MPSS) on microbead arrays. *Nature biotechnology*, *18*(6), 630–634.

Brooks, W. S., Helton, E. S., Banerjee, S., Venable, M., Johnson, L., Schoeb, T. R., Kesterson, R. A., and Crawford, D. F. (2008). G2E3 is a dual function ubiquitin ligase required for early embryonic development. *Journal of Biological Chemistry*, *283*(32), 22304–22315.

Bruel-Jungerman, E., Davis, S., Rampon, C., and Laroche, S. (2006). Long-term potentiation enhances neurogenesis in the adult dentate gyrus. *The Journal of neuroscience*, *26*(22), 5888–5893.

Burgaya, F. and Girault, J.-A. (1996). Cloning of focal adhesion kinase, pp125 FAK, from rat brain reveals multiple transcripts with different patterns of expression. *Molecular brain research*, *37*(1), 63–73.

Byrne, M. J., Putkey, J. A., Waxham, M. N., and Kubota, Y. (2009). Dissecting cooperative calmodulin binding to CaM kinase II: a detailed stochastic model. *Journal of computational neuroscience*, *27*(3), 621–638.

Cao, R., Tsukada, Y.-i., and Zhang, Y. (2005). Role of Bmi-1 and Ring1A in H2A ubiquitylation and Hox gene silencing. *Molecular cell*, *20*(6), 845–854.

Chaillan, F. A., Rivera, S., Marchetti, E., Jourquin, J., Werb, Z., Soloway, P. D., Khrestchatisky, M., and Roman, F. S. (2006). Involvement of tissue inhibition of metalloproteinases-1 in learning and memory in mice. *Behavioural brain research*, *173*(2), 191–198.

Chang, B., Mukherji, S., and Soderling, T. (2001). Calcium/calmodulin-dependent protein kinase II inhibitor protein: localization of isoforms in rat brain. *Neuroscience*, *102*(4), 767–777.

Chau, B. N., Cheng, E. H.-Y., Kerr, D. A., and Hardwick, J. M. (2000). Aven, a Novel Inhibitor of Caspase Activation, Binds Bcl-x L and Apaf-1. *Molecular cell*, *6*(1), 31–40.

Chaves, M., Albert, R., and Sontag, E. D. (2005). Robustness and fragility of Boolean models for genetic regulatory networks. *Journal of theoretical biology*, *235*(3), 431–449.

Chaves, M., Sontag, E. D., and Albert, R. (2006). Methods of robustness analysis for Boolean models of gene control networks. *IEE Proceedings-Systems Biology*, *153*(4), 154–167.

Chawla, S., Hardingham, G. E., Quinn, D. R., and Bading, H. (1998). CBP: a signal-regulated transcriptional coactivator controlled by nuclear calcium and CaM kinase IV. *Science*, *281*(5382), 1505–1509.

Chen, H., Lin, R. J., Schiltz, R. L., Chakravarti, D., Nash, A., Nagy, L., Privalsky, M. L., Nakatani, Y., and Evans, R. M. (1997). Nuclear receptor coactivator ACTR is a novel histone acetyltransferase and forms a multimeric activation complex with P/CAF and CBP/p300. *Cell*, *90*(3), 569–580.

Chen, W. Y., Wang, D. H., Yen, R. C., Luo, J., Gu, W., and Baylin, S. B. (2005). Tumor suppressor HIC1 directly regulates SIRT1 to modulate p53-dependent DNA-damage responses. *Cell*, *123*(3), 437–448.

Chetkovich, D., Gray, R., Johnston, D., and Sweatt, J. (1991). N-methyl-D-aspartate receptor activation increases cAMP levels and voltage-gated Ca2+ channel activity in area CA1 of hippocampus. *Proceedings of the National Academy of Sciences*, *88*(15), 6467–6471.

Chiu, R., Boyle, W. J., Meek, J., Smeal, T., Hunter, T., and Karin, M. (1988). The c-fos protein interacts with c-JunAP-1 to stimulate transcription of AP-1 responsive genes. *Cell*, *54*(4), 541–552.

Christensen, T. S., Oliveira, A. P., and Nielsen, J. (2009). Reconstruction and logical modeling of glucose repression signaling pathways in Saccharomyces cerevisiae. *BMC systems biology*, *3*(1), 7.

Clayton, D. F. (2000). The genomic action potential. *Neurobiology of learning and memory*, *74*(3), 185–216.

Coan, E. and Collingridge, G. (1985). Magnesium ions block an N-methyl-D-aspartate receptor-mediated component of synaptic transmission in rat hippocampus. *Neuroscience letters*, *53*(1), 21–26.

Coba, M. P., Valor, L. M., Kopanitsa, M. V., Afinowi, N. O., and Grant, S. G. (2008). Kinase networks integrate profiles of N-methyl-D-aspartate receptor-mediated gene expression in hippocampus. *Journal of Biological Chemistry*, *283*(49), 34101–34107.

Cohen, P. (1989). The structure and regulation of protein phosphatases. *Annual review of biochemistry*, *58*(1), 453–508.

Cole, A. J., Abu-Shakra, S., Saffen, D. W., Baraban, J. M., and Worley, P. F. (1990). Rapid Rise in Transcription Factor mRNAs in Rat Brain After Electroshock-Induced Seizures. *Journal of neurochemistry*, *55*(6), 1920–1927.

Cole, A. J., Saffen, D. W., Baraban, J. M., and Worley, P. F. (1989). Rapid increase of an immediate early gene messenger RNA in hippocampal neurons by synaptic NMDA receptor activation. *Nature*, *340*(6233), 474–476.

Collingridge, G. and Bliss, T. (1987). NMDA receptors-their role in long-term potentiation. *Trends in Neurosciences*, *10*(7), 288–293.

Collingridge, G., Kehl, S., and McLennan, H. (1983). Excitatory amino acids in synaptic transmission in the Schaffer collateral-commissural pathway of the rat hippocampus. *The Journal of Physiology*, *334*(1), 33.

Contractor, A., Rogers, C., Maron, C., Henkemeyer, M., Swanson, G. T., and Heinemann, S. F. (2002). Trans-synaptic Eph receptor-ephrin signaling in hippocampal mossy fiber LTP. *Science*, *296*(5574), 1864–1869.

Cope, L. M., Irizarry, R. A., Jaffee, H. A., Wu, Z., and Speed, T. P. (2004). A benchmark for Affymetrix GeneChip expression measures. *Bioinformatics*, *20*(3), 323–331.

Cullen, P. J. and Lockyer, P. J. (2002). Integration of calcium and Ras signalling. *Nature Reviews Molecular Cell Biology*, *3*(5), 339–348.

Cunningham, A., Murray, C., O'Neill, L., Lynch, M., and O'Connor, J. (1996). Interleukin-1β (IL-1β) and tumour necrosis factor (TNF) inhibit long-term potentiation in the rat dentate gyrus in vitro. *Neuroscience letters*, *203*(1), 17–20.

Curran, B. and O'Connor, J. (2001). The pro-inflammatory cytokine interleukin-18 impairs long-term potentiation and NMDA receptor-mediated transmission in the rat hippocampus in vitro. *Neuroscience*, *108*(1), 83–90.

Davidich, M. and Bornholdt, S. (2008). Boolean network model predicts cell cycle sequence of fission yeast. *PLoS One*, *3*(2), e1672.

Davies, R. W. (2004). *Molecular Biology of the Neuron (Molecular and Cellular Neurobiology)*. Oxford University Press,.

Dayer, A. G., Ford, A. A., Cleaver, K. M., Yassaee, M., and Cameron, H. A. (2003). Short-term and long-term survival of new neurons in the rat dentate gyrus. *Journal of Comparative Neurology*, *460*(4), 563–572.

De Clerck, Y., Szpirer, C., Aly, M. S., Cassiman, J.-J., Eeckhout, Y., and Rousseau, G. (1992). The gene for tissue inhibitor of metalloproteinases-2 is localized on human chromosome arm 17q25. *Genomics*, *14*(3), 782–784.

De Schutter, E. (2008). Why are computational neuroscience and systems biology so separate? *PLoS computational biology*, *4*(5), e1000078.

de Turco, E. B. R., Tang, W., Topham, M. K., Sakane, F., Marcheselli, V. L., Chen, C., Taketomi, A., Prescott, S. M., and Bazan, N. G. (2001). Diacylglycerol kinase r regulates seizure susceptibility and long-term potentiation through arachidonoyl–inositol lipid signaling. *Proceedings of the National Academy of Sciences*, *98*(8), 4740–4745.

De Wit, J., Sylwestrak, E., O'Sullivan, M. L., Otto, S., Tiglio, K., Savas, J. N., Yates III, J. R., Comoletti, D., Taylor, P., and Ghosh, A. (2009). LRRTM2 interacts with Neurexin1 and regulates excitatory synapse formation. *Neuron*, *64*(6), 799–806.

Deisseroth, K., Bito, H., and Tsien, R. W. (1996). Signaling from synapse to nucleus: postsynaptic CREB phosphorylation during multiple forms of hippocampal synaptic plasticity. *Neuron*, *16*(1), 89–101.

Demmer, J., Dragunow, M., Lawlor, P. A., Mason, S. E., Leah, J. D., Abraham, W. C., and Tate, W. P. (1993). Differential expression of immediate early genes after hippocampal long-term potentiation in awake rats. *Molecular brain research*, *17*(3), 279–286.

Dérijard, B., Hibi, M., Wu, I., Barrett, T., Su, B., Deng, T., Karin, M., Davis, R. J., *et al.* (1994). JNK1: a protein kinase stimulated by UV light and Ha-Ras that binds and phosphorylates the c-Jun activation domain. *Cell*, *76*(6), 1025–1037.

Derrida, B. and Pomeau, Y. (1986). Random networks of automata: a simple annealed approximation. *EPL (Europhysics Letters)*, *1*(2), 45.

Derrida, B. and Stauffer, D. (1986). Phase transitions in two-dimensional Kauffman cellular automata. *EPL (Europhysics Letters)*, *2*(10), 739.

Derrida, B. and Weisbuch, G. (1986). Evolution of overlaps between configurations in random Boolean networks. *Journal de physique*, *47*(8), 1297–1303.

Devi, S., Markandeya, Y., Maddodi, N., Dhingra, A., Vardi, N., Balijepalli, R. C., and Setaluri, V. (2013). Metabotropic glutamate receptor 6 signaling enhances TRPM1 calcium channel function and increases melanin content in human melanocytes. *Pigment cell & melanoma research*, *26*(3), 348–356.

Dolphin, A., Errington, M., and Bliss, T. (1982). Long-term potentiation of the perforant path in vivo is associated with increased glutamate release. *Nature*, *297*, 496–497.

Dong, C., Upadhya, S. C., Ding, L., Smith, T. K., and Hegde, A. N. (2008). Proteasome inhibition enhances the induction and impairs the maintenance of late-phase long-term potentiation. *Learning & memory*, *15*(5), 335–347.

Dragunow, M., Yamada, N., Bilkey, D., and Lawlor, P. (1992). Induction of immediate-early gene proteins in dentate granule cells and somatostatin interneurons after hippocampal seizures. *Molecular brain research*, *13*(1), 119–126.

Drossel, B. (2008). Random Boolean Networks. In H. Schuster (Ed.), *Reviews in Nonlinear Dynamics and Complexity*, Volume 1, 69. Vch Verlagsgesellschaft Mbh.

Edelman, A. M., Mitchelhill, K. I., Selbert, M. A., Anderson, K. A., Hook, S. S., Stapleton, D., Goldstein, E. G., Means, A. R., and Kemp, B. E. (1996). Multiple Ca2+-Calmodulin-dependent protein kinase kinases from rat brain. *Journal of Biological Chemistry*, *271*(18), 10806–10810.

Eisen, M. B., Spellman, P. T., Brown, P. O., and Botstein, D. (1998). Cluster analysis and display of genome-wide expression patterns. *Proceedings of the National Academy of Sciences*, *95*(25), 14863–14868.

el Ghissassi, F., Valsesia-Wittmann, S., Falette, N., Duriez, C., Walden, P. D., and Puisieux, A. (2002). BTG2 (TIS21/PC3) induces neuronal differentiation and prevents apoptosis of terminally differentiated PC12 cells. *Oncogene*, *21*(44), 6772–6778.

Ellinger-Ziegelbauer, H., Brown, K., Kelly, K., and Siebenlist, U. (1997). Direct activation of the stress-activated protein kinase (SAPK) and extracellular signal-regulated protein kinase (ERK) pathways by an inducible mitogen-activated protein kinase/ERK kinase kinase 3 (MEKK) derivative. *Journal of Biological Chemistry*, *272*(5), 2668–2674.

Engert, F. and Bonhoeffer, T. (1999). Dendritic spine changes associated with hippocampal long-term synaptic plasticity. *Nature*, *399*(6731), 66–70.

Enoki, R., Hu, Y.-l., Hamilton, D., and Fine, A. (2009). Expression of long-term plasticity at individual synapses in hippocampus is graded, bidirectional, and mainly presynaptic: optical quantal analysis. *Neuron*, *62*(2), 242–253.

Errington, M., Galley, P., and Bliss, T. V. (2003). Long-term potentiation in the dentate gyrus of the anaesthetized rat is accompanied by an increase in extracellular glutamate: real-time measurements using a novel dialysis electrode. *Philosophical Transactions of the Royal Society of London. Series B: Biological Sciences*, *358*(1432), 675–687.

Espinosa-Soto, C., Padilla-Longoria, P., and Alvarez-Buylla, E. R. (2004). A gene regulatory network model for cell-fate determination during Arabidopsis thaliana flower development that is robust and recovers experimental gene expression profiles. *The Plant Cell Online*, *16*(11), 2923–2939.

Evers, D. M., Matta, J. A., Hoe, H.-S., Zarkowsky, D., Lee, S. H., Isaac, J. T., and Pak, D. T. (2010). Plk2 attachment to NSF induces homeostatic removal of GluA2 during chronic overexcitation. *Nature neuroscience*, *13*(10), 1199–1207.

Fang, Y., Vilella-Bach, M., Bachmann, R., Flanigan, A., and Chen, J. (2001). Phosphatidic acid-mediated mitogenic activation of mTOR signaling. *Science*, *294*(5548), 1942–1945.

Feng, J. and Fan, G. (2009). The role of DNA methylation in the central nervous system and neuropsychiatric disorders. *International review of neurobiology*, *89*, 67–84.

Fenner, B. J., Scannell, M., and Prehn, J. H. (2009). Identification of polyubiquitin binding proteins involved in NF-kB signaling using protein arrays. *Biochimica et Biophysica Acta (BBA)-Proteins and Proteomics*, *1794*(7), 1010–1016.

Fermi, G., Perutz, M., Shaanan, B., and Fourme, R. (1984). The crystal structure of human deoxyhaemoglobin at 1.74 Å resolution. *Journal of molecular biology*, *175*(2), 159–174.

Ferrell, J. E. and Machleder, E. M. (1998). The biochemical basis of an all-or-none cell fate switch in Xenopus oocytes. *Science*, *280*(5365), 895–898.

Fischer, M., Kaech, S., Knutti, D., and Matus, A. (1998). Rapid actin-based plasticity in dendritic spines. *Neuron*, *20*(5), 847–854.

Flavell, S. W. and Greenberg, M. E. (2008). Signaling mechanisms linking neuronal activity to gene expression and plasticity of the nervous system. *Annual review of neuroscience*, *31*, 563.

Fleischmann, A., Hvalby, O., Jensen, V., Strekalova, T., Zacher, C., Layer, L. E., Kvello, A., Reschke, M., Spanagel, R., Sprengel, R., *et al.* (2003). Impaired long-term memory and NR2A-type NMDA receptor-dependent synaptic plasticity in mice lacking c-Fos in the CNS. *The journal of neuroscience*, *23*(27), 9116–9122.

Fliegner, K., Ching, G., and Liem, R. (1990). The predicted amino acid sequence of alpha-internexin is that of a novel neuronal intermediate filament protein. *The EMBO journal*, *9*(3), 749.

Fonseca, R., Nägerl, U., and Bonhoeffer, T. (2006). Neuronal activity determines the protein synthesis dependence of long-term potentiation. *Nature neuroscience*, *9*(4), 478–480.

Fox, J. and Hill, C. (2001). From topology to dynamics in biochemical networks. *Chaos: An Interdisciplinary Journal of Nonlinear Science*, *11*(4), 809–815.

Freudenthal, R. and Romano, A. (2000). Participation of Rel/NF-κB transcription factors in long-term memory in the crab Chasmagnathus. *Brain research*, *855*(2), 274–281.

Freudenthal, R., Romano, A., and Routtenberg, A. (2004). Transcription factor NF-kB activation after in vivo perforant path LTP in mouse hippocampus. *Hippocampus*, *14*(6), 677–683.

Frey, U. and Morris, R. G. (1997). Synaptic tagging and long-term potentiation. *Nature*, *385*(6616), 533–536.

Fukazawa, Y., Saitoh, Y., Ozawa, F., Ohta, Y., Mizuno, K., and Inokuchi, K. (2003). Hippocampal LTP is accompanied by enhanced F-actin content within the dendritic spine that is essential for late LTP maintenance in vivo. *Neuron*, *38*(3), 447–460.

Fukunaga, K., Stoppini, L., Miyamoto, E., and Muller, D. (1993). Long-term potentiation is associated with an increased activity of Ca2+/calmodulin-dependent protein kinase II. *Journal of Biological Chemistry*, *268*(11), 7863–7867.

Fusi, S., Drew, P. J., and Abbott, L. (2005). Cascade models of synaptically stored memories. *Neuron*, *45*(4), 599–611.

Garriga-Canut, M., Roopra, A., and Buckley, N. J. (2001). The basic helix-loop-helix protein, sharp-1, represses transcription by a histone deacetylase-dependent and histone deacetylase-independent mechanism. *Journal of Biological Chemistry*, *276*(18), 14821–14828.

Gat-Viks, I., Tanay, A., Raijman, D., and Shamir, R. (2006). A probabilistic methodology for integrating knowledge and experiments on biological networks. *Journal of Computational Biology*, *13*(2), 165–181.

Gat-Viks, I., Tanay, A., and Shamir, R. (2004). Modeling and analysis of heterogeneous regulation in biological networks. *Journal of Computational Biology*, *11*(6), 1034–1049.

Gentleman, R. C., Carey, V. J., Bates, D. M., Bolstad, B., Dettling, M., Dudoit, S., Ellis, B., Gautier, L., Ge, Y., Gentry, J., *et al.* (2004). Bioconductor: open software development for computational biology and bioinformatics. *Genome biology*, *5*(10), R80.

Gerstein, M. B., Bruce, C., Rozowsky, J. S., Zheng, D., Du, J., Korbel, J. O., Emanuelsson, O., Zhang, Z. D., Weissman, S., and Snyder, M. (2007). What is a gene, post-ENCODE? History and updated definition. *Genome research*, *17*(6), 669–681.

Geschwind, D. and Konopka, G. (2009). Neuroscience in the era of functional genomics and systems biology. *Nature*, *461*(7266), 908–915.

Giaever, G., Chu, A. M., Ni, L., Connelly, C., Riles, L., Veronneau, S., Dow, S., Lucau-Danila, A., Anderson, K., Andre, B., *et al.* (2002). Functional profiling of the Saccharomyces cerevisiae genome. *nature*, *418*(6896), 387–391.

Giese, K. P., Fedorov, N. B., Filipkowski, R. K., and Silva, A. J. (1998). Autophosphorylation at Thr286 of the alpha calcium-calmodulin kinase II in LTP and learning. *Science*, *279*(5352), 870–873.

Gille, H., Kortenjann, M., Thomae, O., Moomaw, C., Slaughter, C., Cobb, M. H., and Shaw, P. E. (1995). ERK phosphorylation potentiates Elk-1-mediated ternary complex formation and transactivation. *The EMBO journal*, *14*(5), 951.

Gille, H., Sharrocks, A. D., and Shaw, P. E. (1992). Phosphorylation of transcription factor p62TCF by MAP kinase stimulates ternary complex formation at c-fos promoter. *Nature*, *358*, 414–417.

Gillespie, D. T. (2007). Stochastic simulation of chemical kinetics. *Annu. Rev. Phys. Chem.*, *58*, 35–55.

Glass, L. and Kauffman, S. A. (1973). The logical analysis of continuous, non-linear biochemical control networks. *Journal of theoretical Biology*, *39*(1), 103–129.

Goelet, P., Castellucci, V. F., Schacher, S., and Kandel, E. R. (1986). The long and the short of long-term memory: A molecular framework. *Nature*, *322*, 419–422.

Gould, E., Beylin, A., Tanapat, P., Reeves, A., and Shors, T. J. (1999). Learning enhances adult neurogenesis in the hippocampal formation. *Nature neuroscience*, *2*(3), 260–265.

Graudenzi, A., Serra, R., Villani, M., Damiani, C., Colacci, A., and Kauffman, S. A. (2011). Dynamical properties of a Boolean model of gene regulatory network with memory. *Journal of Computational Biology*, *18*(10), 1291–1303.

Greenberg, M. E. and Ziff, E. B. (1983). Stimulation of 3T3 cells induces transcription of the c-fos proto-oncogene. *Nature*, *311*(5985), 433–438.

Greengard, P., Allen, P. B., and Nairn, A. C. (1999). Beyond the dopamine receptor: the DARPP-32/protein phosphatase-1 cascade. *Neuron*, *23*(3), 435–447.

Greer, P. L. and Greenberg, M. E. (2008). From synapse to nucleus: calcium-dependent gene transcription in the control of synapse development and function. *Neuron*, *59*(6), 846–860.

Greger, I. H., Ziff, E. B., and Penn, A. C. (2007). Molecular determinants of AMPA receptor subunit assembly. *Trends in neurosciences*, *30*(8), 407–416.

Grover, L. M. and Teyler, T. J. (1990). Two components of long-term potentiation induced by different patterns of afferent activation. *Nature*, *347*(6292), 477–479.

Guan, J.-S., Haggarty, S. J., Giacometti, E., Dannenberg, J.-H., Joseph, N., Gao, J., Nieland, T. J., Zhou, Y., Wang, X., Mazitschek, R., *et al.* (2009). HDAC2 negatively regulates memory formation and synaptic plasticity. *Nature*, *459*(7243), 55–60.

Guzowski, J. F., Lyford, G. L., Stevenson, G. D., Houston, F. P., McGaugh, J. L., Worley, P. F., and Barnes, C. A. (2000). Inhibition of activity-dependent arc protein expression in the rat hippocampus impairs the maintenance of long-term potentiation and the consolidation of long-term memory. *The Journal of neuroscience*, *20*(11), 3993–4001.

Haber, D. A., Sohn, R. L., Buckler, A. J., Pelletier, J., Call, K. M., and Housman, D. E. (1991). Alternative splicing and genomic structure of the Wilms tumor gene WT1. *Proceedings of the National Academy of Sciences*, *88*(21), 9618–9622.

Halt, A. R., Dallapiazza, R. F., Zhou, Y., Stein, I. S., Qian, H., Juntti, S., Wojcik, S., Brose, N., Silva, A. J., and Hell, J. W. (2012). CaMKII binding to GluN2B is critical during memory consolidation. *The EMBO journal*, *31*(5), 1203–1216.

Hanai, Y., Tokuda, H., Ohta, T., Matsushima-Nishiwaki, R., Takai, S., and Kozawa, O. (2006). Phosphatidylinositol 3-kinase/Akt auto-regulates PDGF-BB-stimulated interleukin-6 synthesis in osteoblasts. *Journal of cellular biochemistry*, *99*(6), 1564–1571.

Hanley, J. G. and Henley, J. M. (2005). PICK1 is a calcium-sensor for NMDA-induced AMPA receptor trafficking. *The EMBO journal*, *24*(18), 3266–3278.

Hardingham, G. E., Arnold, F. J., and Bading, H. (2001). A calcium microdomain near NMDA receptors: on switch for ERK-dependent synapse-to-nucleus communication. *Nature neuroscience*, *4*(6), 565–566.

Hartl, F. U. (1996). Molecular chaperones in cellular protein folding. *Nature*, *381*, 571–580.

Harvey, C. D., Yasuda, R., Zhong, H., and Svoboda, K. (2008). The spread of Ras activity triggered by activation of a single dendritic spine. *Science*, *321*(5885), 136–140.

Harvey, I. and Bossomaier, T. (1997). Time out of joint: Attractors in asynchronous random boolean networks. In *Proceedings of the Fourth European Conference on Artificial Life*, 67–75. MIT Press, Cambridge.

Hasty, J., McMillen, D., Isaacs, F., Collins, J., *et al.* (2001). Computational studies of gene regulatory networks: in numero molecular biology. *Nature Reviews Genetics*, *2*(4), 268–279.

Haudek, K. C., Spronk, K. J., Voss, P. G., Patterson, R. J., Wang, J. L., and Arnoys, E. J. (2010). Dynamics of galectin-3 in the nucleus and cytoplasm. *Biochimica et Biophysica Acta (BBA)-General Subjects*, *1800*(2), 181–189.

Håvik, B., Røkke, H., Dagyte, G., Stavrum, A., Bramham, C., and Steen, V. (2007a). Synaptic activity-induced global gene expression patterns in the dentate gyrus of adult behaving rats: Induction of immunity-linked genes. *Neuroscience*, *148*(4), 925–936.

Håvik, B., Røkke, H., Dagyte, G., Stavrum, A.-K., Bramham, C., and Steen, V. (2007b). Synaptic activity-induced global gene expression patterns in the dentate gyrus of adult behaving rats: induction of immunity-linked genes. *Neuroscience*, *148*(4), 925–936.

He, Y., Janssen, W. G., Rothstein, J. D., and Morrison, J. H. (2000). Differential synaptic localization of the glutamate transporter EAAC1 and glutamate receptor subunit GluR2 in the rat hippocampus. *Journal of Comparative Neurology*, *418*(3), 255–269.

Heckscher, E. S., Fetter, R. D., Marek, K. W., Albin, S. D., and Davis, G. W. (2007). NF-κB, IκB, and IRAK control glutamate receptor density at the Drosophila NMJ. *Neuron*, *55*(6), 859–873.

Heller, M. J. (2002). DNA microarray technology: devices, systems, and applications. *Annual review of biomedical engineering*, *4*(1), 129–153.

Herculano-Houzel, S. (2009). The human brain in numbers: a linearly scaled-up primate brain. *Frontiers in human neuroscience*, *3*, 31.

Herculano-Houzel, S. and Lent, R. (2005). Isotropic fractionator: a simple, rapid method for the quantification of total cell and neuron numbers in the brain. *The Journal of neuroscience*, *25*(10), 2518–2521.

Herdegen, T. and Leah, J. (1998). Inducible and constitutive transcription factors in the mammalian nervous system: control of gene expression by Jun, Fos and Krox, and CREB/ATF proteins. *Brain Research Reviews*, *28*(3), 370–490.

Hernandez, A. I., Blace, N., Crary, J. F., Serrano, P. A., Leitges, M., Libien, J. M., Weinstein, G., Tcherapanov, A., and Sacktor, T. C. (2003). Protein Kinase Mζ Synthesis from a Brain mRNA Encoding an Independent Protein Kinase Cζ Catalytic Domain IMPLICATIONS FOR THE MOLECULAR MECHANISM OF MEMORY. *Journal of Biological Chemistry*, *278*(41), 40305–40316.

Hodgkin, A. L. and Huxley, A. F. (1952). A quantitative description of membrane current and its application to conduction and excitation in nerve. *The Journal of physiology*, *117*(4), 500.

Hong, S. J., Li, H., Becker, K. G., Dawson, V. L., and Dawson, T. M. (2004). Identification and analysis of plasticity-induced late-response genes. *Proceedings of the National Academy of Sciences of the United States of America*, *101*(7), 2145–2150.

Hope, B., Kosofsky, B., Hyman, S. E., and Nestler, E. J. (1992). Regulation of immediate early gene expression and AP-1 binding in the rat nucleus accumbens by chronic cocaine. *Proceedings of the National Academy of Sciences*, *89*(13), 5764–5768.

Huang, S. (2001). Genomics, complexity and drug discovery: insights from Boolean network models of cellular regulation. *Pharmacogenomics*, *2*(3), 203–222.

Huang, S. and Ingber, D. E. (2000). Shape-dependent control of cell growth, differentiation, and apoptosis: switching between attractors in cell regulatory networks. *Experimental cell research*, *261*(1), 91–103.

Huang, Y. and Kandel, E. (1994). Recruitment of long-lasting and protein kinase A-dependent long-term potentiation in the CA1 region of hippocampus requires repeated tetanization. *Learning & Memory*, *1*(1), 74.

Huang, Z. and Hahn, J. (2009). Fuzzy modeling of signal transduction networks. *Chemical Engineering Science*, *64*(9), 2044–2056.

Im, H.-I. and Kenny, P. J. (2012). MicroRNAs in neuronal function and dysfunction. *Trends in neurosciences*, *35*(5), 325–334.

Impey, S., Fong, A. L., Wang, Y., Cardinaux, J.-R., Fass, D. M., Obrietan, K., Wayman, G. A., Storm, D. R., Soderling, T. R., and Goodman, R. H. (2002). Phosphorylation of CBP mediates transcriptional activation by neural activity and CaM kinase IV. *Neuron*, *34*(2), 235–244.

Impey, S., Obrietan, K., and Storm, D. R. (1999). Making new connections: role of ERK/MAP kinase signaling in neuronal plasticity. *Neuron*, *23*(1), 11–14.

Ingi, T., Krumins, A. M., Chidiac, P., Brothers, G. M., Chung, S., Snow, B. E., Barnes, C. A., Lanahan, A. A., Siderovski, D. P., Ross, E. M., *et al.* (1998). Dynamic regulation of RGS2 suggests a novel mechanism in G-protein signaling and neuronal plasticity. *The Journal of neuroscience*, *18*(18), 7178–7188.

Inoue, M., Yagishita-Kyo, N., Nonaka, M., Kawashima, T., Okuno, H., and Bito, H. (2010). Synaptic activity–responsive element (SARE). *Communicative and Integrative Biology*, *3*(5), 443–446.

Irizarry, R. A., Bolstad, B. M., Collin, F., Cope, L. M., Hobbs, B., and Speed, T. P. (2003). Summaries of Affymetrix GeneChip probe level data. *Nucleic acids research*, *31*(4), e15–e15.

Irizarry, R. A., Hobbs, B., Collin, F., Beazer-Barclay, Y. D., Antonellis, K. J., Scherf, U., and Speed, T. P. (2003). Exploration, normalization, and summaries of high density oligonucleotide array probe level data. *Biostatistics*, *4*(2), 249–264.

Irwin, N., Chao, S., Goritchenko, L., Horiuchi, A., Greengard, P., Nairn, A. C., and Benowitz, L. I. (2002). Nerve growth factor controls GAP-43 mRNA stability via the phosphoprotein ARPP-19. *Proceedings of the National Academy of Sciences*, *99*(19), 12427–12431.

Janz, R. and Südhof, T. (1999). SV2C is a synaptic vesicle protein with an unusually restricted localization: anatomy of a synaptic vesicle protein family. *Neuroscience*, *94*(4), 1279–1290.

Jeong, H., Mason, S., Barabási, A.-L., and Oltvai, Z. (2001). Lethality and centrality in protein networks. *Nature*, *411*(6833), 41–42.

Jeong, H., Tombor, B., Albert, R., Oltvai, Z. N., and Barabási, A.-L. (2000). The large-scale organization of metabolic networks. *Nature*, *407*(6804), 651–654.

Jin, X., Jin, H. R., Jung, H. S., Lee, S. J., Lee, J.-H., and Lee, J. J. (2010). An Atypical E3 Ligase Zinc Finger Protein 91 Stabilizes and Activates NF-kB-inducing Kinase via Lys63-linked Ubiquitination. *Journal of Biological Chemistry*, *285*(40), 30539–30547.

Joilin, G., Guévremont, D., Ryan, B., Claudianos, C., Cristino, A. S., Abraham, W. C., and Williams, J. M. (2014). Rapid regulation of microRNA following induction of long-term potentiation in vivo. *Frontiers in molecular neuroscience*, *7*.

Jones, M., Errington, M., French, P., Fine, A., Bliss, T., Garel, S., Charnay, P., Bozon, B., Laroche, S., and Davis, S. (2001). A requirement for the immediate early gene Zif268 in the expression of late LTP and long-term memories. *Nature neuroscience*, *4*(3), 289–296.

Kaiser, F. J., Möröy, T., Chang, G. T., Horsthemke, B., and Lüdecke, H.-J. (2003). The RING finger protein RNF4, a co-regulator of transcription, interacts with the TRPS1 transcription factor. *Journal of Biological Chemistry*, *278*(40), 38780–38785.

Kaltschmidt, B. and Kaltschmidt, C. (2009). NFkappaB in the nervous system. *Cold Spring Harbor perspectives in biology*, *1*(3), a001271.

Kandel, E. R. (2001). The molecular biology of memory storage: a dialogue between genes and synapses. *Science*, *294*(5544), 1030–1038.

Kandel, E. R., Schwartz, J. H., Jessell, T. M., *et al.* (2000). *Principles of neural science*, Volume 4. McGraw-Hill New York.

Kang-Park, M.-H., Sarda, M. A., Jones, K. H., Moore, S. D., Shenolikar, S., Clark, S., and Wilson, W. A. (2003). Protein phosphatases mediate depotentiation induced by high-intensity theta-burst stimulation. *Journal of neurophysiology*, *89*(2), 684–690.

Kannan, R., Tetali, P., and Vempala, S. (1997). Simple Markov-chain algorithms for generating bipartite graphs and tournaments. In *Proceedings of the eighth annual ACM-SIAM symposium on Discrete algorithms*, 193–200. Society for Industrial and Applied Mathematics.

Karin, M. and Ben-Neriah, Y. (2000). Phosphorylation meets ubiquitination: the control of NF-κB activity. *Annual review of immunology*, *18*(1), 621–663.

Karlebach, G. and Shamir, R. (2008). Modelling and analysis of gene regulatory networks. *Nat Rev Mol Cell Biol*, *9*(10), 770–780.

Karlsson, F. and Hörnquist, M. (2007). Order or chaos in Boolean gene networks depends on the mean fraction of canalizing functions. *Physica A: Statistical Mechanics and its Applications*, *384*(2), 747–757.

Karpova, A., Sanna, P., and Behnisch, T. (2006). Involvement of multiple phosphatidylinositol 3-kinase-dependent pathways in the persistence of late-phase long term potentiation expression. *Neuroscience*, *137*(3), 833–841.

Kashishian, A., Kazlauskas, A., and Cooper, J. A. (1992). Phosphorylation sites in the PDGF receptor with different specificities for binding GAP and PI3 kinase in vivo. *The EMBO journal*, *11*(4), 1373.

Kato, A., Ozawa, F., Saitoh, Y., Hirai, K., and Inokuchi, K. (1997). vesl, a gene encoding VASP/Ena family related protein, is upregulated during seizure, long-term potentiation and synaptogenesis. *FEBS letters*, *412*(1), 183–189.

Kato, A. S., Gill, M. B., Ho, M. T., Yu, H., Tu, Y., Siuda, E. R., Wang, H., Qian, Y.-W., Nisenbaum, E. S., Tomita, S., *et al.* (2010). Hippocampal AMPA receptor gating controlled by both TARP and cornichon proteins. *Neuron*, *68*(6), 1082–1096.

Kauer, J., Malenka, R., and Nicoll, R. (1988). NMDA application potentiates synaptic transmission in the hippocampus. *Nature*, *334*, 250–252.

Kauffman, K. J., Prakash, P., and Edwards, J. S. (2003). Advances in flux balance analysis. *Current opinion in biotechnology*, *14*(5), 491–496.

Kauffman, S. (1969a). Homeostasis and differentiation in random genetic control networks. *Nature*, *224*, 177–178.

Kauffman, S. (1993). *The origins of order: Self-organization and selection in evolution*. Oxford University Press, USA.

Kauffman, S. (1995). *At home in the universe: The search for the laws of self-organization and complexity*. Oxford University Press.

Kauffman, S., Peterson, C., Samuelsson, B., and Troein, C. (2003). Random Boolean network models and the yeast transcriptional network. *Proceedings of the National Academy of Sciences of the United States of America*, *100*(25), 14796.

Kauffman, S., Peterson, C., Samuelsson, B., and Troein, C. (2004). Genetic networks with canalyzing Boolean rules are always stable. *Proceedings of the National Academy of Sciences of the United States of America*, *101*(49), 17102–17107.

Kauffman, S. A. (1969b). Metabolic stability and epigenesis in randomly constructed genetic nets. *Journal of theoretical biology*, *22*(3), 437–467.

Kauselmann, G., Weiler, M., Wulff, P., Jessberger, S., Konietzko, U., Scafidi, J., Staubli, U., Bereiter-Hahn, J., Strebhardt, K., and Kuhl, D. (1999). The polo-like protein kinases Fnk and Snk associate with a Ca2+-and integrin-binding protein and are regulated dynamically with synaptic plasticity. *The EMBO journal*, *18*(20), 5528–5539.

Kawai, T., Nomura, F., Hoshino, K., Copeland, N. G., Gilbert, D. J., Jenkins, N. A., and Akira, S. (1999). Death-associated protein kinase 2 is a new calcium/calmodulin-dependent protein kinase that signals apoptosis through its catalytic activity. *Oncogene*, *18*(23), 3471–3480.

Kawashima, T., Okuno, H., Nonaka, M., Adachi-Morishima, A., Kyo, N., Okamura, M., Takemoto-Kimura, S., Worley, P. F., and Bito, H. (2009). Synaptic activity-responsive element in the Arc/Arg3. 1 promoter essential for synapse-to-nucleus signaling in activated neurons. *Proceedings of the National Academy of Sciences*, *106*(1), 316–321.

Kelly, A., Lynch, A., Vereker, E., Nolan, Y., Queenan, P., Whittaker, E., O'Neill, L. A., and Lynch, M. A. (2001). The Anti-inflammatory Cytokine, Interleukin (IL)-10, Blocks the Inhibitory Effect of IL-1β on Long Term Potentiation A ROLE FOR JNK. *Journal of Biological Chemistry*, *276*(49), 45564–45572.

Kennedy, M. J. and Ehlers, M. D. (2011). Mechanisms and function of dendritic exocytosis. *Neuron*, *69*(5), 856–875.

Khan, J., Wei, J. S., Ringner, M., Saal, L. H., Ladanyi, M., Westermann, F., Berthold, F., Schwab, M., Antonescu, C. R., Peterson, C., *et al.* (2001). Classification and diagnostic prediction of cancers using gene expression profiling and artificial neural networks. *Nature medicine*, *7*(6), 673–679.

Kim, C.-H. and Lisman, J. E. (1999). A role of actin filament in synaptic transmission and long-term potentiation. *The Journal of neuroscience*, *19*(11), 4314–4324.

Kim, R. H., Flanders, K. C., Reffey, S. B., Anderson, L. A., Duckett, C. S., Perkins, N. D., and Roberts, A. B. (2001). SNIP1 inhibits NF-κB signaling by competing for its binding to the C/H1 domain of CBP/p300 transcriptional co-activators. *Journal of Biological Chemistry*, *276*(49), 46297–46304.

Kimber, W., Deak, M., Prescott, A., and Alessi, D. (2003). Interaction of the protein tyrosine phosphatase PTPL1 with the PtdIns (3, 4) P2-binding adaptor protein TAPP1. *Biochem. J*, *376*, 525–535.

Kinouchi, O. and Copelli, M. (2006). Optimal dynamical range of excitable networks at criticality. *Nature Physics*, *2*(5), 348–351.

Klamt, S., Saez-Rodriguez, J., Lindquist, J., Simeoni, L., and Gilles, E. (2006). A methodology for the structural and functional analysis of signaling and regulatory networks. *BMC bioinformatics*, *7*(1), 56.

Klein, R. (2008). Bidirectional modulation of synaptic functions by Eph/ephrin signaling. *Nature neuroscience*, *12*(1), 15–20.

Klipp, E., Herwig, R., Kowald, A., Wierling, C., and Lehrach, H. (2008). *Systems biology in practice: concepts, implementation and application*. John Wiley & Sons.

Knöll, B. and Nordheim, A. (2009). Functional versatility of transcription factors in the nervous system: the SRF paradigm. *Trends in neurosciences*, *32*(8), 432–442.

Komiya, Y., Kurabe, N., Katagiri, K., Ogawa, M., Sugiyama, A., Kawasaki, Y., and Tashiro, F. (2008). A novel binding factor of 14-3-3 beta functions as a transcriptional repressor and promotes anchorage-independent growth, tumorigenicity, and metastasis. *Journal of Biological Chemistry*, *283*(27), 18753–18764.

Koob, A. (2009). *The Root of Thought: Unlocking Glia¿ the Brain Cell That Will Help Us Sharpen Our Wits, Heal Injury, and Treat Brain Disease*. FT Press.

Kouzarides, T. (2007). Chromatin modifications and their function. *Cell*, *128*(4), 693–705.

Krucker, T., Siggins, G. R., and Halpain, S. (2000). Dynamic actin filaments are required for stable long-term potentiation (LTP) in area CA1 of the hippocampus. *Proceedings of the National Academy of Sciences*, *97*(12), 6856–6861.

Kruijer, W., Cooper, J. A., Hunter, T., and Verma, I. M. (1983). Platelet-derived growth factor induces rapid but transient expression of the c-fos gene and protein. *Nature*, *312*(5996), 711–716.

Kwapis, J. L. and Helmstetter, F. J. (2014). Does PKM (zeta) maintain memory? *Brain research bulletin*, *105*, 36–45.

Langfelder, P. and Horvath, S. (2008). WGCNA: an R package for weighted correlation network analysis. *BMC Bioinformatics*, (1), 559.

Langton, C. G. *et al.* (1992). Life at the edge of chaos. *Artificial life II*, *10*, 41–91.

Larkman, A. and Jack, J. (1995). Synaptic plasticity: hippocampal LTP. *Current Opinion in neurobiology*, *5*(3), 324–334.

Le Gallic, L., Sgouras, D., Beal, G., and Mavrothalassitis, G. (1999). Transcriptional repressor ERF is a Ras/mitogen-activated protein kinase target that regulates cellular proliferation. *Molecular and cellular biology*, *19*(6), 4121–4133.

Lee, K. J., Lee, Y., Rozeboom, A., Lee, J.-Y., Udagawa, N., Hoe, H.-S., and Pak, D. T. (2011). Requirement for Plk2 in orchestrated ras and rap signaling, homeostatic structural plasticity, and memory. *Neuron*, *69*(5), 957–973.

Lee, P., Cohen, J., Becker, K., and Fields, R. (2005). Gene Expression in the Conversion of Early-Phase to Late-Phase Long-Term Potentiation. *Annals of the New York Academy of Sciences*, *1048*(1), 259–271.

Lee, S.-J. R., Escobedo-Lozoya, Y., Szatmari, E. M., and Yasuda, R. (2009). Activation of CaMKII in single dendritic spines during long-term potentiation. *Nature*, *458*(7236), 299–304.

Lee, T., Rinaldi, N., Robert, F., Odom, D., Bar-Joseph, Z., Gerber, G., Hannett, N., Harbison, C., Thompson, C., Simon, I., *et al.* (2002). Transcriptional regulatory networks in Saccharomyces cerevisiae. *Science Signalling*, *298*(5594), 799.

Leonard, A. S., Lim, I. A., Hemsworth, D. E., Horne, M. C., and Hell, J. W. (1999). Calcium/calmodulin-dependent protein kinase II is associated with the N-methyl-D-aspartate receptor. *Proceedings of the National Academy of Sciences*, *96*(6), 3239–3244.

Levenson, J. M., Roth, T. L., Lubin, F. D., Miller, C. A., Huang, I.-C., Desai, P., Malone, L. M., and Sweatt, J. D. (2006). Evidence that DNA (cytosine-5) methyltransferase regulates synaptic plasticity in the hippocampus. *Journal of Biological Chemistry*, *281*(23), 15763–15773.

Li, C. and Wong, W. H. (2001). Model-based analysis of oligonucleotide arrays: expression index computation and outlier detection. *Proceedings of the National Academy of Sciences*, *98*(1), 31–36.

Li, F., Long, T., Lu, Y., Ouyang, Q., and Tang, C. (2004). The yeast cell-cycle network is robustly designed. *Proceedings of the National Academy of Sciences of the United States of America*, *101*(14), 4781–4786.

Li, F. and Tsien, J. Z. (2009). Memory and the NMDA receptors. *The New England journal of medicine*, *361*(3), 302.

Li, L., Carter, J., Gao, X., Whitehead, J., and Tourtellotte, W. G. (2005). The neuroplasticity-associated arc gene is a direct transcriptional target of early growth response (Egr) transcription factors. *Molecular and cellular biology*, *25*(23), 10286–10300.

Lilienbaum, A. and Israël, A. (2003). From calcium to NF-κB signaling pathways in neurons. *Molecular and cellular biology*, *23*(8), 2680–2698.

Lin, C.-l. G., Orlov, I., Ruggiero, A. M., Dykes-Hoberg, M., Lee, A., Jackson, M., and Rothstein, J. D. (2001). Modulation of the neuronal glutamate transporter EAAC1 by the interacting protein GTRAP3-18. *Nature*, *410*(6824), 84–88.

Link, W., Konietzko, U., Kauselmann, G., Krug, M., Schwanke, B., Frey, U., and Kuhl, D. (1995). Somatodendritic expression of an immediate early gene is regulated by synaptic activity. *Proceedings of the National Academy of Sciences*, *92*(12), 5734–5738.

Lisman, J., Yasuda, R., and Raghavachari, S. (2012). Mechanisms of CaMKII action in long-term potentiation. *Nature Reviews Neuroscience*, *13*(3), 169–182.

Lisman, J. E. (1985). A mechanism for memory storage insensitive to molecular turnover: a bistable autophosphorylating kinase. *Proceedings of the National Academy of Sciences*, *82*(9), 3055–3057.

Liu, T., Liu, P. Y., and Marshall, G. M. (2009). The critical role of the class III histone deacetylase SIRT1 in cancer. *Cancer research*, *69*(5), 1702–1705.

Liu, Y., Shepherd, E. G., and Nelin, L. D. (2007). MAPK phosphatases-regulating the immune response. *Nature Reviews Immunology*, *7*(3), 202–212.

Lledo, P.-M., Hjelmstad, G. O., Mukherji, S., Soderling, T. R., Malenka, R. C., and Nicoll, R. A. (1995). Calcium/calmodulin-dependent kinase II and long-term potentiation enhance synaptic transmission by the same mechanism. *Proceedings of the National Academy of Sciences*, *92*(24), 11175–11179.

Lømo, T. (1966). Frequency potentiation of excitatory synaptic activity in the dentate area of the hippocampal formation. *Acta physiologica Scandinavica*, *68*(Suppl. 277), 128.

Lømo, T. (2003). The discovery of long-term potentiation. *Philosophical Transactions of the Royal Society of London. Series B: Biological Sciences*, *358*(1432), 617–620.

Lubin, F. D., Gupta, S., Parrish, R. R., Grissom, N. M., and Davis, R. L. (2011). Epigenetic Mechanisms Critical Contributors to Long-Term Memory Formation. *The Neuroscientist*, *17*(6), 616–632.

Lubin, F. D., Roth, T. L., and Sweatt, J. D. (2008). Epigenetic regulation of BDNF gene transcription in the consolidation of fear memory. *The Journal of Neuroscience*, *28*(42), 10576–10586.

Luque, B. and Solé, R. V. (1997). Phase transitions in random networks: simple analytic determination of critical points. *Physical Review E*, *55*(1), 257.

Lüscher, C., Malenka, R. C., and Nicoll, R. A. (1998). Monitoring glutamate release during LTP with glial transporter currents. *Neuron*, *21*(2), 435–441.

Lyford, G. L., Yamagata, K., Kaufmann, W. E., Barnes, C. A., Sanders, L. K., Copeland, N. G., Gilbert, D. J., Jenkins, N. A., Lanahan, A. A., and Worley, P. F. (1995). Arc, a growth factor and activity-regulated gene, encodes a novel cytoskeleton-associated protein that is enriched in neuronal dendrites. *Neuron*, *14*(2), 433–445.

Lynch, M. (2004). Long-term potentiation and memory. *Physiological reviews*, *84*(1), 87–136.

Lynch, M., Errington, M., Clements, M., Bliss, T., Redini-Del Negro, C., and Laroche, S. (1990). Increases in glutamate release and phosphoinositide metabolism associated with long-term potentiation and classical conditioning. *Progress in brain research*, *83*, 251–256.

Mainen, Z. F., Jia, Z., Roder, J., and Malinow, R. (1998). Use-dependent AMPA receptor block in mice lacking GluR2 suggests postsynaptic site for LTP expression. *Nature neuroscience*, *1*(7), 579–586.

Malenka, R. and Bear, M. (2004). Ltp and ltd: An embarrassment of riches. *Neuron*, *44*(1), 5–21.

Malenka, R. and Nicoll, R. (1999). Long-term potentiation–a decade of progress? *Science*, *285*(5435), 1870.

Maletic-Savatic, M., Malinow, R., and Svoboda, K. (1999). Rapid dendritic morphogenesis in CA1 hippocampal dendrites induced by synaptic activity. *Science*, *283*(5409), 1923–1927.

Malinow, R., Schulman, H., and Tsien, R. W. (1989). Inhibition of postsynaptic PKC or CaMKII blocks induction but not expression of LTP. *Science*, *245*(4920), 862–866.

Mammen, A. L., Kameyama, K., Roche, K. W., and Huganir, R. L. (1997). Phosphorylation of the alpha-amino-3-hydroxy-5-methylisoxazole4-propionic acid receptor GluR1 subunit by calcium/calmodulin-dependent kinase II. *Journal of Biological Chemistry*, *272*(51), 32528–32533.

Man, H.-Y., Wang, Q., Lu, W.-Y., Ju, W., Ahmadian, G., Liu, L., D'Souza, S., Wong, T., Taghibiglou, C., Lu, J., *et al.* (2003). Activation of PI3-kinase is required for AMPA receptor insertion during LTP of mEPSCs in cultured hippocampal neurons. *Neuron*, *38*(4), 611–624.

Manabe, T. and Nicoll, R. A. (1994). Long-term potentiation: evidence against an increase in transmitter release probability in the CA1 region of the hippocampus. *Science*, *265*(5180), 1888–1892.

Manninen, T., Hituri, K., Kotaleski, J. H., Blackwell, K. T., and Linne, M.-L. (2010). Postsynaptic signal transduction models for long-term potentiation and depression. *Frontiers in computational neuroscience*, *4*(152).

Markstein, M., Markstein, P., Markstein, V., and Levine, M. S. (2002). Genome-wide analysis of clustered Dorsal binding sites identifies putative target genes in the Drosophila embryo. *Proceedings of the National Academy of Sciences*, *99*(2), 763–768.

Martin, S., Grimwood, P., and Morris, R. (2000). Synaptic plasticity and memory: an evaluation of the hypothesis. *Annual review of neuroscience*, *23*(1), 649–711.

Matsumura, H., Ito, A., Saitoh, H., Winter, P., Kahl, G., Reuter, M., Krüger, D. H., and Terauchi, R. (2005). SuperSAGE. *Cellular microbiology*, *7*(1), 11–18.

Matsuo, R., Asada, A., Fujitani, K., and Inokuchi, K. (2001). LIRF, a Gene Induced during Hippocampal Long-Term Potentiation as an Immediate-Early Gene, Encodes a Novel RING Finger Protein. *Biochemical and biophysical research communications*, *289*(2), 479–484.

Matsuzaki, M., Honkura, N., Ellis-Davies, G. C., and Kasai, H. (2004). Structural basis of long-term potentiation in single dendritic spines. *Nature*, *429*(6993), 761–766.

Mattick, J. S. and Makunin, I. V. (2006). Non-coding RNA. *Human molecular genetics*, *15*(suppl 1), R17–R29.

Matus, A. (2000). Actin-based plasticity in dendritic spines. *Science*, *290*(5492), 754–758.

May, M. J. and Ghosh, S. (1997). Rel/NF-kappaB and IkappaB proteins: an overview. In *Seminars in cancer biology*, Volume 8, 63–73. Elsevier.

McClelland, J. L., McNaughton, B. L., and O'Reilly, R. C. (1995). Why there are complementary learning systems in the hippocampus and neocortex: insights from the successes and failures of connectionist models of learning and memory. *Psychological review*, *102*(3), 419.

Meberg, P. J., Kinney, W. R., Valcourt, E. G., and Routtenberg, A. (1996). Gene expression of the transcription factor NF-kB in hippocampus: regulation by synaptic activity. *Molecular brain research*, *38*(2), 179–190.

Meffert, M. K., Chang, J. M., Wiltgen, B. J., Fanselow, M. S., and Baltimore, D. (2003). NF-kB functions in synaptic signaling and behavior. *Nature neuroscience*, *6*(10), 1072–1078.

Mercer, T. R., Dinger, M. E., Mariani, J., Kosik, K. S., Mehler, M. F., and Mattick, J. S. (2008). Noncoding RNAs in long-term memory formation. *The Neuroscientist*, *14*(5), 434–445.

Merida, I., Avila-Flores, A., and Merino, E. (2008). Diacylglycerol kinases: at the hub of cell signalling. *Biochem. J*, *409*, 1–18.

Merlo, E., Freudenthal, R., and Romano, A. (2002). The IκB kinase inhibitor sulfasalazine impairs long-term memory in the crab Chasmagnathus. *Neuroscience*, *112*(1), 161–172.

Metzler, M., Li, B., Gan, L., Georgiou, J., Gutekunst, C.-A., Wang, Y., Torre, E., Devon, R. S., Oh, R., Legendre-Guillemin, V., *et al.* (2003). Disruption of the endocytic protein HIP1 results in neurological deficits and decreased AMPA receptor trafficking. *The EMBO journal*, *22*(13), 3254–3266.

Michalski, P. (2013). The delicate bistability of CaMKII. *Biophysical journal*, *105*(3), 794–806.

Michán, S., Li, Y., Chou, M. M.-H., Parrella, E., Ge, H., Long, J. M., Allard, J. S., Lewis, K., Miller, M., Xu, W., *et al.* (2010). SIRT1 is essential for normal cognitive function and synaptic plasticity. *The Journal of Neuroscience*, *30*(29), 9695–9707.

Miller, C. A. and Sweatt, J. D. (2007). Covalent modification of DNA regulates memory formation. *Neuron*, *53*(6), 857–869.

Miller, S. G. and Kennedy, M. B. (1986). Regulation of brain Type II Ca2+ calmodulin-dependent protein kinase by autophosphorylation: A Ca2+-triggered molecular switch. *Cell*, *44*(6), 861–870.

Milo, R., Shen-Orr, S., Itzkovitz, S., Kashtan, N., Chklovskii, D., and Alon, U. (2002). Network motifs: simple building blocks of complex networks. *Science Signaling*, *298*(5594), 824.

Milstein, A. D., Zhou, W., Karimzadegan, S., Bredt, D. S., and Nicoll, R. A. (2007). TARP subtypes differentially and dose-dependently control synaptic AMPA receptor gating. *Neuron*, *55*(6), 905–918.

Misner, D. L. and Sullivan, J. M. (1999). Mechanism of cannabinoid effects on long-term potentiation and depression in hippocampal CA1 neurons. *The journal of Neuroscience*, *19*(16), 6795–6805.

Miyashita, T., Kubik, S., Lewandowski, G., and Guzowski, J. F. (2008). Networks of neurons, networks of genes: an integrated view of memory consolidation. *Neurobiology of learning and memory*, *89*(3), 269–284.

Miyata, S., Mori, Y., and Tohyama, M. (2008). PRMT1 and Btg2 regulates neurite outgrowth of Neuro2a cells. *Neuroscience letters*, *445*(2), 162–165.

Monte, D., Baert, J.-L., Defossez, P.-A., De Launoit, Y., and Stéhelin, D. (1994). Molecular cloning and characterization of human ERM, a new member of the Ets family closely related to mouse PEA3 and ER81 transcription factors. *Oncogene*, *9*(5), 1397–1406.

Moore, J. H. (2005). A global view of epistasis. *Nature genetics*, *37*(1), 13–14.

Morgan, J. I., Cohen, D. R., Hempstead, J. L., and Curran, T. (1987). Mapping patterns of c-fos expression in the central nervous system after seizure. *Science*, *237*(4811), 192–197.

Morgan, J. I. and Curran, T. (1989). Stimulus-transcription coupling in neurons: role of cellular immediate-early genes. *Trends in neurosciences*, *12*(11), 459–462.

Morgan, S. and Teyler, T. (1999). VDCCs and NMDARs underlie two forms of LTP in CA1 hippocampus in vivo. *Journal of neurophysiology*, *82*(2), 736–740.

Morris, M., Saez-Rodriguez, J., Clarke, D., Sorger, P., and Lauffenburger, D. (2011). Training Signaling Pathway Maps to Biochemical Data with Constrained Fuzzy Logic: Quantitative Analysis of Liver Cell Responses to Inflammatory Stimuli. *PLoS computational biology*, *7*(3), e1001099.

Morris, M., Saez-Rodriguez, J., Sorger, P., and Lauffenburger, D. (2010). Logic-based models for the analysis of cell signaling networks. *Biochemistry*, *49*(15), 3216–3224.

Morris, R. (2003). Long-term potentiation and memory. *Philosophical Transactions of the Royal Society of London. Series B: Biological Sciences*, *358*(1432), 643.

Morris, R., Garrud, P., Rawlins, J., and O'Keefe, J. (1982). Place navigation impaired in rats with hippocampal lesions. *Nature*, *297*(5868), 681–683.

Morrison, D. K. and Cutler Jr, R. E. (1997). The complexity of Raf-1 regulation. *Current opinion in cell biology*, *9*(2), 174–179.

Muller, D., Toni, N., and Buchs, P.-A. (2000). Spine changes associated with long-term potentiation. *Hippocampus*, *10*(5), 596–604.

Murphy, T. H., Worley, P. F., and Baraban, J. M. (1991). L-type voltage-sensitive calcium channels mediate synaptic activation of immediate early genes. *Neuron*, *7*(4), 625–635.

Nachman, I., Regev, A., and Friedman, N. (2004). Inferring quantitative models of regulatory networks from expression data. *Bioinformatics*, *20*(suppl 1), i248–i256.

Newman, E. A. (2003). New roles for astrocytes: Regulation of synaptic transmission. *Trends in neurosciences*, *26*(10), 536–542.

Nguyen, P., Abel, T., and Kandel, E. (1994). Requirement of a critical period of transcription for induction of a late phase of LTP. *Science*, *265*(5175), 1104.

Nicoll, R. and Malenka, R. (1995). Contrasting properties of two forms of long-term potentiation in the hippocampus. *Nature*, *377*, 115–118.

Nicoll, R. A., Malenka, R. C., and Kauer, J. A. (1990). Functional comparison of neurotransmitter receptor subtypes in mammalian central nervous system. *Physiological reviews*, *70*(2), 513–565.

Nicoll, R. A. and Roche, K. W. (2013). Long-term potentiation: peeling the onion. *Neuropharmacology*, *74*, 18–22.

Nido, G., Ryan, M., Benuskova, L., and Williams, J. (2015). Dynamical properties of gene regulatory networks involved in long-term potentiation. *Frontiers in Molecular Neuroscience*, *8*(42).

Nido, G., Williams, J., and Benuskova, L. (2012). Bistable properties of a memory-related gene regulatory network. In *Neural Networks (IJCNN), The 2012 International Joint Conference on*, 1602–1607. IEEE.

Nishizuka, Y. (1995). Protein kinase C and lipid signaling for sustained cellular responses. *The FASEB Journal*, *9*(7), 484–496.

Niu, S., Yabut, O., and D'Arcangelo, G. (2008). The Reelin signaling pathway promotes dendritic spine development in hippocampal neurons. *The Journal of Neuroscience*, *28*(41), 10339–10348.

Oda, K., Shiratsuchi, T., Nishimori, H., Inazawa, J., Yoshikawa, H., Taketani, Y., Nakamura, Y., and Tokino, T. (1999). Identification of BAIAP2 (BAI-associated protein 2), a novel human homologue of hamster IRSp53, whose SH3 domain interacts with the cytoplasmic domain of BAI1. *Cytogenetic and Genome Research*, *84*(1-2), 75–82.

O'Donovan, K. J., Tourtellotte, W. G., Millbrandt, J., and Baraban, J. M. (1999). The EGR family of transcription-regulatory factors: progress at the interface of molecular and systems neuroscience. *Trends in neurosciences*, *22*(4), 167–173.

Ogryzko, V. V., Kotani, T., Zhang, X., Schiltz, R. L., Howard, T., Yang, X.-J., Howard, B. H., Qin, J., and Nakatani, Y. (1998). Histone-like TAFs within the PCAF histone acetylase complex. *Cell*, *94*(1), 35–44.

Ohtsuka, K. and Suzuki, T. (2000). Roles of molecular chaperones in the nervous system. *Brain research bulletin*, *53*(2), 141–146.

Okuno, H. (2011). Regulation and function of immediate-early genes in the brain: beyond neuronal activity markers. *Neuroscience research*, *69*(3), 175–186.

Okuno, H., Akashi, K., Ishii, Y., Yagishita-Kyo, N., Suzuki, K., Nonaka, M., Kawashima, T., Fujii, H., Takemoto-Kimura, S., Abe, M., *et al.* (2012). Inverse synaptic tagging of inactive synapses via dynamic interaction of Arc/Arg3. 1 with CaMKIIb. *Cell*, *149*(4), 886–898.

Oldham, M. C., Horvath, S., and Geschwind, D. H. (2006). Conservation and evolution of gene coexpression networks in human and chimpanzee brains. *Proceedings of the National Academy of Sciences*, *103*(47), 17973–17978.

O'Mahony, A., Raber, J., Montano, M., Foehr, E., Han, V., Lu, S., Kwon, H., LeFevour, A., Chakraborty-Sett, S., and Greene, W. (2006). NF-kB/Rel regulates inhibitory and excitatory neuronal function and synaptic plasticity. *Molecular and cellular biology*, *26*(19), 7283–7298.

Opazo, P., Labrecque, S., Tigaret, C. M., Frouin, A., Wiseman, P. W., De Koninck, P., and Choquet, D. (2010). CaMKII triggers the diffusional trapping of surface AMPARs through phosphorylation of stargazin. *Neuron*, *67*(2), 239–252.

Opazo, P., Watabe, A. M., Grant, S. G., and O'Dell, T. J. (2003). Phosphatidylinositol 3-kinase regulates the induction of long-term potentiation through extracellular signal-related kinase-independent mechanisms. *The Journal of neuroscience*, *23*(9), 3679–3688.

Owen, D. J., Collins, B. M., and Evans, P. R. (2004). Adaptors for clathrin coats: structure and function. *Annu. Rev. Cell Dev. Biol.*, *20*, 153–191.

Owens, D. and Keyse, S. (2007). Differential regulation of MAP kinase signalling by dual-specificity protein phosphatases. *Oncogene*, *26*(22), 3203–3213.

Palsson, B. O. (2006). *Systems biology*. Cambridge university press.

Pang, P. T., Teng, H. K., Zaitsev, E., Woo, N. T., Sakata, K., Zhen, S., Teng, K. K., Yung, W.-H., Hempstead, B. L., and Lu, B. (2004). Cleavage of proBDNF by tPA/plasmin is essential for long-term hippocampal plasticity. *Science*, *306*(5695), 487–491.

Panja, D. and Bramham, C. R. (2014). BDNF mechanisms in late LTP formation: a synthesis and breakdown. *Neuropharmacology*, *76*, 664–676.

Park, C., Gong, R., Stuart, J., and Tang, S. (2006). Molecular network and chromosomal clustering of genes involved in synaptic plasticity in the hippocampus. *Journal of Biological Chemistry*, *281*(40), 30195.

Park, J. E., Park, B. C., Kim, H.-A., Song, M., Park, S. G., Lee, D. H., Kim, H.-J., Choi, H.-K., Kim, J.-T., and Cho, S. (2010). Positive regulation of apoptosis signal-regulating kinase 1 by dual-specificity phosphatase 13A. *Cellular and Molecular Life Sciences*, *67*(15), 2619–2629.

Park, P., Volianskis, A., Sanderson, T. M., Bortolotto, Z. A., Jane, D. E., Zhuo, M., Kaang, B.-K., and Collingridge, G. L. (2014). NMDA receptor-dependent long-term potentiation comprises a family of temporally overlapping forms of synaptic plasticity that are induced by different patterns of stimulation. *Philosophical Transactions of the Royal Society B: Biological Sciences*, *369*(1633), 20130131.

Patterson, M. A., Szatmari, E. M., and Yasuda, R. (2010). AMPA receptors are exocytosed in stimulated spines and adjacent dendrites in a Ras-ERK–dependent manner during long-term potentiation. *Proceedings of the National Academy of Sciences*, *107*(36), 15951–15956.

Pearson, H. (2006). Genetics: what is a gene? *Nature*, *441*(7092), 398–401.

Pepke, S., Kinzer-Ursem, T., Mihalas, S., and Kennedy, M. B. (2010). A dynamic model of interactions of Ca2+, calmodulin, and catalytic subunits of Ca2+/calmodulin-dependent protein kinase II. *PLoS computational biology*, *6*(2), e1000675.

Petersen, J. D., Chen, X., Vinade, L., Dosemeci, A., Lisman, J. E., and Reese, T. S. (2003). Distribution of postsynaptic density (PSD)-95 and Ca2+/calmodulin-dependent protein kinase II at the PSD. *The Journal of neuroscience*, *23*(35), 11270–11278.

Petri, C. (1966). Kommunikation mit Automaten. Schriften des IIM 2, Institut für Instrumentelle Mathematik, Bonn, 1962. Technical report, English translation: Technical Report RADCTR-65-377.

Pi, H. J., Otmakhov, N., Lemelin, D., De Koninck, P., and Lisman, J. (2010). Autonomous CaMKII can promote either long-term potentiation or long-term depression, depending on the state of T305/T306 phosphorylation. *The Journal of Neuroscience*, *30*(26), 8704–8709.

Pievani, M., de Haan, W., Wu, T., Seeley, W. W., and Frisoni, G. B. (2011). Functional network disruption in the degenerative dementias. *The Lancet Neurology*, *10*(9), 829–843.

Pilpel, Y., Sudarsanam, P., and Church, G. M. (2001). Identifying regulatory networks by combinatorial analysis of promoter elements. *Nature genetics*, *29*(2), 153–159.

Plant, K., Pelkey, K. A., Bortolotto, Z. A., Morita, D., Terashima, A., McBain, C. J., Collingridge, G. L., and Isaac, J. T. (2006). Transient incorporation of native GluR2-lacking AMPA receptors during hippocampal long-term potentiation. *Nature neuroscience*, *9*(5), 602–604.

Plath, N., Ohana, O., Dammermann, B., Errington, M. L., Schmitz, D., Gross, C., Mao, X., Engelsberg, A., Mahlke, C., Welzl, H., *et al.* (2006). Arc/Arg3. 1 is essential for the consolidation of synaptic plasticity and memories. *Neuron*, *52*(3), 437–444.

Pomerening, J. R., Sontag, E. D., and Ferrell, J. E. (2003). Building a cell cycle oscillator: hysteresis and bistability in the activation of Cdc2. *Nature Cell Biology*, *5*(4), 346–351.

Powers, E. T., Morimoto, R. I., Dillin, A., Kelly, J. W., and Balch, W. E. (2009). Biological and chemical approaches to diseases of proteostasis deficiency. *Annual review of biochemistry*, *78*, 959–991.

Prange, O., Wong, T. P., Gerrow, K., Wang, Y. T., and El-Husseini, A. (2004). A balance between excitatory and inhibitory synapses is controlled by PSD-95 and neuroligin. *Proceedings of the National Academy of Sciences of the United States of America*, *101*(38), 13915–13920.

Price, J. C., Guan, S., Burlingame, A., Prusiner, S. B., and Ghaemmaghami, S. (2010). Analysis of proteome dynamics in the mouse brain. *Proceedings of the National Academy of Sciences*, *107*(32), 14508–14513.

Price, M. A., Rogers, A. E., and Treisman, R. (1995). Comparative analysis of the ternary complex factors Elk-1, SAP-1a and SAP-2 (ERP/NET). *The EMBO journal*, *14*(11), 2589.

Pujadas, L., Gruart, A., Bosch, C., Delgado, L., Teixeira, C. M., Rossi, D., de Lecea, L., Martínez, A., Delgado-García, J. M., and Soriano, E. (2010). Reelin regulates postnatal neurogenesis and enhances spine hypertrophy and long-term potentiation. *The Journal of Neuroscience*, *30*(13), 4636–4649.

Pyle, R. A., Schivell, A. E., Hidaka, H., and Bajjalieh, S. M. (2000). Phosphorylation of synaptic vesicle protein 2 modulates binding to synaptotagmin. *Journal of Biological Chemistry*, *275*(22), 17195–17200.

Qian, Z., Gilbert, M., and Kandel, E. R. (1994). Temporal and spatial regulation of the expression of BAD2, a MAP kinase phosphatase, during seizure, kindling, and long-term potentiation. *Learning & Memory*, *1*(3), 180–188.

Qiu, S., Zhao, L. F., Korwek, K. M., and Weeber, E. J. (2006). Differential reelin-induced enhancement of NMDA and AMPA receptor activity in the adult hippocampus. *The Journal of neuroscience*, *26*(50), 12943–12955.

R Core Team (2013). *R: A Language and Environment for Statistical Computing*. Vienna, Austria: R Foundation for Statistical Computing.

Raber, J., Rola, R., LeFevour, A., Morhardt, D., Curley, J., Mizumatsu, S., VandenBerg, S. R., and Fike, J. R. (2004). Radiation-induced cognitive impairments are associated with changes in indicators of hippocampal neurogenesis. *Radiation research*, *162*(1), 39–47.

Rämö, P., Kesseli, J., and Yli-Harja, O. (2006). Perturbation avalanches and criticality in gene regulatory networks. *Journal of theoretical biology*, *242*(1), 164–170.

Ravasz, E., Somera, A. L., Mongru, D. A., Oltvai, Z. N., and Barabási, A.-L. (2002). Hierarchical organization of modularity in metabolic networks. *science*, *297*(5586), 1551–1555.

Raymond, C. R. (2007). LTP forms 1, 2 and 3: different mechanisms for the 'long' in long-term potentiation. *Trends in neurosciences*, *30*(4), 167–175.

Redondo, R. L. and Morris, R. G. (2010). Making memories last: the synaptic tagging and capture hypothesis. *Nature Reviews Neuroscience*, *12*(1), 17–30.

Reymann, K. and Frey, J. (2007). The late maintenance of hippocampal LTP: Requirements, phases, synaptic tagging, late-associativity and implications. *Neuropharmacology*, *52*(1), 24–40.

Ribeiro, A. S., Kauffman, S. A., Lloyd-Price, J., Samuelsson, B., and Socolar, J. E. (2008). Mutual information in random Boolean models of regulatory networks. *Physical Review E*, *77*(1), 011901.

Rice, D. S. and Curran, T. (2001). Role of the reelin signaling pathway in central nervous system development. *Annual review of neuroscience*, *24*(1), 1005–1039.

Robertson, L. M., Kerppola, T. K., Vendrell, M., Luk, D., Smeyne, R. J., Bocchiaro, C., Morgan, J. I., and Curran, T. (1995). Regulation of c-fos expression in transgenic mice requires multiple interdependent transcription control elements. *Neuron*, *14*(2), 241–252.

Rocca, D. L., Martin, S., Jenkins, E. L., and Hanley, J. G. (2008). Inhibition of Arp2/3-mediated actin polymerization by PICK1 regulates neuronal morphology and AMPA receptor endocytosis. *Nature cell biology*, *10*(3), 259–271.

Roche, K. W., O'Brien, R. J., Mammen, A. L., Bernhardt, J., and Huganir, R. L. (1996). Characterization of multiple phosphorylation sites on the AMPA receptor GluR1 subunit. *Neuron*, *16*(6), 1179–1188.

Roediger, H. L. (1990). Implicit memory: Retention without remembering. *American psychologist*, *45*(9), 1043.

Rojo, A. I., Salinas, M., Martín, D., Perona, R., and Cuadrado, A. (2004). Regulation of Cu/Zn-superoxide dismutase expression via the phosphatidylinositol 3 kinase/Akt pathway and nuclear factor-κB. *The journal of neuroscience*, *24*(33), 7324–7334.

Ronan, J. L., Wu, W., and Crabtree, G. R. (2013). From neural development to cognition: unexpected roles for chromatin. *Nature Reviews Genetics*, *14*(5), 347–359.

Rong, R., Ahn, J.-Y., Huang, H., Nagata, E., Kalman, D., Kapp, J. A., Tu, J., Worley, P. F., Snyder, S. H., and Ye, K. (2003). PI3 kinase enhancer–Homer complex couples mGluRI to PI3 kinase, preventing neuronal apoptosis. *Nature neuroscience*, *6*(11), 1153–1161.

Rosenblum, K., Futter, M., Voss, K., Erent, M., Skehel, P. A., French, P., Obosi, L., Jones, M. W., and Bliss, T. V. (2002). The role of extracellular regulated kinases I/II in late-phase long-term potentiation. *The Journal of neuroscience*, *22*(13), 5432–5441.

Rotenberg, M. and Maines, M. (1990). Isolation, characterization, and expression in Escherichia coli of a cDNA encoding rat heme oxygenase-2. *Journal of Biological Chemistry*, *265*(13), 7501–7506.

Rouach, N., Byrd, K., Petralia, R. S., Elias, G. M., Adesnik, H., Tomita, S., Karimzadegan, S., Kealey, C., Bredt, D. S., and Nicoll, R. A. (2005). TARP gamma-8 controls hippocampal AMPA receptor number, distribution and synaptic plasticity. *Nature neuroscience*, *8*(11), 1525–1533.

Runyan, J. D., Moore, A. N., and Dash, P. K. (2004). A role for prefrontal cortex in memory storage for trace fear conditioning. *The Journal of neuroscience*, *24*(6), 1288–1295.

Ryan, M. M., Mason-Parker, S. E., Tate, W. P., Abraham, W. C., and Williams, J. M. (2011). Rapidly induced gene networks following induction of long-term potentiation at perforant path synapses in vivo. *Hippocampus*, *21*(5), 541–553.

Ryan, M. M., Ryan, B., Kyrke-Smith, M., Logan, B., Tate, W. P., Abraham, W. C., and Williams, J. M. (2012). Temporal Profiling of Gene Networks Associated with the Late Phase of Long-Term Potentiation In Vivo. *PloS one*, *7*(7), e40538.

Saadatpour, A., Albert, I., and Albert, R. (2010). Attractor analysis of asynchronous Boolean models of signal transduction networks. *Journal of theoretical biology*, *266*(4), 641–656.

Sacktor, T. C. (2008). PKMζ, LTP maintenance, and the dynamic molecular biology of memory storage. *Progress in brain research*, *169*, 27–40.

Sacktor, T. C. (2010). How does PKMz maintain long-term memory? *Nature Reviews Neuroscience*, *12*(1), 9–15.

Sacktor, T. C., Osten, P., Valsamis, H., Jiang, X., Naik, M. U., and Sublette, E. (1993). Persistent activation of the zeta isoform of protein kinase C in the maintenance of long-term potentiation. *Proceedings of the National Academy of Sciences*, *90*(18), 8342–8346.

Saez-Rodriguez, J., Alexopoulos, L., Epperlein, J., Samaga, R., Lauffenburger, D., Klamt, S., and Sorger, P. (2009). Discrete logic modelling as a means to link protein signalling networks with functional analysis of mammalian signal transduction. *Molecular systems biology*, *5*(1).

Saez-Rodriguez, J., Alexopoulos, L., and Stolovitzky, G. (2011). Setting the standards for signal transduction research. *Science signaling*, *4*(160), pe10.

Saez-Rodriguez, J., Simeoni, L., Lindquist, J. A., Hemenway, R., Bommhardt, U., Arndt, B., Haus, U.-U., Weismantel, R., Gilles, E. D., Klamt, S., *et al.* (2007). A logical model provides insights into T cell receptor signaling. *PLoS computational biology*, *3*(8), e163.

Saffen, D. W., Cole, A. J., Worley, P. F., Christy, B. A., Ryder, K., and Baraban, J. M. (1988). Convulsant-induced increase in transcription factor messenger RNAs in rat brain. *Proceedings of the National Academy of Sciences*, *85*(20), 7795–7799.

Saghatelyan, A. K., Dityatev, A., Schmidt, S., Schuster, T., Bartsch, U., and Schachner, M. (2001). Reduced perisomatic inhibition, increased excitatory transmission, and impaired long-term potentiation in mice deficient for the extracellular matrix glycoprotein tenascin-R. *Molecular and Cellular Neuroscience*, *17*(1), 226–240.

Saha, R., Wissink, E., Bailey, E., Zhao, M., Fargo, D., Hwang, J., Daigle, K., Fenn, J., Adelman, K., and Dudek, S. (2011). Rapid activity-induced transcription of Arc and other IEGs relies on poised RNA polymerase II. *Nature neuroscience*, *14*(7), 848–856.

Sakane, F., Yamada, K., Kanoh, H., Yokoyama, C., and Tanabe, T. (1990). Porcine diacylglycerol kinase sequence has zinc finger and E–F hand motifs. *Nature*, *344*(6264), 345–348.

Sala, C., Piëch, V., Wilson, N. R., Passafaro, M., Liu, G., and Sheng, M. (2001). Regulation of dendritic spine morphology and synaptic function by Shank and Homer. *Neuron*, *31*(1), 115–130.

Salles, A., Romano, A., and Freudenthal, R. (2014). Synaptic NF-kappa B pathway in neuronal plasticity and memory. *Journal of Physiology-Paris*, *108*(4), 256–262.

Sanhueza, M., Fernandez-Villalobos, G., Stein, I. S., Kasumova, G., Zhang, P., Bayer, K. U., Otmakhov, N., Hell, J. W., and Lisman, J. (2011). Role of the CaMKII/NMDA receptor complex in the maintenance of synaptic strength. *The Journal of Neuroscience*, *31*(25), 9170–9178.

Sanjuán, R., Moya, A., and Elena, S. F. (2004). The contribution of epistasis to the architecture of fitness in an RNA virus. *Proceedings of the National Academy of Sciences of the United States of America*, *101*(43), 15376–15379.

Sanna, P. P., Cammalleri, M., Berton, F., Simpson, C., Lutjens, R., Bloom, F. E., and Francesconi, W. (2002). Phosphatidylinositol 3-kinase is required for the expression but not for the induction or the maintenance of long-term potentiation in the hippocampal CA1 region. *The Journal of neuroscience*, *22*(9), 3359–3365.

Santos, S. D. and Ferrell, J. E. (2008). Systems biology: On the cell cycle and its switches. *Nature*, *454*(7202), 288–289.

Sarkisov, D. V. and Wang, S. S.-H. (2008). Order-dependent coincidence detection in cerebellar Purkinje neurons at the inositol trisphosphate receptor. *The Journal of Neuroscience*, *28*(1), 133–142.

Sarma, V., Wolf, F. W., Marks, R. M., Shows, T. B., and Dixit, V. (1992). Cloning of a novel tumor necrosis factor-alpha-inducible primary response gene that is differentially expressed in development and capillary tube-like formation in vitro. *The Journal of Immunology*, *148*(10), 3302–3312.

Satel, J., Trappenberg, T., and Fine, A. (2009). Are binary synapses superior to graded weight representations in stochastic attractor networks? *Cognitive neurodynamics*, *3*(3), 243–250.

Scannell, J., Burns, G., Hilgetag, C., O'Neil, M., and Young, M. P. (1999). The connectional organization of the cortico-thalamic system of the cat. *Cerebral Cortex*, *9*(3), 277–299.

Schena, M., Shalon, D., Davis, R. W., and Brown, P. O. (1995). Quantitative monitoring of gene expression patterns with a complementary DNA microarray. *Science*, *270*(5235), 467–470.

Schmitz, D., Mellor, J., and Nicoll, R. A. (2001). Presynaptic kainate receptor mediation of frequency facilitation at hippocampal mossy fiber synapses. *Science*, *291*(5510), 1972–1976.

Schulz, S., Siemer, H., Krug, M., and Höllt, V. (1999). Direct evidence for biphasic cAMP responsive element-binding protein phosphorylation during long-term potentiation in the rat dentate gyrus in vivo. *The Journal of neuroscience*, *19*(13), 5683.

Schulze, A. and Downward, J. (2001). Navigating gene expression using microarrays – a technology review. *Nature cell biology*, *3*(8), E190–E195.

Schwanhäusser, B., Busse, D., Li, N., Dittmar, G., Schuchhardt, J., Wolf, J., Chen, W., and Selbach, M. (2011). Global quantification of mammalian gene expression control. *Nature*, *473*(7347), 337–342.

Schwenk, J., Harmel, N., Zolles, G., Bildl, W., Kulik, A., Heimrich, B., Chisaka, O., Jonas, P., Schulte, U., Fakler, B., *et al.* (2009). Functional proteomics identify cornichon proteins as auxiliary subunits of AMPA receptors. *Science*, *323*(5919), 1313–1319.

Schworer, C. M., Rothblum, L., Thekkumkara, T., and Singer, H. (1993). Identification of novel isoforms of the delta subunit of Ca2+/calmodulin-dependent protein kinase II. Differential expression in rat brain and aorta. *Journal of Biological Chemistry*, *268*(19), 14443–14449.

Scott, K. L. and Plon, S. E. (2005). CHES1/FOXN3 interacts with Ski-interacting protein and acts as a transcriptional repressor. *Gene*, *359*, 119–126.

Segal, E., Raveh-Sadka, T., Schroeder, M., Unnerstall, U., and Gaul, U. (2008). Predicting expression patterns from regulatory sequence in Drosophila segmentation. *Nature*, *451*(7178), 535–540.

Serra, R., Villani, M., Barbieri, A., Kauffman, S., and Colacci, A. (2010). On the dynamics of random Boolean networks subject to noise: attractors, ergodic sets and cell types. *Journal of theoretical biology*, *265*(2), 185–193.

Serra, R., Villani, M., Graudenzi, A., and Kauffman, S. A. (2006). On the distribution of small avalanches in random Boolean networks. In *Proceedings of the 4th TICSP workshop on computational systems biology*, 93–96.

Shao, Y., Li, Y., Zhang, J., Liu, D., Liu, F., Zhao, Y., Shen, T., and Li, F. (2010). Involvement of histone deacetylation in MORC2-mediated down-regulation of carbonic anhydrase IX. *Nucleic acids research*, *38*(9), 2813–2824.

Shen, K. and Meyer, T. (1999). Dynamic control of CaMKII translocation and localization in hippocampal neurons by NMDA receptor stimulation. *Science*, *284*(5411), 162–167.

Sheng, M. and Kim, E. (2011). The postsynaptic organization of synapses. *Cold Spring Harbor perspectives in biology*, *3*(12), a005678.

Shepherd, J. D., Rumbaugh, G., Wu, J., Chowdhury, S., Plath, N., Kuhl, D., Huganir, R. L., and Worley, P. F. (2006). Arc/Arg3.1 mediates homeostatic synaptic scaling of AMPA receptors. *Neuron*, *52*(3), 475–484.

Shi, Y.-J., Matson, C., Lan, F., Iwase, S., Baba, T., and Shi, Y. (2005). Regulation of LSD1 histone demethylase activity by its associated factors. *Molecular cell*, *19*(6), 857–864.

Shiraishi-Yamaguchi, Y. and Furuichi, T. (2007). The Homer family proteins. *Genome Biol*, *8*(2), 206.

Shmulevich, I., Dougherty, E. R., Kim, S., and Zhang, W. (2002). Probabilistic Boolean networks: a rule-based uncertainty model for gene regulatory networks. *Bioinformatics*, *18*(2), 261–274.

Shmulevich, I., Kauffman, S. A., and Aldana, M. (2005). Eukaryotic cells are dynamically ordered or critical but not chaotic. *Proceedings of the National Academy of Sciences of the United States of America*, *102*(38), 13439–13444.

Shors, T. J., Miesegaes, G., Beylin, A., Zhao, M., Rydel, T., and Gould, E. (2001). Neurogenesis in the adult is involved in the formation of trace memories. *Nature*, *410*(6826), 372–376.

Siegal-Gaskins, D., Mejia-Guerra, M. K., Smith, G. D., and Grotewold, E. (2011). Emergence of switch-like behavior in a large family of simple biochemical networks. *PLoS computational biology*, *7*(5), e1002039.

Silverman, J., Takai, H., Buonomo, S. B., Eisenhaber, F., and de Lange, T. (2004). Human Rif1, ortholog of a yeast telomeric protein, is regulated by ATM and 53BP1 and functions in the S-phase checkpoint. *Genes & development*, *18*(17), 2108–2119.

Smith, S. (2007). Information processing in cells and tissues. *BioSystems*, *87*(2-3), 99–100.

Smyth, G. K. (2005). Limma: linear models for microarray data. In *Bioinformatics and computational biology solutions using R and Bioconductor*, 397–420. Springer.

Snyder, J., Hong, N., McDonald, R., and Wojtowicz, J. (2005). A role for adult neurogenesis in spatial long-term memory. *Neuroscience*, *130*(4), 843–852.

Soderling, T. R. and Derkach, V. A. (2000). Postsynaptic protein phosphorylation and LTP. *Trends in neurosciences*, *23*(2), 75–80.

Song, C., Havlin, S., and Makse, H. A. (2005). Self-similarity of complex networks. *Nature*, *433*(7024), 392–395.

Song, I., Kamboj, S., Xia, J., Dong, H., Liao, D., and Huganir, R. L. (1998). Interaction of the N-ethylmaleimide–sensitive factor with AMPA receptors. *Neuron*, *21*(2), 393–400.

Squire, L. R. (2009). The legacy of patient HM for neuroscience. *Neuron*, *61*(1), 6–9.

Squire, L. R. and Alvarez, P. (1995). Retrograde amnesia and memory consolidation: a neurobiological perspective. *Current opinion in neurobiology*, *5*(2), 169–177.

Steward, O., Wallace, C. S., Lyford, G. L., and Worley, P. F. (1998). Synaptic Activation Causes the mRNA for the IEG Arc to Localize Selectively near Activated Postsynaptic Sites on Dendrites. *Neuron*, *21*(4), 741–751.

Strack, S., Barban, M. A., Wadzinski, B. E., and Colbran, R. J. (1997). Differential Inactivation of Postsynaptic Density-Associated and Soluble Ca2+/Calmodulin-Dependent Protein Kinase II by Protein Phosphatases 1 and 2A. *Journal of neurochemistry*, *68*(5), 2119–2128.

Strack, S. and Colbran, R. J. (1998). Autophosphorylation-dependent targeting of calcium/calmodulin-dependent protein kinase II by the NR2B subunit of theN-methyl-D-aspartate receptor. *Journal of Biological Chemistry*, *273*(33), 20689–20692.

Strogatz, S. H. (2001). Exploring complex networks. *Nature*, *410*(6825), 268–276.

Sukhatme, V. P., Cao, X., Chang, L. C., Tsai-Morris, C.-H., Stamenkovich, D., Ferreira, P. C., Cohen, D. R., Edwards, S. A., Shows, T. B., Curran, T., *et al.* (1988). A zinc finger-encoding gene coregulated with c-fos during growth and differentiation, and after cellular depolarization. *Cell*, *53*(1), 37–43.

Svoboda, K. and Mainen, Z. (1999). Synaptic [Ca2+]: intracellular stores spill their guts. *Neuron*, *22*(3), 427.

Svoboda, K., Tank, D. W., and Denk, W. (1996). Direct measurement of coupling between dendritic spines and shafts. *Science*, *272*, 716–718.

Tancredi, V., Zona, C., Velotti, F., Eusebi, F., and Santoni, A. (1990). Interleukin-2 suppresses established long-term potentiation and inhibits its induction in the rat hippocampus. *Brain research*, *525*(1), 149–151.

Teng, H., Cai, W., Zhou, L., Zhang, J., Liu, Q., Wang, Y., Dai, W., Zhao, M., and Sun, Z. (2010). Evolutionary mode and functional divergence of vertebrate NMDA receptor subunit 2 genes. *PloS one*, *5*(10), e13342.

Thakar, J., Pilione, M., Kirimanjeswara, G., Harvill, E. T., and Albert, R. (2007). Modeling systems-level regulation of host immune responses. *PLoS computational biology*, *3*(6), e109.

Thiel, G., Mayer, S. I., Müller, I., Stefano, L., and Rössler, O. G. (2010). Egr-1-A Ca 2+-regulated transcription factor. *Cell calcium*, *47*(5), 397–403.

Thomas, G. M. and Huganir, R. L. (2004). MAPK cascade signalling and synaptic plasticity. *Nature Reviews Neuroscience*, *5*(3), 173–183.

Thomas, R. (1973). Boolean formalization of genetic control circuits. *Journal of theoretical biology*, *42*(3), 563–585.

Tiberi, L., Van Den Ameele, J., Dimidschstein, J., Piccirilli, J., Gall, D., Herpoel, A., Bilheu, A., Bonnefont, J., Iacovino, M., Kyba, M., *et al.* (2012). BCL6 controls neurogenesis through Sirt1-dependent epigenetic repression of selective Notch targets. *Nature neuroscience*, *15*(12), 1627–1635.

Tischmeyer, W. and Grimm, R. (1999). Activation of immediate early genes and memory formation. *Cellular and Molecular Life Sciences CMLS*, *55*(4), 564–574.

Tomita, S., Stein, V., Stocker, T. J., Nicoll, R. A., and Bredt, D. S. (2005). Bidirectional synaptic plasticity regulated by phosphorylation of stargazin-like TARPs. *Neuron*, *45*(2), 269–277.

Traynelis, S. F., Wollmuth, L. P., McBain, C. J., Menniti, F. S., Vance, K. M., Ogden, K. K., Hansen, K. B., Yuan, H., Myers, S. J., and Dingledine, R. (2010). Glutamate receptor ion channels: structure, regulation, and function. *Pharmacological reviews*, *62*(3), 405–496.

Ulitsky, I., Gat-Viks, I., and Shamir, R. (2008). MetaReg: a platform for modeling, analysis and visualization of biological systems using large-scale experimental data. *Genome biology*, *9*(1), R1.

Urakubo, H., Sato, M., Ishii, S., and Kuroda, S. (2014). In Vitro Reconstitution of a CaMKII Memory Switch by an NMDA Receptor-Derived Peptide. *Biophysical journal*, *106*(6), 1414–1420.

Valor, L. and Barco, A. (2010). Hippocampal gene profiling: Toward a systems biology of the hippocampus. *Hippocampus*, *22*(5), 929–941.

VanGuilder, H. D., Vrana, K. E., and Freeman, W. M. (2008). Twenty-five years of quantitative PCR for gene expression analysis. *Biotechniques*, *44*(5), 619.

Varga-Weisz, P. D. and Becker, P. B. (1998). Chromatin-remodeling factors: machines that regulate? *Current opinion in cell biology*, *10*(3), 346–353.

Velculescu, V. E., Zhang, L., Vogelstein, B., Kinzler, K. W., *et al.* (1995). Serial analysis of gene expression. *Science*, *270*(5235), 484–487.

Vickers, C., Dickson, K., and Wyllie, D. (2005). Induction and maintenance of late-phase long-term potentiation in isolated dendrites of rat hippocampal CA1 pyramidal neurones. *The Journal of physiology*, *568*(3), 803–813.

Villarreal, D., Do, V., Haddad, E., and Derrick, B. (2002). NMDA receptor antagonists sustain LTP and spatial memory: active processes mediate LTP decay. *nature neuroscience*, *5*(1), 48–52.

Vogel-Ciernia, A. and Wood, M. A. (2014). Neuron-specific chromatin remodeling: a missing link in epigenetic mechanisms underlying synaptic plasticity, memory, and intellectual disability disorders. *Neuropharmacology*, *80*, 18–27.

Volianskis, A., Bannister, N., Collett, V. J., Irvine, M. W., Monaghan, D. T., Fitzjohn, S. M., Jensen, M. S., Jane, D. E., and Collingridge, G. L. (2013). Different NMDA receptor subtypes mediate induction of long-term potentiation and two forms of short-term potentiation at CA1 synapses in rat hippocampus in vitro. *The Journal of physiology*, *591*(4), 955–972.

Volianskis, A. and Jensen, M. S. (2003). Transient and sustained types of long-term potentiation in the CA1 area of the rat hippocampus. *The Journal of physiology*, *550*(2), 459–492.

Wagner, A. (2005). Distributed robustness versus redundancy as causes of mutational robustness. *Bioessays*, *27*(2), 176–188.

Wales, M. M., Biel, M. A., El Deiry, W., Nelkin, B. D., Issa, J.-P., Cavenee, W. K., Kuerbitz, S. J., and Baylin, S. B. (1995). p53 activates expression of HIC-1, a new candidate tumour suppressor gene on 17p13. 3. *Nature medicine*, *1*(6), 570–577.

Wallace, C. S., Lyford, G. L., Worley, P. F., and Steward, O. (1998). Differential intracellular sorting of immediate early gene mRNAs depends on signals in the mRNA sequence. *The Journal of neuroscience*, *18*(1), 26–35.

Waltereit, R., Dammermann, B., Wulff, P., Scafidi, J., Staubli, U., Kauselmann, G., Bundman, M., and Kuhl, D. (2001). Arg3. 1/Arc mRNA induction by Ca2+ and cAMP requires protein kinase A and mitogen-activated protein kinase/extracellular regulated kinase activation. *The Journal of Neuroscience*, *21*(15), 5484–5493.

Wang, J., Gao, Q.-S., Wang, Y., Lafyatis, R., Stamm, S., and Andreadis, A. (2004). Tau exon 10, whose missplicing causes frontotemporal dementia, is regulated by an intricate interplay of cis elements and trans factors. *Journal of neurochemistry*, *88*(5), 1078–1090.

Wang, J.-H. and Feng, D.-P. (1992). Postsynaptic protein kinase C essential to induction and maintenance of long-term potentiation in the hippocampal CA1 region. *Proceedings of the National Academy of Sciences*, *89*(7), 2576–2580.

Wang, J.-H. and Kelly, P. T. (1996). The balance between postsynaptic Ca (2+)-dependent protein kinase and phosphatase activities controlling synaptic strength. *Learning & Memory*, *3*(2-3), 170–181.

Wang, X., Nagl, N., Wilsker, D., Van Scoy, M., Pacchione, S., Yaciuk, P., Dallas, P., and Moran, E. (2004). Two related ARID family proteins are alternative subunits of human SWI/SNF complexes. *Biochem. J*, *383*, 319–325.

Wang, Y. T. and Linden, D. J. (2000). Expression of cerebellar long-term depression requires postsynaptic clathrin-mediated endocytosis. *Neuron*, *25*(3), 635–647.

Watson, M. A. and Milbrandt, J. (1989). The NGFI-B gene, a transcriptionally inducible member of the steroid receptor gene superfamily: genomic structure and expression in rat brain after seizure induction. *Molecular and cellular biology*, *9*(10), 4213–4219.

Watterson, S., Marshall, S., and Ghazal, P. (2008). Logic models of pathway biology. *Drug discovery today*, *13*(9-10), 447–456.

Weaver, D., Workman, C., and Stormo, G. (1999). Modeling regulatory networks with weight matrices. In *Pacific symposium on biocomputing*, Volume 4, 112–123. Citeseer.

Weeber, E. J., Beffert, U., Jones, C., Christian, J. M., Förster, E., Sweatt, J. D., and Herz, J. (2002). Reelin and ApoE receptors cooperate to enhance hippocampal synaptic plasticity and learning. *Journal of Biological Chemistry*, *277*(42), 39944–39952.

Wei, F., Xu, Z. C., Qu, Z., Milbrandt, J., and Zhuo, M. (2000). Role of EGR1 in hippocampal synaptic enhancement induced by tetanic stimulation and amputation. *The Journal of cell biology*, *149*(7), 1325–1334.

Wibrand, K., Messaoudi, E., Håvik, B., Steenslid, V., Løvlie, R., Steen, V. M., and Bramham, C. R. (2006). Identification of genes co-upregulated with Arc during BDNF-induced long-term potentiation in adult rat dentate gyrus in vivo. *European Journal of Neuroscience*, *23*(6), 1501–1511.

Wigström, H. and Gustafsson, B. (1983). Facilitated induction of hippocampal long-lasting potentiation during blockade of inhibition. *Nature*, *301*, 603–604.

Williams, J., Dragunow, M., Lawlor, P., Mason, S., Abraham, W., Leah, J., Bravo, R., Demmer, J., and Tate, W. (1995). Krox20 may play a key role in the stabilization of long-term potentiation. *Molecular brain research*, *28*(1), 87–93.

Winder, D. G., Mansuy, I. M., Osman, M., Moallem, T. M., and Kandel, E. R. (1998). Genetic and pharmacological evidence for a novel, intermediate phase of long-term potentiation suppressed by calcineurin. *Cell*, *92*(1), 25–37.

Wisden, W., Errington, M., Williams, S., Dunnett, S., Waters, C., Hitchcock, D., Evan, G., Bliss, T., and Hunt, S. (1990). Differential expression of immediate early genes in the hippocampus and spinal cord. *Neuron*, *4*(4), 603–614.

Wisden, W. and Seeburg, P. H. (1993). Mammalian ionotropic glutamate receptors. *Current opinion in neurobiology*, *3*(3), 291–298.

Woo, N. H., Duffy, S. N., Abel, T., and Nguyen, P. V. (2003). Temporal spacing of synaptic stimulation critically modulates the dependence of LTP on cyclic AMP-dependent protein kinase. *Hippocampus*, *13*(2), 293–300.

Worley, P., Bhat, R., Baraban, J., Erickson, C., McNaughton, B., and Barnes, C. (1993). Thresholds for synaptic activation of transcription factors in hippocampus: correlation with long-term enhancement. *The Journal of neuroscience*, *13*(11), 4776–4786.

Wu, Z., Irizarry, R. A., Gentleman, R., Murillo, F. M., and Spencer, F. (2004). A model based background adjustment for oligonucleotide expression arrays. *Journal of the American Statistical Association*, *99*(468), 909–917.

Xie, D., Gore, C., Zhou, J., Pong, R.-C., Zhang, H., Yu, L., Vessella, R. L., Min, W., and Hsieh, J.-T. (2009). DAB2IP coordinates both PI3K-Akt and ASK1 pathways for cell survival and apoptosis. *Proceedings of the National Academy of Sciences*, *106*(47), 19878–19883.

Xing, J., Ginty, D. D., and Greenberg, M. E. (1996). Coupling of the RAS-MAPK pathway to gene activation by RSK2, a growth factor-regulated CREB kinase. *Science*, *273*(5277), 959–963.

Yamagata, K., Andreasson, K. I., Kaufmann, W. E., Barnes, C. A., and Worley, P. F. (1993). Expression of a mitogen-inducible cyclooxygenase in brain neurons: regulation by synaptic activity and glucocorticoids. *Neuron*, *11*(2), 371–386.

Yamagata, K., Kaufmann, W., Lanahan, A., Papapavlou, M., Barnes, C., Andreasson, K., and Worley, P. (1994). Egr3/Pilot, a zinc finger transcription factor, is rapidly regulated by activity in brain neurons and colocalizes with Egr1/zif268. *Learning & Memory*, *1*(2), 140–152.

Yamagata, K., Sanders, L. K., Kaufmann, W. E., Yee, W., Barnes, C. A., Nathans, D., and Worley, P. F. (1994). rheb, a growth factor-and synaptic activity-regulated gene, encodes a novel Ras-related protein. *Journal of Biological Chemistry*, *269*(23), 16333–16339.

Yamaguchi, T., Kimura, J., Miki, Y., and Yoshida, K. (2007). The deubiquitinating enzyme USP11 controls an IkappaB kinase alpha (IKKalpha)-p53 signaling pathway in response to tumor necrosis factor alpha (TNFalpha). *Journal of Biological Chemistry*, *282*(47), 33943–33948.

Yao, G., Tan, C., West, M., Nevins, J. R., and You, L. (2011). Origin of bistability underlying mammalian cell cycle entry. *Molecular systems biology*, *7*(1).

Yokote, K., Mori, S., Hansen, K., McGlade, J., Pawson, T., Heldin, C.-H., and Claesson-Welsh, L. (1994). Direct interaction between Shc and the platelet-derived growth factor beta-receptor. *Journal of Biological Chemistry*, *269*(21), 15337–15343.

Yuste, R. and Bonhoeffer, T. (2001). Morphological changes in dendritic spines associated with long-term synaptic plasticity. *Annual review of neuroscience*, *24*(1), 1071–1089.

Zalutsky, R. A. and Nicoll, R. A. (1990). Comparison of two forms of long-term potentiation in single hippocampal neurons. *Science*, *248*(4963), 1619–1624.

Zhang, B., Gaiteri, C., Bodea, L.-G., Wang, Z., McElwee, J., Podtelezhnikov, A. A., Zhang, C., Xie, T., Tran, L., Dobrin, R., *et al.* (2013). Integrated Systems Approach Identifies Genetic Nodes and Networks in Late-Onset Alzheimer's Disease. *Cell*, *153*(3), 707–720.

Zhang, B., Horvath, S., *et al.* (2005). A general framework for weighted gene co-expression network analysis. *Statistical applications in genetics and molecular biology*, *4*(1), 1128.

Zhang, J., Wang, J., Wu, Q., Kuang, W., Huang, X., He, Y., and Gong, Q. (2011). Disrupted brain connectivity networks in drug-naive, first-episode major depressive disorder. *Biological psychiatry*, *70*(4), 334–342.

Zhang, L., Yang, S.-H., and Sharrocks, A. D. (2007). Rev7/MAD2B links c-Jun N-terminal protein kinase pathway signaling to activation of the transcription factor Elk-1. *Molecular and cellular biology*, *27*(8), 2861–2869.

Zhu, C., Johansen, F.-E., and Prywes, R. (1997). Interaction of ATF6 and serum response factor. *Molecular and cellular biology*, *17*(9), 4957–4966.

Ziv, N. E. and Smith, S. J. (1996). Evidence for a role of dendritic filopodia in synaptogenesis and spine formation. *Neuron*, *17*(1), 91–102.

Zola-Morgan, S., Squire, L. R., and Amaral, D. (1986). Human amnesia and the medial temporal region: enduring memory impairment following a bilateral lesion limited to field CA1 of the hippocampus. *The Journal of Neuroscience*, *6*(10), 2950–2967.

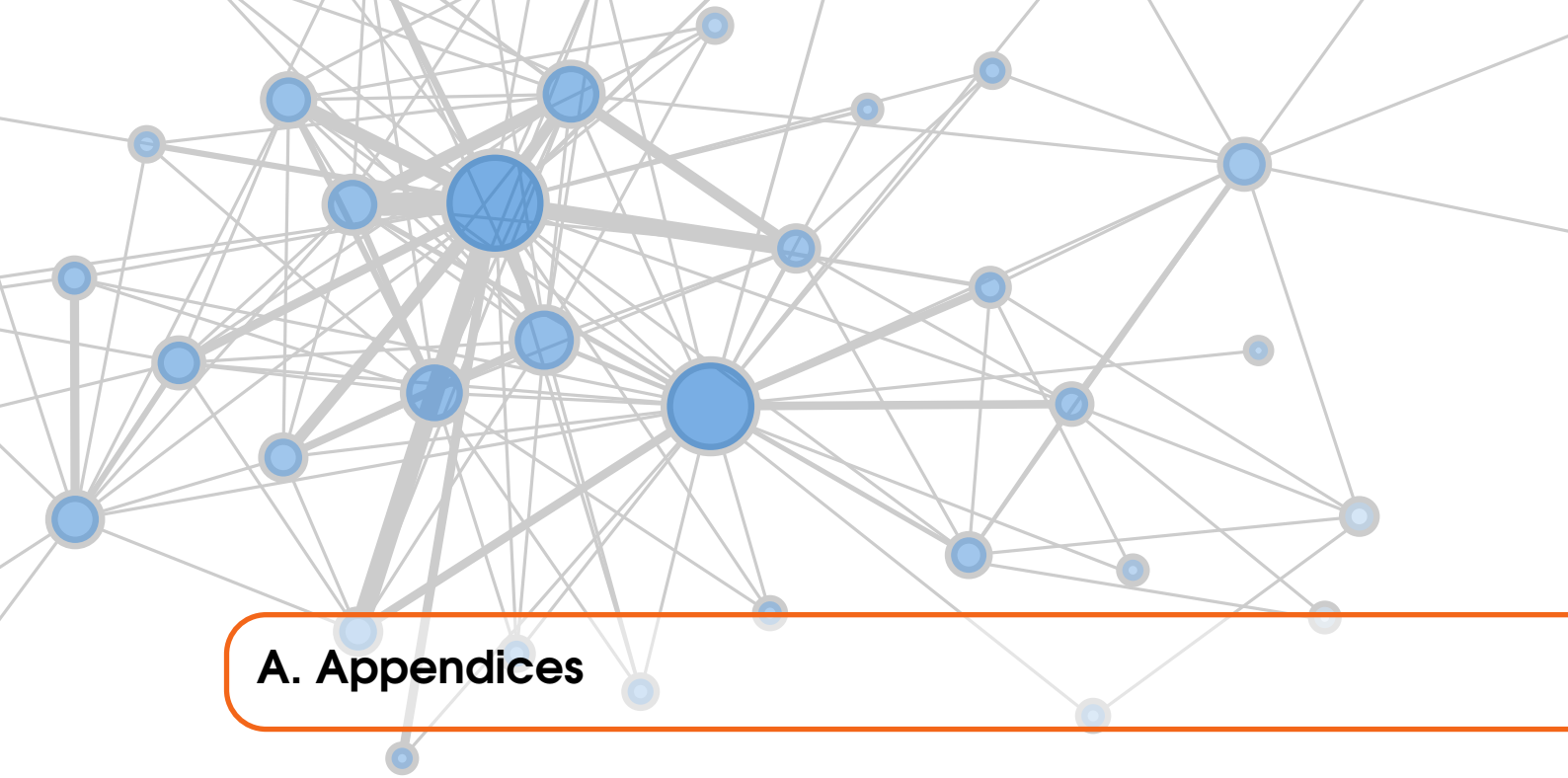

A. Appendices

A.1 List of differentially expressed genes

A.1.1 20 min post-LTP

Top 50 differentially expressed genes, $p - value < 0.05$, $-0.15 < ln(\text{Fold Change}) < 0.15$

	$p - value$	ln(Fold Change)	Gene Symbol
1390166_at	8.80E-05	3.80E-01	
1369053_at	1.50E-03	2.83E-01	Syt2
1382848_at	3.43E-03	-2.49E-01	
1369803_at	3.74E-03	3.12E-01	Ptf1a
1387313_at	4.30E-03	2.77E-01	Myoc
1368657_at	4.67E-03	2.90E-01	Mmp3
1381302_at	5.22E-03	2.21E-01	
1384726_at	5.28E-03	-2.07E-01	
1398033_at	5.44E-03	3.27E-01	
1375816_at	5.46E-03	-3.10E-01	
1382084_at	5.75E-03	3.40E-01	
1391508_at	5.96E-03	2.56E-01	
1396041_at	6.14E-03	3.15E-01	
1382360_at	6.41E-03	2.36E-01	Fzd5
1398162_at	6.55E-03	2.31E-01	
1387974_a_at	6.76E-03	2.10E-01	Slc21a4
1380224_at	7.13E-03	2.02E-01	Eftud2
1370203_at	7.44E-03	2.22E-01	Pgap2
1381214_at	7.45E-03	2.22E-01	
1378870_at	7.95E-03	2.24E-01	
1393206_at	7.99E-03	2.19E-01	
1389645_at	8.05E-03	3.43E-01	Prodh2
1368707_at	8.18E-03	-2.87E-01	Itih4
1377292_at	8.21E-03	2.59E-01	
1386754_at	8.23E-03	2.87E-01	Trim14
1397923_at	8.38E-03	2.01E-01	
1395033_at	9.18E-03	2.28E-01	
1398504_at	9.34E-03	2.41E-01	
1380432_at	9.35E-03	2.26E-01	Cmah
1394127_at	9.53E-03	2.22E-01	
1397256_at	9.55E-03	2.37E-01	
1376083_at	9.82E-03	2.12E-01	Memo1
1378799_at	1.00E-02	-3.22E-01	
1373259_at	1.03E-02	2.32E-01	

1395859_at	1.03E-02	2.30E-01	
1394661_at	1.08E-02	1.72E-01	
1396391_at	1.11E-02	-2.89E-01	
1378990_at	1.12E-02	-3.16E-01	
1394757_at	1.12E-02	-1.99E-01	
1375379_at	1.12E-02	2.49E-01	Tap1
1375322_at	1.12E-02	-2.81E-01	Sema6c
1371034_at	1.13E-02	2.26E-01	Onecut1
1380941_at	1.13E-02	3.49E-01	
1397437_at	1.16E-02	2.33E-01	Arid5a
1369488_at	1.19E-02	-2.20E-01	Fut4
1389502_at	1.19E-02	1.91E-01	
1382936_at	1.19E-02	-2.23E-01	
1370593_at	1.21E-02	1.70E-01	Cyp3a2
1380493_at	1.25E-02	3.59E-01	Tet3
1382461_at	1.29E-02	1.74E-01	Prmt7

A.1.2 5 h post-LTP

Top 50 differentially expressed genes, $p-value < 0.05$, $-0.15 < ln(\text{Fold Change}) < 0.15$

	$p-value$	log_2(Fold Change	Gene Symbol
1384601_at	5.67E-04	2.56E-01	Lrba
1387269_s_at	1.40E-03	2.41E-01	Plaur
1377015_at	1.66E-03	2.68E-01	
1374242_at	1.71E-03	2.45E-01	
1370454_at	1.73E-03	1.33E+00	Homer1
1380252_at	1.96E-03	-2.12E-01	Psmd11
1391414_at	2.00E-03	-3.56E-01	LOC679811
1381256_at	2.14E-03	-2.44E-01	
1374120_at	2.20E-03	-2.26E-01	Slc45a4
1369195_at	2.44E-03	2.14E-01	Fabp2
1390681_at	2.73E-03	3.66E-01	Tgif2
1382197_at	3.33E-03	2.58E-01	Rhod
1382136_at	3.36E-03	-2.20E-01	Slc2a9
1390071_at	3.39E-03	2.45E-01	
1371984_at	4.38E-03	-3.69E-01	Ldb3
1373903_at	4.41E-03	2.08E-01	Rcsd1
1389078_at	4.42E-03	-2.91E-01	Fbxl6
1390693_at	4.83E-03	1.76E-01	
1384849_at	5.07E-03	2.39E-01	
1396339_at	5.47E-03	3.08E-01	
1393621_at	5.51E-03	2.47E-01	
1389514_at	5.56E-03	3.54E-01	Lingo1
1380627_at	5.64E-03	-3.14E-01	
1390147_at	5.65E-03	-1.86E-01	RGD1559904
1384996_at	5.76E-03	4.69E-01	
1397562_at	5.95E-03	1.83E-01	
1384070_at	6.02E-03	-2.96E-01	Gmip
1387395_at	6.37E-03	2.58E-01	Adora2b
1382062_at	6.39E-03	-2.31E-01	Gstcd
1378432_at	6.68E-03	2.57E-01	Pttg1ip
1384902_at	6.82E-03	2.06E-01	
1384555_at	6.84E-03	-2.68E-01	Dennd1c
1389606_at	7.06E-03	-2.28E-01	Anapc1
1371978_at	7.12E-03	-2.03E-01	Osbpl9
1373708_at	7.29E-03	-2.37E-01	Tut1
1371627_at	7.32E-03	-3.13E-01	
1396993_at	7.40E-03	1.98E-01	Hsh2d
1368456_at	7.51E-03	-1.73E-01	Gabrr1
1385256_at	7.54E-03	4.89E-01	
1395733_at	7.65E-03	-1.97E-01	
1382516_at	7.65E-03	-2.43E-01	
1378384_at	7.69E-03	3.55E-01	Ints6
1397658_at	7.79E-03	2.05E-01	
1397009_at	7.90E-03	2.25E-01	
1390385_at	8.33E-03	1.69E-01	Glce
1388422_at	8.43E-03	-2.92E-01	Lims2
1397938_at	8.64E-03	1.99E-01	
1392664_at	9.05E-03	1.68E-01	Gpr182

1396276_at	9.30E-03	-3.30E-01	
1390925_a_at	9.31E-03	-1.66E-01	Igsf3

A.1.3 24 h post-LTP

Top 50 differentially expressed genes, $p-value < 0.05$, $-0.15 < ln(\text{Fold Change}) < 0.15$

	$p-value$	log_2(Fold Change	Gene Symbol
1377104_at	1.44E-04	3.77E-01	
1398135_at	1.49E-04	2.68E-01	
1373252_at	1.51E-04	3.06E-01	Fmnl3
1377641_at	2.24E-04	2.98E-01	Fam29a
1382627_at	2.43E-04	-4.93E-01	
1396642_at	2.43E-04	-4.48E-01	Usp34
1389628_at	2.70E-04	3.53E-01	Plcd3
1377686_at	4.62E-04	-4.25E-01	
1386437_at	5.28E-04	2.43E-01	Txlnb
1396213_at	6.16E-04	2.84E-01	
1381256_at	6.34E-04	3.04E-01	
1379286_at	6.41E-04	-5.19E-01	Rnf152
1373511_at	6.45E-04	-3.28E-01	
1377151_at	9.26E-04	-8.37E-01	
1381633_at	1.09E-03	-2.19E-01	
1384662_at	1.09E-03	2.90E-01	
1393332_at	1.14E-03	3.87E-01	Gfod2
1398539_at	1.26E-03	3.96E-01	
1373483_at	1.46E-03	3.11E-01	Kank3
1370594_at	1.49E-03	-6.26E-01	Igsf1
1390640_at	1.57E-03	3.79E-01	Chtf18
1387348_at	1.61E-03	-5.81E-01	Igfbp5
1387787_at	1.61E-03	4.47E-01	Mylpf
1377847_at	1.67E-03	2.36E-01	
1369858_at	1.87E-03	3.24E-01	Grpr
1397213_at	1.88E-03	2.28E-01	
1382734_at	2.20E-03	4.05E-01	
1389692_at	2.23E-03	2.09E-01	Rab22a
1376728_at	2.42E-03	-7.55E-01	
1368536_at	2.50E-03	-1.26E+00	Enpp2
1381298_at	2.52E-03	2.68E-01	Mcm10
1384603_at	2.58E-03	-7.03E-01	Abca4
1393098_at	2.64E-03	-3.06E-01	Llgl2
1375293_at	2.72E-03	2.56E-01	
1382405_at	2.72E-03	2.56E-01	
1375779_at	2.79E-03	-2.77E-01	
1377073_at	2.81E-03	2.79E-01	LOC100911193
1367504_at	2.84E-03	2.31E-01	
1390294_at	2.99E-03	2.79E-01	Atxn7l4
1396069_at	3.08E-03	2.90E-01	Kdm6a
1384960_at	3.10E-03	2.14E-01	Cftr
1394745_at	3.27E-03	-4.45E-01	
1385136_at	3.33E-03	2.69E-01	Lrrc26
1382069_at	3.39E-03	-2.88E-01	Atp11a
1387889_at	3.39E-03	-1.72E+00	Folr1
1387693_a_at	3.40E-03	-7.20E-01	Slc6a9
1382741_at	3.40E-03	-3.52E-01	Ube3a
1385500_at	3.53E-03	-1.13E+00	RGD1561795
1394830_at	3.57E-03	2.93E-01	
1376568_at	3.61E-03	2.76E-01	

A.2 Top Gene Ontology terms for co-expression networks

Table A.4: *Top Gene Ontology terms for each of the modules ($p < 0.01$)*

Module	GO Term
black_20	positive regulation of receptor-mediated endocytosis regulation of reactive oxygen species metabolic process

Continued on next page

Table A.4 – *Continued from previous page*

Module	GO Term
	regulation of hydrolase activity
	negative regulation of transcription by competitive promoter binding
	energy derivation by oxidation of organic compounds
	ribonucleoside metabolic process
black_24	morphogenesis of a polarized epithelium
	establishment of planar polarity
	establishment of tissue polarity
	post-anal tail morphogenesis
	acetyltransferase activity
	canonical Wnt receptor signaling pathway
black_5H	coated pit
	anion homeostasis
	neuromuscular junction
	sarcolemma
	synapse assembly
	cholesterol metabolic process
black_U	negative regulation of tissue remodeling
	membrane budding
	interleukin-1 secretion
	regulation of interleukin-1 secretion
	protein transport
	response to nitric oxide
blue_20	vitamin metabolic process
	positive regulation of leukocyte activation
	positive regulation of cell activation
	lipid transporter activity
	water-soluble vitamin metabolic process
	secretion of lysosomal enzymes
blue_24	regulation of endocrine process
	endocrine hormone secretion
	retina development in camera-type eye
	cellular response to corticosteroid stimulus
	response to estrogen stimulus
	steroid catabolic process
blue_5H	cellular amino acid biosynthetic process
	vacuolar membrane
	aspartate family amino acid catabolic process
	aspartate family amino acid metabolic process
	positive regulation of oxidoreductase activity
	vacuole
blue_U	nucleus
	protein phosphatase type 2A complex
	phosphoric diester hydrolase activity
	DNA binding
	sequence-specific DNA binding RNApolII TF activity
	dephosphorylation
brown_20	cytoplasmic microtubule
	organic hydroxy compound transport
	Rho guanyl-nucleotide exchange factor activity
	monoamine transport
	microtubule binding
	cilium
brown_24	cofactor transporter activity
	heterocyclic compound binding
	modified amino acid binding
	organic cyclic compound binding
	female meiosis
	cofactor transport
brown_5H	potassium ion transport
	insulin-like growth factor receptor binding
	cell body membrane
	Ras GTPase binding
	response to nutrient
	dendrite cytoplasm
brown_U	regulation of secretion
	plasma membrane
	regulation of multicellular organismal process

Continued on next page

Table A.4 – *Continued from previous page*

Module	GO Term
	cell periphery
	regulation of system process
	negative regulation of secretion
cyan_24	gastric acid secretion
	early endosome to late endosome transport
	single-stranded DNA binding
	negative regulation of pathway-restricted SMAD protein phosphorylation
	acid secretion
	DNA repair
cyan_5H	regulation of DNA methylation
	negative regulation of IkB kinase/NFkB cascade
	DNA alkylation
	DNA methylation
	negative regulation of viral transcription
	osteoblast proliferation
darkgreen_5H	6-phosphofructo-2-kinase activity
	sugar:hydrogen symporter activity
	cation:sugar symporter activity
	phosphofructokinase activity
	cytoplasmic ubiquitin ligase complex
	DNA replication factor A complex
darkgrey_5H	M/G1 transition of mitotic cell cycle
	negative regulation of exit from mitosis
	regulation of extracellular matrix constituent secretion
	positive regulation of extracellular matrix constituent secretion
	glycine metabolic process
	glycine biosynthetic process
darkred_5H	chondroitin sulfate metabolic process
	chondroitin sulfate proteoglycan metabolic process
	lipid phosphorylation
	phosphatidylinositol phosphorylation
	aminoglycan metabolic process
	glycosaminoglycan metabolic process
darkturquoise_5H	negative regulation of protein autophosphorylation
	response to oxidative stress
	response to hydrogen peroxide
	regulation of protein autophosphorylatioon
	response to reactive oxygen species
	oxygen transport
green_20	response to axon injury
	regulation of interphase of mitotic cell cycle
	response to calcium ion
	quaternary ammonium group transport
	reflex
	alcohol binding
green_24	interaction with host
	regulation of gliogenesis
	regulation of organ formation
	adenohypophysis development
	embryonic skeletal system development
	regulation of astrocyte differentiation
green_5H	regulation of amino acid transport
	steroid binding
	xenobiotic metabolic process
	response to xenobiotic stimulus
	cellular response to xenobiotic stimulus
	gamma-aminobutyric acid secretion
green_U	outflow tract septum morphogenesis
	labyrinthine layer morphogenesis
	embryonic placenta morphogenesis
	cranial suture morphogenesis
	craniofacial suture morphogenesis
	lateral sprouting from an epithelium
greenyellow_24	intrinsic to mitochondrial outer membrane
	integral to mitochondrial outer membrane
	superior temporal gyrus development
	tau-protein kinase activity

Continued on next page

Table A.4 – *Continued from previous page*

Module	GO Term
	protein K63-linked ubiquitination
	protein K48-linked ubiquitination
greenyellow_5H	regulation of myeloid leukocyte differentiation
	glycoprotein binding
	macrophage differentiation
	regulation of macrophage differentiation
	response to calcium ion
	protein tyrosine/threonine phosphatase activity
grey60_5H	regulation of branching involved in salivary gland morphogenesis
	cochlea development
lightcyan_24	regulation of cellular response to stress
	optic nerve development
	optic nerve morphogenesis
	optic nerve structural organization
	regulation of eosinophil differentiation
	interleukin-5 receptor binding
lightcyan_5H	pyrimidine nucleotide metabolic process
	pyrimidine nucleoside triphosphate metabolic process
	pyrimidine ribonucleoside triphosphate metabolic process
	pyrimidine ribonucleotide metabolic process
	pyrimidine nucleoside metabolic process
	pyrimidine ribonucleoside metabolic process
lightgreen_5H	regulation of T cell migration
	positive regulation of T cell migration
	tumor necrosis factor superfamily cytokine production
	T cell migration
	regulation of lymphocyte migration
	positive regulation of lymphocyte migration
lightyellow_5H	central nervous system neuron axonogenesis
	establishment of nucleus localization
	nucleus localization
	dendritic spine morphogenesis
	dendritic spine organization
	dendritic spine development
magenta_20	pattern binding
	polysaccharide binding
	protein activation cascade
magenta_24	proteasomal protein catabolic process
	cullin-RING ubiquitin ligase complex
	response to virus
	ubiquitin ligase complex
	defense response to virus
	proteasomal ubiquitin-dependent protein catabolic process
magenta_5H	progesterone receptor signaling pathway
	response to gonadotropin stimulus
	microvillus
	blastocyst development
	epithelial cell differentiation involved in kdney development
	mesenchymal to epithelial transition
magenta_U	integrin binding
	inflammatory response
midnightblue_24	clathrin-coated endocytic vesicle
	chaperone-mediated protein folding
	mitogen-activated protein kinase binding
	negative regulation of B cell activation
	regulation of lymphocyte differentiation
midnightblue_5H	negative regulation of cytokine biosynthetic process
	neutral amino acid transmembrane transporter activity
	actinin binding
	alpha-actinin binding
	neutral amino acid transport
	mesodermal cell differentiation
pink_20	calmodulin-dependent protein kinase activity
	protein serine/threonine kinase activity
	neural crest cell migration
	positive regulation of proteasomal ubiquitin-dependent protein catabolic process
	positive regulation of proteasomal protein catabolic process

Continued on next page

Table A.4 – *Continued from previous page*

Module	GO Term
	Golgi vesicle transport
pink_24	fatty-acyl-CoA binding transporter activity sensory perception of chemical stimulus mannose metabolic process cholesterol storage plasma lipoprotein particle assembly
pink_5H	RNApolII core promoter proximal region sequence-specific DNA binding TF activity involved in negative regulation of transcription RNApolII transcription regulatory region sequence-specific DNA binding TF activity involved in negative regulation of transcription sexual reproduction taurine binding immunoglobulin production activation-induced cell death of T cells
pink_U	mitochondrial transport regulation of intrinsic apoptotic signaling pathway regulation of mitochondrial membrane permeability regulation of release of cytochrome c from mitochondria positive regulation of intrinsic apoptotic signaling pathway. intrinsic apoptotic signaling pathway
purple_24	negative regulation of vascular permeability glycogen granule midbody chemical homeostasis regulation of glycogen catabolic process cAMP-mediated signaling
purple_5H	histone H3-K27 methylation regulation of neutrophil chemotaxis endothelial cell apoptotic process regulation of endothelial cell apoptotic process positive regulation of lymphocyte differentiation regulation of primary metabolic process
red_20	perinuclear region of cytoplasm regulation of axonogenesis dendrite development regulation of neuron projection development regulation of cell projection organization cellular component morphogenesis
red_24	septin complex septin cytoskeleton myeloid leukocyte activation interleukin-23 production regulation of interleukin-23 production negative regulation of interleukin-17 production
red_5H	maternal placenta development regulation of JNK cascade multicellular organismal movement musculoskeletal movement positive regulation of natural killer cell mediated immune response to tumor cell positive regulation of natural killer cell mediated cytotoxicity directed against tumor cell target
red_U	organonitrogen compound metabolic process regulation of GTP catabolic process regulation of GTPase activity positive regulation of GTPase activity cellular amide metabolic process regulation of nucleoside metabolic process
royalblue_5H	chromatin remodeling carboxypeptidase activity cytosolic part exopeptidase activity
salmon_24	striated muscle adaptation positive regulation of steroid biosynthetic process cGMP biosynthetic process rRNA processing rRNA metabolic process

Continued on next page

Table A.4 – *Continued from previous page*

Module	GO Term
	positive regulation of steroid metabolic process
salmon_5H	positive regulation of vasoconstriction ethanolamine-containing compound metabolic process protein targeting to mitochondrion
tan_24	Golgi stack chromosome organization macromolecule methylation mitotic sister chromatid segregation methylation chromatin modification
tan_5H	cellular response to heat neuromuscular synaptic transmission lipoprotein biosynthetic process lipoprotein metabolic process MAPK import into nucleus RNA import into nucleus
turquoise_20	oxidoreductase activity negative regulation of defense response flavin adenine dinucleotide binding regulation of natural killer cell mediated immunity positive regulation of natural killer cell mediated immunity regulation of histone deacetylation
turquoise_24	leading edge membrane negative regulation of protein catabolic process response to external stimulus positive chemotaxis cellular component movement neuron projection membrane
turquoise_5H	DNA catabolic process axoneme SCF ubiquitin ligase complex TBP-class protein binding regulated secretory pathway transcription initiation from RNApolII promoter
turquoise_U	polysaccharide catabolic process glycogen catabolic process glucan catabolic process cellular polysaccharide catabolic process polysaccharide metabolic process methylated histone residue binding
yellow_20	transcription from RNApolI promoter hormone biosynthetic process vascular endothelial growth factor production regulation of vascular endothelial growth factor regulation of transcription from RNApolI promoter positive regulation of protein import into nucleus (translocation)
yellow_24	proteasomal protein catabolic process proteasomal ubiquitin-dependent protein catabolic process cell-cell adhesion involved in gastrulation negative regulation of gene expression transcription cofactor activity negative regulation of macromolecule biosynthetic process
yellow_5H	chromatin DNA binding thyroid hormone receptor activator activity positive regulation of response to interferon-gamma positive regulation of interferon-gamma-mediated signaling pathway electron carrier activity androgen metabolic process
yellow_U	BRCA1-A complex photoreceptor cell maintenance positive regulation of response to DNA damage stimulus visual perception ion channel binding calcium-dependent phospholipid binding